Universitat Autònoma de Barcelona

ROLE OF ADAM17 IN KIDNEY DISEASE: A CLINICAL AND EXPERIMENTAL APPROACH

Vanesa Palau González

ROLE OF ADAM17 IN KIDNEY DISEASE: A CLINICAL AND EXPERIMENTAL APPROACH

Doctoral Thesis submitted by

Vanesa Palau González

For the degree of Doctor

Directors

Dr. Julio Pascual Santos

Dr. Mª José Soler Romeo

Dr. Marta Riera Oliva

Tutor

Dr. Julio Pascual Santos

Doctoral Program in Medicine
Department of Medicine
Universitat Autònoma de Barcelona
Barcelona, November 2020

Els doctors Julio Pascual Santos (director/tutor), Maria José Soler Romeo (directora) i Marta Riera Oliva (directora),

Certifiquen:

Que el treball experimental i la redacció de la memòria de la Tesi Doctoral titulada “Role of ADAM17 in kidney disease: a clinical and experimental approach” han estat realitzats per la Vanesa Palau González sota la seva direcció i consideren que l’esmentada tesi és apta per a ser presentada per optar al grau de Doctora en Medicina per la Universitat Autònoma de Barcelona.

I per a que en quedi constància, signen aquest document.

Dr. Julio Pascual Santos Dra. Maria José Soler Romeo Dra. Marta Riera Oliva

Al meu avi.

ACKNOWLEDGEMENTS

Acknowledgements

Aquesta tesis ha estat possible gràcies a l'ajut i el suport de molts.

En primer lloc, agraeixo als meus directors de tesi el recolzament i la confiança durant aquests 4 anys. Al Dr. Julio Pascual por darme la oportunidad de formar parte de este grupo, por el apoyo y la confiança depositada en mi. A la Dra. Maria José Soler per aportar una visió clínica al projecte, per la motivació per la feina ben feta i per tot el recolzament professional i personal rebut en aquests 4 anys. A la Dra. Marta Riera per tota l'ajuda en el dia a dia al laboratori, per la seva empatia, per tots els moments "fora del lab" per fer pinya i per tot el suport tant a nivell científic com personal. Gràcies a tots!!

To my supervisors in Zurich, Dr. Emmert, Dr. Hoestrup, and specially Dr. Nugraha for giving me the opportunity to join your team during my stay. It was a great experience on a personal and scientific level.

Als meus companys de laboratori, des del primer fins a l'últim, tots heu sigut imprescindibles per aquesta tesi. Al Dr. Sergi Clotet, a la Dra. Lidia Anguiano i a la Marta Rebull perquè vau formar part de la primera etapa al lab quan tant sols era una estudiant de màster. Per tot el que m'heu ensenyat i per tot el que he après de vosaltres. Dr. Budour there is not enough space in these pages to thank you for what you have meant in this thesis. Thank you for all your help in the lab, for your understanding and support, for all the intense conversations we had, for all the plans, for all the travels, for being a great friend. You will always have a place wherever I am. Al David, perquè vam començar junts i hem acabat junts aquesta etapa. Gràcies per tota l'ajuda al lab, per tots els riures i per aguantar-me en els meus millors i pitjors dies. Has estat el millor tècnic que podria haver tingut al costat durant la tesis. A la futura doctora Laura Llinàs, per la seva efusivitat, per tots els "cotilleos", per totes les aventures als congressos i tots els Kit Kats durant aquests 4 anys. A la Dàlia, per la seva positivitat i per encoratjar-me a seguir endavant quan les coses no sortien del tot bé. A tots vosaltres GRÀCIES!

To my Swiss labmates, Erik, Nick, Sofia, Pascal and Vicky. Thank you for your practical help, support and warm humour. You have made staying away from home more enjoyable.

A l'Evelyn, perquè ens vam conèixer en el curs d'animals, entre riures i pors, i des d'aleshores et vas convertir en una amiga. Per la teva simpatia, per tots els moments divertits (entre riures i plors), per totes les "Beer Sessions", per totes les excursions, viatges i plans que hem anat fent durant aquest temps. Estic convençuda de que arribaràs molt lluny com a farmacèutica i allà estaré per celebrar-ho juntes, com sempre.

Al servei de Nefrologia de l'hospital per ser partícip de l'evolució d'aquesta tesi en les sessions i en els congressos i per contribuir amb una visió clínica.

A la Begoña i la Lucía, per la seva paciència i la seva ajuda diària a l'estabulari d'Ubiomex.

A les nenes de la uni, Mireia, Bruna, Laura, Nerea, Maria i Leire, perquè amb vosaltres va començar tot. Per totes les bbq, per totes les escapadetes, per tots els caps d'anys BQ, per totes les festes i per tot el que ha d'arribar. Sous les millors!

A las de toda la vida, Cris, Sara y Anna Maria, porque por muy lejos que estemos, siempre puedo contar con vosotras.

A la meva família, avís, tiets i cosins per animar-me sempre a seguir endavant tot i no entendre moltes vegades de que va això de la tesis i els ratolins. M'heu ensenyat la importància d'encarar aquest projecte amb dedicació i ganes. Al meu avi, perquè estic convençuda de que series l'home més feliç del món el dia de la meva defensa. A la Mercè, per transmetre'm sempre l'energia per seguir endavant i per tota l'ajuda amb la correcció de la tesis. I especialment...

Als meus pares, pel suport incondicional, per la confiança, per aguantar els moments d'estrès, per acompanyar-me sempre en totes les meves decisions. Gracias por estar siempre cuando os he necesitado, por todos los buenos consejos, por dármelo todo.

Al Marc, per estar sempre al meu costat des del primer dia, per tots els viatges a Zurich, per ajudar-me amb les figures, per treure'm sempre un somriure, per ensenyar-me a desconnectar, per animar-me a seguir endavant i per què sé que sempre puc comptar amb tu.

ABBREVIATIONS

Abbreviations

ACE – Angiotensin converting enzyme

ACE2 – Angiotensin converting enzyme 2

ACR – Albumin-to-creatinine ratio

ADAM – A disintegrin and Metalloproteinase

AGEs – advanced glycation end-products

AGT – Angiotensinogen

AKI – Acute kidney injury

ANG – Angiotensin

ARB – Angiotensin II receptor blocker

AT1R – Angiotensin II receptor type 1

AT2R – Angiotensin II receptor type 1

C-terminal – Carboxi-terminal

CKD – Chronic kidney disease

CV – Cardiovascular

CysSL – Cysteine switch-like region

Da – Dalton

DBP – Diastolic blood pressure

DN – Diabetic nephropathy

eADAM17 – Endothelial ADAM17

ECM – Extracellular matrix

EGF – Epidermal growth factor

EGFR – Epidermal growth factor receptor

ESRD – End-stage renal disease

FAK – Focal adhesion kinase

GBM – Glomerular basement membrane

GFR – Glomerular filtration rate

GLUT – Glucose transporter

HB-EGF – Heparin binging EGF-like growth factor

HG – High glucose

HKC-8 – Human proximal tubular cells

IFTA – Interstital fibrosis and tubular atrophy

KO – Knockout

LG – Low glucose

MAPK – p38-mitogen activated protein kinase

M-CSF – macrophage-colony stimulating factor

MCP-1 – Monocyte chemoattractant protein-1

MMPs – Metalloproteases

NOD – Non-obese diabetic

N-terminal – Amino-terminal

PAS – Periodic acid-Schiff

PCR - Polymerase chain reaction

PDGF - Platelet-derived growth factor

PEPCK - Phosphoenolpyruvate carboxykinase

PMA – Phorbol myristate acetate

PVDF – Polyvinylidene fluoride

RAS – Renin-angiotensin system

RFU – Relative fluorescence units

ROS – Reactive oxygen species

RT-qPCR – Quantitative reverse transcriptase PCR

STZ – Streptozotocin

SBP – Systolic blood pressure

tADAM17 – Proximal tubular ADAM17

TAPI – TNF-α processing inhibitor

TGF-α – Transforming growth factor α

TGF-β – Transforming growth factor β

TIMPs – Tissue inhibitors of metalloproteinases

TNF-α – Tumour necrosis factor α

TNFR – TNF-α receptor

UAE – Urinary albumin excretion

UUO – Unilateral ureteral obstruction

WT – Wild-type

WT-1 – Wilms Tumour 1

Zn-BR – Zinc-binding domain region

α-SMA – α-smooth muscle actin

Table of contents

SUMMARY

Summary

Disintegrins and metalloproteinases (ADAMs) are a family of proteinases that function as sheddases. Especially, ADAM17 has been the best studied family member. ADAM17 is highly expressed in renal distal tubules and is increased in the whole kidney, mainly in endothelial and proximal tubular cells, during chronic kidney disease (CKD), diabetic nephropathy (DN) and cardiovascular (CV) disease, among others. Given these premises, three studies have been proposed in this thesis. Firstly, baseline circulating ADAMs activity was analysed in human plasma samples from the NEFRONA Study, which includes CKD patients without previous history of CV disease. Baseline and prospective studies were performed to evaluate the association of circulating ADAMs activity with baseline clinical variables, and with the progression of renal function and CV outcomes. Secondly, the role of endothelial (*eAdam17*) and proximal tubular (*tAdam17*) *Adam17* deletion in renal histology, modulation of the renin angiotensin system (RAS), renal inflammation and fibrosis was studied in a mouse model of type 1 Diabetes Mellitus. Thirdly, the effect of *Adam17* deletion in an *in vitro* 3D cell culture from human proximal tubular cells under high glucose conditions was evaluated. The human study showed that circulating ADAMs activity is a powerful predictor of CKD progression in male patients. Furthermore, circulating ADAMs activity is independently associated with CV events in CKD patients. Within the experimental studies, *eAdam17* deletion attenuates renal fibrosis and inflammation, whereas *tAdam17* deletion decreases podocyte loss, attenuates the RAS, and decreases macrophage infiltration and α-SMA and collagen accumulation. The 3D *in vitro* cell culture reinforced the findings obtained in *tAdam17KO* mice with decreased fibrosis in the *Adam17* knockout spheroids. In conclusion, the manipulation of *Adam17* should be considered as a therapeutic strategy for treating DN. In CKD patients, without previous history of CV disease, circulating ADAMs activity can be useful as a biomarker of renal and CV outcomes.

RESUM

Resum

Les desintegrines i metal·loproteases (ADAMs) són una família de proteïnases que alliberen dominis proteics solubles en un procés conegut com a “shedding”. En concret, l’ADAM17 és el membre de la família millor estudiat. Aquest, es troba altament expressat en les cèl·lules dels túbuls distals i augmenta la seva expressió en totes les cèl·lules del ronyó en la malaltia renal crònica (MRC), la nefropatia diabètica (ND) i la malaltia cardiovascular (CV), entre d’altres. Basant-nos en aquests antecedents, es van dissenyar tres estudis per aquesta tesi doctoral. En primer lloc, es va analitzar l’activitat circulant dels ADAMs en plasmes humans de la cohort NEFRONA que inclou pacients amb MRC sense història prèvia de malaltia CV. Es va avaluar l’associació entre l’activitat circulant dels ADAMs i variables clíniques basals, així com amb la progressió de la funció renal i els events CV. Per altra banda, es va estudiar l’efecte en el ronyó de la deleció de l’*Adam17,* a nivell endotelial (*eAdam17*) o tubular proximal (*tAdam17*), en la histologia, la modulació del sistema renina angiotensina (SRA), la inflamació i la fibrosis en un model murí de diabetis tipus 1. Finalment, en un cultiu 3D de cèl·lules tubulars proximals humanes, en condicions d’alta glucosa, també es va abordar l’efecte de la deleció de *l’Adam17*. L’estudi en humans va demostrar que l’activitat circulant dels ADAMs era un potent predictor de la progressió de MRC en els homes. A més, s’associava de forma independent amb els events CV en els pacients amb MRC. En relació amb els estudis experimentals, es va veure com la deleció específica de l’*eAdam17* atenuava la fibrosis i la inflamació renal, mentre que la deleció del *tAdam17* disminuïa la pèrdua podocitària, atenuava el SRA i disminuïa la infiltració per macròfags així com l’acumulació de α-SMA i col·lagen en el ronyó. El cultiu *in vitro* 3D va reforçar els resultats obtinguts en el model de ratolí *tAdam17KO* on es va observar una disminució de marcadors fibròtics en els esferoides amb deleció de l’*Adam17*. En conclusió, la manipulació de l’*Adam17* podria ser considerada com una estratègia terapèutica en el tractament de la ND. En pacients amb MRC sense events CV previs, l’activitat circulant dels ADAMs podria utilitzar-se com a biomarcador de malalties renals i cardiovasculars.

1. INTRODUCTION

1. Introduction

1.1 Chronic Kidney Disease

Chronic kidney disease (CKD) is a general term for heterogeneous disorders affecting the structure and function of the kidney (1). CKD is increasingly recognized as a global public health problem (2). In the 2017 Global Burden of Disease Study, CKD was the 12th most common cause of death, accounting for 1.2 million deaths worldwide (3). However, it is expected to become the fifth cause of death in 2040 (4).

The definition of CKD is based on the presence of kidney damage for more than 3 months, with or without decreased glomerular filtration rate (GFR) and/or decreased GFR (<60 mL/min per 1.73m^2) for more than 3 months, with or without kidney damage (5,6). Kidney damage refers to a broad range of abnormalities observed during clinical assessment, which may be insensitive and non-specific for the cause of disease but may precede reduction in kidney function. According to the National Kidney Foundation, the prognosis of CKD is characterized in terms of both GFR (Table 1) and albuminuria (Table 2) (5,6).

Table 1: GFR categories in CKD. Adapted from Group KDIGO, *Kidney International Supplements*, 2013 (6).

GFR categories in CKD		
Category	**GFR mL/min/1.73m^2**	**Terms**
G1$^{\$}$	≥90	Normal o high
G2$^{\$}$	60-89	Mildly decreased*
G3a	45-59	Mildly to moderately decreased
G3b	30-44	Moderately to severely decreased
G4	15-29	Severely decreased
G5	<15	Kidney failure

$^{\$}$In the absence of evidence of kidney damage, neither GFR category G1 nor G2 fulfill the criteria for CKD. *Relative to young adult level. Abbreviations: GFR, glomerular filtration rate; CKD, chronic kidney disease.

Table 2: Albuminuria categories in CKD. Adapted from Group KDIGO, *Kidney International Supplements*, 2013 (6).

Albuminuria categories in CKD		
Category	**ACR (mg/g)**	**Terms**
A1	<30	Normal to mildly increased
A2	30-300	Moderately increased*
A3	>300	Severely increased

*Relative to young adult level. Abbreviations: CKD, chronic kidney disease; ACR: albumin-to-creatinine ratio.

One of the important features of CKD is the presence of interstitial infiltrate of inflammatory cells including lymphocytes, macrophages and dendritic cells at early stages followed by tubulointerstitial fibrosis and glomerular sclerosis thereafter (7–9). Systemic or intrarenal inflammation contributes to deregulation of the microvascular response and sustains the production of an array of tubular toxins, leading to tubular injury, nephron dropout, and the onset of CKD. Circulating proinflammatory cytokines activate endothelial cells and leukocytes, resulting in a local amplification of proinflammatory factors and reactive oxygen species (ROS) that induce tissue damage and stimulate the synthesis of fibrogenic cytokines and growth factors affecting cell-surface adhesion molecules and disrupting the glycocalyx layer (8). These inflammation-mediated alterations can induce an accumulation of extracellular matrix (ECM) leading to irreversible interstitial fibrosis, peritubular capillary loss causing tubular hypoxia, tubular injury and nephron failure (8,10).

The increasing prevalence of CKD is partly explained by the increase in the number of risk factors, including population aging, obesity, diabetes, and hypertension (11,12). The high incidence of CKD in the elderly might be partly ascribed to related comorbidities of CKD, such as cardiovascular (CV) diseases or diabetes (13).

To our knowledge, no specific therapy available to recover organ function after chronic damage has been established. Currently, the only treatment for end-stage renal disease (ESRD) is the replacement of renal function by dialysis or kidney transplantation. Therefore, early identification of CKD is urgently needed to prevent disease progression and reduce cardiovascular morbidity and mortality risk (14).

1.2 Diabetic nephropathy

1.2.1 Definition and physiopathology

Diabetic nephropathy (DN) is a microvascular complication of type 1 and type 2 diabetes mellitus that has been classically defined as increased protein excretion in urine (15). Nowadays, DN term is reserved for patients with diabetic lesions confirmed by kidney biopsy (16). DN occurs in 20-40% of patients with diabetes and is the leading cause of CKD in patients starting renal replacement therapy (17). DN is a potentially devastating complication of diabetes, and its incidence has more than doubled in the past decade, largely related to the rising prevalence of obesity and type 2 diabetes. It has been estimated that patients with diabetes have a 12-fold increased risk of ESRD compared to patients without diabetes (18).

1.2.2 Clinical evolution

DN has been categorized into stages based on the values of urinary albumin excretion (UAE). In the early stages of DN there is an increase in the UAE defined as an albumin-to-creatinine ratio (ACR) in urine between 30 and 300mg/g termed microalbuminuria. Subsequently, there is a progressive increase in proteinuria, defined as an ACR > 300mg/g, termed macroalbuminuria and considered as overt DN (19).

Approximately 20-40% of patients with diabetes develop microalbuminuria within 10 to 15 years of the diagnosis of diabetes, and about 80-90% of those patients progress to more advanced stages. Thus, after 15-20 years, macroalbuminuria occurs in approximately 20-40% of patients, and around half of them will present renal insufficiency within 5 years (20,21).

The progressive increase in proteinuria leads to a variable decline in renal function. Once the subject has developed macroalbuminuria, there is a decrease in the GFR (22). Although measurement of albuminuria is essential for the diagnosis of DN, there are some patients who present decreased GFR when ACR values are normal, termed non-proteinuric diabetic kidney disease (23).

The management of DN is based on the multifactorial treatment of its known risk factors: hypertension, hyperglycaemia, smoking, and dyslipidaemia, together with the prevention of the progression from microalbuminuria to macroalbuminuria (15,24).

1.2.3 Stages in the development of diabetic nephropathy

Morgensen *et al.* first characterized the natural evolution of DN into several distinct phases that can be used for both types of diabetes (Table 3) (25). During the first stage, early hypertrophy and hyperfunction can be detected accompanied by an increase in kidney and glomerular size, nephron hypertrophy and hyperplasia. The second stage is characterized by hyperfiltration and is associated with morphological changes including increased glomerular basement membrane (GBM) thickness and mesangial expansion. This second phase is followed by changes in ACR levels in the range of microalbuminuria leading to an incipient diabetic nephropathy (Stage

3). Stage 4 is characterized by persistent and pronounced proteinuria (macroalbuminuria) with declining GFR and increased blood pressure. Finally, gradual deterioration of renal function leads to ESRD (Stage 5).

Table 3: Stages in the development of DN. Adapted from Mogensen *et al. Diabetes,* 1983 (25).

Stage	Designation	Characteristic	GFR (mL/min)	ACR (mg/g)	Blood pressure
Stage 1	Hypertrophy, hyperfunction	Glomerular hyperfiltration	>150	>30	Normal
Stage 2	Silent DN	Increased GBM thickness and mesangial expansion	~150	>30	Normal
Stage 3	Incipient DN	Microalbuminuria	~130	30-299	Incipient increase
Stage 4	Overt DN	Macroalbuminuria	<100	>300	Hypertension
Stage 5	Uremic	ESRD	0-10	>300	Hypertension

Abbreviations: GFR, glomerular filtration rate; ACR: albumin-to-creatinine ratio; DN, diabetic nephropathy; GBM, glomerular basement membrane; ESRD: end-stage renal disease.

1.2.4 Histopathology

From human biopsies of patients affected by DN, Tervaert *et al.* established a uniform classification system containing four specific categories that discriminate glomerular lesions graded I to IV (Table 4) and tubulointerstitial and vascular lesions graded separately (26).

Table 4: Glomerular classification of DN. Adapted from Tervaert *et al.* J Am Soc Nephrol, 2010 (26).

Class	Description
Class I	Mild or nonspecific LM changes and GBM thickening by EM
Class IIa	Mild mesangial expansion
Class IIb	Severe mesangial expansion
Class III	Nodular sclerosis (Kimmelstiel-Wilson lesion)
Class IV	Advanced diabetic glomerulosclerosis

Abbreviations: LM, light microscopy; GBM, glomerular basement membrane; EM, electron microscope.

According to the glomerular classification, GBM thickness which is the first measurable change (Class I), has been detected as early as 1.5 to 2.5 years after the onset of diabetes (27). Mesangial expansion, due to an increase in mesangial matrix, develops later albeit an increase in matrix component of the mesangium can be detected as early as 5 to 7 years after the onset of diabetes (Class II). Both, GBM thickness and mesangial expansion are a consequence of the extracellular matrix local components of collagen types IV and VI, laminin and fibronectin due to their increased production, decreased degradation or both (28,29). In a later stage, diffuse mesangial expansion can be associated with nodular lesions consisting in areas of marked mesangial expansion forming large round fibrillary mesangial zones with palisading of mesangial nuclei around the periphery of the nodule and compression of the associated glomerular capillaries (Kimmelstiel-Wilson nodules) (Class III). Glomerular nodules are areas of marked mesangial expansion, with oval tuft shape, fibrillary appearance and absence of nuclei that contribute to glomerular function loss leading to a congestion of the surrounding capillaries, especially when this lesion progresses to advanced diabetic glomerulosclerosis (Class IV) (27).

Interstitial fibrosis and tubular atrophy (IFTA) and infiltration of mononuclear cells in the interstitium follow glomerular changes in type 1 DN that ultimately lead to ESRD. Tervaert *et al.* scored IFTA together as a percentage of the total involved area of interstitium and tubules and the presence or absence of infiltrated T lymphocytes and macrophages (Table 5). A score of 0 was assigned when the biopsy showed no IFTA, a score of 1 was assigned when less than 25% IFTA was present, a score of 2 was assigned when at least 25% but less than 50% of the biopsy has IFTA, and a score of 3 was assigned when the biopsy has at least 50% IFTA. Absence of interstitial inflammation was scored as 0. A score of 1 was assigned when the infiltrate occurred only around atrophic tubules, and a score of 2 was assigned if the inflammatory infiltrate was also in other areas than around atrophic tubules (26).

In addition to glomerular and tubular lesions, renal vasculature lesions have been also described. Afferent and efferent arteriolar hyalinosis may be present within few years after diabetes onset (30). However, according to Stout *et al.* only hyalinosis of the efferent arteriole is relatively specific for DN. Hyalinosis of the afferent arteriole occurs also in numerous other settings (31). These vascular lesions are characterized by replacement of the smooth muscle cells by plasma proteins such as immunoglobulins, complement, fibrinogen and albumin (30). Tervaert *et al.* scored as 0 if no arteriolar hyalinosis was present, 1 if one arteriole with hyalinosis was present and 2 if more than one arteriole with hyalinosis was observed in the biopsy. Moreover, the presence of nonspecific arteriosclerosis could also be present in the biopsy of DN patients. If no intimal thickening was present in the biopsy, a score of 0 was given. If intimal thickening was less than the thickness of the media, a score of 1 was given. Finally, if

the intimal thickness was greater than the thickness of the media, a score of 2 was given (26) (Table 5).

Table 5: Interstitial and vascular lesions in diabetic nephropathy. Adapted from Tervaert *et al.* J Am Soc Nephrol, 2010 (26).

Lesion	Criteria	Score
Interstitial lesions		
IFTA	No IFTA	0
	<25%	1
	25% to 50%	2
	>50%	3
Interstitial inflammation	Absent	0
	Infiltration only in relation to IFTA	1
	Infiltration in areas without IFTA	2
Vascular lesions		
Arteriolar hyalinosis	Absent	0
	At least one area of arteriolar hyalinosis	1
	More than one area of arteriolar hyalinosis	2
Presence of large vessels	-	Yes/no
Arteriosclerosis	No intimal thickening	0
	Intimal thickening less than thickness of media	1
	Intimal thickening greater than thickness of media	2

Abbreviations: IFTA, interstitial and tubular atrophy.

1.3 Renin-Angiotensin System

The renin-angiotensin system (RAS) plays a fundamental role in the pathophysiology of diabetes and its development and progression (32). The RAS is a coordinated hormonal cascade that regulates blood pressure and fluid balance and has a crucial role in the regulation of the cardiovascular system and the renal function (33). The physiological significance of this system resides in the homeostasis of peripheral vascular resistance as well as the regulation of volume and electrolyte

composition in body fluids. Thus, dysregulations of this system are associated with the development of cardiovascular pathologies, including kidney injury. At the kidney level, the RAS exerts powerful influence and regulates many aspects of renal hemodynamic and transport function including the cortical and medullary circulations, glomerular hemodynamics, and the glomerular filtration coefficient in normal physiological and pathological conditions (34,35).

Classic RAS is initiated by the synthesis and release of renin from the juxtaglomerular apparatus into the plasma. Angiotensinogen (AGT) is formed and secreted by hepatic cells into the circulation. Renin cleaves AGT at the N-terminus to form the inactive decapeptide angiotensin I (ANG I) which is then converted by angiotensin converting enzyme (ACE) to ANG II, a biologically active peptide that interacts with angiotensin II receptor type 1 and type 2 (AT1R and AT2R). Through AT1R, ANG II mediates vasoconstriction, stimulates aldosterone production, enhance myocardial contractility, increases cellular transport, hypertrophy, growth factors synthesis, oxidative stress generation, and changes in gene expression activating multiple intracellular signalling pathways contributing to renal injury (36–38).

In 2000, angiotensin converting enzyme 2 (ACE2), an homologous to ACE, was discovered and the non-classic RAS emerged (39). ACE2 is a type I transmembrane glycoprotein with its catalytic site exposed to the extracellular surface (40,41). It is involved in the generation of alternative ANG peptides in particular by conversion of ANG II to ANG(1-7) and ANG I to ANG(1-9). Thus, while ACE generates ANG II from ANG I through the cleavage of the C-terminal dipeptide His-Leu, ACE2 catalyses the conversion of ANG II into ANG(1-7) by removing the C-terminal amino acid phenylalanine (Figure 1). In addition, ACE2

also cleaves the C-terminal residue of the decapeptide ANG I, thus generating the nonapeptide ANG(1-9), which may be subsequently converted to ANG(1-7) by ACE (42). ANG(1-7) acts via the G protein-coupled receptor Mas (43) and opposes the actions of the ANG II/AT1R axis by increasing nitric oxide and prostaglandins levels, and mediating vasodilation, vascular protection, anti-fibrotic, anti-proliferative and anti-inflammatory effects (44,45).

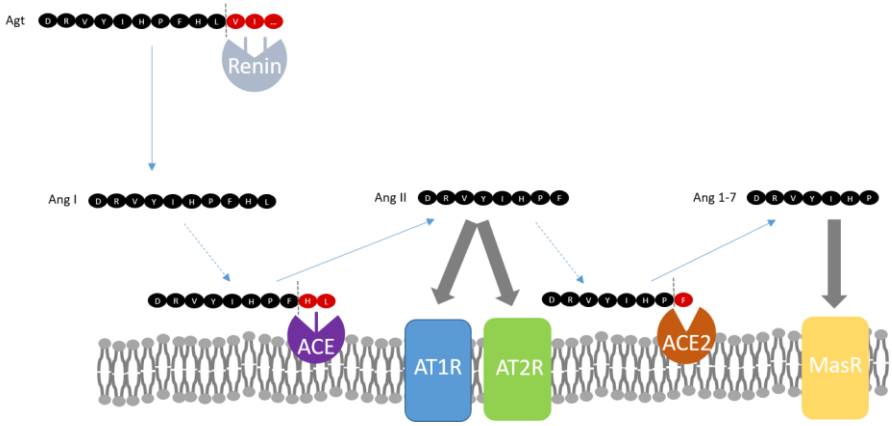

Figure 1: Schematic representation of the RAS system. ACE generates ANG II from ANG I, ACE2 catalyses the conversion of ANG II to ANG(1-7). Abbreviations: ACE, angiotensin-converting enzyme, AT1R, angiotensin II receptor 1; AT2R, angiotensin II receptor 2; MasR, Mas receptor. Adapted from Palau *et al.* AJPR, 2019 (46).

In rat kidney, mRNA for ACE2 has been detected in all nephron segments, except for the thick ascending limb of the loop of Henle, with increased expression in the proximal tubule, the inner medullary collecting ducts and the vasa recta (47). Within the glomerulus, ACE2 is mainly present in podocytes and mesangial cells. Studies in animal and human kidneys have localized ACE2 in both apical brush border and cytoplasm of proximal tubular cells (47–50). It has been reported that the increased levels of ACE2 in the urine most likely reflect release from the proximal tubular epithelium (51).

1.4 Disintegrins and metalloproteinases (ADAMs)

Disintegrins and Metalloproteinases (ADAMs) are membrane-anchored cell surface and secreted proteins (52). The ADAMs play an important role in the regulation of cell phenotype via their effects on cell adhesion, migration and proteolysis and in modulating cell signalling and biological responses (52,53).

ADAMs contain a pro-domain, a metalloproteinase domain, a disintegrin domain, a cysteine domain, an EGF-like domain, a transmembrane domain, and a cytoplasmic tail (54,55). ADAMs are approximately 750 amino acids long and evolutionarily conserved (56). A total of 40 ADAMs have been identified in the mammalian genome, of which 37 are expressed in mice and 21 are expressed in humans. However, only 12 of the human ADAM members are predicted to function as proteases, while the rest do not contain the catalytic-Zn binding domain (HExxHxxGxxH) in their metalloprotease domain and cannot be catalytically active (57,58).

Functional ADAMs are involved in ectodomain shedding of diverse growth factors, cytokines, receptors and adhesion molecules (53). ADAMs enzymatic activities are controlled by post-transcriptionally tissue inhibitors of metalloproteinases (TIMPs) (59). Four TIMP family members have been described: TIMP1, TIMP2, TIMP3, and TIMP4 (60–63). These proteins act as regulators of the activities of different metalloproteases (MMPs) and ADAMs. The TIMPs are able to act as proteinase inhibitors and as signalling molecules (64). The TIMPs share a similar domain structure, composed of an amino-terminal domain and a carboxy-terminal sub-domain. The TIMPs show tissue-specific, constitutive, or inducible expression, which is regulated at the transcriptional level by various cytokines and growth factors. TIMP1 is

widely expressed in many mammalian tissues, notably in the reproductive organs. TIMP2 is constitutively expressed in most tissues but is not inducible by common growth factors. TIMP3 is expressed in many tissues and is often found as a significant matrix protein in the basement membranes of the eye and kidney. TIMP4 has a relatively restricted tissue distribution (in the heart, kidney, ovary, pancreas, colon, testes, brain and adipose tissue) and it plays a role in tissue-specific physiological functions (65).

TIMP1 and TIMP3 gene transcription is upregulated by TPA, TNF-α, and TGF-β, whereas TIMP2 is downregulated by these agents (66). TIMP4 gene expression is upregulated by TGF-β, and IL17, but not by TNF- α or IL-1β (67). TIMP1 is responsible of ADAM10 inhibition, TIMP2 participates in ADAM12 inhibition, TIMP3 inhibits ADAM10, ADAM12 and ADAM17, and TIMP4 participates in ADAM17 and ADAM28 inhibition (68–70).

1.4.1 A disintegrin and metalloproteinase domain 17 (ADAM17): localization and function

A disintegrin and metalloproteinase domain 17 (*ADAM17)* gene is approximately 50kb and contains 19 exons. Chromosomal mapping places ADAM17 on the human chromosome 2p25 and mouse chromosome 12 (71,72). ADAM17 is a type I transmembrane protein with an N-terminal signal sequence followed by a pro-domain with a cysteine switch-like region (CysSL), a metalloproteinase domain with Zinc-binding domain region (Zn-BR) catalytically active, a disintegrin cysteine-rich domain, an EGF-like domain, a single transmembrane domain and a cytoplasmic tail (58,73–76) (Figure 2).

ADAM17 was identified predominantly in two forms, as a full-length inactive protein (100kDa) and as a mature form lacking the pro-domain, the active form (80kDa) (77).

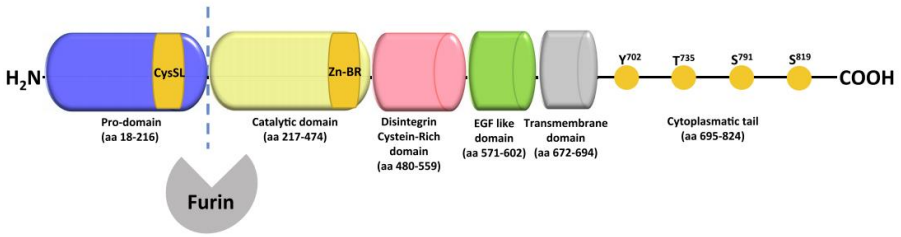

Figure 2: Representation of a disintegrin and metalloproteinase (ADAM)17 domain. The inactive pro-ADAM17 contains a pro-domain, a catalytic domain, disintegrin domain, an EGF-like domain, a transmembrane domain, and a cytoplasmic tail. Furin is needed for ADAM17 maturation and activation by cleaving the pro-domain. Furthermore, Thr^{735} at the cytoplasmic tail is phosphorylated by MAPKs and Erk stimulation. Abbreviations: aa, amino acids; CysSL, Cysteine switch-like region; Zn-Br, Zinc-binding domain region; EGF, epidermal growth factor. Adapted from Palau *et al.* AJPR, 2019 (46).

The ADAM17 zymogen is enzymatically inactive because of the pro-domain interaction with the active site making substrates inaccessible to the catalytic domain (78). Maturation of ADAM17 takes place in lipid rafts from the medial Golgi where the enzyme furin cleaves the ADAM17 pro-domain (79). The cleavage of ADAM17 pro-domain is needed for its activation together with other molecular processes such as phosphorylation events (80). Activation of the Erk or p38-mitogen activated protein kinase (MAPK) pathways increases phosphorylation in Thr^{735} at the cytoplasmic domain, whereas growth factor stimulation increases phosphorylation of Ser^{819} and dephosphorylation of Ser^{791} of the pro-ADAM17. Mutation or dephosphorylation of Ser^{791} enhances phosphorylation at Thr^{735} (81). Phosphorylation of Thr^{735} by p38-MAPK or Erk is necessary for ADAM17 maturation and regulates its cell surface levels (81).

ADAM17 was initially described by Black *et al.* to specifically cleave the precursor of tumour necrosis factor α (pro-TNF-α) (82). Currently, it is known that ADAM17 can also release the ectodomains of a diverse variety of membrane-anchored cytokines, cell adhesion molecules, receptors, ligands, and enzymes, such as, transforming growth factor α (TGF-α), L-selectin, IL-6R and ACE2, among others (58,74,83–86). Proteomic studies of cleavage site specificities have revealed a high preference of ADAM17 for alanine, leucine, and valine residues, and a low preference for proline residues (87,88). Most of the ADAM17 substrates are associated with different diseases such as cardiovascular disease, diabetes, autoimmune diseases, hypertension, and cancer (58,84,85).

ADAM17 is required for normal embryonic development due to ADAM17 deficiency causes defects in eyes, skin, heart, lungs, and hair (89). Peschon *et al.* demonstrated the essentiality of ADAM17 for mammalian development due to epidermal growth factor receptor (EGFR) ligand cleavage and EGFR signalling (89). ADAM17 is widely expressed in various tissues including the brain, heart, kidney, and skeletal muscle and its expression changes during embryonic development and adult life (82). Interestingly, several reports have described circulating ADAM17 activity (90,91). Recently, Scharfenberg *et al.* have postulated that ADAM8 releases ADAM17 into the circulation (92). From ADAM10/17 knockout HEK293T cells, the authors used single or double transfection with ADAM17 or ADAM17/ADAM8 to conclude that ADAM8 was needed to detect ADAM17 shedding that was weakened in ADAM17 single transfected cells.

In CD4 T cells, ADAM17 has been identified as the major protease that mediates IL-6R shedding after T cell receptor activation. The secretion of soluble (sIL-6R) is primarily mediated by shedding of the membrane-bound receptor and correlates with the expression of ADAM17 in CD4 T cells. However, the lack of ADAM17 in CD8 T cells could explain the inability of these cells to produce sIL-6R. The sIL-6R plays an important role in the progression of several autoimmune diseases (93). In type 1 diabetic patients, reduced ADAM17 expression has been found in CD4 T cells resulting in decreased sIL-6R. As a consequence, enhanced T cell responses to IL-6 in type 1 diabetic patients have been reported, in part due to an increase in IL-6R surface expression. Dysregulation of IL-6 responsiveness contributes to altered T cell trafficking (94).

1.4.2 ADAM17 and Renin-Angiotensin System

Chronic activation of the RAS and increased binding of ANG II to AT1R leads to ADAM17 activation, promoting inflammation and hypertension (95–97). When ADAM17 catalyses ACE2 ectodomain shedding, ANG II is accumulated and the compensatory axis of the RAS is compromised (Figure 3).

Increased ACE2 ectodomain into the circulation and urine has been found in diabetic mice (98,99) and in patients with CKD, diabetic nephropathy, or diabetic renal transplant (100–103). Interestingly, experimental studies have shown that ADAM17 and ACE2 are increased and colocalize in the apical side of the proximal tubule brush-border membrane in the diabetic kidney (99,104). Moreover, Lautrette *et al.* demonstrated that ANG II causes induction and redistribution of ADAM17 to the apical membranes of distal tubules (96). Consequently, active forms of ACE2 from the kidney proximal tubular and distal cells

are shed by ADAM17 increasing urinary ACE2 in diabetic mice (99,104,105), strongly suggesting that the primary source of elevated urinary ACE2 in diabetic kidney is of tubular origin (106,107). Urinary ACE2 excretion correlates positively with the progression of diabetic renal injury, represented by progressive albuminuria, mesangial matrix expansion, and renal fibrosis in type 2 diabetic mice (99). In agreement, urinary ACE2 shedding is increased together with albuminuria in CKD patients with type 2 diabetes (101,107). Gutta *et al.* suggested that the detection of urinary ACE2 could become an indicator of renal injury before the presence of microalbuminuria. They demonstrated increased urinary ACE2 activity and urinary ADAM17 in diabetic patients with normoalbuminuria, microalbuminuria and macroalbuminuria (108).

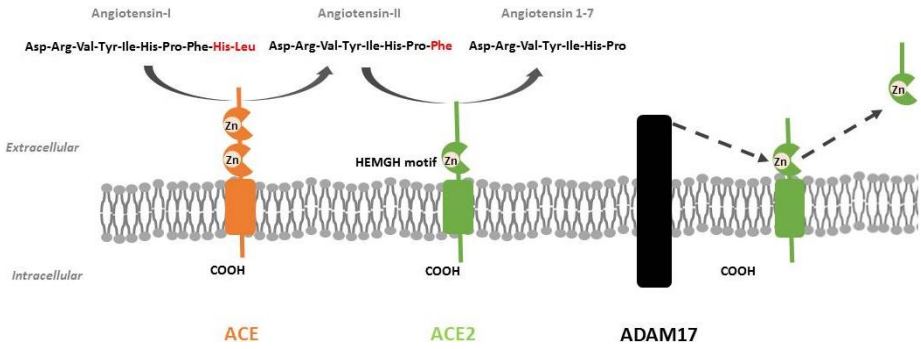

Figure 3: A simplified representation of the renin angiotensin system pathway. Whereas ACE converts ANG I to ANG II, ACE2 converts ANG II to Ang(1–7). ACE2 is cleaved by ADAM17, producing a soluble form of ACE2. Abbreviations: Zn, zinc; ACE, angiotensin converting enzyme; ACE2, angiotensin converting enzyme 2; ADAM17, a disintegrin and metalloproteinase domain 17. Adapted from Palau *et al.* AJPR, 2019 (46).

There is evidence of different mechanisms for inhibiting ACE2 shedding. Insulin treatment in type 1 diabetic mice and rosiglitazone treatment in type 2 diabetic mice normalizes hyperglycaemia and attenuates urinary ACE2 shedding, albuminuria and renal ADAM17

expression (99,104). Moreover, the administration of high doses of paricalcitol normalizes renal ADAM17 protein expression and circulating ACE2 activity in type 1 non-obese diabetic (NOD) mice demonstrating that paricalcitol could be a negative regulator of the RAS (98). These results are reinforced by previous studies of Dusso *et al.* which demonstrated that paricalcitol can be a negative regulator of ADAM17 activity (109). *In vitro* studies proved that TNF-α processing inhibitor (TAPI)-1 and 2, synthetic ADAM17 inhibitors, decreases ACE2 shedding into the cell media induced by stimulation of the cells with high D-glucose, ANG II or phorbol myristate acetate (PMA). However, TAPI-1 and TAPI-2 had no effect on constitutive (not stimulated) ACE2 release (86,110). In contrast, Salem *et al.* reported constitutive inhibition of ACE2 shedding into the media by TAPI-1 (104) and Grobe *et al.* shown reduced basal ACE2 shedding after ADAM17 gene silencing (111).

1.4.3 ADAM17 in chronic kidney disease

There is increasing evidence on the pathophysiological role of ADAM17 in CKD. By activating TNF-α and EGFR ligands, ADAM17 has a crucial role in inflammatory and proliferative processes both of which contribute in the development of CKD (112) (Figure 4). Kefaloyianni *et al.* suggested an interplay of both physiological ADAM17 downstream pathways, the EGFR pathway (with strong evidence for a role of amphiregulin), and the TNF-α pathway establishing sustained inflammation and tubular EGFR activation leading to fibrosis (113).

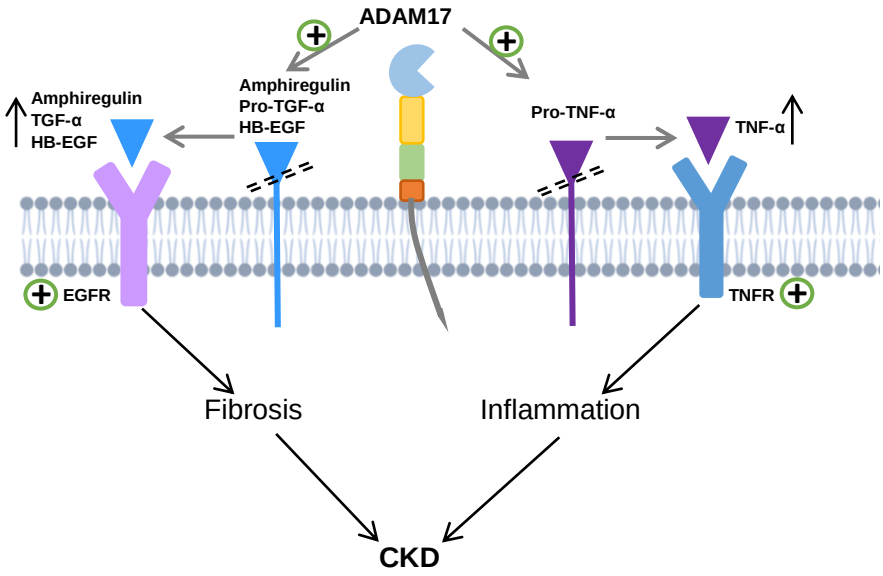

Figure 4: Schematic representation of the activation of EGFR and TNFR signalling pathways by ADAM17. Abbreviations: ADAM17, a disintegrin and metalloproteinase domain 17; TGF-α, transforming growth factor alpha; HB-EGF, heparin binding EGF-like growth factor; TNF-α, tumour necrosis factor alpha; EGFR, epidermal growth factor receptor; TNFR, tumour necrosis factor alpha receptor; CKD, chronic kidney disease.

Over the course of ischemic acute kidney injury (AKI), a variety of cell types (endothelial cells, neutrophils, T cells, macrophages, tubular cells, and pericytes) play important roles in injury and repair (114). However, injury to the proximal tubule cell is sufficient to induce CKD and fibrosis (115). Injured tubular cells drive inflammation and fibrosis by releasing pro-inflammatory cytokines including TNF-α and by producing profibrotic factors, in particular transforming growth factor β (TGF-β) (116,117).

Elevated levels of TNF-α receptors (TNFR) are predictive of disease progression in patients with DN. In type 1 and type 2 diabetes, elevated circulating TNFRs levels are associated with progression to CKD stage

3 or higher (118,119). Further, patients in haemodialysis with increased circulating TNFRs present higher risk of all-cause and/or cardiovascular mortality (120).

After kidney injury, tubular repair mechanisms involve the activation of EGFR. It is widely expressed in the kidney, including the glomeruli, proximal tubules, and cortical and medullary collecting ducts (121). EGFR activation is beneficial in the early phases of epithelial repair in AKI (day 1–2 after injury). However, sustained activation of EGFR beyond the initial injury repair phase (days to weeks after injury) has been linked to kidney fibrosis in mouse models of bilateral ischemic AKI and unilateral ureteral obstruction (UUO) (122–126). Persistent activation of EGFR and its downstream pathways, in particular MAPK, increases production of TGF-β (123,126). This seems to be the major growth factor that promotes fibroblasts tubular epithelial cell phenotype changes into mesenchymal-like phenotype (myofibroblasts) which express α-smooth muscle actin (α-SMA) (127). Interstitial myofibroblasts proliferate and contribute to the secretion of ECM pro-fibrotic components, driving interstitial fibrosis and functional disruption of nephrons (128).

In human biopsy studies, ADAM17 expression was found significantly upregulated in various chronic fibrotic kidney diseases, including diabetic nephropathy, and many forms of glomerular disease (129). ADAM17 expression levels in the proximal tubule correlated positively with the extent of macrophage ingress and interstitial fibrosis and correlated negatively with glomerular filtration rate suggesting that the ADAM17 activity positively correlates with functional decline (130).

1.4.4 ADAM17 in diabetic nephropathy

In control human kidneys, ADAM17 mRNA staining is predominantly negative in proximal tubules, mesangium and endothelium. Glomerular parietal cells and podocytes are moderately positive. In contrast, distal tubules present strong ADAM17 expression. In diabetic patients, ADAM17 mRNA is upregulated in the endothelium, proximal tubules, peritubular capillaries, glomerular mesangium, glomerular parietal epithelium, and interstitial inflammatory cells (129). In the same line, *in vitro* studies have shown that high concentrations of glucose mimicking the diabetic milieu increase ADAM17 protein expression in podocytes, glomerular endothelial cells, mesangial cells, and proximal tubular epithelial cells (131–133).

TNF-α is a prime inducer and driver of renal microinflammation and thus is believed to play a central role in the activation of pro-inflammatory molecules during the progression of DN (134). TNF-α after cleavage by ADAM17 activation is released into the circulation and binds to TNFR1 or TNFR2 and modulates a complex series of immune and inflammatory responses (135,136). Hyperglycaemia and advanced glycation end-product (AGEs) are potent inducers of TNF-α production in almost all resident kidney cells, including mesangial cells, podocytes, glomerular endothelial and tubular cells (134,137,138). However, TNF-α is predominantly synthesized by infiltrating T-cells and monocytes or macrophages (134). In DN, TNF-α can amplify the renal inflammatory response by inducing the cells to release other cytokines, growth factors and pro-inflammatory chemokines, such as, IL-8, monocyte chemoattractant protein-1 (MCP-1) and macrophage-colony stimulating factor (M-CSF) in an autocrine and paracrine manner. Furthermore, TNF-α can directly activate NADPH oxidase leading to

local generation of ROS via phosphodiesterase-dependent mechanisms (134).

Hyperglycaemia plays an important role in EGFR activation leading to renal fibrosis by interaction with TGF-β signalling pathway (139). EGFR is widely expressed in the mammalian kidney, including the glomeruli, proximal tubules, and cortical and medullary collecting ducts (121). Of the several EGFR ligands that can be shed by ADAM17, TGF-α, heparin binding EGF-like growth factor (HB-EGF) and amphiregulin have been implicated in the pathogenesis of DN (89,130,140).

Li *et al.* suggested that focal adhesion kinase (FAK) is an upstream key mediator of ADAM17 activation through the recruitment of both Src and Erk, with subsequent phosphorylation of ADAM17 at two sides in its C-terminal. Y^{702} is phosphorylated by Src and T^{735} by Erk. Phosphorylation at both sites enhances association of ADAM17 with FAK and is required for downstream pro-fibrotic effects. High glucose also leads to increased furin-mediated processing of ADAM17 to its mature form and increased translocation of mature ADAM17 to the membrane (141). Thus, high glucose activates ADAM17 in kidney cells stimulating the release of ligands for the EGFR inducing pro-fibrotic TGF-β and Akt production boosting the activation of fibroblasts into myofibroblasts contributing to ECM production (122,142–147). Moreover, ADAM17 itself, through activation of the EGFR and downstream PI3K/Akt and Erk activation, induces its own up-regulation. This describes an amplification loop that augments the fibrotic response (148).

Experimental studies in diabetic mice reported higher infiltration of macrophages and T-lymphocytes in kidneys from type 1 diabetic mice (149–151). Moreover, inflammatory and fibrotic markers such as TNF-

α, TNFR1, TNFR2, ICAM1, VCAM1, TGF-β, α-SMA, collagen IV and fibronectin are increased in diabetic mice (149,150,152). TNF-α produced by macrophages plays an important role in the pathogenesis of DN. Awad *et al.* demonstrated that using a TNF-α neutralizing antibody or specific TNF-α depletion in macrophages prevents from renal hypertrophy and reduces albuminuria and plasma creatinine in type 1 diabetic mice. Moreover, TNFR1 and TNFR2 gene expression and protein levels and glomerular macrophage infiltration are decreased in those animal models (152). EGFR deletion in podocytes of diabetic mice attenuates albuminuria and podocyte loss. Moreover, TGF-β signalling pathway was markedly inhibited giving rise to reduced fibronectin accumulation in the glomeruli (122).

1.5 Murine models of type 1 diabetic nephropathy

Several studies have been focused in developing animal models to assess the evolution of DN and the molecular mechanisms implicated in the progression of the disease, as well as the positive and negative effects of new therapeutic strategies. However, few animal models mimic the human DN. Although these models of diabetic kidney disease exhibit albuminuria, glomerular hyperfiltration and some of the mild pathological changes, reports of renal failure and severe pathological renal lesions in these mice or rats resulting from diabetes are lacking (153,154).

1.5.1 Non-obese diabetic mice model

The NOD mice model develop spontaneous autoimmune destruction of β cells that mimics human type 1 diabetes (154). NOD mice develop spontaneous insulinitis at the age of 4-5 weeks, and overt diabetes emerges at the age of 24-30 weeks when most of the pancreatic β cells

are destroyed (155). There is a marked sex difference in the incidence of diabetes in the NOD mouse. The cumulative incidence of the onset up to 30 weeks of age is 80% in females and less than 20% in males (154,156). Insulin treatment is required for surviving long periods of time to prevent mice from dying of dehydration (154,155).

This model exhibits a number of clinical features of human type 1 diabetes including hyperglycaemia, glycosuria, polyuria, and polydipsia (155). Diabetic NOD mice show albuminuria, mild changes in glomeruli and structural alteration of the proximal straight tubules (155,157) (Figure 5).

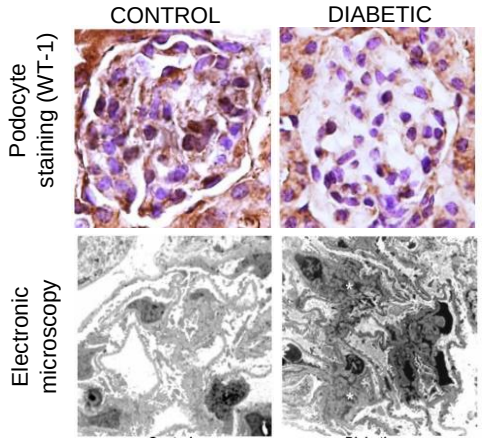

Figure 5: Glomerular lesions in female NOD mice after 40 days of diabetes. Podocyte number was markedly reduced in diabetic mice as compared to controls. Ultrastructural analysis revealed an increased mesangial volume and glomerular basement membrane thickness in diabetic mice. Abbreviations: WT-1, wilms tumour 1. Adapted from Riera *et al.* Plos One, 2014 (157).

1.5.2 Streptozotocin-induced mice model

Streptozotocin (STZ)-induced type 1 diabetes has been widely used as a model of DN. STZ is composed of a glucosamine-nitrosourea and synthesized by *Streptomyces achromogenes*. It is transported into the pancreatic β cells via glucose transporter 2 (GLUT2) resulting in

changes in the DNA of the pancreatic β cells comprising its fragmentation. It is known that the main reason for STZ-induced β cells death is alkylation of DNA (154,158). DNA damage causes the activation of poly ADP-ribosylation that leads to depletion of cellular NAD+ and ATP. As a result, superoxide radicals are formed, and reactive oxygen species (ROS) and a simultaneous cytosolic calcium overload leads to acute necrosis of pancreatic β cells (154).

Animal models receiving STZ to induce type 1 diabetes, have been shown to develop albuminuria and increased serum creatinine together with histological lesions associated with DN such as glomerular hypertrophy, mesangial expansion, arteriolar hyalinosis or nodular glomerulosclerosis (154,159,160) (Figure 6).

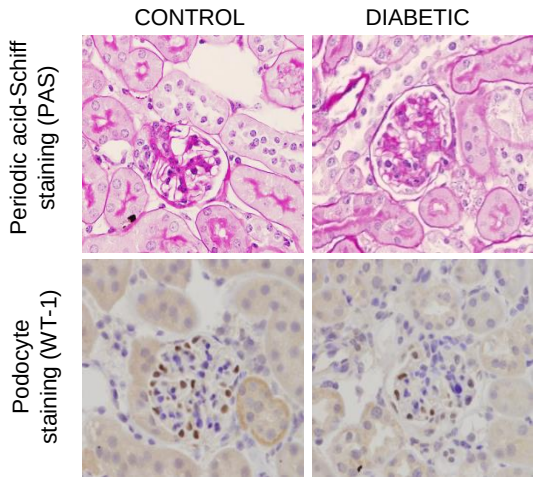

Figure 6: Glomerular lesions in the male STZ mice after 19 weeks of diabetes. Glomerular tuft area and mesangial index were increased in diabetic male mice. The proportion of podocytes was significantly decreased in diabetic mice. Abbreviations: PAS, periodic acid-Schiff; WT-1, wilms tumour 1. Adapted from Clotet *et al.* J Hypertens, 2016 (160).

There are two different protocols for STZ diabetes induction: (1) A high dose STZ protocol consisting in a single dose of STZ (150-200mg/Kg)

injected intraperitoneally and (2) a multiple low dose protocol consisting in 40-60mg/Kg for 5 consecutive days (154). Both protocols exhibit similar levels of hyperglycaemia within 1 to 2 weeks. Using low-dose STZ, levels of albuminuria are generally lower than with high-dose STZ. In addition, no loss of podocyte markers after completion of the low-dose STZ regimen have been observed suggesting that this regimen has no toxic effects on podocytes (154).

The STZ-induced is considered an established model of pancreatic toxicity, deeply studied and reproducible, that resembles several features of kidney disease described in human DN (155). However, there is evidence of differential susceptibility to diabetic nephropathy in inbred mice. Some strains such as DBA/2J and KK/HIJ are more prone to develop diabetic nephropathy after STZ administration. In contrast, C57BL/6 mice appear to be more resistant to diabetic nephropathy development (153).

Although requiring some adjustments depending on the strain employed, the possibility of dose adjustment notably increase the versatility of this model and allow a better method optimization, which is a clear advantage when working with a high number of experimental groups.

1.5.3 Akita ($Ins2^{WT/C96Y}$) mice model

The insulin-2 Akita ($Ins2^{Akita}$) mice is a genetically modified model of type 1 diabetes (161,162). These mice develop pancreatic β cell failure because of β cell-selective proteotoxicity resulting from misfolding of insulin2. Pancreatic islets from $Ins2^{Akita}$ mice are depleted of β cells, and those remaining β cells release very little mature insulin (154,155,163). This mutation exists on the C57BL/6 and C3H/He

strains (164). Histopathological lesions of DN, namely mesangial matrix expansion and GBM thickening, have been described in the Akita mouse model, with no evidence for mesangiolysis or nodular mesangial sclerosis (155,165). Interestingly, a sexual dimorphism is observed in $Ins2^{Akita}$ mice. Hyperglycaemia is substantially higher in male mice than in female mice (154,155).

1.5.4 OVE26 mice model

The OVE26 mouse on the FVB background is a transgenic mouse model of severe early-onset type 1 diabetes (155). These mice exhibit severe hyperglycaemia 2 to 3 weeks after birth due to pancreatic damage caused by overexpression of calmodulin transgene regulated by the insulin promotor (155,166).

OVE26 mice presented increasing albuminuria, hypoalbuminemia, increased GFR, and hypertension. These mice develop morphological changes of advanced DN such as enlarged glomeruli, nodular and diffuse expansion of the mesangial matrix, GBM thickening, diffuse and nodular glomerulosclerosis, nodules similar to Kimmelstiel-Wilson nodules, expansion of tubules, atrophy of tubular cells, interstitial infiltration of mononuclear cells, and tubulointerstitial fibrosis (155,167,168).

2. HYPOTHESIS

2. Hypothesis

ADAMs are a family of metalloproteinases that process a wide variety of substrates and its expression increases in several diseases. One of the most relevant ADAMs, is ADAM17 which was initially described as the enzyme responsible of TNF-α shedding. However, it is known that it can also release the ectodomains of a diverse variety of molecules such as cytokines, growth factors, cell adhesion molecules, and ACE2 among others. It has been shown that circulating ACE2 activity is altered in CKD patients, correlates with classical CV risk factors, and it is associated with higher risk for silent atherosclerosis. However, circulating ADAMs have not been extensively studied in patients with CKD.

Diabetic nephropathy is the leading cause of CKD in patients starting renal replacement therapy and is associated with increased cardiovascular mortality and loss of kidney function. Hyperglycaemia induces ADAM17 activation increasing it expression in the kidney, especially in distal tubular epithelial cells, but also in endothelial cells and renal proximal tubular epithelial cells. The increase of ADAM17 in the kidney induces glomerular alterations, renal fibrosis and inflammation. However, the role of ADAM17 on modulating these pathways has not been addressed.

Considering all this previous knowledge we hypothesize that (1) circulating ADAMs activity is altered in CKD patients without previous history of cardiovascular disease and it may correlate with renal disease progression and cardiovascular events; and (2) specific endothelial and renal proximal tubular *Adam17* deletion may protect type 1 diabetic mice from kidney inflammation and fibrosis.

3. OBJECTIVES

3. Objectives

Main Objective

- To study the modulation of ADAMs and ADAM17 in two different approaches of renal disease, human chronic kidney disease and experimental type 1 diabetic nephropathy, respectively.

Specific Objectives

1. Clinical studies

- To analyse basal circulating ADAMs activity in CKD patients without previous history of CV disease included in the NEFRONA Study and evaluate its association with baseline clinical parameters.
- To assess whether basal circulating ADAMs activity correlates with renal disease progression after 2 years of follow-up and with cardiovascular events after 4 years of follow-up.

2. Experimental studies

- To evaluate the effect of endothelial and proximal tubular *Adam17* deletion on glomerular injury, RAS components, and inflammatory and fibrotic processes in STZ mice.
- To assess the effect of *Adam17* deletion on fibrotic markers in an *in vitro* 3D model of human proximal tubular cells.

4. MATERIALS AND METHODS

4. Materials and methods

4.1 Clinical study

4.1.1 Patients and study design

A total of 2570 subjects from the NEFRONA project were included in the study. The NEFRONA project is an observational, prospective (a four-year follow-up) and multicentre study. From October 2009 to June 2011 patients with CKD (eGFR <60ml/min/1.73m^2) were recruited across Spain. The selection of kidney patients was carried out using a consecutive sampling of the patients arriving from outpatient nephrology clinics, which represent the entire health care system of the Spanish public network. Patients without CKD were recruited from different Spanish community health centres. Male and female patients without cardiovascular disease (angina pectoris, acute myocardial infarction, ischemic stroke, cerebral infarction, subarachnoid haemorrhage, intracerebral haemorrhage, cardiac insufficiency, atherosclerosis of extremities with intermittent claudication and abdominal aortic aneurysm) with ages ranging from 18 to 74 were included in the study (169,170). Exclusion criteria were pregnancy, human immunodeficiency virus infection, a history of transplantation, previous history of carotid artery disease, patients with active infections and/or hospitalized in the last month and current illness that presumes the absence of follow-up or survival expectation <1year (171).

The protocol was reviewed and approved by the ethical review board of each hospital and each participant signed an informed consent document before being included in the study.

Patients were classified into three groups according to their GFR estimated by MDRD-4 (Table 6).

Table 6: Classification of patients included in the study.

	Control group (CONT)	CKD stage 3 to 5 group (CKD3-5)	Dialysis group (haemodialysis or peritoneal dialysis) (CKD5D)
GFR	≥ 60 mL/min/1.73m^2	< 60 mL/min/1.73m^2	-
Number of patients	569	1463	538

Abbreviations: CONT, control; CKD, chronic kidney disease; CKD3-5, non-dialysis patients with chronic kidney disease stage 3 to 5; CKD5D, dialysis patients; GFR, glomerular filtration rate.

Recruiting investigators completed a questionnaire with the patients' clinical data, including socio-demographic variables, specific data of the kidney disease, family history of early CV disease, CV risk factors (namely smoking, diabetes, hypertension or dyslipidaemia) and current medications. An itinerant team from the NEFRONA Study, comprising two technicians and a nurse, carried out a physical and a vascular examination that included height, weight and measurement of SBP and DBP, carotid and femoral ultrasonography and ankle brachial index (ABI) measurement. Biochemical parameters were obtained from a routine fasting blood test taken no more than three months apart from the vascular explorations. In haemodialysis patients, samples were obtained before the second dialysis session of the week. EDTA-anticoagulated plasma samples were collected from all patients and controls and sent to the biobank of the Renal Research Network (REDinRen), where they were centrifuged at 3000g and stored at -80ºC (171).

Plasma samples were then sent from the REDinRen biobank to our laboratory for the determination of baseline circulating ADAMs enzymatic activity.

To study the modulation of circulating ADAMs in the NEFRONA population, three analyses were performed at three time points: baseline, 2-year follow-up, and 4-year follow-up.

a) Baseline analysis

At baseline the following variables were recorded and studied in the 2570 patients:

- Clinical variables: age, gender, history of diabetes, hypertension, dyslipidaemia, smoking (active smokers over the last month) and body weight.
- Analytical variables: glycosylated haemoglobin and estimated glomerular filtration rate.
- Current treatments: ACE inhibitors, ARBs and insulin treatment.

b) 2-year follow-up analysis

Progression of renal disease was determined as a 30% increase in serum creatinine or dialysis requirement after 2 years of follow-up. For this assessment, 538 patients following a dialysis program at baseline were excluded. Therefore, a total of 2032 patients were included in the study. 934 patients were included in the analysis of increase in serum creatinine and 1453 patients were included in the analysis of dialysis requirement (Figure 7).

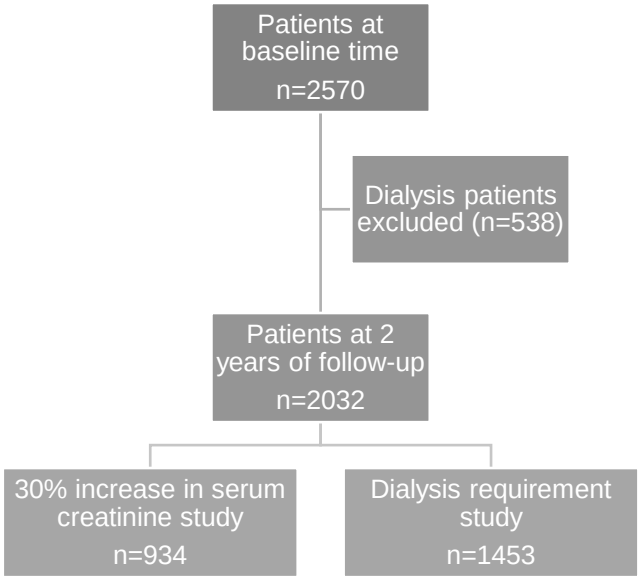

Figure 7: Flow chart of patients included in the analysis of increasing serum creatinine and dialysis requirement studies after 2 years of follow-up.

In addition, analyses of the composite renal outcome that included a 30% increase of the serum creatinine level and/or the initiation of renal replacement therapy were performed.

c) 4-year follow-up analysis

All patients with CKD were monitored every six months for the appearance of CV disease, which were recorded according to the ninth version of the International Statistical Classification of Disease (ICD-9) (171).

CV events were assessed at 4 years of follow-up in the CKD group. 576 patients were excluded due to control patients or loss of follow-up. Thus, a total of 1994 patients were included in the study (Figure 8).

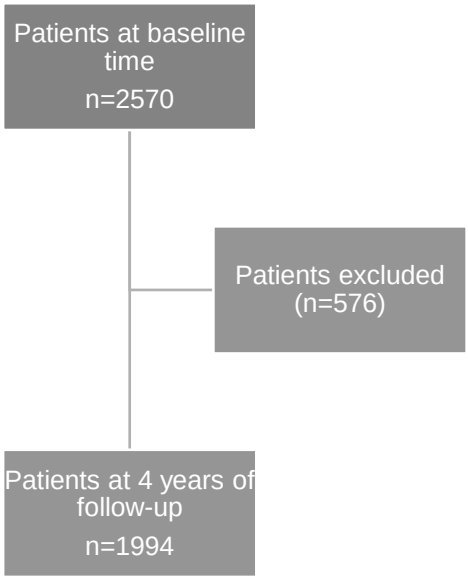

Figure 8: Flow chart of patients included in the analysis of cardiovascular after 48 months of follow-up. Abbreviations: CV, cardiovascular.

4.1.2 Circulating ADAMs enzymatic activity

The ADAMs fluorescent enzymatic assay was performed at baseline using the fluorescence-quenched ADAMs substrate (Mca-Pro-Leu-Ala-Gln-Ala-Val-Dpa-Arg-Ser-Ser-Ser-Arg-NH_2 (R&D Systems)). The Dpa group quenches Mca fluorescence until the enzyme hydrolyses the substrate by cleavage at Ala-Val. This substrate is mainly cut by ADAM17, however, it can also be cleaved by other related enzymes such as ADAM8, ADAM9, and ADAM10.

Concisely, a total of 10μL of plasma were incubated with an appropriate reaction buffer consisting of 50mM acetic acid, pH 4.5 and 100mM sodium chloride in a black 96-well plate. Samples were then incubated with 10μM of the quenched fluorescent substrate in the reaction buffer (final volume 200μL) at 37ºC for 16 hours. The circulating ADAMs activity were read using a fluorescence plate reader (Tecan Infinite 200 reader) at λ_{ex}=320nm and λ_{em}=400nm. All experiments were carried out

in duplicate, and results were expressed as RFU/μL plasma/hour. Intra-assay variability was 3.46±0.2% and interassay variability was 4.92±0.5%.

4.1.3 Statistical analysis

Statistical analyses were performed using the SPSS version 23.0 for Windows (IBM, Armonk) as well as STATA version 15 (StataCorp, College Station). Normality of the continuous variables was assessed by normal probability plots. Continuous variables that followed a normal distribution were expressed as mean ± standard error (SE), whereas non-normal variables were expressed as median [interquartile range (IQR)]. Categorical variables were expressed as frequency and percentage and differences by group were evaluated by the non-parametric Mann-Whitney test and by the chi-square or Fisher's exact test for categorical variables. P-values<0.05 were considered statistically significant.

a) Baseline analysis

Median regression analysis was performed to evaluate circulating ADAMs activity by baseline renal function and other clinical characteristics.

b) 2-year follow-up analysis

Multivariate logistic regression analyses were used to identify independent predictors of worsening renal function and dialysis. These analyses were adjusted by diabetes, age (<65 versus ≥65 years), and smoking.

c) 4-year follow-up analysis

Survival was plotted on Kaplan–Meier curves and comparisons between groups were evaluated using the log-rank tests. Probability of survival was stratified according to ADAMs activity, diabetes, sex, age (<65 versus ≥65 years), smoking, and baseline renal function. Multivariate Cox regression analyses were assessed to identify risk factors for CV and mortality events. The proportional hazard assumption, checked by examining Schoenfeld residuals (for overall model and variable by variable), was not violated.

4.2 *In vivo* study

4.2.1 Housing

C57BL/6 male mice were housed in groups of three in ventilated cages with 15-20 air renewals per hour with *ad libitum* access to mouse chow and water under 12:12 hour light:dark cycle. The Ethical Committee of Animal Experimentation of the Barcelona Biomedical Research Park and the Catalan Government approved all procedures (DMAH n. 9302).

4.2.2 *Adam17* deletion

ADAM17 expression is increased in endothelial and proximal tubular cells of DN patients. However, the effect of specifically blocking *Adam17* on endothelial or proximal tubular cells in DN has not been previously addressed. For that reason, we conditionally deleted *Adam17* in endothelial (*eAdam17*) or renal proximal tubular (*tAdam17*) cells in C57BL/6 mice. For the generation of specific *Adam17KO* mice we used $Adam17^{Fl/Fl}$ mice (kindly provided by Dr. Elaine W. Raines, Washington University, USA) (172). The $Adam17^{Fl/Fl}$ mice presented two *loxP* sites surrounding exon 5 of the *Adam17* gene (Figure 11).

Exon 5 was selected for deletion as it encodes for the carboxyl-terminus of the prodomain, upstream of the mature protein, and excision of the sequence results in a frame shift (172).

For specific *eAdam17* deletion, Adam17$^{Fl/Fl}$ mice were crossed with tamoxifen-inducible platelet-derived growth factor (Pdgf)-iCreER mice (kindly provided by Dr. Marcus Fruttiger, University College London, UK) (173). In the presence of tamoxifen, the iCreER, driven by the PDGF promoter (specific of endothelial cells), translocates to the nucleus and mediates loxP-specific recombination events at the exon 5 of the *Adam17* gene, only in endothelial cells.

Tamoxifen preparation was performed as previously described (174). Briefly, tamoxifen (Sigma) was dissolved in 100% ethanol by heating at 65ºC to obtain a final concentration of 200mg/mL. Deletion of the floxed *Adam17* allele in adult male mice was induced by four intraperitoneal injections (every 2 days starting at the age of 10 weeks) of 0.1mg tamoxifen/g body weight, dissolved in corn oil (Sigma). One extra dose was administered to mice four weeks after the first dose.

The generation of specific *tAdam17KO* mice occurred spontaneously by crossing Adam17$^{Fl/Fl}$ mice and spontaneous phosphoenolpyruvate carboxykinase (Pepck)-CreER mice and ROSA26-driven LacZ-Cre reporter mice (kindly provided by Dr. Volker Haase, Vanderbilt University, USA) (175). The *Pepck-CreER* transgene contains a mutated version of the PEPCK promoter, which reduces *Pepck* expression in the liver by 60% and increases *Pepck* expression in the kidney by 10-fold in transgenic mice (176). Therefore, recombination occurred principally in renal proximal tubular cells. The ROSA26-driven LacZ-Cre reporter presented β-galactosidase activity after an STOP

codon flanked by *loxP* sites and it has been used as a positive control for recombination (Figure 9).

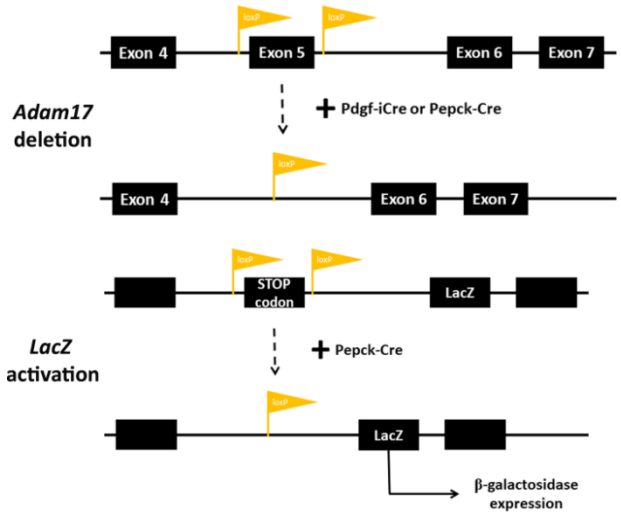

Figure 9: Schematic representation of the targeting construct, showing replacement of the loxP sites for Cre-mediated recombination on the *Adam17* and *LacZ* genes. Abbreviations: ADAM17, a disintegrin and metalloproteinase domain 17; Pdgf, platelet-derived growth factor; iCre, inducible Cre recombinase, Pepck, phosphoenolpyruvate carboxykinase; LacZ, lactose operon Z.

4.2.3 Genotyping

4.2.3.1 DNA extraction

DNA extraction and isolation were performed using Wizard® Genomic DNA Purification Kit (Promega), following manufacturer's instructions. Briefly, tissue was lysated by O/N enzymatic digestion at 55ºC with 250µL of nuclei lysis solution, adding 60µL of 0.5M ethylenediamine-tetraacetic acid (EDTA) pH 8.5 and 8.75µL of proteinase K (20mg/mL). Samples were incubated with 100µL of protein precipitation solution for 5 minutes while chilled in ice. After 4 minutes of centrifugation at 16000 x *g*, nucleic acids in the supernatant were transferred in a new tube. For DNA precipitation, 300µL of isopropanol were added followed by 2 minutes centrifugation at 16000 x *g*. Precipitated DNA was washed with

600µL of 70% ethanol and centrifuged for 1 minute at 16000 x *g* to obtain a DNA pellet. Ethanol excess was removed and the samples were dried at room temperature (RT). The dried pellet was resuspended in 50µL of rehydration solution and incubated at 65ºC for 60 minutes. Finally, samples were stored at 4ºC.

4.2.3.2 Polymerase chain reaction

Genotyping of *Adam17KO* mice was carried out by classic PCR. The polymerase chain reaction (PCR) is a technique for amplifying DNA that generates thousands to millions of copies of a particular DNA sequence. The method relies on thermal cycling, consisting of cycles of repeated heating and cooling of the reaction for DNA melting, primer annealing and enzymatic elongation of the newly synthetized DNA strain. The elongation reaction is usually catalysed by a heat-stable DNA polymerase, such as Taq polymerase. As PCR progresses, the DNA generated is itself used as a template for replication, setting in motion a chain reaction in which the DNA template is exponentially amplified.

In our studies, PCR reaction was performed using 10-40ng of DNA in a final volume of 15µL. The reagents and the conditions employed for the preparation of the PCR mix are depicted in Table 7.

Table 7: Reagents used for the genotyping PCR reaction. For each reagent, the volume employed per tube is specified.

Reagents	Volume (µL)/tube
10x NH_4 Buffer	1.5
50mM $MgCl_2$	0.35
100mM dNTPs	0.04
Forward primer 100µM	0.04
Reverse primer 100µM	0.04
ddH_2O	12.74
Taq polymerase	0.09
Sample	0.2

Abbreviations: dNTPs, deoxyribose nucleoside triphosphate.

PCR was performed for *Adam17*, *Pdgf-iCreER*, *Pepck-CreER and LacZ* genes. For each of the genes, one extra tube was included in which ddH_2O water was added instead of sample as negative control. Primer sequences used for the amplification of the genes of interest are depicted in Table 8.

Table 8: Primers used for *Adam17*, *Pdgf-iCreER*, *Pepck-CreER* and *LacZ* genes amplification.

Gene	Forward primer sequence (5' → 3')	Reverse primer sequence (5' → 3')
Adam17	ATAGGGAGCCAAGTGTGATGG	CACATACTTGCCTACAAGCCAG
Pdgf	CCAGCCGCCGTCGCAACT	GCCGCCGGGATCACTCTCG
Pepck	CGGTGCTAACCAGCGTTTTC	TGGGCGGCATGGTGCAAGTT
LacZ	CGG TGA TGG TGC TGC GTT GG	GAA TCA GCA ACC GCT TGC CG

Abbreviations: *Adam17,* a disintegrin and metalloproteinase domain 17; *Pdgf*, platelet-derived growth factor; *Pepck,* phosphoenolpyruvate carboxykinase; *LacZ,* lactose operon Z.

PCRs were programmed in a thermocycler (TProfessional Basic, Biometra) following specific settings depending on each gene. The steps for each PCR are depicted in the tables below (Table 9-12).

Table 9: PCR program used for *Adam17* gene amplification. Denaturing, annealing and elongation of the sequences were performed during 30 cycles.

PCR for *Adam17* gene			
Step	**Temperature**	**Time (min:sec)**	**Nº of cycles**
Initialization	94ºC	05:00	
Denaturing	94ºC	00:45	30
Annealing	54ºC	00:45	
Elongation	72ºC	00:35	
Final elongation	72ºC	05:00	
Cooling	8ºC	-	

Abbreviations: *Adam17,* a disintegrin and metalloproteinase domain 17.

Table 10: PCR program used for *Pdgf-iCreER* gene amplification. Denaturing, annealing and elongation of the sequences were performed during 28 cycles.

PCR for *Pdgf-iCreER* gene			
Step	**Temperature**	**Time (min:sec)**	**Nº of cycles**
Initialization	94ºC	05:00	
Denaturing	94ºC	00:45	28
Annealing	59ºC	00:45	
Elongation	72ºC	00:40	
Final elongation	72ºC	05:00	
Cooling	8ºC	-	

Abbreviations: *Pdgf*, platelet-derived growth factor; iCre, inducible Cre recombinase fused to an estrogen receptor.

Table 11: PCR program used for *Pepck-CreER* gene amplification. Denaturing, annealing and elongation of the sequences were performed during 28 cycles.

PCR for *Pepck-CreER* gene			
Step	**Temperature**	**Time (min:sec)**	**Nº of cycles**
Initialization	94ºC	05:00	
Denaturing	94ºC	00:45	28
Annealing	58ºC	00:45	
Elongation	72ºC	00:30	
Final elongation	72ºC	05:00	
Cooling	8ºC	-	

Abbreviations: *Pepck,* phosphoenolpyruvate carboxykinase; CreER, spontaneous Cre recombinase fused to an estrogen receptor.

Table 12: PCR program used for *LacZ* gene amplification. Denaturing, annealing and elongation of the sequences were performed during 28 cycles.

PCR for *LacZ* gene			
Step	**Temperature**	**Time (min:sec)**	**Nº of cycles**
Initialization	94ºC	05:00	
Denaturing	94ºC	00:45	28
Annealing	58ºC	00:30	
Elongation	72ºC	00:30	
Final elongation	72ºC	05:00	
Cooling	8ºC	-	

Abbreviations: *LacZ,* lactose operon Z.

After the PCR, samples were loaded into a 1% agarose gel (Promega) in TBE1x buffer (220mM Tris; 180mM Borate; 5mM EDTA; pH 8.3). GelRed® (Biotium) was employed as intercalating nucleic acid stain. This substance supposes a less toxic and more sensitive alternative to ethidium bromide. Amplicons were separated depending on its molecular weight (MW) and visualized under the ultraviolet light in a ChemiDocTM transilluminator (Biorad). 1Kb DNA Ladder (Sigma) was used as a MW marker.

4.2.4 Diabetes induction

Diabetes was induced to 12-week-old mice following the High Dose STZ induction protocol with some modifications (https://www.diacomp.org). Before STZ administration, mice were weighted and fasted for 4 hours with full access to water. STZ solution was freshly prepared by mixing 18.75mg of STZ (Sigma) with 840µL of 0.05M sodium citrate buffer (final concentration: 22.32mg/mL). To avoid drug degradation (15-20 minutes after preparation), freshly STZ solution was injected intraperitoneally to mice at a 150mg/kg dose in two consecutive weeks.

Mice were considered diabetic when blood glucose levels were higher than 250mg/dL twice after the first 2 weeks of STZ administration.

4.2.5 Experimental design

To evaluate the impact of specific *Adam17* deletion and diabetes in our animal model, we performed two different *Adam17* knockouts models. The experimental design is detailed below.

4.2.5.1 Endothelial Adam17 deletion in type 1 diabetic mice

As mentioned before, *eAdam17* deletion was induced through five intraperitoneal injections of tamoxifen to 10-week-old male C57BL/6 mice. At 12 weeks of age, type 1 diabetes was induced by two intraperitoneal doses of STZ. Citrate buffer was used as vehicle and given to controls. Mice were followed for 19 weeks after diabetes onset (Figure 10). During this period, blood glucose and body weight were monitored every 2 weeks under 3h-fasted animals.

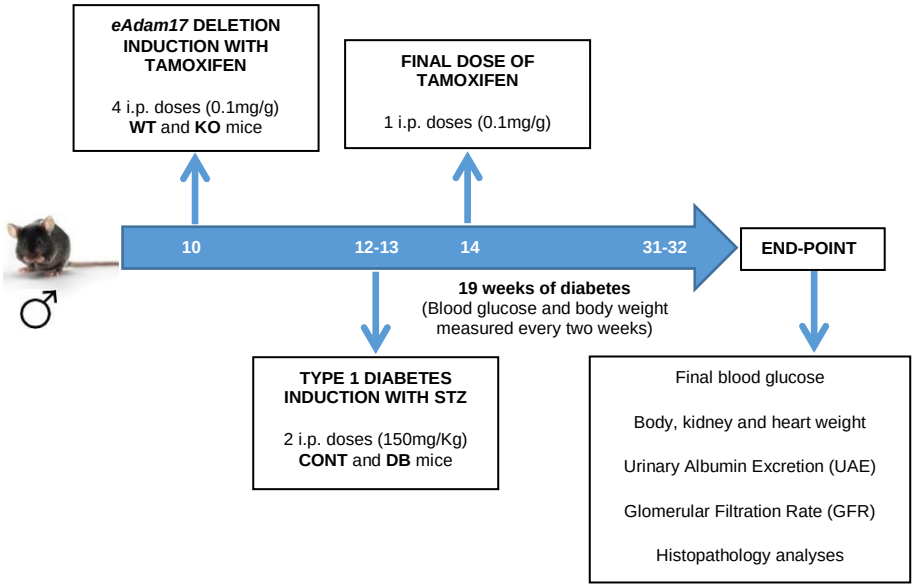

Figure 10: Experimental design for study 1. The timeline shows the most relevant aspects regarding *eAdam17* deletion and diabetes induction, follow-up, and main analysis performed at the end-point of the study. The study was made up of four different groups, CONT-WT, DB-WT, CONT-KO and DB-KO mice. Abbreviations: *Adam17*, endothelial *Adam17*; i.p, intraperitoneal; WT, wild-type; KO, knockout; CONT, control; DB, diabetic.

4.2.5.2 Proximal tubular Adam17 deletion in type 1 diabetic mice

As stated before, *tAdam17* deletion occurred spontaneously without tamoxifen injection needed. As in Study 1, type 1 diabetes was induced to 12-week-old mice by two intraperitoneal doses of STZ. Citrate buffer

was used as vehicle and given to controls. Mice were followed for 19 weeks (Figure 11). During this period, blood glucose and body weight were monitored every 2 weeks under 3h fasting conditions.

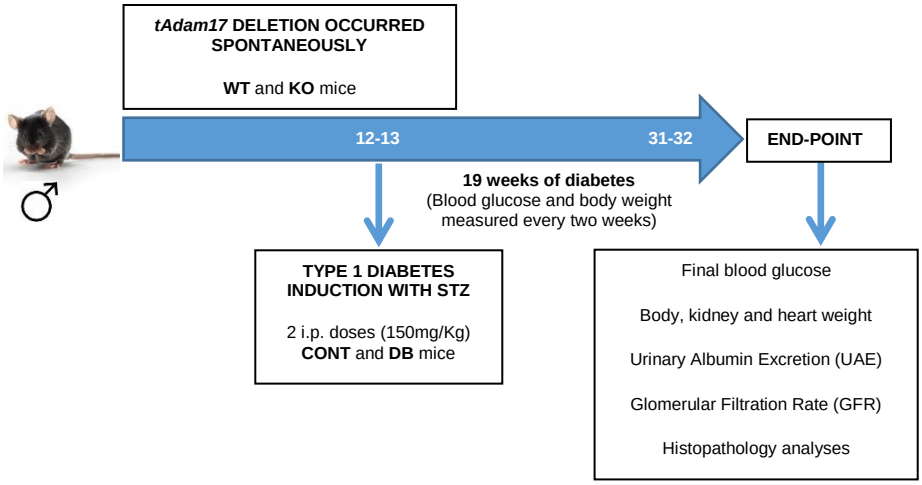

Figure 11: Experimental design for study 2. The timeline shows the most relevant aspects regarding *tAdam17* deletion, diabetes induction and duration, and main analysis performed at the end-point of the study. The study was made up of four different groups, WT-CONT, WT-DB, KO-CONT and KO-DB mice. Abbreviations: *tAdam17*, proximal tubular *Adam17*; i.p, intraperitoneal; WT, wild-type; KO, knockout; CONT, control; DB, diabetic.

4.2.6 Systolic and diastolic blood pressure and heart rate measurement

Systolic blood pressure (SBP), diastolic blood pressure (DBP) and heart rate were measured using the non-invasive tail-cuff method (CODA^{TM}; Kent Scientific Corporation, Torrington, CT). Values were obtained from conscious-trained mice on six consecutive morning sessions by the same research assistant. Mice were placed on a heating platform at 33ºC in an acrylic restrainer. A tail-cuff and pulse sensor was introduced along the tail. The tail cuff is connected to a cylinder of compressed air through an arrangement of inlet and outlet valves that allow inflation and deflation of the cuff at a constant rate.

Results were calculated as the mean from the valid values of 20 measurements in each session and expressed in millimetres of mercury (mmHg), for SBP and DBP, and beats per minute (bpm), for heart rate.

4.2.7 Glomerular filtration rate

GFR was estimated using clearance kinetics of plasma FITC-inulin after a single bolus injection, as previously described (157). 60mg of FITC-inulin (Sigma) were dissolved in 1.2mL of 0.9% NaCl by heating the solution in boiling water. To remove FITC not bound to inulin, the solution was filled into a 1000Da cut-off dialysis membrane (VWR). The dialysis membrane filled with the FITC-inulin was suspended in a container with 1L of 0.9% NaCl for 24h at room temperature. Prior to use, the dialyzed solution was filtered through a 0.2µm filter (Millipore).

Dialyzed 5% FITC-inulin was injected to conscious mice through the tail vein (3.74µL/g body weight). Blood was collected at 3, 7, 10, 15, 35, 55, and 75 minutes after injection into heparinized capillary blood collection Microvette® system tubes (Sarstedt).

Blood samples were centrifuged at 6000 x *g* for 30 minutes. For each animal, 5µL of plasma from each time point were loaded into a black 96-well plate with 95µL of 0.5M HEPES, pH 7.4. To determine the total fluorescence emitted by the inulin, 0.25µL of the same inulin injected to the mice were loaded into an additional well with 4.75µL of non-fluorescent mice plasma and 95µL of 0.5M HEPES, pH 7.4. Plasma fluorescence was read using the Tecan Infinite 200 reader (λ_{ex}=485nm, λ_{em}=538nm).

The decay in plasma fluorescence levels was fit to a two-phase decay curve using nonlinear regression (GraphPad Prism, GraphPad Software) as previously described (177). The initial-rapid decay phase

represents redistribution of the tracer from the intravascular compartment to the extracellular fluid. Systemic elimination also occurs, but the distribution process is relatively dominant during the initial phase. During the later phase, slower decay in tracer concentration predominantly reflects systemic clearance from the plasma. GFR was calculated using the equation:

$$GFR = \frac{I}{\frac{A}{\alpha} + \frac{B}{\beta}}$$

I represents the amount of FITC-inulin delivered by the bolus injection, A and B are the y-intercept values of the two decay rates, and α and β are the decay constants for the distribution and elimination phases, respectively. GFR values were expressed as µL/min/g.

4.2.8 Urinary Albumin Excretion

UAE was determined by the ACR on morning spot urine, obtained through abdominal massage and collected in microcentrifuge tubes during three consecutive days at the end of the follow-up. A commercial ELISA kit was used for albumin quantification (Albuwell M; Exocell) and a colorimetric assay kit was used to quantify creatinine levels (Creatinine Colorimetric Assay, Caiman). ACR values were expressed as µg of albumin/mg of creatinine.

4.2.8.1 Albumin levels determination

Albuwell M is an indirect competitive enzyme-linked immunosorbent assay (ELISA) designed to monitor kidney function in mice by measurement of urinary albumin. The assay is performed in 96-well plates coated with mouse albumin (stationary phase), where urine sample (fluid phase) is added. The antigen in urine samples (albumin)

is recognized by the primary antibody, a specific rabbit anti-murine albumin antibody conjugated to horseradish peroxidase (anti-mouse Albumin Ab-HRP). This primary antibody binds to the albumin of the fluid phase or to that immobilized in the stationary phase. After washing, only the antibody-conjugate that has bound to the albumin of the stationary phase remains in the well. Given that it is an indirect competitive assay, albumin molecules in urine samples compete with the stationary albumin for binding to the primary antibody. Thus, colour intensity is inversely proportional to the concentration in urine samples.

In detail, 50µL of standard curve point or diluted sample (1/13) were loaded in duplicate into albumin-coated wells. Afterwards, 50µL of primary anti-mouse Albumin Ab-HRP was added to every well and incubated for 30 minutes at room temperature. Liquid was then removed from the wells and the plate was washed 10 times with an appropriate wash buffer: 0.15M NaCl, 0.05% Tween-20 and ddH_2O. After washing, 100µL of colour developer were added to the wells. After 5 minutes, addition of 100µL of acid stopped the colorimetric reaction. Absorbance was then read in Tecan Infinite 200 reader at 450 nm. Results were expressed as µg albumin/mL.

4.2.8.2 Creatinine levels determination

Creatinine detection was performed in the same urine samples according to the manufacturer's instructions. Picric acid in an alkaline medium reacts with creatinine from the urine sample to form a complex with the alkaline picrate. Intensity of the colour formed is directly proportional to the amount of creatinine present in the sample.

Briefly, 15µL of standard curve point or diluted urine (1/20) were added to a 96-well plate and mixed with 150µL of alkaline picrate solution. After 10 minutes of incubation at RT, absorbance was determined in

Tecan Infinite 200 at 500nm (initial absorbance reading). Then, 5µL of acid reagent were added to each of the wells. After 20 minutes of incubation at room temperature, absorbance was read at 500nm (final absorbance reading). Results were expressed as mg creatinine/dL.

4.2.9 Necropsy

After 19 weeks of follow-up, animals were anesthetized with sodium pentobarbital diluted 1/10 in saline (20 mg/mL) at a dose of 45 mg/kg. Blood was collected by intracardiac puncture. Afterward, mice were perfused with cold phosphate-saline buffer (PBS) by transcardiac puncture to flush out blood. Kidneys and heart were removed, weighed, and processed for several purposes. Half of one kidney was fixed in 10% neutral-buffered formalin solution (Sigma) and processed for paraffin embedding according to standard procedures. The other half of the kidney was snap-frozen in liquid nitrogen embedded in an optimal cutting temperature (OCT) medium compound. The remaining tissue was snap-frozen and kept at -80ºC until it was used. Blood samples were centrifuged for 10 minutes at 8000 x *g* at 10ºC and serum was transferred and maintained at -20ºC until used.

4.2.10 Molecular studies

4.2.10.1 Evaluation of renal morphology in PAS-stained samples

To evaluate the presence of structural alterations in tubular and glomerular compartments, deparaffinized kidney sections were stained with periodic acid–Schiff (PAS) by our pathologist (Dr. Gimeno) as previously described (178). For each mouse, twenty microphotographs of the central section of the glomeruli were taken at 40x magnification with an Olympus BX61 microscope. Only glomeruli showing the vascular pole were considered for the analyses in order to avoid

tangential cuts. Glomerular area, glomerular tuft area, and mesangial area (Figure 12) were determined by ImageJ software. Finally, mesangial index was calculated as mesangial area/glomerular tuft area.

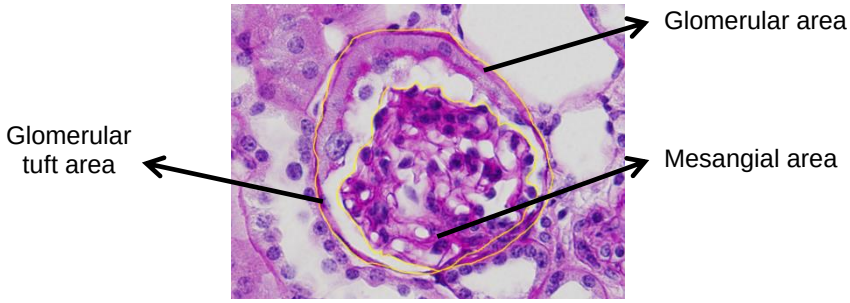

Figure 12: Glomerular morphology. Glomerular area, glomerular tuft area and mesangial area are indicated in the microphotograph.

For each animal, the mean value for glomerular tuft area, mesangial area and mesangial index was calculated.

4.2.10.2 Immunohistochemistry

For ADAM17 immunolocalization, OCT-embedded tissues were cut into 8µm-sections in a cryostat (Leica Biosystem). Sections were fixed on 4X formalin for 10 minutes at room temperature and then washed in PBS 1X. Endogenous peroxidase activity was blocked by incubating renal sections with 3% H_2O_2 in methanol for 10 minutes. After blocking, samples were washed twice with PBS 1X for 5 minutes. Unspecific binding was prevented by incubation with a blocking solution containing 10% goat serum (Sigma) for 1 hour at RT. Primary antibody against ADAM17 and HRP-conjugated anti-rabbit IgG as secondary antibody diluted in blocking solution were used. Representative images were taken at 10x magnifications for the arteries and 20x magnifications for the renal cortex using an Olympus BX61 microscope.

Paraffin-embedded tissues were cut into 3µm-sections with a rotatory microtome (Leica Biosystem). For immunohistochemistry, excess of paraffin was melted by incubating the sections in a stove at 60ºC for 30 minutes. Sections were then deparaffinized in xylene (2x15 minutes) and rehydrated through graded alcohols at 100% (2x10 minutes), 96% (1 minute), 70% (1 minute) and 50% (1 minute). Sections were then kept in ddH_2O for 5 minutes. For antigen retrieval, kidney sections were boiled in 10mM sodium citrate buffer (pH 6.0), in a pressure cooker (100ºC). After antigen retrieval, samples were cooled for 30 minutes. Endogenous peroxidase activity was blocked by incubating renal sections with 3%H_2O_2 in PBS 1X for 20 minutes. Samples were washed twice with TBS 1X for 5 minutes. Unspecific binding was prevented by incubation with a blocking solution containing bovine serum albumin (BSA, Sigma) and goat serum (Sigma) for 1 hour at RT. For protein immunolocalization, samples were incubated with specific primary antibodies diluted in blocking solution. HRP-conjugated anti-rabbit IgG, anti-mouse IgG, and anti-rat IgG were used as secondary antibodies.

β-galactosidase staining was performed as a positive control of recombination to confirm specific proximal tubular *Adam17* deletion and validate the animal model. Representative images were taken at 10x magnifications with an Olympus BX61 microscope.

Podocyte number was determined on renal sections stained for Wilms Tumour 1 (WT-1). Twenty microphotographs per animal of the central area of the glomeruli were taken at 40x magnification with an Olympus BX61 microscope. From these images, WT-1 positive and WT-1 negative nuclei were counted in a double blinded fashion (Figure 13).

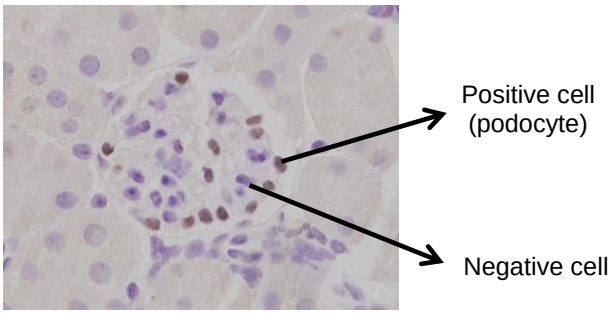

Figure 13: Glomerular podocytes determined by WT-1 staining. Brown cells are podocytes (positive nuclei) and haematoxylin-counterstained (purple) cells are other glomerular cells (negative nuclei).

Tubulointerstitial fibrosis was evaluated by cortical staining with α-smooth muscle actin (α-SMA). In order to prevent non-specific binding of the anti-mouse secondary antibody to murine immunoglobulins, samples were incubated for 1h with Fab Goat anti-mouse IgG (Jackson ImmunoResearch) diluted 1/10 in PBS 1X. This step was performed prior to the incubation with blocking solution. For each kidney section, 6 microphotographs of the renal cortex were taken at 10x magnification with an Olympus BX61 microscope. Positive α-SMA staining was quantified by ImageJ Software and expressed as mean grey value (MGV). This analysis was performed in a double blinded fashion.

Macrophage infiltration in the kidney was evaluated by renal staining with F4/80. For each kidney section, 6 microphotographs of the renal cortex were taken at 20x magnification with an Olympus BX61 microscope. Positive nuclei for F4/80 were counted in a double blinded fashion.

The specific conditions for optimized detection of our proteins of interest, including the antigen retrieval conditions, time of boiling, blocking solution composition, and primary antibodies dilution and incubation time, are detailed in Table 13.

Table 13: Proteins analysed by immunohistochemistry. Conditions for optimal staining are provided.

Protein	Antigen retrieval	BS	Primary antibody			
			Origin Incubation	Reference	Dilution	
ADAM17	-	10% GS, PBS1X	Rabbit polyclonal	ab2051 (Abcam)	1/100	1h, RT
β-GAL	0.01M citrate pH6.0, 10 minutes	1% BSA, 1% FBS, PBS1X	Rabbit polyclonal	A11132 (Invitrogen)	1/2500	O/N, 4ºC
WT-1	0.01M citrate pH6.0, 5 minutes	3% BSA, 3% GS, TBS1X	Rabbit polyclonal	sc-192 (SantaCruz Biotechnology)	1/1000	O/N, 4ºC
α-SMA	0.01M citrate pH6.0, 10 minutes	1% BSA, TBS1X	Mouse monoclonal	A-2547 (Sigma)	1/1000	1h, RT
F4/80	0.01M citrate pH6.0, 5 minutes	3% BSA, 3% GS, TBS1X	Rat monoclonal	123101 (Biolegend)	1/500	1h, RT

Abbreviations: ADAM17, a disintegrin and metalloproteinase domain 17; β-GAL, beta-galactosidase; WT-1, wilms tumour 1; α-SMA, alpha-smooth muscle actin; BS, blocking solution; PBS, phosphate-buffered saline; BSA, bovine serum albumin; FBS, fetal bovine serum; GS, goat serum; O/N, overnight; RT, room temperature; TBS, Tris-buffered saline.

After primary antibody incubation, kidney sections were washed in TBS 1X or PBS 1X depending on the composition of the blocking solution. After washing, sections were incubated with secondary antibodies. Incubation conditions are depicted in Table 14.

Table 14: Secondary antibodies used in immunohistochemistry. Conditions for optimal staining are provided.

	Secondary antibody			
	Origin Incubation	Reference	Dilution	
Anti-Rabbit IgG-HRP	Goat polyclonal	P0448 (Dako)	1/200	1h, RT
Anti-Mouse IgG-HRP	Goat polyclonal	P0447 (Dako)	1/200	1h, RT
Anti-Rat IgG-Peroxidase	Rabbit polyclonal	A5795 (Sigma)	1/200	1h, RT

Abbreviations: IgG, immunoglobulin G; HRP, horseradish peroxidase; RT, room temperature.

Binding of all antibodies was detected by oxidation of 3,3'-Diaminobenzidine (DAB) using the Liquid DAB+Substrate Chromogen System (Dako). Samples were counterstained with haematoxylin (15 seconds) and dehydrated through graded alcohols. Finally, stained sections were dried and preserved with DPX mounting media (Sigma).

4.2.10.3 Picrosirius red staining

To evaluate collagen accumulation, picrosirius red staining was performed on 4.5μm kidney sections. Briefly, deparaffined samples were incubated for 5 minutes in acidified water (0.5% acetic acid in ddH_2O water) and then transferred to a container with 0.1% picrosirius red reagent (Direct Red 81 Dye, Sigma) for 1h. Stained samples were rinsed three times with acidified water and dipped in ddH_2O water. Finally, sections were dehydrated through graded alcohols and mounted with DPX media. Tubulointerstitial collagen accumulation was semi-quantitatively measured (0-4 score) as previously described (179). All analyses were performed in a double blinded fashion. Representative images were taken at 10x magnifications with an Olympus BX61 microscope.

4.2.10.4 Protein extraction

Kidney cortex samples (25-50mg) were homogenized through a syringe in extraction buffer consisting on 50mM HEPES pH 7.4, 150mM NaCl, 0.5% Triton X-100, 0.025mM $ZnCl_2$, 0.1mM Pefabloc SC Plus (Roche), and EDTA-free protease inhibitor cocktail tablet (Roche). For phosphorylated protein detection, samples were homogenized in extraction buffer containing 25mM HEPES pH 7.5, 150mM NaCl, 1% Triton X-100, 10mM $MgCl_2$, 1mM EDTA pH 8.5, 10% glycerol, 0.1mM Pefabloc SC Plus (Roche), EDTA-free protease inhibitor cocktail tablet

(Roche), and phosphatase inhibitor cocktail (Sigma) at 1% final concentration. Protein extracts were clarified by centrifugation at 14000 x *g* for 10 minutes at 4°C.

4.2.10.5 Protein quantification

Protein concentration was determined using the Micro BCA™ Protein Assay Kit (ThermoFisher Scientific Pierce®). This technique is based on Biuret reaction, which consists on the reduction of the copper ions ($Cu^{2+} \rightarrow Cu^{1+}$) in an alkaline environment in the presence of protein in the samples (180). The colorimetric reaction that takes place after addition of BCA allows the detection of the Cu^{1+} cation.

Briefly, 150µL of diluted protein extracts (1/750 in ddH2O water) and BSA standard curve were loaded into 96-well plates. 150µL of a working solution containing BCA and Cu^{2+} were then added to each well, and plates were incubated for 2h at 37ºC. Absorbance was measured by spectrophotometry at a wavelength of 562nm in a Tecan Infinite 200 reader. Absorbance values were extrapolated in the standard curve, and protein concentration in the sample was expressed as µg of protein/µL of sample.

4.2.10.6 Western Blot

Western blot is an analytical technique that uses gel electrophoresis to separate denatured proteins by molecular weight. Then, proteins are transferred to an absorbent membrane and incubated with specific antibodies.

For protein detection, a total of 15µg of protein diluted in appropriate sample buffer (21mM Tris-HCl pH 6.8, 6% SDS, 34% glycerol, 19% β-mercaptoethanol and bromophenol blue) and denatured for 10 minutes at 100ºC were loaded in acrylamide/bisacrylamide gels (4% for the

stacking gel and 7% for the separating gel) (Table 15). A protein ladder (Precision Plus Protein Dual Colour Standard, BIO-RAD) was loaded as a molecular weight marker that enables the determination of our protein size. After loading all the samples and the protein ladder, electrophoresis was performed in a specific running buffer (25mM Tris, 192mM Glycine and 0,1% SDS).

Table 15: Components used to obtain the acrylamide/bisacrylamide gels.

Stacking gel (4% acrylamide/bisacrylamide)	Separating gel (7% acrylamide/bisacrylamide)
4% SDS + 0.5M Tris-HCl pH 6.8: 0.888mL	**4%SDS + 1.5M Tris-HCl pH 8.8:** 1.880mL
30% Acrylamide: 0.475mL	**30% Acrylamide:** 1.770mL
ddH_2O: 2.125mL	**ddH_2O:** 3.879mL
10% APS: 25µL	**10% APS:** 50µL
TEMED: 5µL	**TEMED:** 10µL

Abbreviations: SDS, Sodium dodecyl sulfate; HCl, hydrochloric acid; ddH_2O, double-distilled water; APS, ammonium persulfate; TEMED, N,N,N′,N′-tetramethyl ethylenediamine.

Following electrophoresis, samples were transferred into polyvinylidene fluoride (PVDF) membranes (Immobilon-P Millipore, Merck, Germany), previously activated with pure methanol during 15 seconds. Protein transfer was performed in a semi-dry system (Trans-Blot® Turbo™, Biorad) during 30 minutes at 1 Ampere in an appropriate transfer buffer (25mM Tris, 192mM de Glycine pH 8.3 and 10% methanol). Membranes were incubated in blocking solution containing 5% skimmed milk (SM) in TBST 0.1% for 1h at RT. After blocking nonspecific binding sites, primary antibody incubation was carried out O/N at 4ºC. After washing in TBST 0.1%, the membranes were incubated with the corresponding secondary antibody during 1h at room temperature. Protein bands were detected by chemiluminescence with Clarity Western ECL Substrate (Bio-Rad) on Curix RP2 films (AGFA-

CURIX). Control for protein loading was performed by reblotting the membranes with primary antibody against α-tubulin during 1h at room temperature. Following detection, films were scanned and bands were quantified by densitometry with Image J software. The specific conditions for optimized detection of our proteins of interest are detailed in Table 16.

Table 16: Antibodies used for Western blot protein analyses. Conditions for optimal staining are provided.

	Primary antibody			Secondary antibody			
	Origin	Reference	Dilution		Origin	Reference	Dilution
pAKT Ser473	Rabbit polyclonal	9271S (Cell Signaling)	1/1000 BSA 2.5%	**Anti-Rabbit IgG-HRP**	Goat polyclonal	P0448 (Dako)	1/2000 SM 1%
AKT	Rabbit polyclonal	9272S (Cell Signaling)	1/2000 BSA 2.5%	**Anti-Rabbit IgG-HRP**	Goat polyclonal	P0448 (Dako)	1/4000 SM 1%
TGF-β	Rabbit polyclonal	3711S (Cell Signaling)	1/1000 BSA 2.5%	**Anti-Rabbit IgG-HRP**	Goat polyclonal	P0448 (Dako)	1/6000 SM 1%
ADAM17	Rabbit polyclonal	ab2051 (Abcam)	1/3000 SM 2.5%	**Anti-Rabbit IgG-HRP**	Goat polyclonal	P0448 (Dako)	1/6000 SM 1%
α-tubulin	Rabbit polyclonal	GTX112141 (Genetex)	1/20000 SM 1%	**Anti-Rabbit IgG-HRP**	Goat polyclonal	P0448 (Dako)	1/6000 SM 1%

Abbreviations: pAKT, phosphorylated protein kinase B; TGF-β, tumour growth factor beta; ADAM17, a disintegrin and metalloproteinase domain 17; BSA, bovine serum albumin; IgG, immunoglobulin G; HRP, horseradish peroxidase; SM, skimmed milk.

4.2.10.7 Soluble TNF-α ELISA

The TNF-α levels were measured in mouse serum using the Mouse TNF-α Quantikine ELISA Kit (R&D Systems). According to manufacturer's instructions, 50µL of mouse serum were incubated with 50µL of Assay Diluent for 2h in a 96 well polystyrene microplates coated with a monoclonal antibody specific for mouse TNF-α. After washing unbound substances, 100µL of an enzyme-linked polyclonal antibody specific for mouse TNF-α conjugated to horseradish

peroxidase with preservatives were added and incubated for 2h. Then, after washing, 100µL of a Substrate Solution containing stabilized hydrogen peroxide and stabilized chromogen were added and incubated for 30 minutes. The enzyme reaction yields a blue product that turns yellow when 100µL of the Stop Solution was added. Finally, optical density of each well was determined using the Tecan Infinite 200 reader at 450nm. Wavelength correction was set at 570nm. Results were calculated using the standard curve provided by the kit and expressed as pg/mL.

4.2.10.8 ACE2 enzymatic activity

The ACE2 fluorescent enzymatic assay was performed using the ACE2-quenched fluorogenic substrate, Mca-Ala-Pro-Lys(Dnp)-OH (Enzo LifeSciences). The Dnp group quenches Mca fluorescence until the enzyme hydrolyses the substrate by cleavage at Pro-Lys. Enzymatic activity of ACE2 was determined in serum and kidney tissue from all experimental groups.

For serum, 2µL of sample were incubated with assay buffer (100mM Tris-HCl pH 7.5, 600mM NaCl, 10µM $ZnCl_2$) in the presence of protease inhibitors (100µM captopril, 5µM amastatin, 5µM bestatin and 10µM Z-Pro-prolinal) in a black 96-well plate. Samples were incubated with 10µM of the fluorogenic substrate in assay buffer (final volume 100µL) at 37 ºC for 16 hours. Plates were read in Tecan Infinite 200 reader (λ_{ex}=320nm, λ_{em}=400nm). Results were expressed as RFU/µL/hour.

For kidney tissue, after protein concentration measurement, samples were diluted in the same ACE2 assay buffer used for serum samples. To each well, 1µg of protein in 50µL of assay buffer was added and the reaction was initiated by addition of 50µL of the fluorogenic substrate at

a final concentration of 5µM. ACE2 enzymatic activity was determined after 4 hours of incubation at 37ºC. Results were expressed as RFU/µg/hour.

4.2.11 Gene expression analysis

4.2.11.1 RNA extraction

Total RNA was extracted from frozen kidney cortex using Tripure Isolation Reagent (Roche). Following manufacturer's instructions, 40-50mg of tissue were homogenized with 800µL of Tripure through a syringe and incubated for 5 minutes at room temperature to ensure the dissociation of nucleoprotein complexes. Then, 160µL of chloroform were added to each tube. Samples were shacked vigorously for 15 seconds and incubated for 10 minutes at room temperature. To separate RNA (aqueous phase) from DNA (interphase) and proteins (red organic phase), samples were centrifuged at 12000 x *g* for 15 minutes at 6ºC. After centrifugation, aqueous phase was transferred to a new centrifuge tube with 400µL of isopropanol. Samples were incubated for 5 minutes at room temperature to allow RNA precipitation and centrifuged at 12000 x *g* for 10 minutes at 6ºC. Supernatant was discarded and 1mL of ethanol 75% was added to the pellet and centrifuged at 7500 x *g* for 5 minutes at 6ºC. This process was repeated twice and excess of ethanol from the RNA pellet was removed by air-drying for 30 minutes. Finally, RNA pellet was resuspended in 50µL of RNase-free water.

4.2.11.2 cDNA synthesis

RNA concentration, quality and purity were analysed with NanoDrop (ND-1000V3.3). Acceptable purity was considered when A_{260}/A_{280} ratio

was 1.6 to 2.0. For our analysis, RNA concentration was higher than 100µg/µL in all samples.

First-strand cDNA was synthesized from 1µg of RNA using the High-Capacity cDNA Reverse Transcription Kit (Applied Biosystems, Foster City, CA). Appropriate volumes of RNA and RNase-free water were mixed with 10µL of RT Master Mix 2x to obtain a final volume reaction of 20µL (Table 17).

Table 17: Components of the RT Master Mix 2x.

Reagents	Volume (µL/sample)
10X RT Buffer	2.0µL
25X dNTP Mix (100mM)	0.8µL
10X RT Random Primers	2.0µL
MultiScribe™ Reverse Transcriptase	1.0µL
RNase Inhibitor	1.0µL
RNase-free H_2O	3.2µL

Abbreviations: RT, room temperature; dNTP, deoxyribose nucleoside triphosphate.

Retrotranscription was performed in a thermocycler (TProfessional Basic, Biometra) by incubating for 10 minutes at 25ºC, 120 minutes at 37ºC and 5 minutes at 85ºC.

4.2.11.3 Real-time quantitative PCR (RT-qPCR)

The RT-qPCR uses the same methodology as the classical PCR but a fluorophore is included in this mixture. The thermocycler includes a fluorometer that detects this fluorescence in real time as the thermal cycler runs, giving readings throughout the amplification process of the PCR. The RT-qPCR was performed using SYBR Green I Master Mix 2x (Roche) which contains FastStart Taq DNA Polymerase and DNA double-strand-specific SYBR Green I dye which binds all double-stranded DNA that are being generated throughout the cycles allowing product detection and characterization. The reaction was carried out in

LightCycler 480 multiwell-384 plates (Roche). The reagents employed and the composition of the reaction mix is described in Table 18.

Table 18: Reagents used for the RT-qPCR. For each reagent, the volume employed per sample, as well as its final concentration, is specified.

Reagent	Volume (µL/sample)	Final concentration
SYBRGreen Master Mix 2X	5.0	1x
Forward primer (100µM)	0.025	0.25µM
Reverse primer (100µM)	0.025	0.25µM
ddH_2O	2.95	-
cDNA sample (diluted 1/50)	2.0	-

The RT-qPCR was performed in the LightCycler 480 System (Roche) following the settings described in Table 19.

Table 19: RT-qPCR settings in the LightCycler® 480 System.

Step	Temperature	Ramp Rate	Time
1. Pre-incubation	95ºC	4.8ºC/s	5 minutes
2. Amplification (45 cycles)			
Denaturing	95ºC	4.8ºC/S	10 seconds
Annealing	58ºC	2.5ºC/s	20 seconds
Elongation	72ºC	4.8ºC/s	20 seconds
3. Melting			
Denaturing	95ºC	4.8ºC/s	5 seconds
Annealing	58ºC	2.5ºC/s	1 minute
Denaturing	95ºC	0.11ºC/s	-
4. Cooling	40ºC	2.5ºC/s	10 seconds

Gene expression for genes related to the RAS, fibrosis, and inflammation was determined. The sequences of primers were as follows (Table 20). Relative quantification of target genes was normalized by an endogenous control or housekeeping gene (*Gapdh*) using the ΔΔCt method as previously described (181).

Table 20: Primers used for RT-qPCR analysis.

Gene	Forward (5'-3')	Reverse (5'-3')
Agt	CGTGCCCCTAGGTGAGAGAG	TCCAAGTCAGGAGGTCGTTC
At1ra	CAAAGCTTGCTGGCAATGTA	ACTGGTCCTTTGGTCGTGAG
At2r	TAATCAGCCTAGCCATTGGTTT	TGTTCTCGGGGGAGTAAGTAAA
Ccl5	CTGCTGCTTTGCCTACCTCT	GTGACAAACACGACTGCAAGAT
Col I	GCA GGT TCA CCT ACT CTG TCC T	CTT GCC CCA TTC ATT TGT CT
Col IV	TGT CCA TGG CAC CCA TCT CT	CAC AAA CCG CAC ACC TGC TA
Fn	GCCACCGGAGTCTTTACTACC	TCTCTGTCACCTCGGTGTTG
Gapdh	TCA TTG ACC TCA ACT ACA TGG TCT	CTT GAC TGT GCC GTT GAA TTT
Hb-egf	TGGTGGCTGTAGTACTGTCGTC	TCATAACCTCCTCTCCTGTGGT
Tgfα	AGGAAGAGAAGCCAGCATGT	GCAGTGATGGCTTGCTTCTT
Tgfβ1	CAACAACGCCATCTATGAGAAA	CTTCCCGAATGTCTGACGTATT
Tnfα	GACTAGCCAGGAGGGAGAACAG	CAGTGAGTGAAAGGGACAGAACCT
Tnfr1	ACGAATCACTCTGCTCCGTG	TCGCAAGGTCTGCATTGTCA

Abbreviations: *Agt,* angiotensinogen; *At1r*, angiotensin II receptor type 1A; *At2r*, angiotensin II receptor type 2; *Ccl5*, chemokine (C-C motif) ligand 5; *Col I*, collagen I, *Col IV*, collagen IV; *Fn*, fibronectin; *Gapdh*, glyceraldehyde-3-phosphate dehydrogenase; *Hb-egf*, heparin binding EGF-like growth factor; *Tgfα*, transforming growth factor alpha; *Tgfβ1*, transforming growth factor beta-1*; Tnfα*, tumour necrosis factor alpha; *Tnfr1*, tumour necrosis factor alpha receptor 1.

4.3 *In vitro* study

To reinforce our *in vivo* observations, we studied the role of *Adam17* deletion and high glucose against fibrosis in organoids from human kidney proximal tubular cells (HKC-8). For this purpose a three dimensional (3D) *in vitro* cell culture with HKC-8 spheroids incubated in low glucose, high glucose, and mannitol medium was performed.

Like traditional two-dimensional (2D)-cell culture, three-dimensional (3D) *in vitro* cell culture technology shares the advantages of being accessible to microscopic examination, chemical intervention, and biological manipulation. They have the added benefit of closer resembling physiological tissue organization and are therefore a powerful tool to investigate fundamental questions regarding morphogenesis, physiology, and disease dynamics (182,183).

4.3.1 Cell type and cell culture conditions

Adherent HKC-8 cells kindly provided by Dr. Nugraha (Switzerland) are a human-derived renal proximal tubular cell line that provides a useful model system for the study of human renal cell function (184).

For our studies, HKC-8 cells were cultured in Dulbecco's Modified Eagle's Medium/Nutrient Mixture F-12 Ham (DMEM/F12) which is a 50:50 mixture of DMEM and Ham's F12 media. The medium was supplemented with 5.5mM glucose, 2.5% fetal bovine serum (FBS), 1% Insulin-Transferrin-Selenium, 100U/mL Penicillin and 100µg/mL streptomycin. Culture conditions were maintained at 37°C in a humidified atmosphere containing 5% CO2. Cells were verified as mycoplasma-free using a commercial test kit (Qiagen).

4.3.2 CRISPR/Cas9 for *Adam17* silencing

Adam17 deletion on HKC-8 cells was performed using the human TACE CRISPR/Cas 9 KO plasmid (SantaCruz Biotechnology) consisting of a pool of 3 plasmids. Each plasmid encodes a GFP protein, a Cas9 nuclease and a target-specific 20nt guide RNA (gRNA) designed for maximum knockout efficiency (Figure 14).

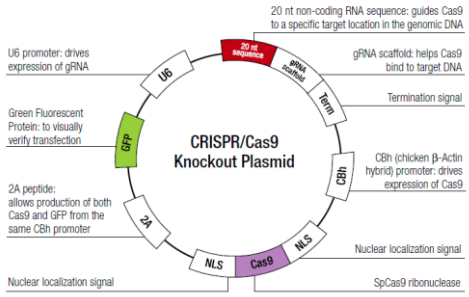

Figure 14: Schematic representation of one of the plasmids of the TACE CRISPR/Cas9 KO plasmids.

Transfection was performed following manufacturer's instructions. 24h prior to transfection, $1.5x10^5$cells were seeded in a 6-well plate in antibiotic-free DMEM/F12 medium.

The day of transfection, 0.5µg of Plasmid DNA (0.1µg/µL) were diluted into Opti-MEM™ medium to bring the final volume to 150µL (solution A). The solution was mixed and incubated for 5 minutes at room temperature. For each transfection, 5µL of transfection reagent (SantaCruz Biotechnology) were diluted into Opti-MEM™ medium to bring final volume to 150µL (solution B). The solution was mixed and incubated for 5 minutes at room temperature. After incubation, solution A was mixed with solution B and the complex was incubated for 20 minutes at room temperature. Afterwards the complex was added to the cells growing in monolayer and gently mixed by swirling the plate. The day after after transfection, medium was replaced with fresh antibiotic-free DMEM/F12.

4.3.3 Cell sorting

Three days after transfection, cells were selected by positive GFP sorting. Cells were resuspended in 400µL PBS + 1% FBS and filtered directly before sorting using cell strainer caps in 5mL FACS tubes (Corning). Non-transfected cells were used as control to estimate background signals. Cell sorting was performed using the FACSAria III sorter (BD Biosciences). 600 GFP-positive cells were collected in 5mL FACS tubes with complete DMEM/F12 medium and centrifuged at 300 x *g* for 5 minutes. After medium aspiration, cells were resuspended in complete DMEM/F12 medium and seeded in a single well of a 24-well plate.

4.3.4 3D cell culture set up

To obtain the 3D HKC-8 spheroids, the 3D Life dextran hydrogel kit (BioCat) was functionalized with RGD peptide (BioCat) following the manufacturer's instructions. The HKC-8 single cell suspension (around 57,600 cells) was mixed with the RGD-functionalized dextran hydrogel and crosslinked with PEG-based crosslinker provided in the kit.

Briefly, cells were trypsinized and a cell suspension of $3.6x10^5$cells/mL was prepared. 30mmol/L Mal-dextran, 10x concentrated buffer (CB) pH 5.5 and 3mmol/L thiol Arg-Gly-Asp (RGD) peptide were combined in a sterile tube with ddH_2O (Table 21). The mixture was incubated for 10 minutes at room temperature. After incubation, cell suspension was added to the mixture. For gel formation, 3.25µL of 20mmol/L polyethylene glycol (PEG)-link and 61.75µL of the mixture were combined and spotted as small droplets in the cell culture 24-well plate. To allow gelation, the spots were incubated for 10 minutes at RT. After incubation, 700µL of DMEM/F12 low glucose medium were added to neutralize the acidic pH. Medium was exchanged 30 minutes later and every 48h.

Table 21: Reagents used to obtain the 3D cell spheroids. Volumes and final concentration are specified.

Reagent	Volume (µL)	Final concentration
ddH_2O	288	-
10X CB pH 5.5	80	1X
Mal-dextran (30mmol/L)	64	2mmol/L
Thiol RGD peptide (3mmol/L)	320	1mmol/L
Cell suspension ($3.6x10^5$cells/mL)	160	-

Abbreviations: CB, concentrated buffer; RGD, Arg-Gly-Asp peptide.

After 13 days of seeding, the spheroids were incubated for 72h with either final concentration of 35mM D-glucose (HG, high glucose), 5mM D-glucose (LG, low glucose) or 35mM mannitol (M) as osmotic control.

4.3.5 Immunofluorescence in 3D-tubular spheroids

The quality of the established 3D cell culture of mature HKC-8 spheroids was assessed by aquaporin 1 (AQP1) and glucose transporter 1 (GLUT-1) staining. Immunofluorescence for fibrotic markers such as type IV collagen and α-SMA was performed on HKC-8 spheroids. HKC-8 spheroids in hydrogel were fixed in a 4% formaldehyde solution (ThermoFisher Scientific) for 30 minutes. The spheroids were then permeabilized and blocked with 0.2% saponin (Sigma), 3% BSA and 20% FCS for 30 minutes. After blocking, the spheroids were incubated with primary and secondary antibodies for 1h as depicted in Table 22. The samples were then mounted with FluorSave Reagent (Merck Chemicals) to minimize laser-induced photo bleaching.

Table 22: Primary and secondary antibodies used for immunofluorescence in 3D-tubular spheroids. Conditions for optimal staining are provided.

	Primary antibodies			Secondary antibodies		
	Origin	**Ref**	**Dilution**	**Origin**	**Ref**	**Dilution**
AQP1	Mouse monoclonal	sc-32737 (SantaCruz)	1/1000, BS	Goat polyclonal	A32723, Alexa 488, (ThermoFisher)	1/500, PBS1X
GLUT1	Rabbit polyclonal	ab652 (Abcam)	1/500, BS	Goat polyclonal	A11011, Alexa 568 (ThermoFisher)	1/500, PBS1X
α-SMA	Mouse monoclonal	A5228 (Sigma)	1/1000, BS	Goat polyclonal	A32723, Alexa 488, (ThermoFisher)	1/500, PBS 1X
Type IV collagen	Mouse monoclonal	C1926 (Sigma)	1/1000, BS	Goat polyclonal	A32723 Alexa 488, ThermoFisher	1/500, PBS1X

Abbreviations: AQP1, aquaporin 1; BS, blocking solution; PBS, phosphate-buffered saline; GLUT1, glucose transporter 1; α-SMA, alpha-smooth muscle actin.

Microscopy images were acquired using a HC APO CS2 20x/0.75 IMM on a Leica SP8 inverted confocal microscope. The 3D image stack was reconstructed using Imaris Software. The study included four spheroids per group. Eight to ten images were taken from each spheroid.

4.3.6 Statistical analysis

Statistical analyses were performed using the SPSS version 23.0 0 for Windows (IBM, Armonk). Non-parametric Kruskal-Wallis tests were performed for multiple comparisons between groups. In addition, Non-parametric Mann-Whitney tests were used for group-to-group comparisons. Significance was defined as $P<0.05$ and values were expressed as mean±SD.

5. RESULTS

5. Results

5.1 Study 1: Clinical Study

5.1.1 Cohort description

A total of 2570 patients from the NEFRONA Study were included in the analysis. Of them, 2001 were CKD patients without previous history of CV disease and 569 were control patients. The CKD patients were divided into two groups, patients not requiring dialysis (CKD3-5, n=1463) and patients in dialysis, either haemodialysis or peritoneal dialysis (CKD5D, n=538). Characteristics of studied subjects are shown in Table 23. Briefly, CKD patients (CKD3–5 and CKD5D patients) had a higher prevalence of diabetes, hypertension, and dyslipidaemia than controls. Interestingly, CKD5D patients were younger, thinner and had less prevalence of diabetes, hypertension, and dyslipidaemia than CKD3-5 patients. As expected, CKD3-5 presented a significantly lower GFR as compared with control subjects. Regarding therapy treatments, the percentage of patients in RAS blockade and insulin therapy was lower in the control group than in CKD patients.

Table 23: Description of basal NEFRONA cohort. Values are expressed as mean±SD, and categorical variables are represented by the number and the percentage of patients.

					P-value		
	Total population n=2570	**CONT n=569**	**CKD3-5 n=1463**	**CKD5D n=538**	**CONT vs CKD3-5**	**CONT vs CKD5D**	**CKD3-5 vs CKD5D**
Age (years)	59.3±12.66	56.1±11.41	61.9±12.13	55.75±13.63	**p<0.001**	p=0.845	**p<0.001**
Male/Female	1554/1016	316/253	912/551	326/212	**p<0.001**	p=0.088	p=0.477
Diabetes	586 (22.8%)	68 (12%)	420 (28.7%)	98 (18.2%)	**p<0.001**	**p=0.004**	**p<0.001**
Hypertension	2001 (77.8%)	219 (38.5%)	1323 (90.4%)	459 (85.3%)	**p<0.001**	**p<0.001**	**p=0.001**
Dyslipidaemia	1500 (58.4%)	208 (36.6%)	1013 (69.2%)	279 (51.9%)	**p<0.001**	**p<0.001**	**p<0.001**
Smoking	517 (20.1%)	118 (20.7%)	280 (19.1%)	119 (22.1%)	p=0.415	p=0.576	p=0.139
Body weight (kg)	76.4±15.18	76.7±14.98	77.8±14.89	72.2±15.39	p=0.087	**p<0.001**	**p<0.001**
Glycosylated haemoglobin (%)	6.0±1.21	5.7±1.06	6.3±1.23	5.6±1.04	**p<0.001**	p=0.111	**p<0.001**
GFR (mL/min/1.73m^2)	48.2±29.94	89.8±17.58	32.0±13.76	-	**p<0.001**	-	-
ACEi treatment	679 (26.4%)	57 (10%)	517 (35.3%)	105 (19.5%)	**p<0.001**	**p<0.001**	**p<0.001**
ARB treatment	1115 (43.4%)	128 (22.5%)	819 (55.9%)	168 (31.2%)	**p<0.001**	**p=0.001**	**p<0.001**
Insulin treatment	320 (12.5%)	8 (1.4%)	233 (15.9%)	79 (14.7%)	**p<0.001**	**p<0.001**	p=0.497

Abbreviations: CONT, control patients; CKD3-5, non-dialysis patients chronic kidney disease stage 3 to 5; CKD5D, dialysis patients; GFR, glomerular filtration rate; ACEi, angiotensin-converting enzyme inhibitor; ARB, angiotensin II receptor blockers.

5.1.2 Baseline circulating ADAMs activity in CKD patients

Baseline soluble plasma ADAMs (sADAMs) activity was significantly increased in CKD3-5 and CKD5D patients as compared with the control group. In addition, circulating ADAMs activity was found to be significantly increased in CKD5D patients compared with CKD3-5 patients (Figure 15A). It should be noted that circulating ADAMs activity increased as renal function worsened (Figure 15B).

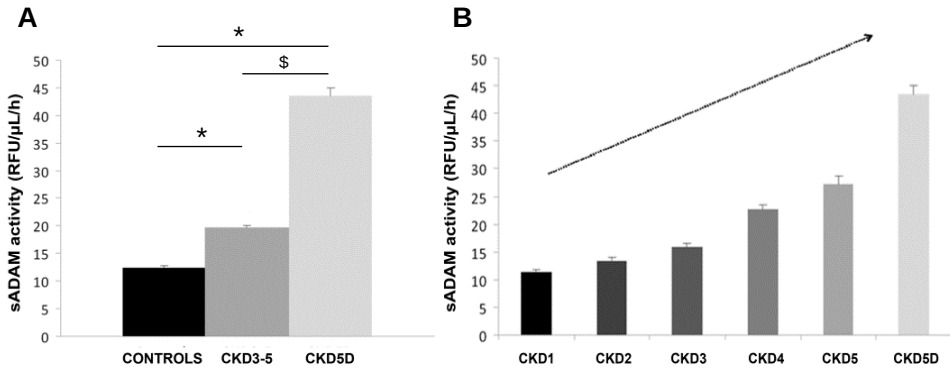

Figure 15: Circulating ADAM activity in studied subjects. A) Circulating ADAMs activity was higher in CKD3-5 and CKD5D patients as compared with the control group (P<0.001) and in CKD5D compared with CKD3-5 patients (P<0.001). Continuous variables are expressed as mean±SE. B) Circulating ADAMs activity classified into all CKD stages and CKD5D patients. Abbreviations: sADAM, soluble plasma ADAMs; CKD, chronic kidney disease; CKD5D, dialysis patients. *P≤0.05 CKD vs controls; $P≤0.05 CKD5D vs CKD3-5.

Median regression analyses were performed to identify independent predictors of circulating ADAMs activity in the studied groups (Table 24). After adjustment for clinical variables (including sex, age, hypertension, diabetes, dyslipidaemia, and smoking) and treatments (RAS blockade and insulin therapies), baseline renal function and smoking were significantly associated with circulating ADAMs activity.

Table 24: Median regression analysis of circulating ADAMs activity by baseline renal function and other clinical characteristics. Dependent variable: circulating ADAMs median.

	Standardized coefficient β [95% CI]	P-value
CKD stages		
Control	0 (Reference)	
CKD3-5	3.61(1.46-5.76)	**0.001**
CKD5D	22.77(20.36-25.18)	**0.000**
Sex		
Female	0 (Reference)	
Male	-0.04(-1.53-1.44)	0.956
Age (≥65 years)	-0.06(-0.12-0.00)	0.052
Hypertension	1.13(-1.09-3.36)	0.321
Diabetes	-1.60(-4.00-0.80)	0.191
Dyslipidaemia	0.89(-0.68-2.45)	0.267
ACEi treatment	-0.84(-2.63-0.94)	0.355
ARB treatment	0.87(-0.81-2.55)	0.311
Insulin treatment	0.30(-2.71-3.30)	0.847
Smoking	1.89(0.07-3.72)	**0.042**

Abbreviations: CKD3-5, non-dialysis patients with chronic kidney disease stage 3 to 5; CKD5D, dialysis patients; ACEi, angiotensin-converting enzyme inhibitors; ARB, angiotensin II receptor blockers.

5.1.3 Circulating ADAMs activity and renal disease progression after 2-year follow-up

For the prospective study at 2 years of follow-up, a total of 2032 CKD patients from the baseline study were included. From these CKD patients, 934 were included in the serum creatinine outcome study, where 109 patients (11.7%) had a serum creatinine increase of ≥30%. 1453 patients were included in the dialysis requirement outcome study, where 117 (8.1%) started with renal replacement therapy.

Baseline circulating ADAMs activity was significantly higher in patients with a ≥30% increase in serum creatinine levels after 2 years of follow-up compared with stable renal function patients (Figure 16A). In addition, circulating ADAMs activity was also significantly higher in

patients that needed dialysis after 2 years compared with patients that remained dialysis free (Figure 16B). Taken together, patients in whom CKD progressed presented a higher baseline circulating ADAMs activity as compared with patients with stable kidney function (Figure 16C).

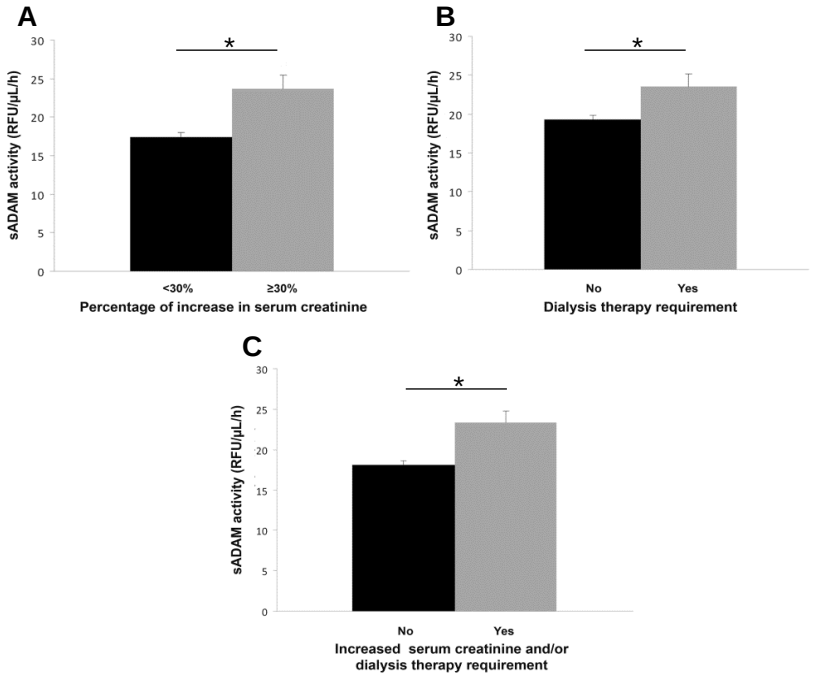

Figure 16: Circulating ADAMs activity in CKD patients with increased serum creatinine and/or dialysis requirement. A) Circulating ADAMs activity was higher in CKD patients with 30% increased serum creatinine compared with stable patients. B) Circulating ADAMs activity was increased in CKD patients that needed dialysis therapy in comparison with patients that maintained kidney function. C) Circulating ADAMs activity was increased in CKD patients with 30% increased serum creatinine and/or needed dialysis requirement. Continuous variables are expressed as mean±SE. *P≤0.05 ≥30% vs <30 and Yes vs No. Abbreviations: sADAM, soluble plasma ADAMs.

For the multivariate analyses at 2-year follow-up, stratified baseline circulating ADAMs activity according to the median value was used (low-level sADAM: <14.9 and high-level sADAM: ≥14.9). Multivariate logistic regression analysis demonstrated an interaction between sex and baseline circulating ADAMs activity (Table 25).

Table 25: Multivariate logistic regression analysis of sADAM17 activity for predicting the worsening of renal function and dialysis requirement.

	30% increase in serum creatinine				Dialysis requirement				Composite renal endpoint			
	Unadjusted OR (95% CI)	P-value	Adjusted OR (95% CI)	P-value	Unadjusted OR (95% CI)	P-value	Adjusted OR (95% CI)	P-value	Unadjusted OR (95% CI)	P-value	Adjusted OR (95% CI)	P-value
sADAM17 median (≥14.9)	1.96(1.3-2.94)	**0.000**	1.10(1.21-2.76)	0.768	2.02(1.36-2.99)	**0.000**	1.16(0.67-2.00)	0.607	2.16(1.59-2.92)	**0.000**	1.18(0.75-1.86)	0.481
Diabetes	0.89(0.56-1.41)	0.617	1.01(0.63-1.63)	0.953	0.98(0.64-1.49)	0.915	1.15(0.75-1.78)	0.517	1.03(0.74-1.43)	0.885	1.15(0.81-1.63)	0.433
Age (≥65 years)	0.61(0.40-0.91)	**0.016**	0.68(0.45-1.05)	0.081	0.52(0.35-0.77)	**0.001**	0.57(0.38-0.86)	**0.007**	0.57(0.42-0.77)	**0.000**	0.66(0.48-0.91)	**0.010**
Sex (male)	0.79(0.52-1.19)	0.253	0.50(0.27-0.94)	**0.031**	0.57(0.39-0.83)	**0.003**	0.32(0.17-0.61)	**0.001**	0.64(0.47-0.86)	**0.003**	0.37(0.23-0.60)	**0.000**
sADAM17 median by Sex	1.78(1.17-2.68)	**0.007**	2.34(1.02-5.40)	**0.046**	1.39(0.94-2.07)	0.100	2.59(1.16-5.79)	**0.021**	1.67(1.22-2.28)	**0.001**	2.57(1.39-4.78)	**0.003**
Smoking	1.36(0.83-2.21)	0.219	1.25(0.76-2.10)	0.398	1.24(0.79-1.96)	0.354	1.18(0.73-1.89)	0.506	0.73(0.51-1.05)	0.091	1.31(0.89-1.92)	0.170

Abbreviations: Abbreviation: OR, Odds ratio; CI, confidence interval; sADAMs, soluble plasma ADAMs.

Considering this interaction, we decided to perform a sex-stratified analysis. The multivariate analysis was adjusted by diabetes, age and smoking, and as shown in Table 26, increased circulating ADAMs activity was independently associated with CKD progression only in males.

Table 26: Multivariate logistic regression analysis of circulating ADAMs activity for predicting the worsening of renal function and dialysis separating males and females. Results are expressed as odd ratio (OR) and 95% confidence intervals (95% CI).

	30% increase in serum creatinine in males				30% increase in serum creatinine in females			
	Unadjusted OR (95% CI)	**P-value**	**Adjusted OR (95% CI)**	**P-value**	**Unadjusted OR (95% CI)**	**P-value**	**Adjusted OR (95% CI)**	**P-value**
sADAMs median (≥14.9)	2.72(1.59-4.66)	**0.000**	2.72(1.58-4.68)	**0.000**	1.17(0.62-2.20)	0.635	1.00 (0.52-1.91)	0.992
Diabetes	0.92(0.52-1.66)	0.793	0.99(0.54-1.82)	0.989	0.85(0.40-1.80)	0.665	1.03(0.47-2.23)	0.941
Age (≥65years)	0.89(0.53-1.49)	0.653	1.04(0.61-1.80)	0.874	0.32(0.16-0.66)	**0.002**	0.33(0.16-0.70)	**0.004**
Smoking	1.29(0.70-2.34)	0.414	1.23(0.66-2.30)	0.508	1.71(0.73-3.99)	0.215	1.21(0.51-2.91)	0.663
	Dialysis requirement in males				**Dialysis requirement in females**			
	Unadjusted OR (95% CI)	**P-value**	**Adjusted OR (95% CI)**	**P-value**	**Unadjusted OR (95% CI)**	**P-value**	**Adjusted OR (95% CI)**	**P-value**
sADAMs median (≥14.9)	3.20(1.77-5.77)	**0.000**	3.00(1.65-5.46)	**0.000**	1.26(0.73-2.18)	0.398	1.22(0.71-2.12)	0.471
Diabetes	1.10(0.62-1.94)	0.742	1.31(0.73-2.36)	0.366	0.93(0.49-1.74)	0.811	0.98(0.51-1.86)	0.947
Age (≥65years)	0.46(0.26-0.79)	**0.006**	0.53(0.63-0.94)	**0.032**	0.62(0.36-1.08)	0.091	0.58(0.33-1.03)	0.063
Smoking	2.00(1.14-3.50)	**0.015**	1.78(1.00-3.16)	**0.049**	0.63(0.24-1.62)	0.336	0.50(0.19-1.33)	0.166
	Composite renal end point in males				**Composite renal end point in females**			
	Unadjusted OR (95% CI)	**P-value**	**Adjusted OR (95% CI)**	**P-value**	**Unadjusted OR (95% CI)**	**P-value**	**Adjusted OR (95% CI)**	**P-value**
sADAMs median (≥14.9)	0.32(2.11-4.87)	**0.000**	3.15(2.06-4.81)	**0.000**	1.27(0.81-1.99)	0.302	1.13(0.71-1.79)	0.618
Diabetes	0.93(0.60-1.43)	0.726	1.23(0.78-1.95)	0.368	1.14(0.68-1.93)	0.618	0.94(0.59-1.76)	0.942
Age (≥65years)	0.67(0.46-1.00)	**0.005**	0.83(0.54-1.27)	0.383	0.48(0.30-0.76)	**0.002**	0.47(0.29-0.78)	**0.003**
Smoking	1.69(1.09-2.63)	**0.019**	1.57(0.99-2.48)	0.056	0.90(0.45-1.79)	0.762	1.15(0.57-2.34)	0.692

Abbreviation: OR, Odds ratio; CI, confidence interval; sADAMs, soluble plasma ADAMs.

5.1.4 Circulating ADAMs and cardiovascular outcomes after 4-year follow-up

A total of 1994 CKD patients from the baseline study were included in the CV outcome study after 4-years of follow-up. From those CKD patients, 181 (9.0%) presented a CV event and had a mean follow-up of 41±16 months. For the overall survival analyses at 4-year follow-up, stratified baseline circulating ADAMs activity according to the median value was used.

High-level circulating ADAMs (sADAM≥14.9) group had significantly worse estimated CV event free survival than the low-level group (sADAM<14.9). Using the log-rank test to compare these two Kaplan-Meier survival curves, significant differences were found ($p<0.001$) (Figure 17A).

As expected, patients in dialysis presented worse CV event free survival than CKD3-5 patients (Figure 17B). Also, male had worse CV event free survival than females (Figure 17C). Diabetic patients had worse CV event free survival than non-diabetic patients (Figure 17D), and older age (≥65 years) was a worsening factor for CV event free survival (Figure 17E). However, no difference was found when comparing smoking and non-smoking patients (Figure 17F).

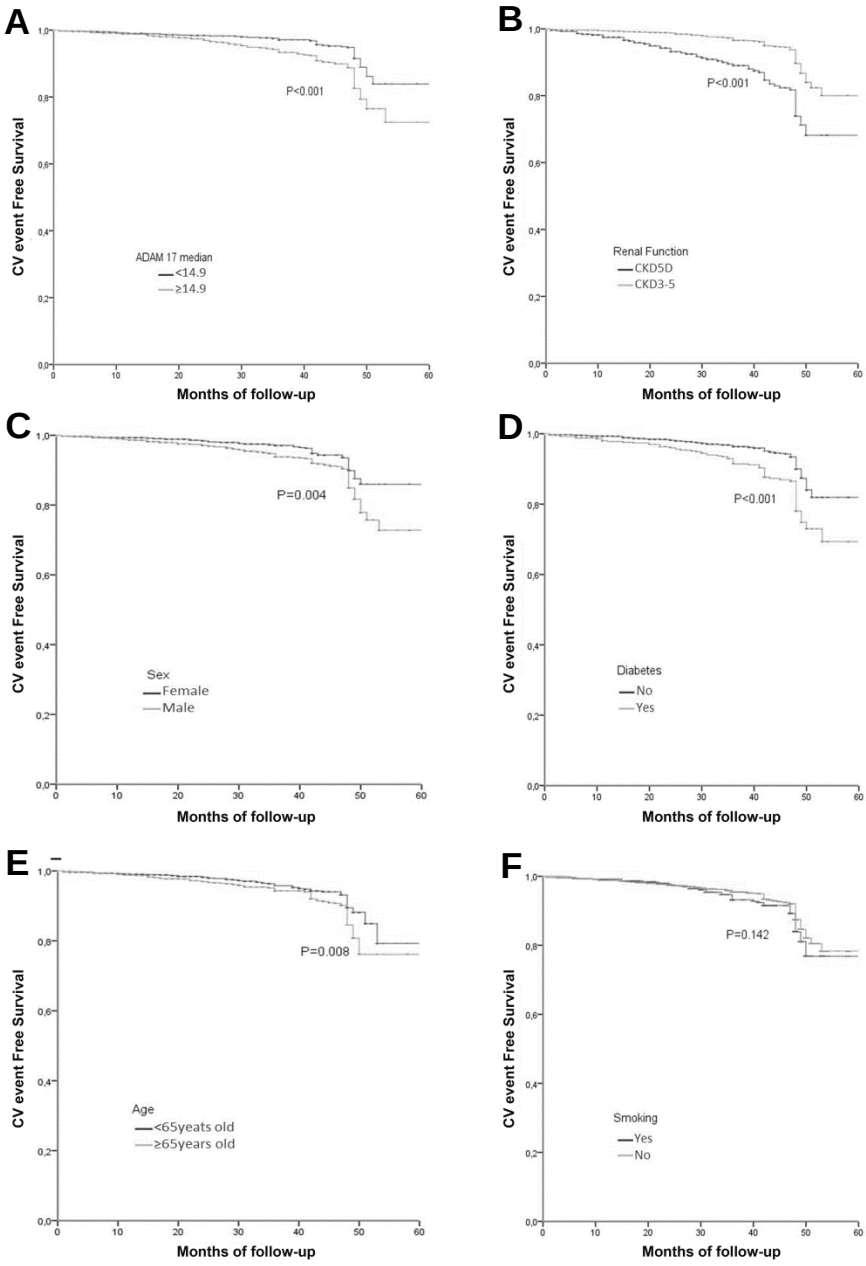

Figure 17: Actuarial survival curves of cardiovascular events after 48 months of follow-up. A) ADAMs activity; B) renal function; C) sex; D) diabetes; E) age; F) smoking. Abbreviations: CV, cardiovascular; CKD5D, dialysis patients; CKD3-5, non-dialysis patients with chronic kidney disease stage 3 to 5.

Risk factors of CV events were analysed in CKD3-5 patients after 4-year follow-up using the multivariate Cox regression model. As shown in table 27 increased circulating ADAMs activity, male sex, diabetes, being older than 65 years old, and CKD progression were significantly associated with CV events after adjusting for sex, diabetes, hypertension, age, dialysis, and smoking.

Table 27: Multivariate COX regression analysis of circulating ADAM activity for predicting risk factors for CV events. Results are expressed as hazard ratio (HR) and 95% confidence interval (95% CI).

	Adjusted HR (95%CI)	P-value
sADAMs median (≥14.9)	1.71 (1.22-2.40)	**0.002**
Sex (male)	1.53 (1.10-2.12)	**0.011**
Diabetes	2.15 (1.58-2.91)	**0.000**
Hypertension	1.18 (0.70-2-02)	0.548
Age (≥65 years)	1.65 (1.20-2.26)	**0.002**
CKD stages CKD3-5 CKD5D	2.60 (1.87-3.61)	**0.000**
Smoking	1.30 (0.91-1.86)	0.148

Abbreviations: HR, hazard ratio; CI, confidence interval; sADAMs, soluble plasma ADAMs; CKD, chronic kidney disease; CKD3-5, non-dialysis patients with chronic kidney disease stage 3 to 5; CKD5D, dialysis patients.

5.2 Study 2: *In vivo* study

5.2.1 Genotype

The *Adam17* gene had up to two bands of 400Kb and 600Kb depending on mice genotype. *Adam17*$^{Fl/Fl}$ mice presented a 600Kb band, *Adam17*$^{+/+}$ mice presented a 400Kb band and heterozygote mice presented both bands (Figure 18A). Amplification of *Pdgf-iCreER*, *Pepck-CreER* and *LacZ* by PCR allowed us to differ between the presence and the absence of the gene. *Pdgf-iCreER* (Figure 18B),

Pepck-CreER and *LacZ* (Figure 18C) appeared as a unique band of 430Kb, 500Kb and 500Kb, respectively.

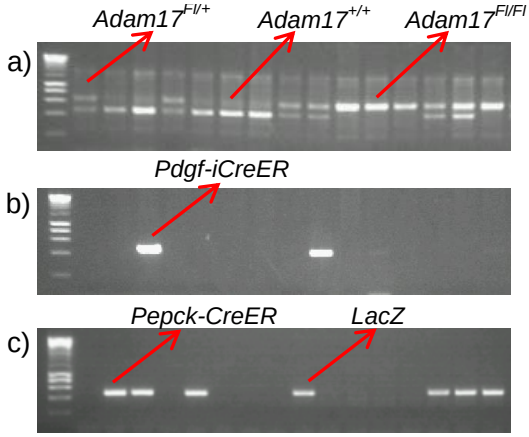

Figure 18: Representative photograph of PCR amplification products. A) *Adam17*$^{Fl/Fl}$ mice presented a 600Kb band, *Adam17*$^{+/+}$ mice presented a 400Kb band and ADAM17$^{Fl/+}$ mice presented both bands. B) Positive *Pdgf-iCreER* appeared as a unique band of 430Kb. C) *Pepck-CreER* and *LacZ* appeared as a unique band of 500Kb. Abbreviations: Adam17, a disintegrin and metalloproteinase domain 17; Pdgf, platelet-derived growth factor; iCreER, tamoxifen-inducible Cre recombinase fused to an estrogen receptor; Pepck, phosphoenolpyruvate carboxykinase; CreER, spontaneous Cre recombinase fused to an estrogen receptor; LacZ, lactose operon Z.

5.2.2 Confirmation of endothelial and renal proximal tubular *Adam17* deletion

Firstly, to ascertain that knockout mice presented genetic changes in the *Adam17* gene, qPCR analyses from renal cortex were performed. *Adam17* gene expression was downregulated in *tAdam17KO* mice (Figure 19B). However, no differences were observed on *eAdam17KO* mice (Figure 19A) due to the low proportion of endothelial cells in the renal cortex. It is largely known that the majority of the renal cortex (around 90%) is formed by tubular cells (185).

Secondly, endothelial and renal proximal tubular *Adam17* deletion was assessed by immunohistochemistry on OCT-embedded kidneys. As verified in Figure 19C, *eAdam17WT* and *tADAM17WT* mice presented

positive staining for ADAM17 in all kidney cells. Nevertheless, endothelial cells from the renal arteries of *eAdam17KO* mice were negative for ADAM17 staining and proximal tubular cells in *tAdam17KO* mice presented a more diffuse ADAM17 staining. These results demonstrated that we have generated knockout mice for ADAM17 on endothelial and renal proximal tubular cells.

In addition, a β-galactosidase staining as control of recombination was performed. *tAdam17* mice presented the ROSA26-driven LacZ-Cre reporter with β-galactosidase activity after a STOP codon flanked by loxP sites. For this reason, only the *tAdam17KO* mice presented positive β-galactosidase staining (Figure 19C).

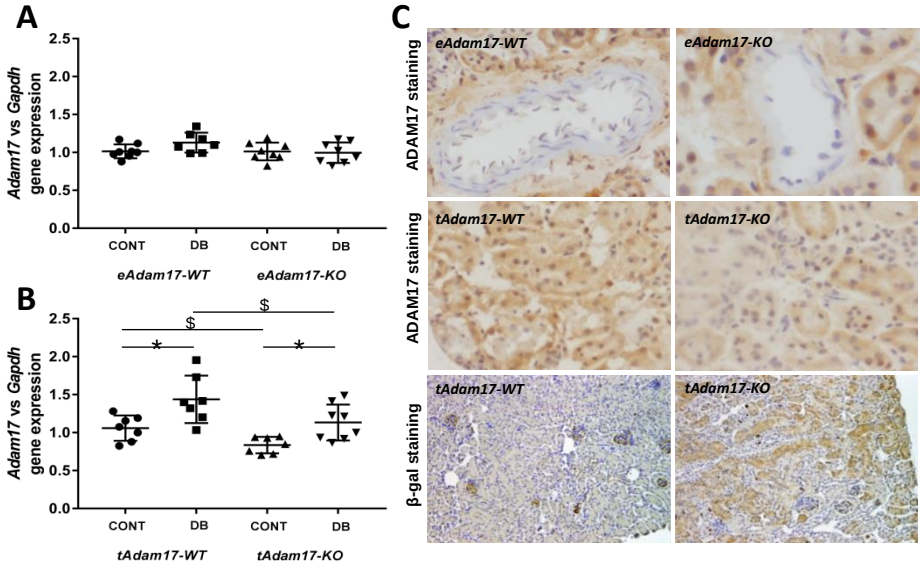

Figure 19: Confirmation of *Adam17* deletion on endothelial and renal proximal tubular cells. A) *Adam17* gene expression in *eAdam17* mice. B) *Adam17* gene expression in *tAdam17* mice. C) Representative images of ADAM17 immunohistochemistry in *eAdam17* and *tAdam17* mice and β-galactosidase staining in *tAdam17* mice. Data are expressed as mean±SD. Abbreviations: CONT, control; DB, diabetic; *eAdam17*, endothelial *Adam17*; *tAdam17,* proximal tubular *Adam17*; *Gapdh*, glyceraldehyde-3-Phosphate dehydrogenase; WT, wild-type; KO, knockout. *p<0.05 DB vs CONT, $ p<0.05 KO vs WT.

5.2.3 Physiological parameters

We studied the effect of *Adam17* deletion on endothelial and renal proximal tubular cells in diabetic nephropathy after 19 weeks of type 1 diabetes induction. During the follow-up, blood glucose and body weight (BW) were monitored every 2 weeks after 4h fasting. As shown in Figure 20, all mice receiving STZ showed significantly higher blood glucose levels and lower body weight as compared to their controls. The hyperglycaemia was maintained throughout all the follow-up.

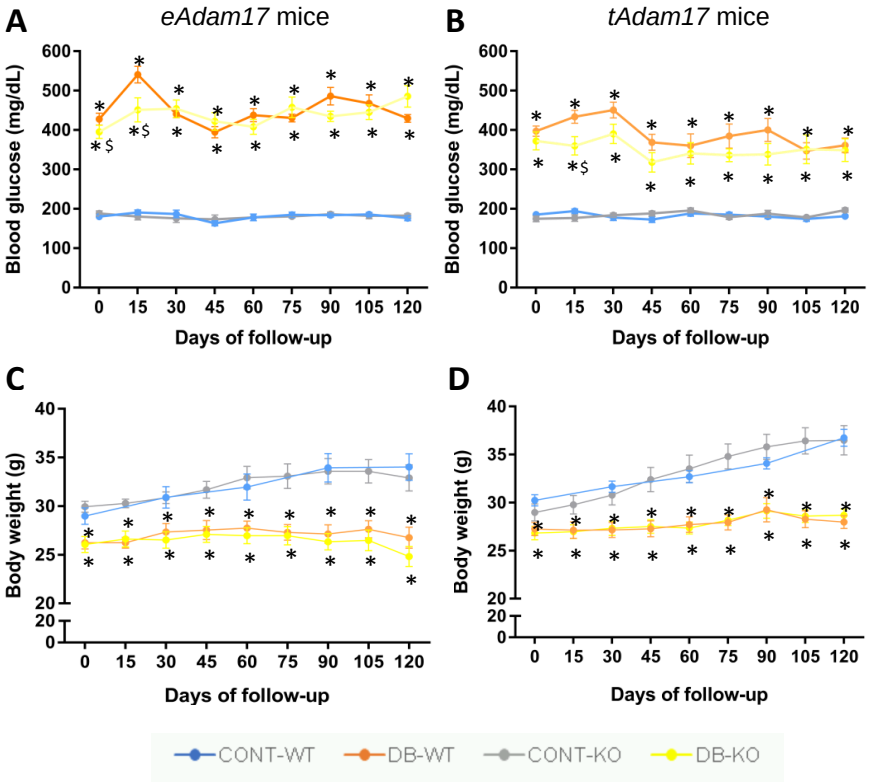

Figure 20: Blood glucose and body weight were assessed every two weeks and after 3h of fasting in all experimental groups. A) Blood glucose levels in *eAdam17* mice. B) Blood glucose levels in *tAdam17* mice. C) Body weight in *eAdam17* mice (D) Body weight in *tAdam17* mice. For these experiments, 8-12 animals were analysed in each group. Data are expressed as mean±SD. Abbreviations: *eAdam17*, endothelial *Adam17*; *tAdam17*, proximal tubular *Adam17*; CONT, control; WT, wild-type; DB, diabetic; KO, knockout. *****p<0.05 DB vs CONT. $p<0.05 KO vs WT.

Differences between diabetic and non-diabetic animals regarding blood glucose and body weight were also maintained at the end of the follow-up, under non-fasting conditions (Table 26).

At the end of the study, renal hypertrophy was evaluated by calculating kidney weight to body weight (KW/BW). Diabetic animals presented higher KW/BW ratio than their controls. Interestingly, proximal tubular *Adam17* deletion in diabetic mice was accompanied by lower KW/BW ratio as compared to diabetic wild-type mice. This decrease on KW/BW suggested a reduced hypertrophy on diabetic *tAdam17* knockout mice. Heart weight to body weight (HW/BW) ratio was significantly increased in *eAdam17KO* mice as compared with wild-type mice (Table 28).

Table 28: Blood glucose, body weight, KW/BW and HW/BW ratios were measured after 19 weeks of diabetes. Non-fasting blood glucose was determined at the end of the study; body weight, kidney weight, and heart weight were recorded in all experimental groups. Data are expressed as mean±SD.

***eAdam17* model**				
	CONT-WT	**DB-WT**	**CONT-KO**	**DB-KO**
BG (mg/dL)	194.11±30.22	591.71±21.71*	201.33±43.14	536.10±87.81*
BW (g)	34.61±5.37	26.35±3,61*****	33.09±3.34	24.16±2,70*****
KW/BW	0.97±0.19	1.45±0.31*****	1.00±0.11	1.41±0.16*****
HW/BW	0.44±0.09	0.37±0.06	0.52±0.07$	0.46±0.11$
***tAdam17* model**				
	CONT-WT	**DB-WT**	**CONT-KO**	**DB-KO**
BG (mg/dL)	212.85±37.80	580.22±37.61*	216.22±31.15	551.64±60.14*
BW (g)	34.38±4.45	28.35±3.27*****	34.94±4.40	27.50±2.15*****
KW/BW	1.07±0.17	1.35±0.15*****	1.00±0.10	1.25±0.20***$**
HW/BW	0.44±0.09	0.37±0.09	0.44±0.07	0.42±0.09

Abbreviations: *eAdam17*, endothelial *Adam17*; *tAdam17*, proximal tubular *Adam17*; CONT, control; WT, wild-type; DB, diabetic; KO, knockout; BG, blood glucose; BW, body weight; KW/BW, kidney weight to body weight ratio; HW/BW, heart weight to body weight ratio. *****p<0.05 DB vs CONT. $p<0.05 KO vs WT.

Albumin-to-creatinine ratio (ACR) in the spot urine sample was determined to evaluate albuminuria at the end of the follow-up. All diabetic mice presented increased ACR as compared with control mice.

No differences were observed between wild-type and *Adam17* knockout mice. Unexpected results were obtained when analysing GFR. No significant differences were observed between diabetic and non-diabetic groups. However, *eAdam17* deletion decreased GFR in the diabetic mice as compared with wild-type mice (Table 29).

Table 29: Albumin-to-creatinine ratio and glomerular filtration rate were measured after 19 weeks of diabetes. Data are expressed as mean±SD.

***eAdam17* model**				
	CONT-WT	**DB-WT**	**CONT-KO**	**DB-KO**
ACR (µg Alb/mg Crea)	31.89±20.61	457.90±430.46*****	30.29±14.47	250.21±291.99*****
GFR (µL/min/g)	34.91±19.08	31.35±24.92	29.58±21.63	13.28±8.66$
***tAdam17* model**				
	CONT-WT	**DB-WT**	**CONT-KO**	**DB-KO**
ACR (µg Alb/mg Crea)	42.89±24.54	180.66±134.13*****	42.34±26,14	227.31±180.87*****
GFR (µL/min/g)	47.12±25.23	38.10±21.99	51.73±19.32	37.97±21.38

Abbreviations: *eAdam17*, endothelial *Adam17*; *tAdam17*, proximal tubular *Adam17*; CONT, control; WT, wild-type; DB, diabetic; KO, knockout; ACR, albumin-to-creatinine ratio; GFR, glomerular filtration rate. *****p<0.05 DB vs CONT. $p<0.05 KO vs WT.

5.2.4 Blood pressure

SBP, DBP and heart rate were measured in diabetic and control conscious mice. Non statistical differences were observed between diabetic and non-diabetic groups when analysing SBP and DBP. However, in diabetic mice, *tAdam17* deletion decreases SBP as compared with diabetic wild-type mice. In addition, all diabetic mice presented lower heart rate than non-diabetic mice in both animal models (Table 30).

Table 30: Primary hemodynamic parameters: systolic blood pressure, diastolic blood pressure, and heart rate. Data are expressed as mean±SD.

***eAdam17* model**				
	CONT-WT	**DB-WT**	**CONT-KO**	**DB-KO**
SBP (mmHg)	94.51±9.34	91.39±5.81	92.76±6.37	94.05±5.10
DBP (mmHg)	70.42±8.02	66.16±5.21	69.17±5.43	67.23±5.65
Heart rate (bpm)	730.27±31.03	656.21±38.96*	703.11±27.15	640.32±56.79*
***tAdam17* model**				
	CONT-WT	**DB-WT**	**CONT-KO**	**DB-KO**
SBP (mmHg)	94.97±6.89	93.48±4.75	92.89±7.05	88.46±7.06$
DBP (mmHg)	70.67±6.62	68.22±4.89	68.28±6.87	64.82±6.60
Heart rate (bpm)	706.30±27.40	649.89±31.24*	712.46±33.18	689.30±41.65*

Abbreviations: *eAdam17*, endothelial *Adam17*; *tAdam17*, proximal tubular *Adam17*; CONT, control; WT, wild-type; DB, diabetic; KO, knockout; SBP, systolic blood pressure; DBP, diastolic blood pressure; mmHg, millimetres of mercury; bpm, beats per minute. *****p<0.05 DB vs CONT. $p<0.05 KO vs WT.

5.2.5 Impact of *Adam17* deletion and diabetes on glomerular histological alterations

Histologic assessment of PAS-stained kidney samples revealed a significant increase in glomerular area, matrix mesangial expansion and mesangial index in all diabetic wild-type mice. This increase in glomerular area, mesangial matrix expansion and mesangial index was attenuated in diabetic knockout mice (Figure 21). Moreover, among diabetic animals, *eAdam17KO* mice exhibited significantly decreased mesangial matrix expansion and mesangial index as compared with diabetic wild-type mice (Figure 21C, E).

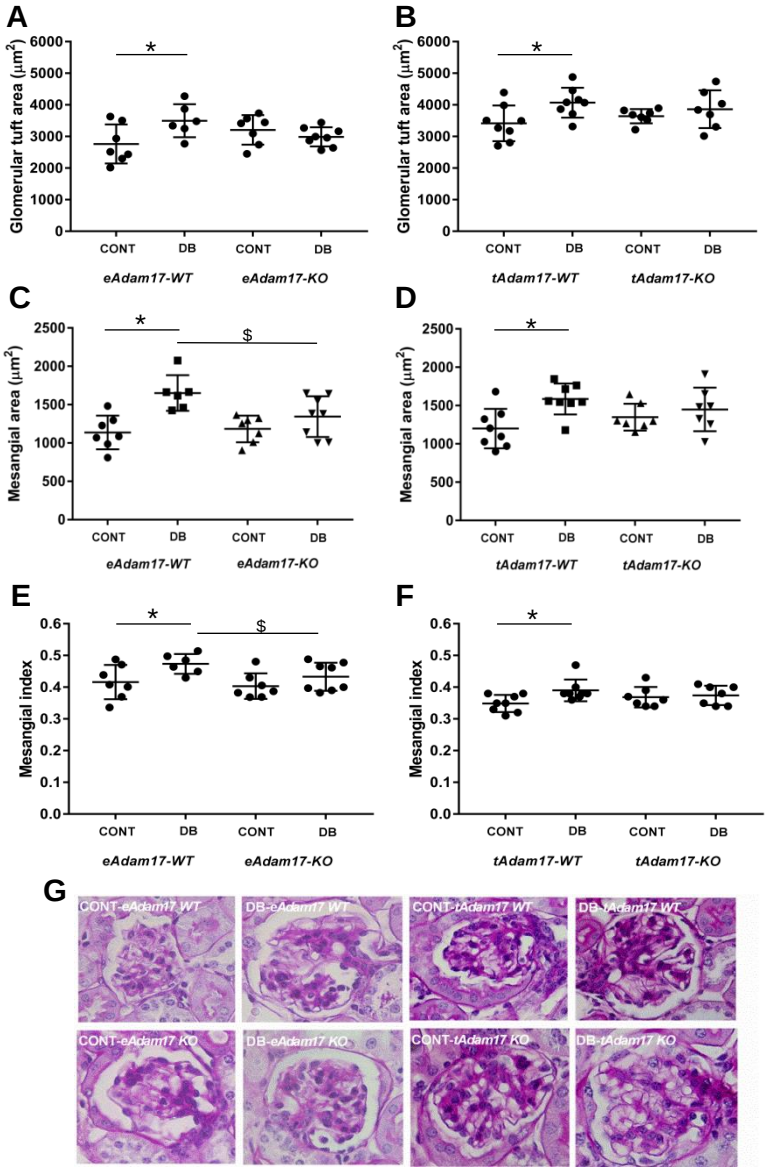

Figure 21: Influence of diabetes and endothelial or proximal tubular *Adam17* deletion on glomerular structural alterations. Periodic Acid-Schiff (PAS) staining was performed on kidney sections from all experimental groups. A) Glomerular area in *eAdam17* mice. B) Glomerular area in *tAdam17* mice. C) Mesangial area in *eAdam17* mice. D) Mesangial area in *tAdam17* mice. E) Mesangial index in *eAdam17* mice. F) Mesangial index in *tAdam17* mice. G) Representative images depicting PAS staining from all experimental groups. Data are expressed as mean±SD. Abbreviations: *eAdam17*, endothelial *Adam17*; *tAdam17*, proximal tubular *Adam17*; CONT, control; WT, wild-type; DB, diabetic; KO, knockout. *p<0.05 DB vs CONT, $ p<0.05 KO vs WT.

When studying the epithelial glomerular cells, the proportion of cells identified as podocytes, was significantly decreased in diabetic groups as compared to controls. Consistent with ameliorated diabetic glomerulopathy, diabetic *tAdam17KO* displayed lower podocyte loss as compared with diabetic WT mice (Figure 22).

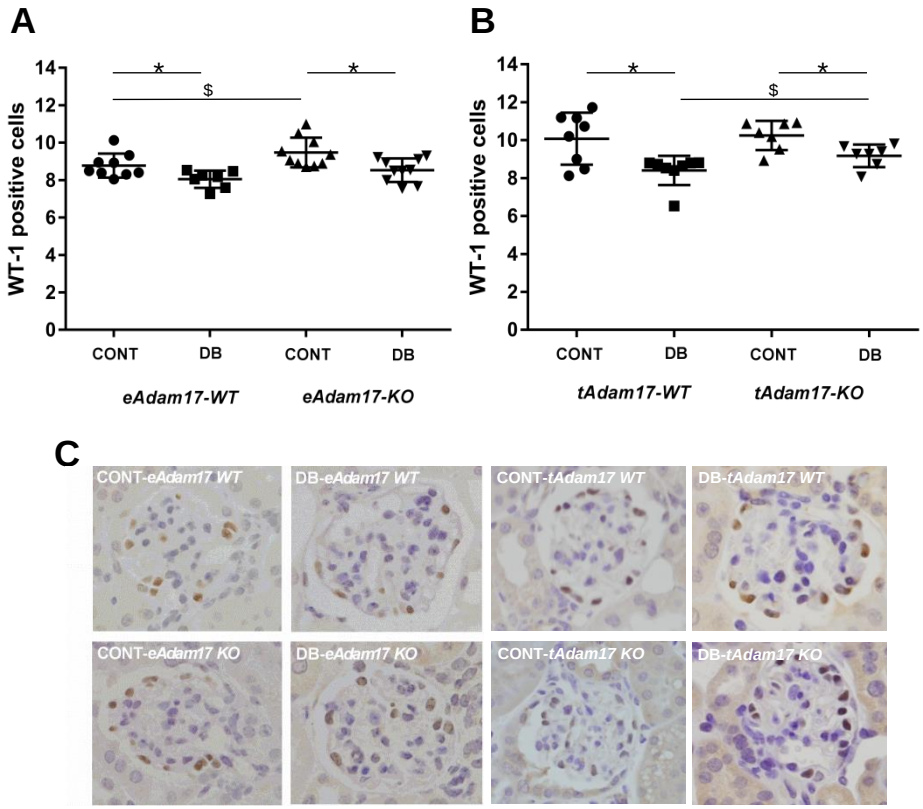

Figure 22: Influence of diabetes and endothelial or proximal tubular *Adam17* deletion on podocyte loss. Podocyte number is represented as the number of positive cells per glomerulus after WT-1 immunostaining. A) Glomerular podocyte number in *eAdam17* mice. B) Glomerular podocyte number in *tAdam17* mice. C) Representative images depicting WT-1 staining from all experimental groups. Data are expressed as mean±SD. Abbreviations: *eAdam17*, endothelial *Adam17*; *tAdam17*, proximal tubular *Adam17*; CONT, control; WT, wild-type; DB, diabetic; KO, knockout; WT-1, wilms tumour 1. *p<0.05 DB vs CONT, $ p<0.05 KO vs WT.

5.2.6 ADAM17 and the Renin Angiotensin System

Circulating ACE2 enzymatic activity was increased in all diabetic mice. Interestingly, *tAdam17* deletion in diabetic mice reduces circulating ACE2 activity as compared with diabetic wild-type mice (Figure 23A, B).

Renal ACE2 enzymatic activity was increased in diabetic mice (Figure 23C, D). Interestingly, *eAdam17* deletion exacerbates renal ACE2 activity in diabetic mice (Figure 23C), while *tAdam17* deletion attenuates the increase in renal ACE2 activity in diabetic mice (Figure 23D).

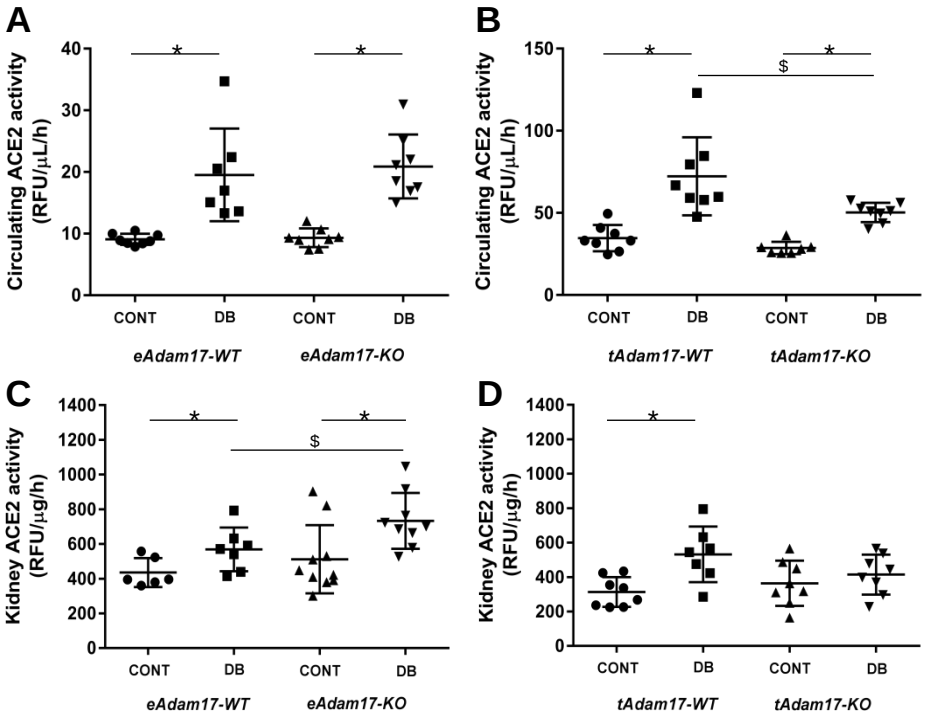

Figure 23: Influence of diabetes and endothelial or proximal tubular *Adam17* deletion on ACE2 enzymatic activity. A) Circulating ACE2 activity in *eAdam17* mice. B) Circulating ACE2 activity in *tAdam17* mice. C) Renal ACE2 activity in *eAdam17* mice. D) Renal ACE2 activity in *tAdam17* mice. Data are expressed as mean±SD. Abbreviations: *eAdam17*, endothelial *Adam17*; *tAdam17*, proximal tubular *Adam17*; CONT, control; WT, wild-type; DB, diabetic; KO, knockout; ACE2, angiotensin converting enzyme 2. *p<0.05 DB vs CONT, $ p<0.05 KO vs WT.

To better understand the molecular mechanisms underlying the differential effect of endothelial and proximal tubular *Adam17* deletion on the renal RAS, we analysed gene expression of different RAS components. Focusing on the initial components of the RAS, *Agt* gene expression was upregulated in all diabetic mice (Figure 24A, B). Regarding ANG II receptors, *At1r* gene expression was downregulated in all diabetic *eAdam17* mice (Figure 24C). Surprisingly, no differences were observed between groups in the *tAdam17* mice, although there was a tendency to decrease *At1r* gene expression in diabetic mice (Figure 24D). In contrast, *At2r* gene expression was increased in all diabetic wild-type mice and the effect of diabetes was lost in the knockout groups (Figure 24E, F).

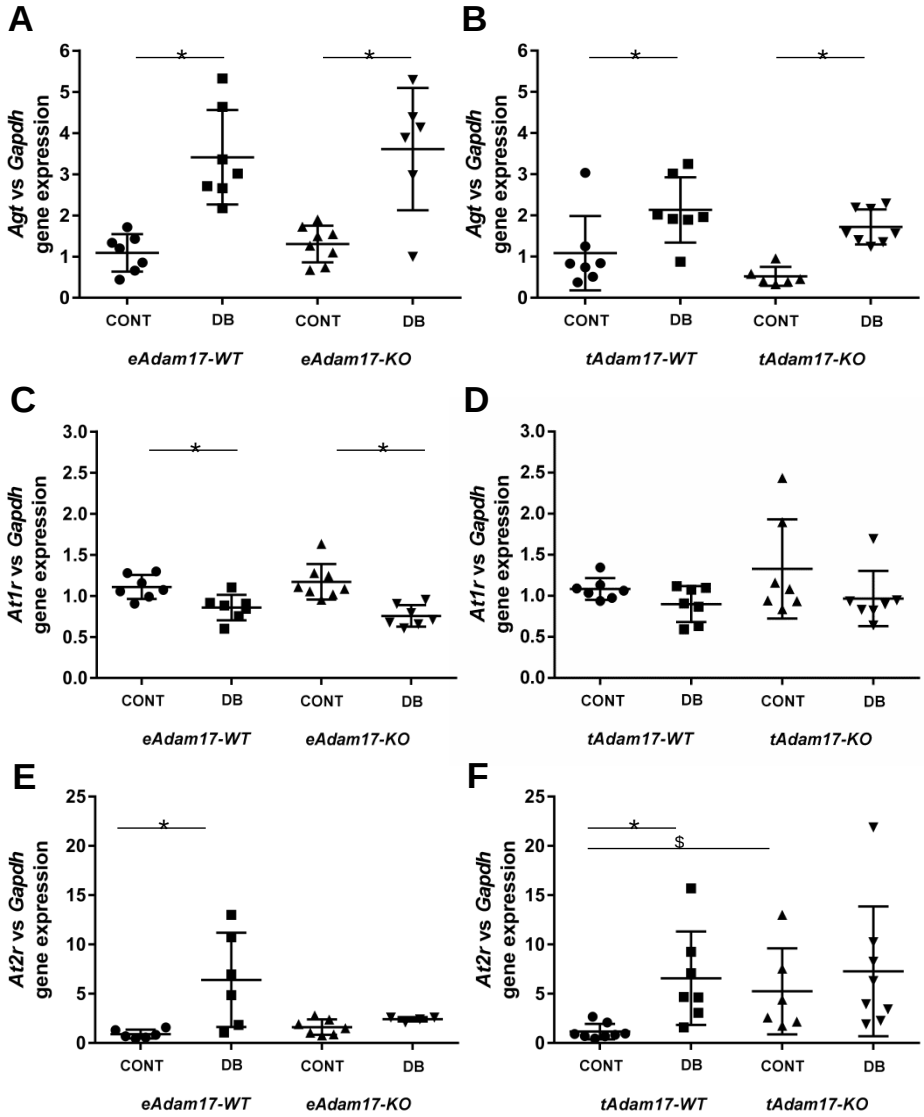

Figure 24: Influence of diabetes and endothelial or proximal tubular *Adam17* deletion on gene expression of the Renin Angiotensin System components. A) *Agt* gene expression on *eAdam17* mice. B) *Agt* gene expression on *tAdam17* mice. C) *At1r* gene expression on *eAdam17* mice. D) *At1r* gene expression on *tAdam17* mice. E) *At2r* gene expression on *eADAM17* mice. F) *At2r* gene expression on *tAdam17* mice. Data are expressed as mean±SD. Abbreviations: *eAdam17*, endothelial *Adam17*; *tAdam17*, proximal tubular *Adam17*; CONT, control; WT, wild-type; DB, diabetic; KO, knockout; Agt, angiotensinogen, At1r, angiotensin II receptor 1; At2r, angiotensin II receptor 2; Gapdh, glyceraldehyde-3-phosphate dehydrogenase. *p<0.05 DB vs CONT, $ p<0.05 KO vs WT.

5.2.7 Role of ADAM17 and diabetes on renal inflammation

To evaluate whether *Adam17* deletion in endothelial or renal proximal tubular cells affects renal inflammation, we analysed the expression of TNF-α in mouse serum by ELISA and renal gene expression of different pro-inflammatory markers (*Tnf-α*, *Tnfr1*, *Tnfr2*, *Ccl2,* and *Ccl5*) by RT-qPCR technique.

Circulating TNF-α levels were significantly increased in diabetic wild-type mice as compared to controls. Interestingly, this rise was not observed in diabetic knockout mice. Moreover, among diabetic animals, *eAdam17-* and *tAdam17-KO mice exhibited* significantly decreased TNF-α levels as compared with diabetic wild-type mice (Figure 25).

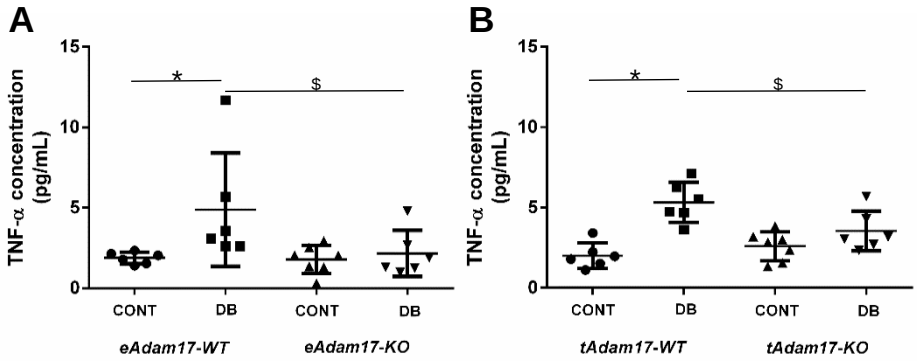

Figure 25: Influence of diabetes and endothelial or proximal tubular *Adam17* deletion on circulating TNF-α levels. A) Circulating TNF-α levels on *eAdam17* mice. B) Circulating TNF-α levels on *tAdam17* mice. Data are expressed as mean±SD. Abbreviations: *eAdam17*, endothelial *Adam17*; *tAdam17*, proximal tubular *Adam17*; CONT, control; WT, wild-type; DB, diabetic; KO, knockout; TNF-α, tumour necrosis factor alpha. *p<0.05 DB vs CONT, $ p<0.05 KO vs WT.

As depicted in Figure 26, hyperglycaemia was accompanied by a significant increase in *Tnf-α*, *Tnfr1* and *Tnfr2* mRNA levels. Interestingly, diabetic *eAdam17KO* mice presented decreased *Tnf-α* and increased *Tnfr1* gene expression as compared with *eAdam17WT* mice (Figure 26A,C).

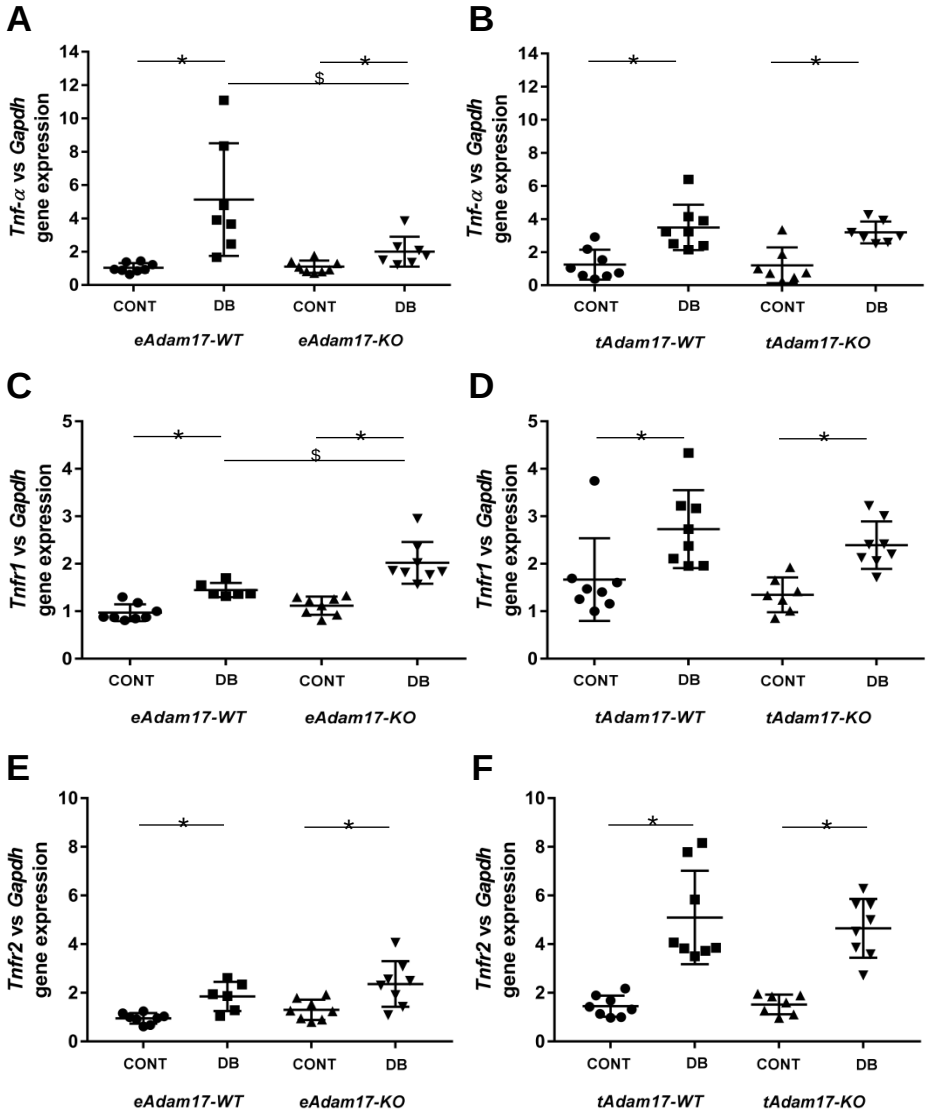

Figure 26: Influence of diabetes and endothelial or proximal tubular *Adam17* deletion on *Tnf-α*, *Tnfr1* and *Tnfr2* gene expression. A) *Tnf-α* gene expression on *eAdam17* mice. B) *Tnf-α* gene expression on *tAdam17* mice. C) *Tnfr1* gene expression on *eAdam17* mice. D) *Tnfr1* gene expression on *tAdam17* mice. E) *Tnfr2* gene expression on *eADAM17* mice. F) *Tnfr2* gene expression on *tAdam17* mice. Data are expressed as mean±SD. Abbreviations: *eAdam17*, endothelial *Adam17*; *tAdam17*, proximal tubular *Adam17*; CONT, control; WT, wild-type; DB, diabetic; KO, knockout; Tnf-α, tumour necrosis factor alpha; Tnfr1, tumour necrosis factor alpha receptor 1; Tnfr2; tumour necrosis factor alpha receptor 2; Gapdh, glyceraldehyde-3-phosphate dehydrogenase. *p<0.05 DB vs CONT, $ p<0.05 KO vs WT.

A similar pattern was observed when studying chemokine (C-C motif) ligand 2 (*Ccl2*) and chemokine (C-C motif) ligand 5 (*Ccl5*) gene expression. While hyperglycaemia induced an increase in *Ccl2 and Ccl5* gene expression, *Adam17* deletion in endothelial cells attenuates *Ccl5* upregulation in diabetic mice (Figure 27).

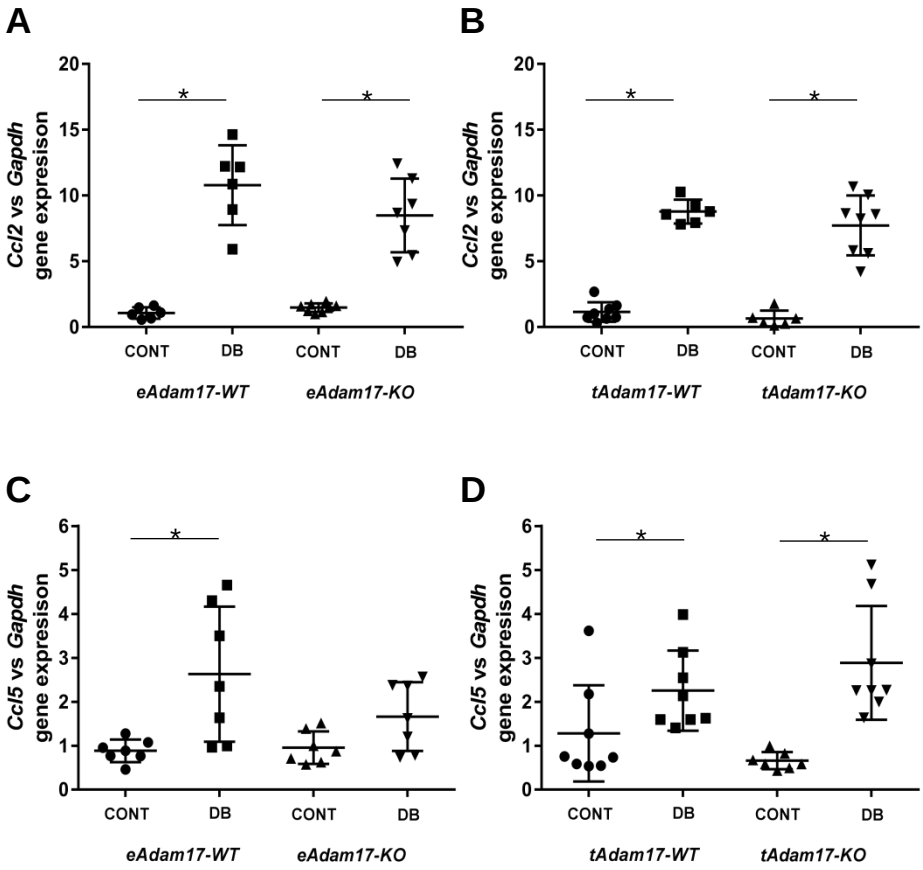

Figure 27: Influence of diabetes and endothelial or proximal tubular *Adam17* deletion on *Ccl2* and *Ccl5* gene expression. A) *Ccl2* gene expression on *eAdam17* mice. B) *Ccl2* gene expression on *tAdam17* mice. C) *Ccl5* gene expression on *eAdam17* mice. D) *Ccl5* gene expression on *tAdam17* mice. Data are expressed as mean±SD. Abbreviations: *eAdam17*, endothelial *Adam17*; *tAdam17*, proximal tubular *Adam17*; CONT, control; WT, wild-type; DB, diabetic; KO, knockout; Ccl2, C-C motif chemokine ligand 2; Ccl5, C-C motif chemokine ligand 5; Gapdh, glyceraldehyde-3-phosphate dehydrogenase. *p<0.05 DB vs CONT.

Our next aim was to determine macrophage infiltration in the kidney. Therefore, the expression of F4/80 was assessed by immunohistochemistry. All diabetic wild-type mice presented higher renal macrophage infiltration as compared with control mice. Interestingly, both endothelial and proximal tubular *Adam17* deletion reduced macrophage infiltration in diabetic mice compared with diabetic wild-type mice (Figure 28).

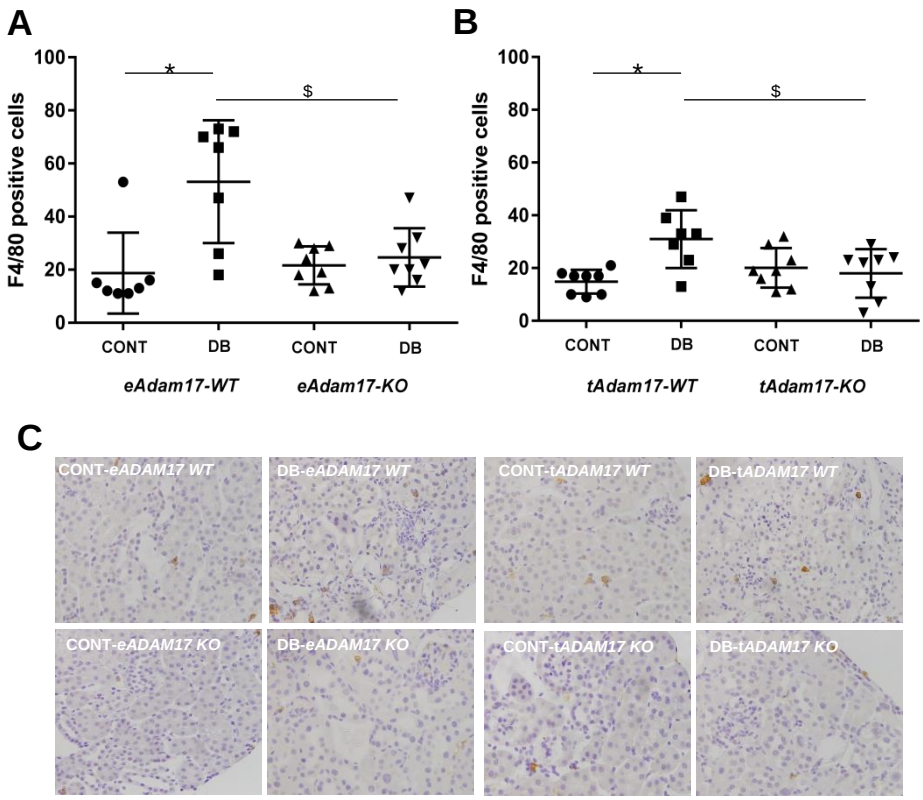

Figure 28: Influence of diabetes and endothelial or proximal tubular *Adam17* deletion on macrophage infiltration. A) F4/80 immunostaining on *eAdam17* mice. B) F4/80 immunostaining on *tAdam17* mice. C) Representative images of F4/80 immunostaining for each experimental group. Original magnification x20. Data are expressed as mean±SD. Abbreviations: *eAdam17*, endothelial *Adam17*; *tAdam17*, proximal tubular *Adam17*; CONT, control; WT, wild-type; DB, diabetic; KO, knockout. *p<0.05 DB vs CONT, $ p<0.05 KO vs WT.

5.2.8 Role of ADAM17 and diabetes on renal fibrosis

To assess whether abrogating *Adam17* ameliorates renal fibrosis, gene expression for different fibrotic markers related to the EGFR signalling pathway was performed. To get started, *Tgf-α* and *Hb-egf* gene expression were analysed as substrates of the EGFR signalling pathway. Although hyperglycaemia induced upregulation of *Tgf-α* gene expression (Figure 29A,B), no differences were observed between groups on *Hb-egf* gene expression (Figure 29C,D).

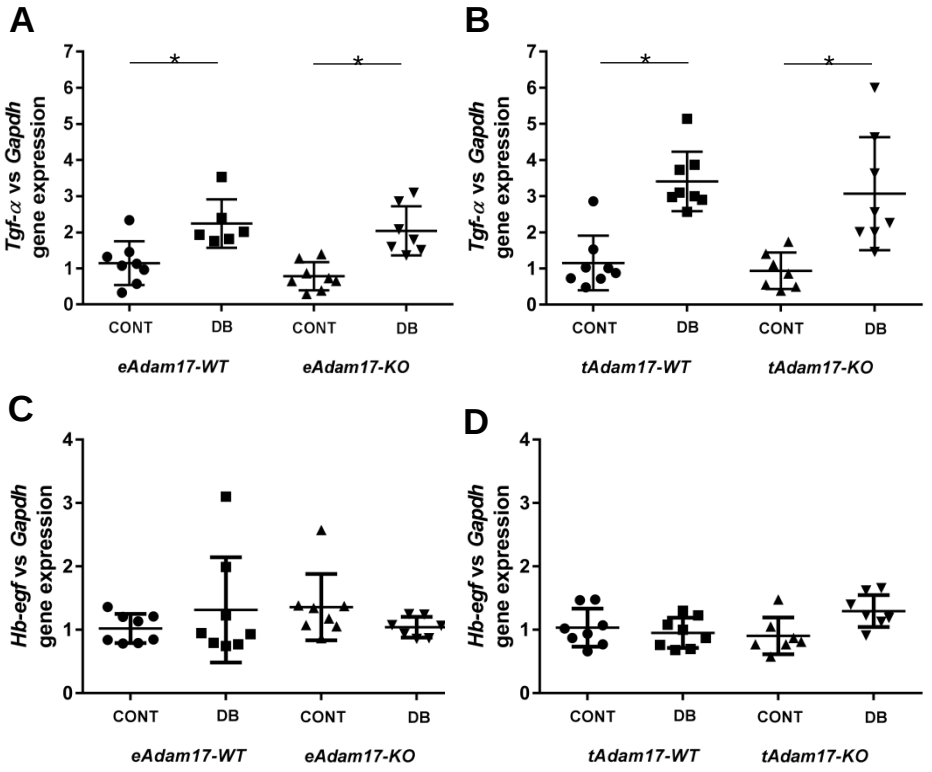

Figure 29: Influence of diabetes and endothelial or proximal tubular *Adam17* deletion on EGFR substrates gene expression. A) *Tgf-α* gene expression on *eAdam17* mice. B) *Tgf-α* gene expression on *tAdam17* mice. C) *Hb-egf* gene expression on *eAdam17* mice. D) *Hb-egf* gene expression on *tAdam17* mice. Data are expressed as mean±SD. Abbreviations: *eAdam17*, endothelial *Adam17*; *tAdam17*, proximal tubular *Adam17*; CONT, control; WT, wild-type; DB, diabetic; KO, knockout; Tgf-α, transforming growth factor alpha; Hb-egf, heparin-binding EGF-like growth factor; Gapdh, glyceraldehyde-3-phosphate dehydrogenase. *p<0.05 DB vs CONT.

When analysing downstream effectors of the EGFR signalling pathway, we observed that *Tgf-β* gene expression was upregulated in diabetic mice except for the *eAdam17KO* mice. Interestingly, only endothelial *Adam17* deletion ameliorated diabetes effect on renal *Tgf-β* gene expression (Figure 30).

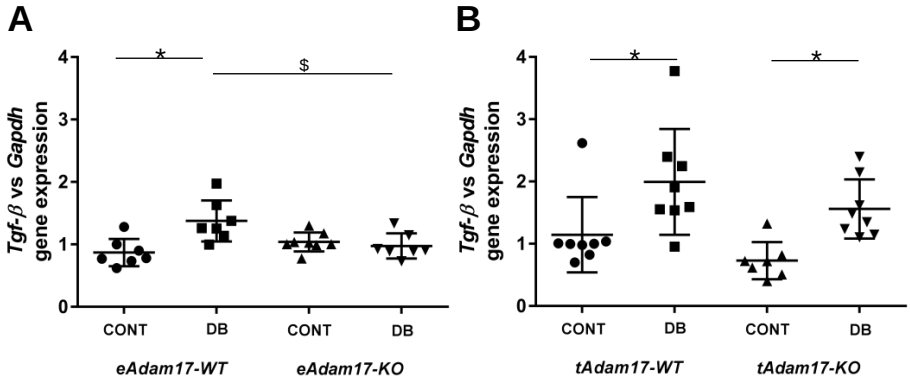

Figure 30: Influence of diabetes and endothelial or proximal tubular *Adam17* deletion on *Tgf-β* gene expression. A) *Tgf-β* gene expression on *eAdam17* mice. B) *Tgf-β* gene expression on *tAdam17* mice. Data are expressed as mean±SD. Abbreviations: *eAdam17*, endothelial *Adam17*; *tAdam17*, proximal tubular *Adam17*; CONT, control; WT, wild-type; DB, diabetic; KO, knockout; Tgf-β, transforming growth factor beta; Gapdh, glyceraldehyde-3-phosphate dehydrogenase. *p<0.05 DB vs NoDB. *p<0.05 DB vs CONT, $ p<0.05 KO vs WT.

When considering protein expression, only diabetic wild-type mice exhibited increased TGF-β (Figure 31). Surprisingly, diabetic *eAdam17KO* mice presented lower TGF-β protein expression than control mice (Figure 31A). Moreover, both endothelial and proximal tubular *Adam17* deletion reduced or attenuated TGF-β production in diabetic mice (Figure 31A, B).

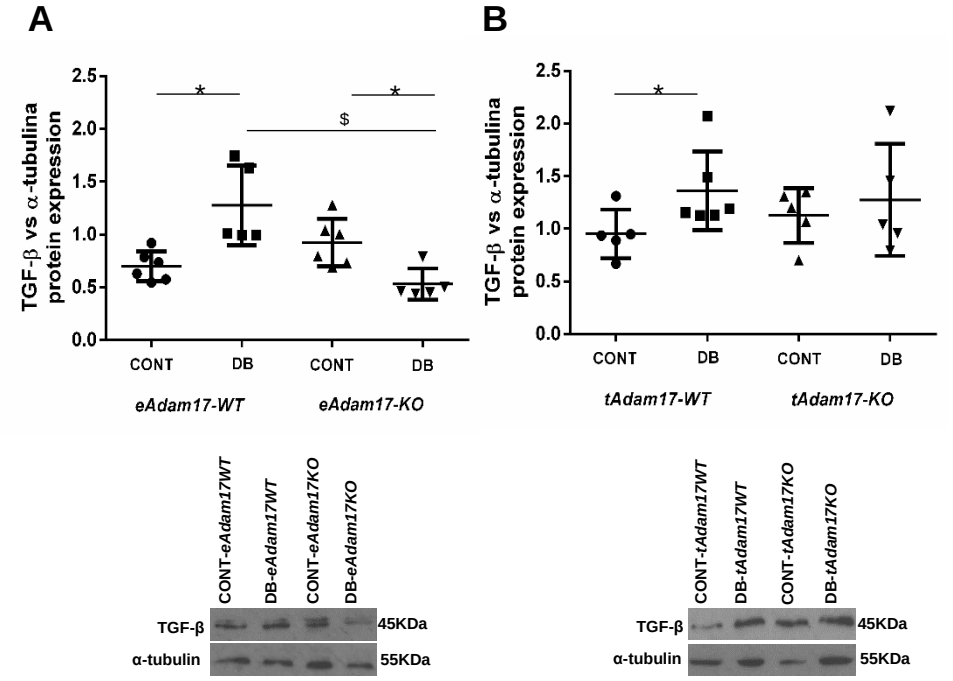

Figure 31: Influence of diabetes and endothelial or proximal tubular *Adam17* deletion on *Tgf-β* protein expression. A) TGF-β protein expression on *eAdam17* mice. B) TGF-β protein expression on *tAdam17* mice. Data are expressed as mean±SD. Abbreviations: *eAdam17*, endothelial *Adam17*; *tAdam17*, proximal tubular *Adam17*; CONT, control; WT, wild-type; DB, diabetic; KO, knockout; Tgf-β, transforming growth factor beta; Gapdh, glyceraldehyde-3-phosphate dehydrogenase. *p<0.05 DB vs NoDB. *p<0.05 DB vs CONT, $ p<0.05 KO vs WT.

Real time-PCR assay also exhibited a remarkable increase in *type I collagen, type IV collagen* and *fibronectin* genes in diabetic mice (Figure 32). Again, *eAdam17* deletion attenuates diabetes effect on *type I collagen* (Figure 32A) and *fibronectin* gene expression (Figure 32E).

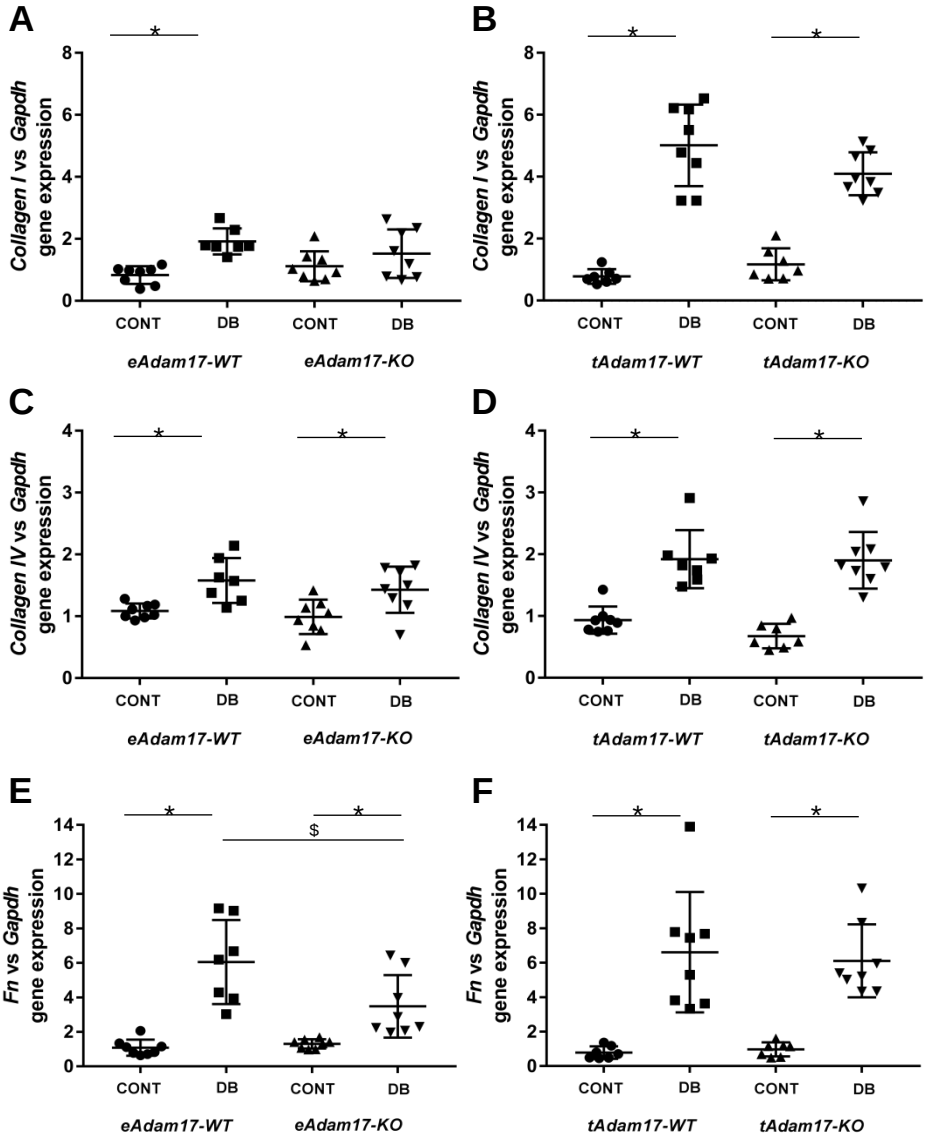

Figure 32: Influence of diabetes and endothelial or proximal tubular *Adam17* deletion on gene expression from different fibrotic markers. A) *Collagen I* gene expression on *eAdam17* mice. B) *Collagen I* gene expression on *tAdam17* mice. C) *Collagen IV* gene expression on *eAdam17* mice. D) *Collagen IV* gene expression on *tAdam17* mice. E) *Fn* gene expression on *eAdam17* mice. F) *Fn* gene expression on *tAdam17* mice. Data are expressed as mean±SD. Abbreviations: *eAdam17*, endothelial *Adam17*; *tAdam17*, proximal tubular *Adam17*; CONT, control; WT, wild-type; DB, diabetic; KO, knockout; Fn, fibronectin; Gapdh, glyceraldehyde-3-phosphate dehydrogenase. *p<0.05 DB vs CONT. *p<0.05 DB vs CONT, $ p<0.05 KO vs WT.

To gain insight into the role of *Adam17* deletion and diabetes on renal fibrosis, we examined cortical α-SMA expression and collagen depositions in the studied groups. As depicted in Figure 33, diabetes induced increased α-SMA accumulation in the interstitial compartment of both animal models. However, this effect of diabetes was lost on diabetic *eAdam17* knockout mice (Figure 33A). Interestingly, diabetic *tAdam17* knockout mice presented lower α-SMA staining in the renal cortex in comparison with diabetic wild-type mice (Figure 33B). Diabetic *eAdam17* knockout mice tended to decrease α-SMA staining in comparison with diabetic wild-type mice without reaching statistical significance (p=0.06).

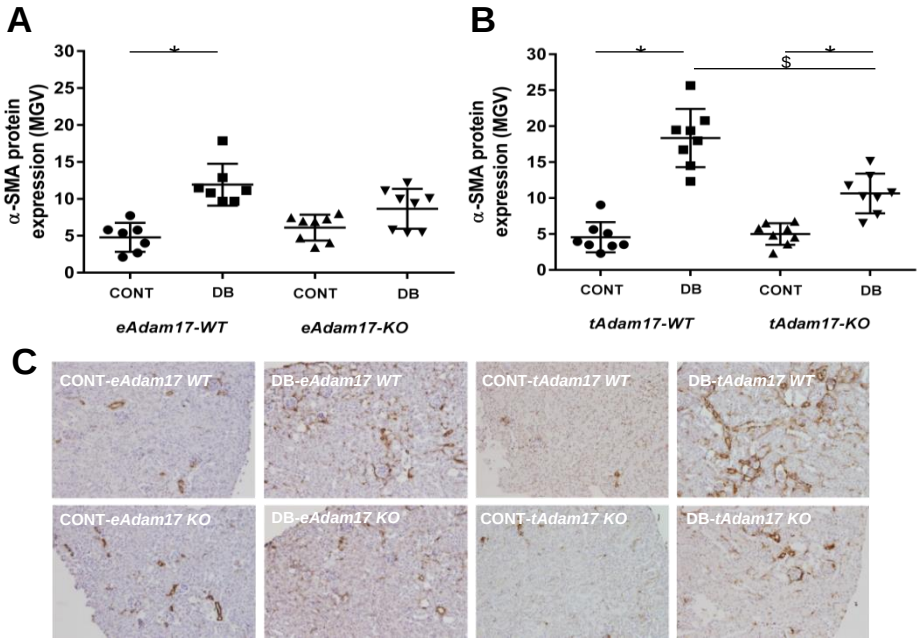

Figure 33: Influence of diabetes and endothelial or proximal tubular *Adam17* deletion on α-SMA immunostaining. A) α-SMA immunostaining on *eAdam17* mice. B) α-SMA immunostaining on *tAdam17* mice. C) Representative images of α-SMA immunostaining from all experimental groups. Original magnification x10. Data are expressed as mean±SD. Abbreviations: *eAdam17*, endothelial *Adam17*; *tAdam17*, proximal tubular *Adam17*; CONT, control; WT, wild-type; DB, diabetic; KO, knockout; α-SMA, alpha smooth muscle actin. *p<0.05 DB vs CONT. *p<0.05 DB vs CONT, $ p<0.05 KO vs WT.

In concordance with gene expression data, semiquantitative scoring of collagen deposition showed increased accumulation of collagen fibres in diabetic mice. In contrast to the gene expression profiles, protein levels of collagen were downregulated by endothelial and proximal tubular *Adam17* deletion in diabetic mice (Figure 34).

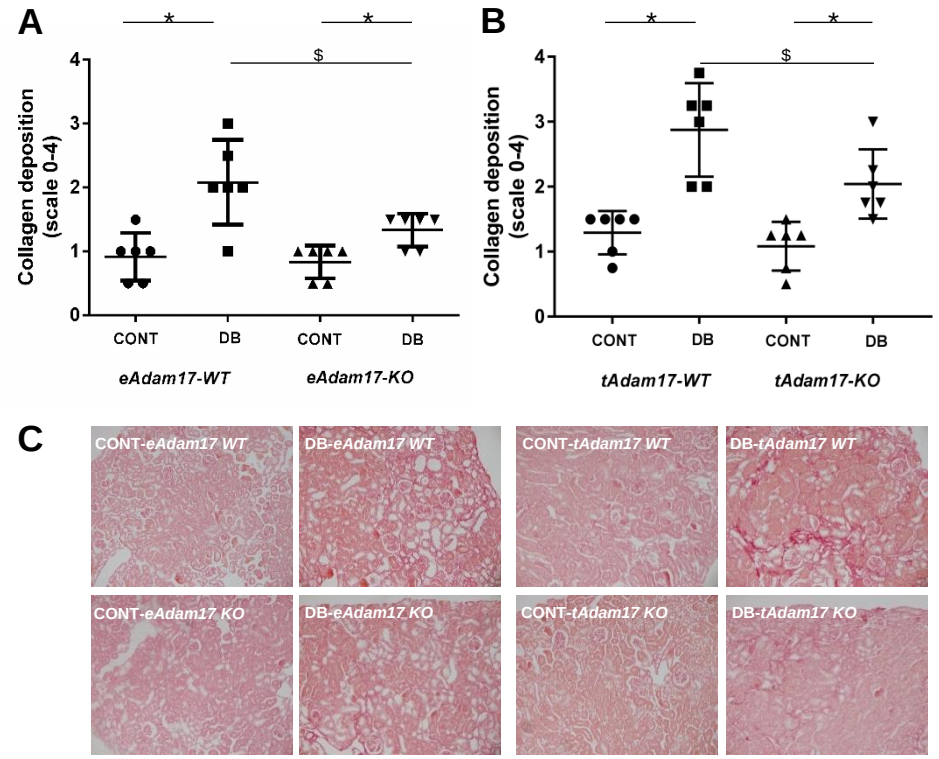

Figure 34: Influence of diabetes and endothelial or proximal tubular *Adam17* deletion on cortical collagen depositions. A) Collagen deposition on *eAdam17* mice. B) Collagen deposition on *tAdam17* mice. Picrosirius red staining was measured in a semiquantitative manner. C) Representative images of picrosirius red staining from all experimental groups. Original magnification x10. Data are expressed as mean±SD. Abbreviations: *eAdam17*, endothelial *Adam17*; *tAdam17*, proximal tubular *Adam17*; CONT, control; WT, wild-type; DB, diabetic; KO, knockout.*p<0.05 DB vs CONT, $ p<0.05 KO vs WT.

Afterwards, our goal was to study Akt protein expression, as an important signalling pathway related to cell growth and migration processes. PI3K/Akt are downstream signalling mediators of the EGFR

that have been demonstrated that are important in glucose-induced pro-fibrotic responses in the kidney (186). While all diabetic mice exhibited a significantly increased pAkt/Akt ratio in renal tissue, *eAdam17* deletion attenuated diabetes effect on pAkt/Akt ratio (Figure 35A). Instead, no effect of *tAdam17* deletion was observed, all diabetic mice exhibited an increased pAkt/Akt ratio (Figure 35B).

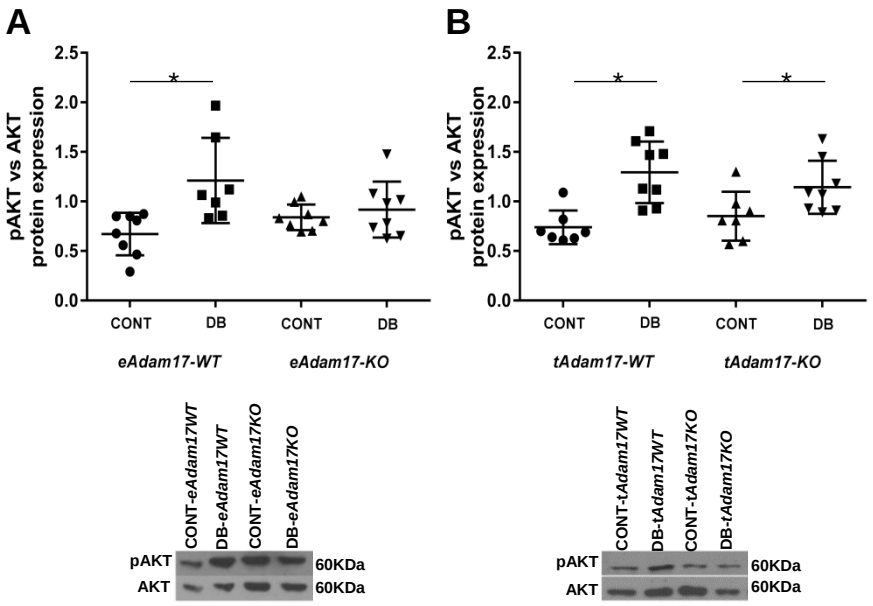

Figure 35: Influence of diabetes and endothelial or proximal tubular *Adam17* deletion on pAKT/AKT ratio. A) pAKT/AKT ratio on *eAdam17* mice. B) pAKT/AKT ratio on *tAdam17* mice. Results are expressed as a ratio of densitometry of pAKT and densitometry of AKT. Data are expressed as mean±SD. Abbreviations: *eAdam17*, endothelial *Adam17*; *tAdam17*, proximal tubular *Adam17*; CONT, control; WT, wild-type; DB, diabetic; KO, knockout; pAKT, phosphorylated protein kinase B; AKT, protein kinase B.*p<0.05 DB vs CONT.

5.3 *In vitro* study

5.3.1 *Adam17* deletion of HKC-8 spheroids

Adam17 gene was deleted on HKC-8 cells using the CRISPR/Cas9 technology. To select positive transfected cells, a cell sorting was performed. As depicted in Figure 36, GFP+ cells were selected by cell sorting as positive transfected cells.

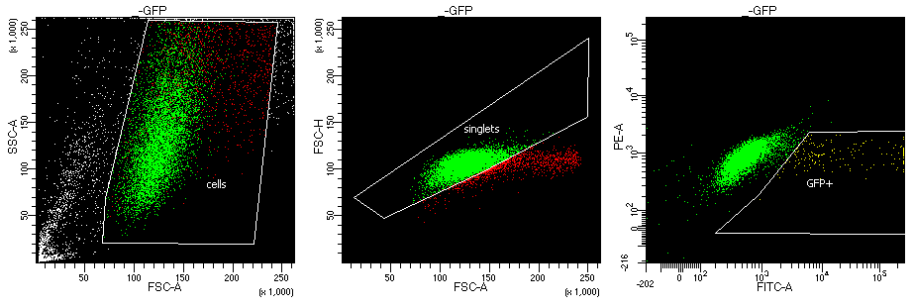

Figure 36: Cell-sorting images. Only GFP+ cells were selected as positive transfected cells and considered *Adam17* knockout. These cells were seeded for carrying out the experiments.

To confirm *Adam17* deletion in HKC-8 cells after CRISPR/Cas9 silencing and GFP+ sorting, we tested by immunoblotting the presence of ADAM17 in wild-type and knockout cells.

Protein analyses proved downregulation of *Adam17* in knockout cells. As shown in Figure 37, cells silenced with the CRISPR/Cas9 technique had significantly lower ADAM17 protein expression compared to wild-type cells.

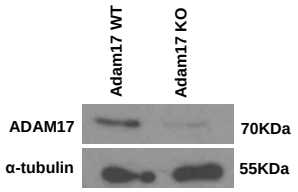

Figure 37: Immunoblotting for ADAM17 in HKC-8 cells. ADAM17 protein band appeared at 70KDa. α-tubulin was used as control for protein loading. Abbreviations: ADAM17, a disintegrin and metalloproteinase domain 17.

5.3.2 Developing an in vitro 3D human renal microenvironment

We developed a stepwise in vitro 3D co-culture system made up of one layer of polyethylene glycol (PEG)-crosslinked dextran hydrogels containing polarized human kidney tubular cell (HKC-8) spheroids. Upon seeding in dextran hydrogel the HKC-8 cells gathered to form cell aggregates. After 6 to 9 days, lumen formation in the spheroid core commenced and by day 12, the majority of structures contained a central hollow lumen surrounded by a uniform layer of columnar epithelium (Figure 38).

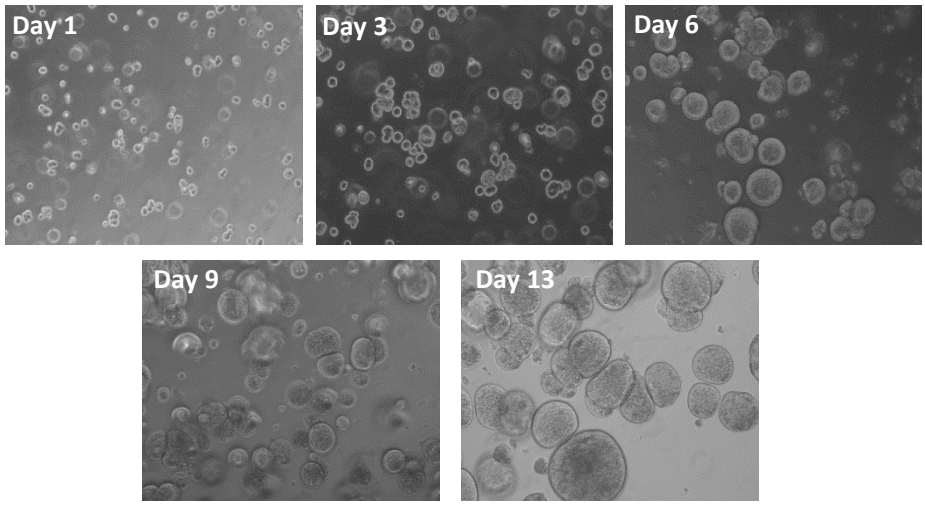

Figure 38: **Bright field images of single cell suspension HKC-8 cells seeded in dextran hydrogel forming HKC-8 spheroids after 13 days.** All images were taken at x10 magnification.

5.3.3 Confirmation of renal proximal tubular phenotype in HKC-8 spheroids.

To test the quality of the established 3D cell culture system, mature HKC-8 spheroids for the proximal tubular transporters, glucose transporter 1 (GLUT-1) and aquaporin 1 (AQP1), were assessed. The

spheroids expressed both markers supporting the proximal tubular phenotype (Figure 39).

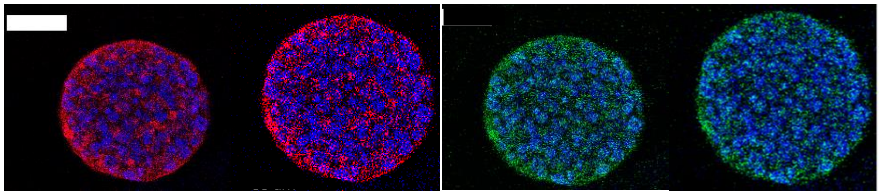

Figure 39: Functional characterization of HKC-8 spheroids. Immunofluorescence staining for GLUT1 (left panel, red) and AQP1 (right panel, green) in *Adam17* wild-type and knockout spheroids. Nuclei staining with DAPI are represented in blue. Scale bar 50µm.

5.3.4 Fibrosis is decreased in Adam17-deleted HKC-8 spheroids

To further analyse the effect of *Adam17* deletion on renal fibrosis in a diabetic microenvironment a 3D *in vitro* culture with HKC-8 incubated for 72h with LG, HG, or M resembling the in vivo human kidney diabetic microenvironment was performed.

In concordance with our results in mice, high glucose concentration induced α-SMA and type IV collagen accumulation. Interestingly, spheroids lacking *Adam17* presented lower α-SMA and type IV collagen expression compared with wild-type cells (Figure 40).

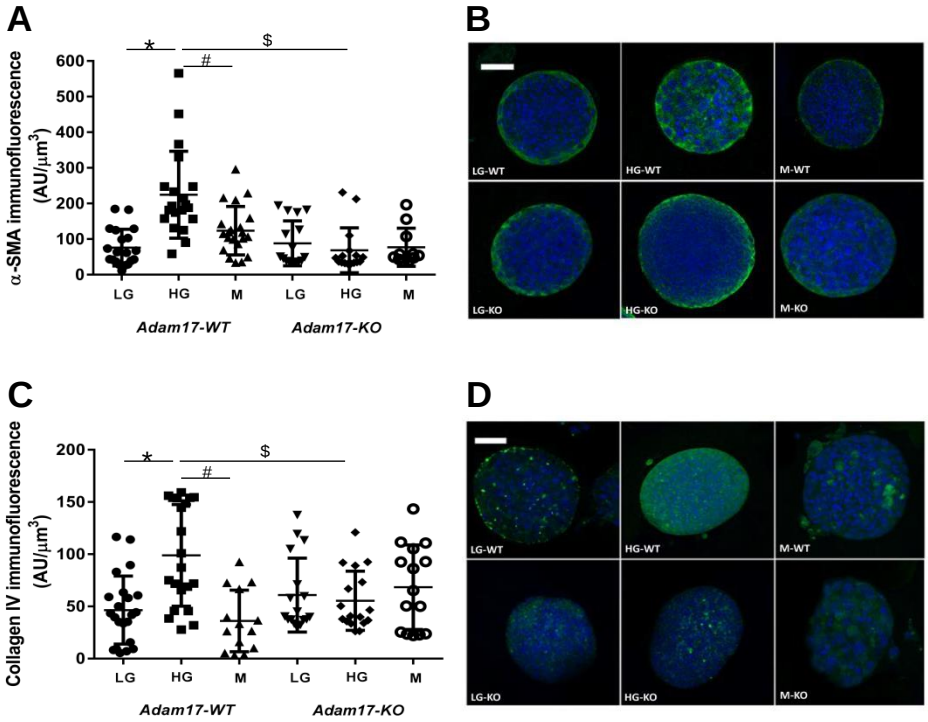

Figure 40: Influence of high glucose medium and *Adam17* deletion on α-SMA and collagen IV immunofluorescence staining. A) α-SMA immunofluorescence staining in HKC8 spheroids. B) Representative images of the α-SMA immunofluorescence staining. C) Type IV collagen immunofluorescence staining in HKC8 spheroids. D) Representative images of the type IV collagen immunofluorescence staining. Scale bar 50μm. Data are expressed as mean±SD. Abbreviations: α-SMA, alpha smooth muscle actin; LG, low glucose; HG, high glucose; M, mannitol; WT, wild-type; KO, knockout.*****p<0.05 HG vs LG, $p<0.05 KO vs WT, #p<0.05 M vs HG.

6. DISCUSSION

6. Discussion

Our study in humans, to our knowledge, is the first assessing circulating ADAMs activity in patients with CKD. We demonstrate that circulating ADAMs activity correlates with baseline renal function in CKD patients without previous history of CV disease. In addition, in non-dialysis patients, circulating ADAMs activity is a powerful predictor for CKD progression in male patients. Furthermore, circulating ADAMs activity is independently associated with CV events in CKD patients after 4 years of follow-up.

Our study has included a large sample size of CKD patients without previous history of CV disease. The study participants were enrolled from more than 80 Spanish centres, representing patients from various clinical settings. CKD5D patients were younger, thinner and had less prevalence of diabetes, hypertension and dyslipidaemia than CKD3-5 patients. This could be explained by an incidence-prevalence bias, since as renal dysfunction progresses, patients with worse CV disease have a lower possibility of staying free of CV events, and hence, of being recruited for the NEFRONA Study.

Previous studies in other pathologies, including Alzheimer's, autoimmune diseases, and atherosclerosis, were interested in circulating ADAMs activity (91,187,188). However, studies that addressed ADAMs activity in chronic kidney disease are lacking. Yet, an interest in ADAM17 expression, related to kidney disease, has been reported. Renal ADAM17 protein levels increased in acute and chronic kidney injury and stimulated TNFR and EGFR signalling pathways by releasing TNF-α and EGFR substrates into the circulation (130). As shown before, the binding of TNF-α and EGFR substrates to their receptors activate downstream signalling pathways that control

inflammatory, immune responses, apoptosis, and fibrosis (136,189,190).

Kefaloyianni *et al.* demonstrated that ADAM17 protein expression correlates positively with fibrotic markers such as α-SMA and collagen fibres in kidney biopsies from AKI and CKD patients. In addition, in urine from those patients, amphiregulin, TNFR1, and TGFα were upregulated as compared with controls. These results suggested that ADAM17 is involved in acute and chronic fibrotic kidney disease in humans by activating its main physiological downstream pathways, EGFR and TNFα/TNFR (130).

To our knowledge, we were the first to assess circulating ADAMs activity in plasma from CKD patients and controls with normal renal function. It is worth mentioning that the ADAMs activity that was detected includes mainly ADAM17 activity but also includes related enzymes such as ADAM8, ADAM9 and ADAM10. CKD patients presented higher circulating ADAMs activity than controls. Furthermore, patients in dialysis (CKD5D) presented higher circulating ADAMs activity as compared with CKD3-5 patients. These results demonstrated that circulating ADAMs activity progressively increases as renal function worsens. In agreement, Bertram *et al.* demonstrated that circulating ADAM17 protein level and activity are increased in patients with active ANCA-associated vasculitis, suggesting a model in which increased plasma ADAM17 correlates with enhanced proteolytic activity and disease progression (90). They determined circulating ADAM17 protein level by immunoassay and circulating ADAM17 activity by using a different fluorogenic substrate recognized by ADAM17, but also by ADAM10 and other MMPs (191). The increased circulating ADAM17 or

ADAMs in the setting of active ANCA-associated vasculitis and in advanced CKD may be related in part to its direct role in inflammation.

Interestingly, several studies focused on ADAM17 inhibition to prevent inflammation have been performed. Inhibition of ADAM17 by vitamin D prevents renal inflammatory and fibrotic lesions, along with systemic inflammation, with a potential effect on decreasing the risk of CV mortality (109). In agreement with those findings, previous studies of our group have demonstrated that paricalcitol, a vitamin D analogue, inhibits renal ADAM17 expression in an experimental model of type 1 diabetic nephropathy (98). Recently, in a mice model of microbial sepsis, Mishra *et al.* demonstrated that the blockage of ADAM17 using a monoclonal antibody reduced bacterial levels, increased the number of recruited neutrophils at sites of infection and provide higher resistance to sepsis (192). In line with these findings, previous studies of these group have shown that gene-targeting of ADAM17 in leukocytes reduced circulating cytokines and chemokines levels, increased neutrophil recruitment and bacterial clearance and decreased mortality during sepsis (193–195).

Early identification of CKD patients likely to progress to end-stage renal disease may become an important tool for daily clinical practice. Current measures including creatinine level, estimated GFR and proteinuria are not sufficient in order to detect patients at risk for CKD progression. Thus, for the last decade, there have been a lot of studies focused on finding new biomarkers of CKD progression, such as soluble TNF-like weak (sTWEAK), asymmetric dimethylarginine, symmetric dimethylarginine, uromodulin, kidney injury molecule-1, neutrophil gelatinase–associated lipocalin, and endotrophin (169,196,197). In our study, we demonstrate that baseline circulating

ADAMs activity correlates with baseline renal function in CKD patients. In addition, when CKD progression was prospectively studied after 2 years of follow-up, it has been shown that circulating ADAMs activity was significantly higher in patients with a ≥30% increase in serum creatinine levels and in patients that needed dialysis. Interestingly, we found an interaction between circulating ADAMs activity and sex for increasing serum creatinine, dialysis requirement and composite renal outcome. Consequently, circulating ADAMs activity was a marker for worsening renal function and dialysis initiation but only in males. These results suggested that inflammation is altered in CKD patients and may be a marker of its progression in males. According to these sex differences, within the NEFRONA study, it has been previous demonstrated that males had significantly increased ACE2 activity when compared with females in all studied groups (198). Other NEFRONA groups found that fasting serum phosphate levels within the normal range were strong predictors of the presence of atheromatous plaque in men with CKD3–5, suggesting that the association between serum phosphate levels and CV disease in CKD may be different according to sex (199).

Cardiovascular disease is the leading cause of morbidity and mortality in CKD patients (11,12,200). Several studies have demonstrated that ADAMs are associated with cardiovascular outcomes. The junctional molecules, vascular endothelial (VE)-cadherin and junctional adhesion molecule A, which play a crucial role in vascular permeability and leukocyte transmigration are ADAM10/17 substrates (201,202). Additionally, ADAM10/17 have been shown to shed the platelet receptors glycoprotein (GP) I and GPVI which are important in thrombus formation (203). Furthermore, both proteases have been proved to be involved in the cleavage of CX3CL1 and CXCL16, which

are chemotactic proteins. Intercellular adhesion molecule 1 (ICAM-1) and vascular cell adhesion molecule 1 (VCAM-1) are two other essential leukocyte adhesion molecules that can be shed by ADAM17 and are involved in the atherosclerotic lesion (204,205). Furthermore, many soluble forms of ADAMs substrates, like sICAM, sVCAM, sRAGE (receptor for advanced glycation end-products), sCD40L, sIL6R and TNFα, have been reported to correlate with clinical events of cardiovascular disease and were identified as potential biomarkers (206–208). In the NEFRONA population the combination of vascular calcification biomarkers (osteoprotegerin and osteopontin) and the inflammatory soluble tumour necrosis factor-like weak inducer of apoptosis (sTWEAK) have been associated with the risk of CV events in CKD patients. The combination of all of them demonstrated a good discriminative power, suggesting that marker combination would better stratify risk of CV events in CKD (209). In concordance with the sTWEAK finding, it has been demonstrated that circulating ADAMs activity is independently associated with CV events in CKD patients without a previous history of CV disease after 4 years of follow-up. In agreement with our results, Rizza *et al.* demonstrated a clear correlation between ADAM17 circulating substrates and second major cardiovascular events in human subjects with atherosclerosis; also suggesting that circulating ADAM17 activity predicts CV events in a population with a previous history of atherosclerosis (187).

In summary, this is the first time that circulating ADAMs activity was measured in CKD patients and associated with the presence of CV events, serum creatinine levels and dialysis therapy initiation. Therefore, circulating ADAMs activity is a promising predictor and a potential target for renal and CV events in CKD patients without a previous history of CV disease. If further confirmed, measurement of

circulating ADAMs activity could help clinicians to identify patients at risk of renal and CV events and help them to initiate strategies to prevent deleterious kidney and CV outcomes. It is worth mentioning that fluorescence resonance energy transfer (FRET) substrates, like the one used in our experiments, can be cleaved by multiple proteases. New methods such as proteolytic activity matrix analysis (PrAMA) allow determining the activities of particular enzymes in complex mixtures of MMPs and ADAMs. PrAMA method overcomes issues of non-specificity and allows the combined cleavage of multiple FRET substrates in parallel. The method distinguishes closely related enzymes from each other with high accuracy becoming a better option when analysing enzymatic activities (210–212).

Our experimental study in type 1 diabetic mice is, to our knowledge, the first analysing the effect of specific *Adam17* deletion on endothelial and renal proximal tubular cells in a STZ mice model. Moreover, we are the first to asses the effect of *Adam17* deletion in human kidney 3D spheroids incubated in medium containing high glucose concentration.

Previous studies have demonstrated that high glucose induces increase of ADAM17 protein expression in different renal cells, namely glomerular endothelial cells, mesangial cells, proximal tubular epithelial cells, and podocytes (129,131,132,148). Since endothelium dysfunction has been posited to play an important role in the pathogenesis of DN and renal proximal tubular cells also contribute to generating important kidney injury signals, we aimed to study the effect of conditional endothelial and renal proximal tubular *Adam17* deletion on type 1 diabetic mice. For this purpose, STZ-induced C57BL/6 mice were used as a model of DN. Many physiological, functional and histological

lesions of DN such as hyperglycaemia, albuminuria, and glomerular lesions have been reported in this animal model (154).

In the male mice used in our study, STZ administration led to hyperglycaemia, body weight loss, decrease in heart rate, renal hypertrophy, polyuria, albuminuria, and cortical fibrosis. However, as previously evidenced in studies carried out by our group (160,213), no differences between diabetic and non-diabetic male mice were observed on SBP and DBP after 19 weeks of follow-up. Interestingly, a slight reduction on SBP was detected after *tAdam17* deletion in diabetic mice as compared with wild-type mice. This suggests that these vasodilatory effects would be ascribed to different balance in RAS components in the *tAdam17KO* mice.

Determination of GFR is integral to the assessment of renal function. The use of sensitive radioisotopic methods is complicated by convenience and safety issues. For this reason, inulin has been widely used to determine GFR and it is considered a gold standard marker of glomerular filtration, being freely filtered and neither reabsorbed nor secreted by the tubules (214). FITC labelling of inulin has made it possible to detect minute quantities of inulin in blood from immobilized mice (215). In the present study FITC-inulin has been used to monitor GFR in conscious mice. Previous studies using STZ mice reported increased GFR in diabetic mice (160,177,213). However, Qi *et al.* demonstrated that the genetic background in inbred mouse strains significantly affects the progression of GFR. While some diabetic strains had an increase in GFR only during the first few weeks of diabetes, others maintained an increase in GFR until old age (153). These results could in part explain why we did not observed significant differences in the GFR between our diabetic and control mice at 19 weeks of

diabetes. Maybe the increased in GFR in diabetic mice occurred earlier and that could well explain why not significant changes have been detected. To confirm this hypothesis, GFR should have been measured at different time points. Interestingly, a significant reduction was observed in diabetic *eAdam17KO mice* compared with wild-type diabetic mice suggesting that endothelial *Adam17* deletion tend to prevent glomerular hyperfiltration in diabetic mice.

In humans, microalbuminuria is a major risk factor for progressive renal function decline in DN and is thought to be the first step in an inevitable progression to proteinuria and renal failure (216–218). Thus, reduction of albuminuria is a major target for renoprotective therapy in DN. Zhang *et al.* demonstrated a slight reduction in ACR levels in monotherapy with paricalcitol (219), an analogue of the active form of vitamin D with ADAM17 inhibition properties (98,220). In STZ-diabetic rats, treatment with paricalcitol and aliskiren lowered ACR compared to untreated diabetic rats (221). In contrast, our study showed that *Adam17* deletion either in endothelial or renal proximal tubular cells was unable to prevent albuminuria in the STZ model. The lack of effect on albuminuria in *Adam17* knockout mice might be ascribed to the huge ACR variability among animals in the same study group. Albuminuria is a determination that exerts a high deviation also in humans (222,223). In addition, in animals, the contamination with faeces and the collection method by morning urine spots increase its variability (224). Even so, a complete *Adam17* knockout model could help us to discern whether *Adam17* deletion prevents type 1 diabetic mice from developing proteinuria.

To determine cardiac hypertrophy, HW/BW ratio was evaluated. Endothelial *Adam17* deficiency caused an increase in the ratio HW/BW in both diabetic and non-diabetic mice. Wilson *et al.* were the first to

report cardiac defects in e*Adam17KO* mice. However, they described an increase in HW/BW due to an expansion of the left ventricle resulting in cardiomegaly. Ablation of *Adam17* in endothelial cells reduced the spectrum of cardiac defects (172).

Regarding renal hypertrophy, all diabetic mice presented a higher KW/BW ratio. Herein, we demonstrated that *tAdam17* deletion in diabetic mice reduced the KW/BW ratio which was compatible with reduced hypertrophy. These results are in concordance with previous studies from our group that demonstrated that paricalcitol administration decreased KW/BW in non-obese diabetic (NOD) mice (98). Moreover, Dusso *et al.* were among the first to demonstrate that paricalcitol administration can downregulate ADAM17 activity and protein expression in rat (109,220). Taken together, it is possible that either pharmacological inhibition or *Adam17* deletion may exert a protective effect in the diabetic kidney by attenuating renal hypertrophy.

At glomerular level, previous studies reported the presence of glomerular and mesangial matrix expansion when studying type 1 diabetic mice (213,225,226). Our histological analyses revealed glomerular alterations in diabetic mice due to an increase of the glomerular tuft area and mesangial expansion which were confirmed by an increase in mesangial index. Instead, after *eAdam17* and *tAdam17* deletion, diabetes-induced glomerular hypertrophy and mesangial matrix expansion were lost. These results suggested that tissue-specific deletion of *Adam17,* from either vascular endothelial cells or proximal tubular cells, protected glomeruli from diabetic deleterious effect. Several studies have described macrophage infiltration in the glomeruli of diabetic animals, which may contribute to the development of glomerular inflammation (227,228). In the same line, Bruneval *et al.*

have described macrophage infiltration in the glomeruli of ApoE knockout mice, a model of hypercholesterolemia. They presume that macrophage infiltration might be mediated by local activation of glomerular endothelial cells. These infiltrate macrophages could transform into foam cells, which may contribute to the development of the mesangial expansion observed in apoE null mice (229). In this sense, *Adam17* deletion in endothelial or proximal tubular cells may be protecting from mesangial expansion by decreasing glomerular inflammation in type 1 diabetic mice.

Our group and others have widely demonstrated podocyte loss in type 1 diabetic mice (150,157,160,230). In this line, in the current study, we observed a decrease in the number of podocytes in the glomeruli of all diabetic mice. Interestingly, Guo *et al.* described TNF-α as a key mediator of high glucose-activated macrophages to induce podocytes apoptosis (228). This may explain why we observed a decrease in podocyte loss in diabetic *tAdam17KO* mice. Blocking renal *Adam17* at a proximal tubular level might have induced a tubular-glomerular feedback recovery that lead to podocyte protection during DN by blocking TNF-α signalling. Moreover, Hasegawa *et al.* proved that molecular changes in proximal tubular cells affected contiguous cells including podocytes. In particular, specific deletion of Sirtuin-1 in proximal tubular cells of STZ mice led to a reduction of Sirtuin-1 and an increase in Claudin-1 levels in podocytes (231). Claudin-1 has been associated to podocyte effacement and albuminuria. Instead, Sirtuin-1 exerts anti-apoptotic effects on the kidney, protecting it against albuminuria and renal dysfunction in DN, preventing podocytes, endothelial cells, and tubular epithelial cells from dying and downregulating the expression of Claudin-1 (232).

ADAM17 plays an important role in the regulation of the renin angiotensin system. Within the RAS, ACE2 counterbalances the vasoconstrictor adverse effects of ANG II by converting it into ANG(1-7) (233). Several studies have explored the relationship between ACE2 and ADAM17 in experimental models of DN (99,104,105). Lambert *et al.* were the first to show an ACE2 proteolytic shedding occurring in the extracellular juxtamembrane region of human embryonic kidney cells (HEK293) and the release of an enzymatic active ectodomain (86). Moreover, Salem *et al.* demonstrated that in diabetic Akita mice, not only do ACE2 and ADAM17 colocalize in the apical site of the proximal tubule brush-border, but that urinary ACE2 and renal ADAM17 levels are increased as well. They proposed that elevated levels of urinary ACE2 observed in diabetic mice may be due to a rise in ectodomain shedding of renal ACE2 mediated by ADAM17 in the tubular membrane (104). These alterations on urinary ACE2 levels were attenuated after insulin treatment demonstrating that hyperglycaemia leads to ADAM17 upregulation and ACE2 shedding into the urine.

The increase in serum ACE2 activity in diabetes has been widely described (157,234–236). As expected, we observed increased circulating ACE2 activity in diabetic mice. Proximal tubular *Adam17* deletion decreased ACE2 circulating activity in diabetic mice demonstrating that in the absence of ADAM17 in the renal proximal tubule, less ACE2 ectodomain can be shed into the circulation. These results confirm that ACE2 origin is mainly tubular and maybe shed from the proximal tubule membrane resulting somehow in an increased circulating ACE2. In concordance, Riera *et al.* have previously demonstrated that paricalcitol administration in NOD mice results in significantly decreased circulating ACE2 activity in diabetic mice (98). Moreover, the same study described a reduction in SBP in the diabetic

mice, consistent with what was mentioned above about the positive effect of *tAdam17* deletion on SBP reduction. It should be pointed out that no differences were observed on circulating ACE2 activity when deleting endothelial *Adam17*. This may be related to the fact that probably distal and proximal tubular cells are contributing to ACE2 shedding into the circulation.

In concordance with previous studies (157,234,237), we observed that diabetic mice presented increased kidney ACE2 activity. This upregulation of ACE2 activity in renal cortex of diabetic mice could be a compensatory mechanism that might have a beneficial effect counterbalancing the deleterious effect of ANG II accumulation. This compensatory mechanism is in line with what we observed on *At1r* and *At2r* gene expression. Lower *At1r* and higher *At2r* gene expression in diabetic mice may be balancing ANG II accumulation. Interestingly, after *eAdam17* deletion, a further increase in renal ACE2 activity was detected in diabetic mice as compared with diabetic wild-type mice. These data suggested that because of diabetes, more ACE2 was produced at tubular level and, due to the deletion of endothelial *Adam17*, less ACE2 shedding occurred from the endothelium, resulting in ACE2 accumulation in the renal cortex. In contrast, *tAdam17* deletion attenuated the increase of renal ACE2 activity in diabetic mice. We surmise that *tAdam17* deletion attenuates ACE2 shedding leading to more ANG II degradation and, therefore, decreased activation of inflammatory signalling pathways in diabetic mice. The relation between ANG II and inflammation in the diabetic kidney has been widely described (238–241). Hence, we hypothesized that as the inflammatory state is attenuated, an increase on renal ACE2 activity is not required. For that reason, renal ACE2 activity in diabetic *tAdam17KO* mice is similar to the control group. These results demonstrated that the RAS

signalling in the renal cortex could be modulated by specific deletion of *Adam17*.

Hyperglycaemia stimulates inflammatory cells to release pro-inflammatory cytokines into the kidney leading to the recruitment of fibroblasts that will initiate the fibrotic process (147). ADAM17 is associated with the shedding of most pro-inflammatory and pro-fibrotic substrates, receptors, and enzymes (58,83,84). Thus, targeting the specific inflammatory and fibrotic pathways could be an effective approach for the management of DN. ADAM17 upregulation leads to the activation of TNFR and EGFR signalling pathways stimulating its substrates shedding and inducing protein matrix accumulation ending in renal inflammation and fibrosis (84,129,131,142). In agreement, we observed an increase in soluble TNF-α in diabetic wild-type mice that was reduced when a specifically deletion of *Adam17* at an endothelial or renal proximal tubular level was induced. These results suggested that blocking *Adam17* at a renal level during DN is sufficient to prevent TNF-α shedding and attenuate renal inflammation. When analysing gene expression, an increase on *Tnf-α*, *Tnfr1* and *Tnfr2* was observed in diabetic mice. In addition, *eAdam17* deletion decreased renal *Tnf-α* gene expression and increased *Tnfr1* gene expression in diabetic *eAdam17KO* mice. These results may be due to a possible negative feedback since the decreased in the release of TNF-α into the circulation could be well explained by the absence of ADAM17. In these circumstances, more TNFR1 may be needed to balance the downstream signalling pathway.

Omote *et al.* have shown increased renal macrophage infiltration in diabetic KK-Ay mice by counting F4/80-positive cells. This increase was attenuated after 8 weeks of etanercept treatment, an effective inhibitor

of TNF-α (242,243). In line with these results, we observed increased macrophage infiltration in the kidneys of diabetic wild-type mice. Instead, both *eAdam17* and *tAdam17* deletion reduced F4/80 immunostaining in diabetic mice as compared with diabetic wild-type mice. Additionally, *eAdam17KO* mice were protected against the increase of *Ccl5* gene expression, also known as RANTES, which encodes a protein with a potent chemoattractant effect for eosinophils, basophils, monocytes, effector memory T cells, B cells, NK cells, and immature dendritic cells. In agreement with our data, Kefaloyianni *et al.* showed a reduction on TNF-α cleavage that correlates with lower inflammatory markers, macrophages, and neutrophil infiltration in the kidney from total *Adam17KO* mice (130). This attenuation of inflammatory markers suggests that *Adam17* deletion ameliorates kidney inflammation by decreasing TNFR and EGFR signalling. Sustained chronic EGFR activation is a definitive feature of the fibrotic response after AKI and in CKD (124,130,244). ADAM17 releases the active ectodomains of EGFR ligands in injured renal proximal tubular cells. Accordingly, EGFR is persistently activated and induces the pro-inflammatory response favouring kidney fibrosis (113,130). EGFR ligands are found to be below-affinity (TGF-α, epiregulin, epigen, and amphiregulin) or high-affinity EGFR ligands (HG-EGF). However, only low-affinity EGFR ligands can be responsible for sustained profibrotic EGFR activation *in vivo* after kidney fibrosis (113). In concordance with those findings, we observed that diabetic mice presented higher renal *Tgf-α* gene expression but no differences were observed regarding *Hb-egf* gene expression demonstrating that only *Tgf-α* gene expression is upregulated due to our model of chronic diabetic nephropathy.

EGFR hyperactivation induces renal fibrosis by stimulating TGF-β signalling (122). Activation of the TGF-β signalling pathway favours

diabetic nephropathy progression through enhancing synthesis of collagen, fibronectin, and laminin and blocking matrix metalloproteinase-mediated extracellular matrix degradation. Hence, TGF-β contributes to extracellular matrix accumulation (245,246). *In vitro* experiments revealed that mesangial cells exposed to high glucose milieu increased ADAM17 expression and induced EGFR transactivation, resulting in renal fibrosis and TGF-β upregulation. Further, it has been demonstrated that EGFR transactivation and Akt phosphorylation are required for TGF-β upregulation by high glucose (143). In addition, the PI3K/Akt signalling pathway has been associated with collagen I production by mesangial cells and fibroblasts exposed to high glucose levels (142,143,247). Moreover, EGFR, Akt, TGF-β, FN and collagen I protein expression have been found to be upregulated in glomeruli in several experimental models of type 1 diabetes (122,142). In concordance, we also found increased *Tgf-β, Fn,* and collagen I gene expression and increased TGF-β and pAKT protein expression in diabetic mice. Also, increased collagen fibres accumulation was found in diabetic mice by Picrosirius red staining. Previous studies from Overstreet *et al.* showed that TGF-β protein expression in tubular epithelial cells decreased after erlotinib administration, an EGFR tyrosine kinase inhibitor (244). Furthermore, Chen *et al.* demonstrated that specific EGFR deletion in podocytes slowed down glomerular fibronectin accumulation by blocking TGF-β upregulation in type 1 diabetic mice (122). In line with these findings, we observed that only *eAdam17* deletion prevents the activation of pAKT and the upregulation of *Tgf-β, Fn,* and *collagen I* gene expression in the diabetic renal cortex. However, both *eAdam17* and *tAdam17* deletion protects against TGF-β and collagen accumulation in the diabetic kidney. It is worth mentioning that Picrosirius red staining could be used to differentiate between type

I, II and III collagens under polarized light microscope as every type of collagen is stained in a different colour (248,249). When analysing the Picrosirius red staining under light microscopy, all collagen fibres were seen in red (250). Type I and type III collagen are not normally synthesized in healthy kidneys, but together with type IV collagen, markedly increased in pathological conditions (251,252). Type III collagen has been associated with human glomerulopathies such as mesangial nodular and focal segmental glomerulosclerosis. However, type I collagen accumulation is widely accepted as a major component of fibrotic tissues (251,253). Considering this collagen distribution, we surmise that the collagen fibres observed in the diabetic kidney by Picrosirius red staining are mostly type I collagen fibres.

In normal adult kidney, the most abundant protein component of glomerular and tubular basement membranes is type IV collagen (251,254) and its production has been attributed predominantly to tubular epithelial cells (255,256). Xu *et al.* showed that type IV collagen and TGF-β gene and protein expression increased in type 1 diabetic mice while EGFR blocking reduced TGF-β and type IV collagen gene and protein expression (257). In this line, immunofluorescence on HKC-8 spheroids presented increased accumulation of type IV collagen when incubated with high glucose medium. Instead, *Adam17* deletion decreased type IV collagen in the spheroids incubated under high glucose conditions. These findings suggest that in *Adam17*-deleted spheroids, EGFR activation is reduced due to less shedding of the EGFR substrates. Hence, TGF-β signalling is downregulated and the HKC-8 produce less type IV collagen.

Persistent activation of the EGFR signalling pathway has been demonstrated to promote increased α-SMA immunostaining in

myofibroblasts, while genetic reduction of EGFR kinase activity hindered α-SMA accumulation (244). In this line, both *eAdam17* and *tAdam17* deletion prevents the accumulation of α-SMA in diabetic mice. In an experimental model of ischemia–reperfusion, Kefaloyianni *et al.* demonstrated that proximal tubular *Adam17* knockout mice presented lower α-SMA expression after kidney injury (113). Altogether, these results suggested that both endothelial and proximal tubular *Adam17* deletion could slow down renal fibrosis during DN. Immunofluorescence on HKC-8 spheroids reinforced those findings. Incubation of the spheroids with high glucose induced a significant increase in α-SMA staining. However, a significant decrease of this fibrotic marker was observed after *Adam17* deletion. These results strengthen the fact that proximal tubular *Adam17* deletion exerts a higher effect on blocking kidney fibrosis at a protein level.

In conclusion, this study shows that tissue-specific *Adam17* deletion protects against renal inflammation and/or fibrosis. Precisely, diabetic mice lacking specific endothelial *Adam17* displayed attenuated renal inflammation and ameliorated renal fibrosis. *Adam17* deletion in the renal proximal tubular cells of diabetic mice attenuated podocyte loss, RAS, renal inflammation and fibrosis in terms of macrophage infiltration, collagen and α-SMA accumulation. The results obtained when studying fibrotic markers on a renal proximal tubular 3D *in vitro* cell culture strengthen the animal findings. All things considered, these results suggest that the manipulation of *Adam17* should be considered as a therapeutic strategy for treating DN.

7. CONCLUSIONS

7. Conclusions

1. Baseline circulating ADAMs activity is increased in CKD3-5 patients and CKD5D patients without previous study of CV disease and is associated with baseline renal function and smoking.
2. The prospective study demonstrates an independent association between baseline ADAMs activity and CKD progression only in males at 2 years of follow-up. This suggests that ADAMs activity may serve as a biomarker to predict CKD progression in male patients.
3. Baseline ADAMs activity is associated to a higher risk of CV events at 4 years of follow-up.
4. In the animal model of type 1 diabetes, mice lacking endothelial *Adam17* display attenuated renal inflammation, ameliorated renal fibrosis, and consequently protection against DN.
5. In the animal model of type 1 diabetes, mice lacking proximal tubular *Adam17* display decreased podocyte loss, attenuated RAS, reduced macrophage infiltration, and reduced collagen and α-SMA accumulation, demonstrating protection against DN.
6. The 3D human kidney proximal tubular cells (HKC-8) model with *Adam17* deletion is a good model to reinforce animal findings. *Adam17* downregulation decreases α-SMA and type IV Collagen accumulation only when cultured cells were exposed to hyperglycaemic stimulus without the presence of any other cell type.

8. LIMITATIONS AND FUTURE PERSPECTIVES

8. Limitations and future perspectives

8.1 Limitations

In the clinical study, only patients without history of CV events were included in the NEFRONA project due to the study was aimed at primary prevention of CV events. Furthermore, a relatively low number of CV and renal events were reported during the follow-up which might limit the statistical power of our analysis. In addition, at a technical level, the fluorescent substrate that was used to analyse ADAMs activity is a fluorescence resonance energy transfer (FRET) substrate that can be cleaved by multiple proteases (ADAM17, ADAM10, ADAM8, and ADAM9). Interestingly, researchers have developed new methods with proteolytic activity matrix analysis (PrAMA) that overcomes issues of non-specificity and allows the combined cleavage of multiple FRET substrates in parallel (210–212).

In the animal model of DN, urine collection may be a limiting point in the determination of albuminuria. Although it seems that albuminuria tends to decrease in diabetic *eAdam17* knockout mice, it did not reach statistical significance, probably due to the high standard error observed. Collecting urine from metabolic cages instead from the morning urinary spot could be more informative.

Another limitation in the *in vivo* study is the use of FITC-inulin for GFR estimation. More accurate techniques can be used for the estimation of GFR in conscious mice. The use of FITC-sinistrin instead of FITC-inulin does not require prior dialysis, and would be advantageous as it can be measured transcutaneously by using a special miniaturized device.

8.2 Future perspectives

In this thesis circulating ADAMs activity has been proposed as a possible biomarker of CKD progression on male patients and of long-term CV events in CKD patients. Furthermore, experimental studies in a model of type 1 diabetic nephropathy have revealed that specific *Adam17* deletion in endothelial or renal proximal tubular cells protects from renal inflammation and fibrosis. Given the direct association between ADAM17 and kidney disease, future studies should be performed:

- To analyse circulating ADAM17 activity together with other possible biomarkers of CV disease (soluble TWEAK, phosphorus, osteoprotegerin, osteopontin…) in patients from the NEFRONA study to create a panel of biomarkers for CV disease in CKD patients.
- To evaluate the influence of sex on ADAM17 modulation and its relation with inflammatory and fibrotic markers in clinical and experimental models of CKD.
- To deepen in the TNFR and EGFR signalling pathways in experimental models of diabetes with upregulation or deprivation of ADAM17 to comprehend the complexity of ADAM17 effects in the diabetic kidney.
- To dissect the role of ADAM17 in cell death in order to elucidate if ADAM17 is directly associated with alterations in apoptotic or necrotic pathways in experimental models of DN.

9. BIBLIOGRAPHY

9. Bibliography

1. Levey AS, Coresh J. Chronic kidney disease. Lancet. 2012;379:165–80.

2. Levey AS, Atkins R, Coresh J, Cohen EP, Collins AJ, Eckardt KU, et al. Chronic kidney disease as a global public health problem: Approaches and initiatives - A position statement from Kidney Disease Improving Global Outcomes. Kidney Int. 2007;72:247–59.

3. Bikbov B, Purcell CA, Levey AS, Smith M, Abdoli A, Abebe M, et al. Global, regional, and national burden of chronic kidney disease, 1990–2017: a systematic analysis for the Global Burden of Disease Study 2017. Lancet. 2020;395:709–33.

4. Zoccali C, Blankestijn PJ, Bruchfeld A, Capasso G, Fliser D, Fouque D, et al. Children of a lesser god: Exclusion of chronic kidney disease patients from clinical trials. Nephrol Dial Transplant. 2019;34:1112–4.

5. National Kidney Foundation. K/DOQI clinical practice guidelines for chronic kidney disease: evaluation, classification, and stratification. Am J Kidney Dis. 2002;39:1–266.

6. Group KDIGO (KDIGO) CW. KDIGO 2012 Clinical Practice Guideline for the Evaluation and Management of Chronic Kidney Disease. Kidney International Supplements. 2013;3:1–150.

7. Ricardo SD, Van Goor H, Eddy AA. Macrophage diversity in renal injury and repair. J Clin Invest. 2008;118:3522–30.

8. Eddy AA. Progression in chronic kidney disease. Adv Chronic Kidney Dis. 2005;12:353–65.

9. Vielhauer V, Kulkarni O, Reichel CA, Anders HJ. Targeting the recruitment of monocytes and macrophages in renal disease. Semin Nephrol. 2010;30:318–33.

10. Hodgkins KS, Schnaper HW. Tubulointerstitial injury and the progression of chronic kidney disease. Pediatr Nephrol. 2012;27:901–9.

11. Gregg EW, Garfield S, Cheng YJ, Geiss L, Saydah S, Barker L, et al. Trends in death rates among U.S. adults with and without diabetes between 1997 and 2006: Findings from the National Health Interview Survey. Diabetes Care. 2012;35:1252–7.

12. Ong KL, Cheung BMY, Man YB, Lau CP, Lam KSL. Prevalence, awareness, treatment, and control of hypertension among United States adults 1999-2004. Hypertension. 2007;49:69–75.

13. Zhang QL, Rothenbacher D. Prevalence of chronic kidney disease in population-based studies: Systematic review. BMC Public Health. 2008;8:117.

14. Jha V, Garcia-Garcia G, Iseki K, Li Z, Naicker S, Plattner B, et al. Chronic kidney disease: Global dimension and perspectives. Lancet. 2013;382:260–72.

15. Gross JL, de Azevedo MJ, Silveiro SP, Canani LH, Caramori ML, Zelmanovitz T. Diabetic nephropathy: diagnosis, prevention, and treatment. Diabetes Care. 2005;28:164–76.

16. Bermejo S, García-Carro C, Soler MJ. Diabetes and renal disease—should we biopsy? Nephrol Dial Transplant. 2019;gfz248.

17. Reutens AT. Epidemiology of Diabetic Kidney Disease. Med Clin North Am. 2013;97:1–18.

18. Shah L, Burgner A. Diabetic kidney disease. Nephrol Secrets Fourth Ed. 2019;209–15.

19. Gross JL, De Azevedo MJ, Silveiro SP, Canani LH, Caramori ML, Zelmanovitz T. Diabetic nephropathy: Diagnosis, prevention, and treatment. Diabetes Care. 2005;28:164–76.

20. Mora-Fernández C, Domínguez-Pimentel V, de Fuentes MM, Górriz JL, Martínez-Castelao A, Navarro-González JF. Diabetic kidney disease: From physiology to therapeutics. J Physiol. 2014;592:3997–4012.

21. Hasslacher CH, Ritz E, Wahl P, Michael C. Similar Risks of Nephropathy in Patients with Type I or Type II Diabetes Mellitus. Nephrol Dial Transplant. 1989;4:859–63.

22. Viberti G, Wheeldon NM. Microalbuminuria reduction with valsartan in patients with type 2 diabetes mellitus: A blood pressure-independent effect. Circulation. 2002;106:672–8.

23. Zelmanovitz T, Gerchman F, Balthazar AP, Thomazelli FC, Matos JD, Canani LH. Diabetic nephropathy. Diabetol Metab Syndr. 2009;1:10.

24. García-Carro C, Vergara A, Agraz I, Jacobs-Cachá C, Espinel E, Seron D, et al. The New Era for Reno-Cardiovascular Treatment in Type 2 Diabetes. J Clin Med. 2019;8:864.

25. Mogensen CE, Christensen CK, Vittinghus E. The stages in diabetic renal disease. With emphasis on the stage of incipient diabetic nephropathy. Diabetes. 1983;32:64–78.

26. Tervaert TWC, Mooyaart AL, Amann K, Cohen AH, Cook HT, Drachenberg CB, et al. Pathologic classification of diabetic nephropathy. J Am Soc Nephrol. 2010;21:556–63.

27. Fioretto P, Mauer M. Histopathology of Diabetic Nephropathy. Semin Nephrol. 2007;27:195–207.

28. Kim Y, Kleppel MM, Mauer SM, Michael AF, Butkowski R, Wieslander

J. Differential expression of basement membrane collagen chains in diabetic nephropathy. Am J Pathol. 1991;138:413–20.

29. Falk RJ, Scheinman JI, Mauer SM, Michael AF. Polyantigenic expansion of basement membrane constituents in diabetic nephropathy. Diabetes. 1983;32:34–9.

30. Harris RD, Steffes MW, Bilous RW, Sutherland DER, Mauer SM. Global glomerular sclerosis and glomerular arteriolar hyalinosis in insulin dependent diabetes. Kidney Int. 1991;40:107–14.

31. Stout LC, Kumar S, Whorton EB. Insudative lesions-Their pathogenesis and association with glomerular obsolescence in diabetes: A dynamic hypothesis based on single views of advancing human diabetic nephropathy. Hum Pathol. 1994;25:1213–27.

32. Anderson S, Jung FF, Ingelfinger JR. Renal renin-angiotensin system in diabetes: Functional, immunohistochemical, and molecular biological correlations. Am J Physiol - Ren Fluid Electrolyte Physiol. 1993;265:477–86.

33. Roscioni SS, Heerspink HJL, De Zeeuw D. The effect of RAAS blockade on the progression of diabetic nephropathy. Nat Rev Nephrol. 2014;10:77–87.

34. Navar LG. Intrarenal renin-angiotensin system in regulation of glomerular function. Curr Opin Nephrol Hypertens. 2014;23:38–45.

35. Peach MJ. Renin angiotensin system: Biochemistry and mechanisms of action. Physiol Rev. 1977;57:313–70.

36. Brewster UC, Perazella MA. The renin-angiotensin-aldosterone system and the kidney: Effects on kidney disease. Am J Med. 2004;116:263–72.

37. Ferrario CM. Role of angiotensin II in cardiovascular disease - Therapeutic implications of more than a century of research. JRAAS - J Renin-Angiotensin-Aldosterone Syst. 2006;7:3–14.

38. Kobori H, Nangaku M, Navar LG, Nishiyama A. The intrarenal renin-angiotensin system: From physiology to the pathobiology of hypertension and kidney disease. Pharmacol Rev. 2007;59:251–87.

39. Donoghue M, Hsieh F, Baronas E, Godbout K, Gosselin M, Stagliano N, et al. A Novel Angiotensin-Converting Enzyme-Related Carboxypeptidase (ACE2) Converts Angiotensin I to Angiotensin 1-9. Circ Res. 2000;87:1–9.

40. Eriksson U, Danilczyk U, Penninger JM. Just the beginning: Novel functions for angiotensin-converting enzymes. Curr Biol. 2002;12:745–52.

41. Tipnis SR, Hooper NM, Hyde R, Karran E, Christie G, Turner AJ. A human homolog of angiotensin-converting enzyme: Cloning and functional expression as a captopril-insensitive carboxypeptidase. J Biol Chem. 2000;275:33238–43.

42. Paul M, Mehr AP, Kreutz R. Physiology of local renin-angiotensin systems. Physiol Rev. 2006;86:747–803.

43. Santos RAS, Simoes e Silva AC, Maric C, Silva DMR, Machado RP, De Buhr I, et al. Angiotensin-(1-7) is an endogenous ligand for the G protein-coupled receptor Mas. Proc Natl Acad Sci U S A. 2003;100:8258–63.

44. Santos RAS, Ferreira AJ, Simões E Silva AC. Recent advances in the angiotensin-converting enzyme 2-angiotensin(1-7)-Mas axis. Exp Physiol. 2008;93:519–27.

45. Bindom SM, Lazartigues E. The sweeter side of ACE2: Physiological evidence for a role in diabetes. Mol Cell Endocrinol. 2009;302:193–202.

46. Palau V, Pascual J, Soler MJ, Riera M. Role of ADAM17 in kidney disease. Am J Physiol Physiol. 2019;317:333–42.

47. Li N, Zimpelmann J, Cheng K, Wilkins JA, Burns KD. The role of angiotensin converting enzyme 2 in the generation of angiotensin 1-7 by rat proximal tubules. Am J Physiol - Ren Physiol. 2005;288:353–62.

48. Lely AT, Hamming I, van Goor H, Navis GJ. Renal ACE2 expression in human kidney disease. J Pathol. 2004;204:587–93.

49. Hamming I, Cooper ME, Haagmans BL, Hooper NM, Korstanje R, Osterhaus ADME, et al. The emerging role of ACE2 in physiology and disease. J Pathol. 2007;212:1–11.

50. Ye M, Wysocki J, William J, Soler MJ, Cokic I, Batlle D. Glomerular Localization and Expression of Angiotensin-Converting Enzyme 2 and Angiotensin-Converting Enzyme: Implications for Albuminuria in Diabetes. J Am Soc Nephrol. 2006;17:3067–75.

51. Shaltout HA, Westwood BM, Averill DB, Ferrario CM, Figueroa JP, Diz DI, et al. Angiotensin metabolism in renal proximal tubules, urine, and serum of sheep: evidence for ACE2-dependent processing of angiotensin II. AJP Ren Physiol. 2006;292:82–91.

52. Blobel CP. ADAMs: Key components in egfr signalling and development. Nat Rev Mol Cell Biol. 2005;6:32–43.

53. Edwards DR, Handsley MM, Pennington CJ. The ADAM metalloproteinases. Mol Aspects Med. 2009;29:258–89.

54. Giebeler N, Zigrino P. A disintegrin and metalloprotease (ADAM): Historical overview of their functions. Toxins (Basel). 2016;8:122.

55. Klein T, Bischoff R. Active metalloproteases of the a disintegrin and metalloprotease (ADAM) family: Biological function and structure. J Proteome Res. 2011;10:17–33.

56. Kato T, Hagiyama M, Ito A. Renal ADAM10 and 17: Their Physiological and Medical Meanings. Front Cell Dev Biol. 2018;6:153.

57. Takeda S. ADAM and ADAMTS family proteins and snake venom metalloproteinases: A structural overview. Toxins (Basel). 2016;8:155.

58. Gooz M. ADAM-17: The enzyme that does it all. Crit Rev Biochem Mol Biol. 2010;45:146–69.

59. Reiss K, Ludwig A, Saftig P. Breaking up the tie: Disintegrin-like metalloproteinases as regulators of cell migration in inflammation and invasion. Pharmacol Ther. 2006;111:985–1006.

60. Greene J, Wang M, Liu YE, Raymond LA, Rosen C, Shi YE. Molecular cloning and characterization of human tissue inhibitor of metalloproteinase 4. J Biol Chem. 1996;271:30375–80.

61. Docherty AJP, Lyons A, Smith BJ, Wright EM, Stephens PE, Harris TJR, et al. Sequence of human tissue inhibitor of metalloproteinases and its identity to erythroid-potentiating activity. Nature. 1985;318:66–9.

62. Pavloff N, Staskus PW, Kishnani NS, Hawkes SP. A new inhibitor of metalloproteinases from chicken: ChIMP-3. A third member of the TIMP family. J Biol Chem. 1992;267:17321–6.

63. Stetler-Stevenson WG, Brown PD, Onisto M, Levy AT, Liotta LA. Tissue inhibitor of metalloproteinases-2 (TIMP-2) mRNA expression in tumor cell lines and human tumor tissues. J Biol Chem. 1990;265:13933–8.

64. Brew K, Nagase H. The tissue inhibitors of metalloproteinases (TIMPs): An ancient family with structural and functional diversity. Biochim Biophys Acta - Mol Cell Res. 2010;1803:55–71.

65. Murphy G. Tissue inhibitors of metalloproteinases. Genome Biol. 2011;12:233.

66. Fassina G, Ferrari N, Brigati C, Benelli R, Santi L, Noonan D, et al. Tissue inhibitors of metalloproteases: Regulation and biological activities. Clin Exp Metastasis. 2000;18:111–20.

67. Huang W. Enhanced Expression of Tissue Inhibitor of Metalloproteinases-4 Gene in Human Osteoarthritic Synovial Membranes and Its Differential Regulation by Cytokines in Chondrocytes. Open Rheumatol J. 2011;5:81–7.

68. Amour A, Hutton M, Knäuper V, Slocombe PM, Webster A, Butler M, et al. Inhibition of the metalloproteinase domain of mouse TACE. Ann N Y Acad Sci. 1999;878:728–31.

69. Jacobsen J, Visse R, Sørensen HP, Enghild JJ, Brew K, Wewer UM, et al. Catalytic properties of ADAM12 and its domain deletion mutants. Biochemistry. 2008;47:537–47.

70. Amour A, Knight CG, Webster A, Slocombe PM, Stephens PE, Knäuper V, et al. The in vitro activity of ADAM-10 is inhibited by TIMP-1 and TIMP-3. FEBS Lett. 2000;473:275–9.

71. Poindexter K, Castner BJ, Means G, Copeland NG, Gilbert DJ, Jenkins NA, et al. Characterization of the cDNA and gene for mouse tumour necrosis factor α converting enzyme (TACE/ADAM17) and its location to mouse chromosome 12 and human chromosome 2p25. Cytokine. 1999;11:541–51.

72. Hirohata S, Seldin MF, Apte SS. Chromosomal assignment of two ADAM genes, TACE (ADAM17) and MLTNB (ADAM19), to human chromosomes 2 and 5, respectively, and of Mltnb to mouse chromosome 11. Genomics. 1998;54:178–9.

73. Niu A, Wang B, Li YP. TNFα Shedding in Mechanically Stressed Cardiomyocytes is Mediated by Src Activation of TACE. J Cell Biochem. 2015;116:559–65.

74. Ohtsu H, Dempsey PJ, Eguchi S. ADAMs as mediators of EGF receptor transactivation by G protein-coupled receptors. Am J Physiol - Cell Physiol. 2006;291:1–10.

75. Xu J, Mukerjee S, Cristiane CR, Carvalho-Galvão A, Cruz JC, Balarini CM, et al. A disintegrin and metalloprotease 17 in the cardiovascular and central nervous systems. Front Physiol. 2016;7:469.

76. Patel IR, Attur MG, Patel RN, Stuchin SA, Abagyan RA, Abramson SB, et al. TNF-α convertase enzyme from human arthritis-affected cartilage: Isolation of cDNA by differential display, expression of the active enzyme, and regulation of TNF-α. J Immunol. 1998;160:4570–9.

77. Gilles S, Zahler S, Welsch U, Sommerhoff CP, Becker BF. Release of TNF-α during myocardial reperfusion depends on oxidative stress and is prevented by mast cell stabilizers. Cardiovasc Res. 2003;60:608–16.

78. Milla ME, Leesnitzer MA, Moss ML, Clay WC, Luke Carter H, Miller AB, et al. Specific sequence elements are required for the expression of functional tumor necrosis factor-α-converting enzyme (TACE). J Biol Chem. 1999;274:30563–70.

79. Tellier E, Canault M, Rebsomen L, Bonardo B, Juhan-Vague I, Nalbone G, et al. The shedding activity of ADAM17 is sequestered in lipid rafts. Exp Cell Res. 2006;312:3969–80.

80. Zhang Z, Kolls JK, Oliver P, Good D, Schwarzenberger PO, Joshi MS, et al. Activation of tumor necrosis factor-alpha-converting enzyme-mediated ectodomain shedding by nitric oxide. J Biol Chem.

2000;275:15839–44.

81. Xu P, Derynck R. Direct Activation of TACE-Mediated Ectodomain Shedding by p38 MAP Kinase Regulates EGF Receptor-Dependent Cell Proliferation. Mol Cell. 2010;37:551–66.

82. Black RA, Rauch CT, Kozlosky CJ, Peschon JJ, Slack JL, Wolfson MF, et al. A metalloproteinase disintegrin that releases tumour-necrosis factor-α from cells. Nature. 1997;385:729–33.

83. Giricz O, Calvo V, Peterson EA, Abouzeid CM, Kenny PA. TACE-dependent TGFα shedding drives triple-negative breast cancer cell invasion. Int J Cancer. 2013;133:2587–95.

84. Menghini R, Fiorentino L, Casagrande V, Lauro R, Federici M. The role of ADAM17 in metabolic inflammation. Atherosclerosis. 2013;228:12–7.

85. Schlöndorff J, Becherer JD, Blobel CP. Intracellular maturation and localization of the tumour necrosis factor α convertase (TACE). Biochem J. 2000;347:131–8.

86. Lambert DW, Yarski M, Warner FJ, Thornhill P, Parkin ET, Smith AI, et al. Tumor necrosis factor-α convertase (ADAM17) mediates regulated ectodomain shedding of the severe-acute respiratory syndrome-coronavirus (SARS-CoV) receptor, angiotensin-converting enzyme-2 (ACE2). J Biol Chem. 2005;280:30113–9.

87. Caescu CI, Jeschke GR, Turk BE. Active-site determinants of substrate recognition by the metalloproteinases TACE and ADAM10. Biochem J. 2009;424:79–88.

88. Tucher J, Linke D, Koudelka T, Cassidy L, Tredup C, Wichert R, et al. LC-MS based cleavage site profiling of the proteases ADAM10 and ADAM17 using proteome-derived peptide libraries. J Proteome Res. 2014;13:2205–14.

89. Peschon JJ, Slack JL, Reddy P, Stocking KL, Sunnarborg SW, Lee DC, et al. An essential role for ectodomain shedding in mammalian development. Science (80-). 1998;282:1281–4.

90. Bertram A, Lovric S, Engel A, Beese M, Wyss K, Hertel B, et al. Circulating ADAM17 Level Reflects Disease Activity in Proteinase-3 ANCA-Associated Vasculitis. J Am Soc Nephrol. 2015;26:2860–70.

91. Sun Q, Hampel H, Blennow K, Lista S, Levey A, Tang B, et al. Increased plasma TACE activity in subjects with mild cognitive impairment and patients with Alzheimer's disease. J Alzheimers Dis. 2014;41:877–86.

92. Scharfenberg F, Helbig A, Sammel M, Benzel J, Schlomann U, Peters F, et al. Degradome of soluble ADAM10 and ADAM17 metalloproteases. Cell Mol Life Sci. 2020;77:331–50.

93. Briso EM, Dienz O, Rincon M. Cutting Edge: Soluble IL-6R Is Produced by IL-6R Ectodomain Shedding in Activated CD4 T Cells. J Immunol. 2008;180:7102–6.

94. Hundhausen C, Roth A, Whalen E, Chen J, Schneider A, Long SA, et al. Enhanced T cell responses to IL-6 in type 1 diabetes are associated with early clinical disease and increased IL-6 receptor expression. Sci Transl Med. 2016;8:356ra119.

95. Patel VB, Clarke N, Wang Z, Fan D, Parajuli N, Basu R, et al. Angiotensin II induced proteolytic cleavage of myocardial ACE2 is mediated by TACE/ADAM-17: A positive feedback mechanism in the RAS. J Mol Cell Cardiol. 2014;66:167–76.

96. Lautrette A, Li S, Alili R, Sunnarborg SW, Burtin M, Lee DC, et al. Angiotensin II and EGF receptor cross-talk in chronic kidney diseases: A new therapeutic approach. Nat Med. 2005;11:867–74.

97. Xia H, Sriramula S, Chhabra KH, Lazartigues E. Brain angiotensin-converting enzyme type 2 shedding contributes to the development of neurogenic hypertension. Circ Res. 2013;113:1087–96.

98. Riera M, Anguiano L, Clotet S, Roca-Ho H, Rebull M, Pascual J, et al. Paricalcitol modulates ACE2 shedding and renal ADAM17 in NOD mice beyond proteinuria. Am J Physiol Physiol. 2016;310:534–46.

99. Chodavarapu H, Grobe N, Somineni HK, Salem ESB, Madhu M, Elased KM. Rosiglitazone Treatment of Type 2 Diabetic db/db Mice Attenuates Urinary Albumin and Angiotensin Converting Enzyme 2 Excretion. PLoS One. 2013;8:e62833.

100. Soro-Paavonen A, Gordin D, Forsblom C, Rosengard-Barlund M, Waden J, Thorn L, et al. Circulating ACE2 activity is increased in patients with type 1 diabetes and vascular complications. J Hypertens. 2012;30:375–83.

101. Mizuiri S, Aoki T, Hemmi H, Arita M, Sakai K, Aikawa A. Urinary angiotensin-converting enzyme 2 in patients with CKD. Nephrology. 2011;16:567–72.

102. Wang G, Lai FMM, Lai KB, Chow KM, Kwan CHB, Li KTP, et al. Urinary mRNA expression of ACE and ACE2 in human type 2 diabetic nephropathy. Diabetologia. 2008;51:1062–7.

103. Xiao F, Hiremath S, Knoll G, Zimpelmann J, Srivaratharajah K, Jadhav D, et al. Increased urinary angiotensin-converting enzyme 2 in renal transplant patients with diabetes. PLoS One. 2012;7:e37649.

104. Salem ESB, Grobe N, Elased KM. Insulin treatment attenuates renal ADAM17 and ACE2 shedding in diabetic Akita mice. Am J Physiol - Ren Physiol. 2014;306:629–39.

105. Somineni HK, Boivin GP, Elased KM. Daily exercise training protects against albuminuria and angiotensin converting enzyme 2 shedding in db/db diabetic mice. J Endocrinol. 2014;221:235–51.

106. Wysocki J, Garcia-Halpin L, Ye M, Maier C, Sowers K, Burns KD, et al. Regulation of urinary ACE2 in diabetic mice. Am J Physiol - Ren Physiol. 2013;305:600–11.

107. Liang Y, Deng H, Bi S, Cui Z, Lata A, Zheng D, et al. Urinary angiotensin converting enzyme 2 increases in patients with type 2 diabetic mellitus. Kidney Blood Press Res. 2015;40:101–10.

108. Gutta S, Grobe N, Kumbaji M, Osman H, Saklayen M, Li G, et al. Increased urinary angiotensin converting enzyme 2 and neprilysin in patients with type 2 diabetes. Am J Physiol Physiol. 2018;315:263–74.

109. Dusso A, Arcidiacono MV, Yang J, Tokumoto M. Vitamin D inhibition of TACE and prevention of renal osteodystrophy and cardiovascular mortality. J Steroid Biochem Mol Biol. 2010;121:193–8.

110. Xiao F, Zimpelmann J, Agaybi S, Gurley SB, Puente L, Burns KD. Characterization of angiotensin-converting enzyme 2 ectodomain shedding from mouse proximal tubular cells. PLoS One. 2014;9:e85958.

111. Grobe N, Di Fulvio M, Kashkari N, Chodavarapu H, Somineni HK, Singh R, et al. Functional and molecular evidence for expression of the renin angiotensin system and ADAM17-mediated ACE2 shedding in COS7 cells. Am J Physiol - Cell Physiol. 2015;308:767–77.

112. Göoz M. ADAM Proteases as Novel Therapeutic Targets in Chronic Kidney Disease. In: Göoz M, editor. Chronic Kidney Disease. Croatia: InTech; 2012. p. 3–12.

113. Kefaloyianni E, Raja MRK, Schumacher J, Muthu ML, Krishnadoss V, Waikar SS, et al. Proximal tubule-derived amphiregulin amplifies and integrates profibrotic EGF receptor signals in kidney fibrosis. J Am Soc Nephrol. 2019;30:2370–83.

114. Bonventre J V., Yang L. Cellular pathophysiology of ischemic acute kidney injury. J Clin Invest. 2011;121:4210–21.

115. Grgic I, Campanholle G, Bijol V, Wang C, Sabbisetti VS, Ichimura T, et al. Targeted proximal tubule injury triggers interstitial fibrosis and glomerulosclerosis. Kidney Int. 2012;82:172–83.

116. Liu J, Krautzberger AM, Sui SH, Hofmann OM, Chen Y, Baetscher M, et al. Cell-specific translational profiling in acute kidney injury. J Clin Invest. 2014;124:1242–54.

117. Bonventre J V., Zuk A. Ischemic acute renal failure: An inflammatory disease? Kidney Int. 2004;66:480–5.

118. Gohda T, Niewczas MA, Ficociello LH, Walker WH, Skupien J, Rosetti F, et al. Circulating TNF receptors 1 and 2 predict stage 3 CKD in type 1 diabetes. J Am Soc Nephrol. 2012;23:516–24.

119. Niewczas MA, Gohda T, Skupien J, Smiles AM, Walker WH, Rosetti F, et al. Circulating TNF receptors 1 and 2 predict ESRD in type 2 diabetes. J Am Soc Nephrol. 2012;23:507–15.

120. Gohda T, Maruyama S, Kamei N, Yamaguchi S, Shibata T, Murakoshi M, et al. Circulating TNF Receptors 1 and 2 Predict Mortality in Patients with End-stage Renal Disease Undergoing Dialysis. Sci Rep. 2017;7:43520.

121. Bryer MD, Redha R, Breyer JA. Segmental distribution of epidermal growth factor binding sites in rabbit nephron. Am J Physiol - Ren Fluid Electrolyte Physiol. 1990;259:553–8.

122. Chen J, Chen JK, Harris RC. EGF receptor deletion in podocytes attenuates diabetic nephropathy. J Am Soc Nephrol. 2015;26:1115–25.

123. Chen J, Chen J-K, Nagai K, Plieth D, Tan M, Lee T-C, et al. EGFR Signaling Promotes TGF -Dependent Renal Fibrosis. J Am Soc Nephrol. 2012;23:215–24.

124. Tang J, Liu N, Zhuang S. Role of epidermal growth factor receptor in acute and chronic kidney injury. Kidney Int. 2013;83:804–10.

125. Tang J, Liu N, Tolbert E, Ponnusamy M, Ma L, Gong R, et al. Sustained activation of EGFR triggers renal fibrogenesis after acute kidney injury. Am J Pathol. 2013;183:160–72.

126. Liu N, Guo J-K, Pang M, Tolbert E, Ponnusamy M, Gong R, et al. Genetic or Pharmacologic Blockade of EGFR Inhibits Renal Fibrosis. J Am Soc Nephrol. 2012;23:854–67.

127. Wang W, Koka V, Lan HY. Transforming growth factor-β and Smad signalling in kidney diseases. Nephrology. 2005;10:48–56.

128. Humphreys BD, Lin SL, Kobayashi A, Hudson TE, Nowlin BT, Bonventre J V., et al. Fate tracing reveals the pericyte and not epithelial origin of myofibroblasts in kidney fibrosis. Am J Pathol. 2010;176:85–97.

129. Melenhorst WB, Visser L, Timmer A, van den Heuvel MC, Stegeman CA, van Goor H. ADAM17 upregulation in human renal disease: a role in modulating TGF-α availability? Am J Physiol Physiol. 2009;297:781–90.

130. Kefaloyianni E, Muthu ML, Kaeppler J, Sun X, Sabbisetti V, Chalaris A, et al. ADAM17 substrate release in proximal tubule drives kidney fibrosis. JCI Insight. 2016;1:e87023.

131. Ford BM, Eid AA, Gooz M, Barnes JL, Gorin YC, Abboud HE. ADAM17 mediates Nox4 expression and NADPH oxidase activity in the kidney cortex of OVE26 mice. AJP Ren Physiol. 2013;305:323–32.

132. Lattenist L, Ochodnický P, Ahdi M, Claessen N, Leemans JC, Satchell SC, et al. Renal endothelial protein C receptor expression and shedding during diabetic nephropathy. J Thromb Haemost. 2016;14:1171–82.

133. Taniguchi K, Xia L, Goldberg HJ, Lee KWK, Shah A, Stavar L, et al. Inhibition of src kinase blocks high glucose-induced EGFR transactivation and collagen synthesis in mesangial cells and prevents diabetic nephropathy in mice. Diabetes. 2013;62:3874–86.

134. Sun L, Kanwar YS. Relevance of TNF-α in the context of other inflammatory cytokines in the progression of diabetic nephropathy. Kidney Int. 2015;88:662–5.

135. Lampropoulou IT, Stangou M, Papagianni A, Didangelos T, Iliadis F, Efstratiadis G. TNF- α and microalbuminuria in patients with type 2 diabetes mellitus. J Diabetes Res. 2014;2014:394206.

136. Al-Lamki RS, Mayadas TN. TNF receptors: Signaling pathways and contribution to renal dysfunction. Kidney Int. 2015;87:281–96.

137. Lai KN, Leung JCK, Chan LYY, Saleem MA, Mathieson PW, Lai FM, et al. Activation of podocytes by mesangial-derived TNF-α: Glomerulo-podocytic communication in IgA nephropathy. Am J Physiol - Ren Physiol. 2008;294:945–55.

138. Dong X, Swaminathan S, Bachman LA, Croatt AJ, Nath KA, Griffin MD. Resident dendritic cells are the predominant TNF-secreting cell in early renal ischemia-reperfusion injury. Kidney Int. 2007;71:619–28.

139. Chen J, Chen J-K, Harris RC. Angiotensin II Induces Epithelial-to-Mesenchymal Transition in Renal Epithelial Cells through Reactive Oxygen Species/Src/Caveolin-Mediated Activation of an Epidermal Growth Factor Receptor-Extracellular Signal-Regulated Kinase Signaling Pathway. Mol Cell Biol. 2012;32:981–91.

140. Sahin U, Weskamp G, Kelly K, Zhou HM, Higashiyama S, Peschon J, et al. Distinct roles for ADAM10 and ADAM17 in ectodomain shedding of six EGFR ligands. J Cell Biol. 2004;164:769–79.

141. Li R, Wang T, Walia K, Gao B, Krepinsky JC. Regulation of profibrotic responses by ADAM17 activation in high glucose requires its C-terminus and FAK. J Cell Sci. 2018;131:jcs208629.

142. Wu D, Peng F, Zhang B, Ingram AJ, Gao B, Krepinsky JC. Collagen I induction by high glucose levels is mediated by epidermal growth factor receptor and phosphoinositide 3-kinase/Akt signalling in mesangial cells. Diabetologia. 2007;50:2008–18.

143. Wu D, Peng F, Zhang B, Ingram AJ, Kelly DJ, Gilbert RE, et al. PKC- 1 Mediates Glucose-Induced Akt Activation and TGF- 1 Upregulation in Mesangial Cells. J Am Soc Nephrol. 2009;20:554–66.

144. Wu D, Peng F, Zhang B, Ingram AJ, Kelly DJ, Gilbert RE, et al. EGFR-PLCgamma1 signaling mediates high glucose-induced PKCbeta1-Akt activation and collagen I upregulation in mesangial cells. Am J Physiol Ren Physiol. 2009;297:822–34.

145. Li JH, Huang XR, Zhu HJ, Johnson R, Lan HY. Role of TGF-β signaling in extracellular matrix production under high glucose conditions. Kidney Int. 2003;63:2010–9.

146. Haneda M, Koya D, Isono M, Kikkawa R. Overview of glucose signaling in mesangial cells in diabetic nephropathy. J Am Soc Nephrol. 2003;14:1374–82.

147. Kanasaki K, Taduri G, Koya D. Diabetic nephropathy: The role of inflammation in fibroblast activation and kidney fibrosis. Front Endocrinol (Lausanne). 2013;4:1–15.

148. Li R, Uttarwar L, Gao B, Charbonneau M, Shi Y, Chan JSD, et al. High glucose up-regulates ADAM17 through HIF-1α in mesangial cells. J Biol Chem. 2015;290:21603–14.

149. Chow FY, Nikolic-Paterson DJ, Atkins RC, Tesch GH. Macrophages in streptozotocin-induced diabetic nephropathy: Potential role in renal fibrosis. Nephrol Dial Transplant. 2004;19:2987–96.

150. Wang W, Jiang S, Tang X, Cai L, Epstein PN, Cheng Y, et al. Sex differences in progression of diabetic nephropathy in OVE26 type 1 diabetic mice. Biochim Biophys Acta - Mol Basis Dis. 2020;1866:165589.

151. Chow FY, Nikolic-Paterson DJ, Ma FY, Ozols E, Rollins BJ, Tesch GH. Monocyte chemoattractant protein-1-induced tissue inflammation is critical for the development of renal injury but not type 2 diabetes in obese db/db mice. Diabetologia. 2007;50:471–80.

152. Awad AS, You H, Gao T, Cooper TK, Nedospasov SA, Vacher J, et al. Macrophage-derived Tumor Necrosis Factor-α mediates diabetic renal injury HHS Public Access. Kidney Int. 2015;88:722–33.

153. Qi Z, Fujita H, Jin J, Davis LS, Wang Y, Fogo AB, et al. Characterization of susceptibility of inbred mouse strains to diabetic nephropathy. Diabetes. 2005;54:2628–37.

154. Breyer MD, Böttinger E, Brosius FC, Coffman TM, Harris RC, Heilig CW, et al. Mouse models of diabetic nephropathy. J Am Soc Nephrol. 2005;16:27–45.

155. Kong LL, Wu H, Cui WP, Zhou WH, Luo P, Sun J, et al. Advances in

murine models of diabetic nephropathy. J Diabetes Res. 2013;2013:797548.

156. Makino S, Kunimoto K, Muraoka Y, Mizushima Y, Katagiri K, Tochino Y. Breeding of a non-obese, diabetic strain of mice. Exp Anim. 1980;29:1–13.

157. Riera M, Márquez E, Clotet S, Gimeno J, Roca-Ho H, Lloreta J, et al. Effect of insulin on ACE2 activity and kidney function in the non-obese diabetic mouse. PLoS One. 2014;9:e84683.

158. Szkudelski T. The mechanism of alloxan and streptozotocin action in B cells of the rat pancreas. Physiol Res. 2001;50:537–46.

159. Tesch GH, Allen TJ. Rodent models of streptozotocin-induced diabetic nephropathy. Nephrology. 2007;12:261–6.

160. Clotet S, Soler MJ, Rebull M, Gimeno J, Gurley SB, Pascual J, et al. Gonadectomy prevents the increase in blood pressure and glomerular injury in angiotensin-converting enzyme 2 knockout diabetic male mice. Effects on renin-angiotensin system. J Hypertens. 2016;34:1752–65.

161. Yoshioka M, Kayo T, Ikeda T, Koizumi A. A novel locus, Mody4, distal to D7Mit189 on chromosome 7 determines early-onset NIDDM in nonobese C57BL/6 (Akita) mutant mice. Diabetes. 1997;46:887–94.

162. Wang J, Takeuchi T, Tanaka S, Kubo SK, Kayo T, Lu D, et al. A mutation in the insulin 2 gene induces diabetes with severe pancreatic β-cell dysfunction in the Mody mouse. J Clin Invest. 1999;103:27–37.

163. Ron D. Proteotoxicity in the endoplasmic reticulum: Lessons from the Akita diabetic mouse. J Clin Invest. 2002;109:443–5.

164. Haseyama T, Fujita T, Hirasawa F, Tsukada M, Wakui H, Komatsuda A, et al. Complications of IgA nephropathy in a non-insulin-dependent diabetes model, the Akita mouse. Tohoku J Exp Med. 2002;198:233–44.

165. Gurley SB, Mach CL, Stegbauer J, Yang J, Snow KP, Hu A, et al. Influence of genetic background on albuminuria and kidney injury in Ins2+/C96Y(Akita) mice. Am J Physiol - Ren Physiol. 2010;298:788–95.

166. Epstein PN, Overbeek PA, Means AR. Calmodulin-induced early-onset diabetes in transgenic mice. Cell. 1989;58:1067–73.

167. Xu J, Huang Y, Li F, Zheng S, Epstein PN. FVB mouse genotype confers susceptibility to OVE26 diabetic albuminuria. Am J Physiol - Ren Physiol. 2010;299:487–94.

168. Zheng S, Noonan WT, Metreveli NS, Coventry S, Kralik PM, Carlson EC, et al. Development of late-stage diabetic nephropathy in OVE26 diabetic mice. Diabetes. 2004;53:3248–57.

169. Fernández-Laso V, Sastre C, Valdivielso JM, Betriu A, Fernández E, Egido J, et al. Soluble TWEAK and major adverse cardiovascular events in patients with CKD. Clin J Am Soc Nephrol. 2016;11:413–22.

170. Junyent M, Martínez M, Borrs M, Coll B, Valdivielso JM, Vidal T, et al. Predicting cardiovascular disease morbidity and mortality in chronic kidney disease in Spain. the rationale and design of NEFRONA: A prospective, multicenter, observational cohort study. BMC Nephrol. 2010;11:1–8.

171. Priu MJ, Martínez M, Borrás M, Betriu A, Coll B, Craver L, et al. Usefulness of imaging techniques and novel biomarkers in the prediction of cardiovascular risk in patients with chronic kidney disease in Spain: The NEFRONA project. Nefrologia. 2010;30:119–26.

172. Wilson CL, Gough PJ, Chang CA, Chan CK, Frey JM, Liu Y, et al. Endothelial deletion of ADAM17 in mice results in defective remodeling of the semilunar valves and cardiac dysfunction in adults. Mech Dev. 2013;130:272–89.

173. Claxton S, Kostourou V, Jadeja S, Chambon P, Hodivala-Dilke K, Fruttiger M. Efficient, inducible cre-recombinase activation in vascular endothelium. Genesis. 2008;46:74–80.

174. Batlle R, Alba-Castellón L, Loubat-Casanovas J, Armenteros E, Francí C, Stanisavljevic J, et al. Snail1 controls TGF-β responsiveness and differentiation of mesenchymal stem cells. Oncogene. 2013;32:3381–9.

175. Rankin EB, Tomaszewski JE, Haase VH. Renal cyst development in mice with conditional inactivation of the von Hippel-Lindau tumor suppressor. Cancer Res. 2006;66:2576–83.

176. Patel YM, Yun JS, Liu J, McGrane MM, Hanson RW. An analysis of regulatory elements in the phosphoenolpyruvate carboxykinase (GTP) gene which are responsible for its tissue-specific expression and metabolic control in transgenic mice. J Biol Chem. 1994;269:5619–28.

177. Qi Z, Whitt I, Mehta A, Jin J, Zhao M, Harris RC, et al. Serial determination of glomerular filtration rate in conscious mice using FITC-inulin clearance. Am J Physiol - Ren Physiol. 2004;286:590–6.

178. Mcmanus JFA. Histological and histochemical uses of periodic acid. Biotech Histochem. 1948;23:99–108.

179. Junqueira LCU, Bignolas G, Brentani RR. Picrosirius staining plus polarization microscopy, a specific method for collagen detection in tissue sections. Histochem J. 1979;11:447–55.

180. Gornall AG, Bardawill CJ, David MM. Determination of serum proteins by means of the biuret reaction. J Biol Chem. 1949;177:751–66.

181. Livak KJ, Schmittgen TD. Analysis of relative gene expression data

using real-time quantitative PCR and the 2-ΔΔCT method. Methods. 2001;25:402–8.

182. Benam KH, Dauth S, Hassell B, Herland A, Jain A, Jang K-J, et al. Engineered In Vitro Disease Models. Annu Rev Pathol Mech Dis. 2015;10:195–262.

183. Choi SH, Kim YH, Hebisch M, Sliwinski C, Lee S, D'Avanzo C, et al. A three-dimensional human neural cell culture model of Alzheimer's disease. Nature. 2014;515:274–8.

184. Nugraha B, Mohr MA, Ponti A, Emmert MY, Weibel F, Hoerstrup SP, et al. Monitoring and manipulating cellular crosstalk during kidney fibrosis inside a 3D in vitro co-culture. Sci Rep. 2017;7:14490.

185. Nilsson LM, Zhang L, Bondar A, Svensson D, Wernerson A, Brismar H, et al. Prompt apoptotic response to high glucose in SGLT-expressing renal cells. Am J Physiol - Ren Physiol. 2019;316:1078–89.

186. Rayego-Mateos S, Rodrigues-Diez R, Morgado-Pascual JL, Valentijn F, Valdivielso JM, Goldschmeding R, et al. Role of epidermal growth factor receptor (EGFR) and its ligands in kidney inflammation and damage. Mediators Inflamm. 2018;2018:8739473.

187. Rizza S, Copetti M, Cardellini M, Menghini R, Pecchioli C, Luzi A, et al. A score including ADAM17 substrates correlates to recurring cardiovascular event in subjects with atherosclerosis. Atherosclerosis. 2015;239:459–64.

188. Zhu H, Sun X, Zhu L, Hu F, Shi L, Li Z, et al. The expression and clinical significance of different forms of Mer receptor tyrosine kinase in systemic lupus erythematosus. J Immunol Res. 2014;2014:431896.

189. Speeckaert MM, Speeckaert R, Laute M, Vanholder R, Delanghe JR. Tumor necrosis factor receptors: Biology and therapeutic potential in kidney diseases. Am J Nephrol. 2012;36:261–70.

190. Zhuang S, Liu N. EGFR signaling in renal fibrosis. Kidney Int Suppl. 2014;4:70–4.

191. Neumann U, Kubota H, Frei K, Ganu V, Leppert D. Characterization of Mca-Lys-Pro-Leu-Gly-Leu-Dpa-Ala-Arg-NH2, a fluorogenic substrate with increased specificity constants for collagenases and tumor necrosis factor converting enzyme. Anal Biochem. 2004;328:166–73.

192. Mishra HK, Ma J, Mendez D, Hullsiek R, Pore N, Walcheck B. Blocking adam17 function with a monoclonal antibody improves sepsis survival in a murine model of polymicrobial sepsis. Int J Mol Sci. 2020;21:6688.

193. Long C, Wang Y, Herrera AH, Horiuchi K, Walcheck B. In vivo role of leukocyte ADAM17 in the inflammatory and host responses during E. coli -mediated peritonitis. J Leukoc Biol. 2010;87:1097–101.

194. Mishra HK, Johnson TJ, Seelig DM, Walcheck B. Targeting ADAM17 in leukocytes increases neutrophil recruitment and reduces bacterial spread during polymicrobial sepsis. J Leukoc Biol. 2016;100:999–1004.

195. Long C, Hosseinkhani MR, Wang Y, Sriramarao P, Walcheck B. ADAM17 activation in circulating neutrophils following bacterial challenge impairs their recruitment. J Leukoc Biol. 2012;92:667–72.

196. Rysz J, Gluba-Brzózka A, Franczyk B, Jablonowski Z, Cialkowska-Rysz A. Novel biomarkers in the diagnosis of chronic kidney disease and the prediction of its outcome. Int J Mol Sci. 2017;18:1702.

197. Rasmussen DGK, Fenton A, Jesky M, Ferro C, Boor P, Tepel M, et al. Urinary endotrophin predicts disease progression in patients with chronic kidney disease. Sci Rep. 2017;7:17328.

198. Anguiano L, Riera M, Pascual J, Valdivielso JM, Barrios C, Betriu A, et al. Circulating angiotensin-converting enzyme 2 activity in patients with chronic kidney disease without previous history of cardiovascular disease. Nephrol Dial Transplant. 2015;30:1176–85.

199. Martín M, Valls J, Betriu A, Fernández E, Valdivielso JM. Association of serum phosphorus with subclinical atherosclerosis in chronic kidney disease. Sex makes a difference. Atherosclerosis. 2014;241:264–70.

200. Sarnak MJ, Levey AS, Schoolwerth AC, Coresh J, Culleton B, Hamm LL, et al. Kidney Disease as a Risk Factor for Development of Cardiovascular Disease: A Statement From the American Heart Association Councils on Kidney in Cardiovascular Disease, High Blood Pressure Research, Clinical Cardiology, and Epidemiology and Prevention. Circulation. 2003;42:1050–65.

201. Koenen RR, Pruessmeyer J, Soehnlein O, Fraemohs L, Zernecke A, Schwarz N, et al. Regulated release and functional modulation of junctional adhesion molecule A by disintegrin metalloproteinases. Blood. 2009;113:4799–809.

202. Donners MMPC, Wolfs IMJ, Olieslagers S, Mohammadi-Motahhari Z, Tchaikovski V, Heeneman S, et al. A Disintegrin and Metalloprotease 10 is a novel mediator of vascular endothelial growth factor-induced endothelial cell function in angiogenesis and is associated with atherosclerosis. Arterioscler Thromb Vasc Biol. 2010;30:2188–95.

203. Matthews AL, Noy PJ, Reyat JS, Tomlinson MG. Regulation of A disintegrin and metalloproteinase (ADAM) family sheddases ADAM10 and ADAM17: The emerging role of tetraspanins and rhomboids. Platelets. 2017;28:333–41.

204. Garton KJ, Gough PJ, Philalay J, Wille PT, Blobel CP, Whitehead RH, et al. Stimulated shedding of vascular cell adhesion molecule 1 (VCAM-1) is mediated by tumor necrosis factor-α-converting enzyme (ADAM

17). J Biol Chem. 2003;278:37459–64.

205. Tsakadze NL, Sithu SD, Sen U, English WR, Murphy G, D'Souza SE. Tumor necrosis factor-α-converting enzyme (TACE/ADAM-17) mediates the ectodomain cleavage of Intercellular Adhesion Molecule-1 (ICAM-1). J Biol Chem. 2006;281:3157–64.

206. Demerath E, Towne B, Blangero J, Siervogel RM. The relationship of soluble ICAM-1, VCAM-1, P-selectin and E-selectin to cardiovascular disease risk factors in healthy men and women. Ann Hum Biol. 2001;28:664–78.

207. Lazo M, Halushka MK, Shen L, Maruthur N, Rebholz CM, Rawlings AM, et al. Soluble receptor for advanced glycation end products and the risk for incident heart failure: The Atherosclerosis Risk in Communities Study. Am Heart J. 2015;170:961–7.

208. Lobbes MBI, Lutgens E, Heeneman S, Cleutjens KBJM, Kooi ME, van Engelshoven JMA, et al. Is there more than C-reactive protein and fibrinogen?. The prognostic value of soluble CD40 ligand, interleukin-6 and oxidized low-density lipoprotein with respect to coronary and cerebral vascular disease. Atherosclerosis. 2006;187:18–25.

209. Bozic M, Méndez-Barbero N, Gutiérrez-Muñoz C, Betriu A, Egido J, Fernández E, et al. Combination of biomarkers of vascular calcification and sTWEAK to predict cardiovascular events in chronic kidney disease. Atherosclerosis. 2018;270:13–20.

210. Conrad C, Miller MA, Bartsch JW, Schlomann U, Lauffenburger DA. Simultaneous detection of metalloprotease activities in complex biological samples using the PrAMA (proteolytic activity matrix assay) method. Methods Mol Biol. 2017;1574:243–53.

211. Miller MA, Barkal L, Jeng K, Herrlich A, Moss M, Griffith LG, et al. Proteolytic Activity Matrix Analysis (PrAMA) for simultaneous determination of multiple protease activities. Integr Biol. 2011;3:422–38.

212. Yoneyama T, Gorry M, Miller MA, Gaither-Davis A, Lin Y, Moss ML, et al. Modification of proteolytic activity matrix analysis (PrAMA) to measure ADAM10 and ADAM17 sheddase activities in cell and tissue lysates. J Cancer. 2017;8:3916–32.

213. Clotet-Freixas S, Soler MJ, Palau V, Anguiano L, Gimeno J, Konvalinka A, et al. Sex dimorphism in ANGII-mediated crosstalk between ACE2 and ACE in diabetic nephropathy. Lab Investig. 2018;98:1237–49.

214. Gaspari F, Perico N, Remuzzi G. Measurement of glomerular filtration rate. Kidney Int Suppl. 1997;51:151–4.

215. Lorenz JN, Gruenstein E. A simple, nonradioactive method for evaluating single-nephron filtration rate using FITC-inulin. Am J Physiol - Ren Physiol. 1999;276:172–7.

216. Mogensen CE, Christensen CK. Predicting Diabetic Nephropathy in Insulin-Dependent Patients. N Engl J Med. 1984;311:89–93.

217. Viberti GC, Jarrett RJ, Keen H. Microalbuminuria as predictor of nephropathy in diabetics. Lancet. 1982;1:1430–2.

218. Perkins BA, Ficociello LH, Silva KH, Finkelstein DM, Warram JH, Krolewski AS. Regression of microalbuminuria in type 1 diabetes. N Engl J Med. 2003;348:2285–93.

219. Zhang Z, Zhang Y, Ning G, Deb DK, Kong J, Yan CL. Combination therapy with AT1 blocker and vitamin D analog markedly ameliorates diabetic nephropathy: Blockade of compensatory renin increase. Proc Natl Acad Sci U S A. 2008;105:15896–901.

220. Arcidiacono MV, Yang J, Fernandez E, Dusso A. The induction of C/EBP' 2 contributes to vitamin D inhibition of ADAM17 expression and parathyroid hyperplasia in kidney disease. Nephrol Dial Transplant. 2015;30:423–33.

221. Eren Z, Günal MY, Bakir EA, Coban J, Çałlayan B, Ekimci N, et al. Effects of paricalcitol and aliskiren combination therapy on experimental diabetic nephropathy model in rats. Kidney Blood Press Res. 2014;39:581–90.

222. Leong A, Ekinci EI, Nguyen C, Milne M, Hachem M, Dobson M, et al. Long-term intra-individual variability of albuminuria in type 2 diabetes mellitus: Implications for categorization of albumin excretion rate. BMC Nephrol. 2017;18:355.

223. Chadban S, Howell M, Twigg S, Thomas M, Jerums G, Cass A, et al. Assessment of kidney function in type 2 diabetes. Nephrology. 2010;15:S146–61.

224. Giralt-López A, Den Bosch MM Van, Vergara A, García-Carro C, Seron D, Jacobs-Cachá C, et al. Revisiting experimental models of diabetic nephropathy. Int J Mol Sci. 2020;21:3587.

225. Wong DW, Oudit GY, Reich H, Kassiri Z, Zhou J, Liu QC, et al. Loss of angiotensin-converting enzyme-2 (Ace2) accelerates diabetic kidney injury. Am J Pathol. 2007;171:438–51.

226. Oudit GY, Liu GC, Zhong JC, Basu R, Chow FL, Zhou J, et al. Human recombinant ACE2 reduces the progression of diabetic nephropathy. Diabetes. 2010;59:529–38.

227. Sassy-Prigent C, Heudes D, Mandet C, Bélair MF, Michel O, Perdereau B, et al. Early glomerular macrophage recruitment in streptozotocin-induced diabetic rats. Diabetes. 2000;49:466–75.

228. Guo Y, Song Z, Zhou M, Yang Y, Zhao Y, Liu B, et al. Infiltrating macrophages in diabetic nephropathy promote podocytes apoptosis via

TNF-α-ROS-p38MAPK pathway. Oncotarget. 2017;8:53276–87.

229. Bruneval P, Bariéty J, Bélair MF, Mandet C, Heudes D, Nicoletti A. Mesangial expansion associated with glomerular endothelial cell activation and macrophage recruitment is developing in hyperlipidaemic apoE null mice. Nephrol Dial Transplant. 2002;17:2099–107.

230. Xiao T, Guan X, Nie L, Wang S, Sun L, He T, et al. Rapamycin promotes podocyte autophagy and ameliorates renal injury in diabetic mice. Mol Cell Biochem. 2014;394:145–54.

231. Hasegawa K, Wakino S, Simic P, Sakamaki Y, Minakuchi H, Fujimura K, et al. Renal tubular sirt1 attenuates diabetic albuminuria by epigenetically suppressing claudin-1 overexpression in podocytes. Nat Med. 2013;19:1496–504.

232. Wang W, Sun W, Cheng Y, Xu Z, Cai L. Role of sirtuin-1 in diabetic nephropathy. J Mol Med. 2019;97:291–309.

233. Varagic J, Ahmad S, Nagata S, Ferrario CM. ACE2: Angiotensin II/angiotensin-(1-7) balance in cardiac and renal injury. Curr Hypertens Rep. 2014;16:420.

234. Wysocki J, Ye M, Soler MJ, Gurley SB, Xiao HD, Bernstein KE, et al. ACE and ACE2 activity in diabetic mice. Diabetes. 2006;55:2132–9.

235. Tikellis C, Bialkowski K, Pete J, Sheehy K, Su Q, Johnston C, et al. ACE2 Deficiency Modifies Renoprotection Afforded by ACE Inhibition in Experimental Diabetes. Diabetes. 2008;57:1018–25.

236. Yamaleyeva LM, Gilliam-Davis S, Almeida I, Brosnihan KB, Lindsey SH, Chappell MC. Differential regulation of circulating and renal ACE2 and ACE in hypertensive mRen2.Lewis rats with early-onset diabetes. AJP Ren Physiol. 2012;302:1374–84.

237. Ye M, Wysocki J, Naaz P, Salabat MR, LaPointe MS, Batlle D. Increased ACE 2 and Decreased ACE Protein in Renal Tubules from Diabetic Mice: A Renoprotective Combination? Hypertension. 2004;43:1120–5.

238. Donate-Correa J, Luis-Rodríguez D, Martín-Núñez E, Tagua VG, Hernández-Carballo C, Ferri C, et al. Inflammatory Targets in Diabetic Nephropathy. J Clin Med. 2020;9:458.

239. Feng Q, Liu D, Lu Y, Liu Z. The Interplay of Renin-Angiotensin System and Toll-Like Receptor 4 in the Inflammation of Diabetic Nephropathy. J Immunol Res. 2020;2020:6193407.

240. Takao T, Horino T, Matsumoto R, Shimamura Y, Ogata K, Inoue K, et al. Possible roles of tumor necrosis factor-α and angiotensin II type 1 receptor on high glucose-induced damage in renal proximal tubular cells. Ren Fail. 2015;37:160–4.

241. Jialal I, Kaur H. The role of toll-like receptors in diabetes-induced inflammation: Implications for vascular complications. Curr Diab Rep. 2012;12:172–9.

242. Omote K, Gohda T, Murakoshi M, Sasaki Y, Kazuno S, Fujimura T, et al. Role of the TNF pathway in the progression of diabetic nephropathy in KK-Ay mice. Am J Physiol - Ren Physiol. 2014;306:1335–47.

243. Venegas-Pont M, Manigrasso MB, Grifoni SC, Lamarca BB, Maric C, Racusen LC, et al. Tumor necrosis factor-α antagonist etanercept decreases blood pressure and protects the kidney in a mouse model of systemic lupus erythematosus. Hypertension. 2010;56:643–9.

244. Overstreet JM, Wang Y, Wang X, Niu A, Gewin LS, Yao B, et al. Selective activation of epidermal growth factor receptor in renal proximal tubule induces tubulointerstitial fibrosis. FASEB J. 2017;31:4407–21.

245. McLennan S V., Fisher E, Martell SY, Death AK, Williams PF, Lyons JG, et al. Effects of glucose on matrix metalloproteinase and plasmin activities in mesangial cells: Possible role in diabetic nephropathy. Kidney Int Suppl. 2000;77:81–7.

246. Ayo SH, Radnik RA, Garoni JA, Glass WF, Kreisberg JI. High glucose causes an increase in extracellular matrix proteins in cultured mesangial cells. Am J Pathol. 1990;136:1339–48.

247. Uttarwar L, Peng F, Wu D, Kumar S, Gao B, Ingram AJ, et al. HB-EGF release mediates glucose-induced activation of the epidermal growth factor receptor in mesangial cells. Am J Physiol - Ren Physiol. 2011;300:F921-FF931.

248. Junqueira LCU, Cossermelli W, Brentani R. Differential Staining of Collagens Type I, II and III by Sirius Red and Polarization Microscopy. Arch Histol Jpn. 1978;41:267–74.

249. Dayan D, Hiss Y, Hirshberg A, Bubis JJ, Wolman M. Are the polarization colors of Picrosirius red-stained collagen determined only by the diameter of the fibers? Histochemistry. 1989;93:27–9.

250. Vogel B, Siebert H, Hofmann U, Frantz S. Determination of collagen content within picrosirius red stained paraffin-embedded tissue sections using fluorescence microscopy. MethodsX. 2015;2:124–34.

251. Alexakis C, Maxwell P, Bou-Gharios G. Organ-specific collagen expression: Implications for renal disease. Nephron - Exp Nephrol. 2006;102:71–5.

252. He X, Zhang T, Tolosa M, Goru SK, Chen X, Misra PS, et al. A new, easily generated mouse model of diabetic kidney fibrosis. Sci Rep. 2019;9:12549.

253. Bülow RD, Boor P. Extracellular Matrix in Kidney Fibrosis: More Than Just a Scaffold. J Histochem Cytochem. 2019;67:643–61.

254. Nerlich A, Schleicher E. Immunohistochemical localization of extracellular matrix components in human diabetic glomerular lesions. Am J Pathol. 1991;139:889–99.

255. Razzaque MS, Koji T, Horita Y, Nishihara M, Harada T, Nakane PK, et al. Synthesis of type III Collagen and type IV collagen by tubular epithelial cells in diabetic nephropathy. Pathol Res Pract. 1995;191:1099–104.

256. Lam S, van der Geest RN, Verhagen NAM, Daha MR, van Kooten C. Secretion of collagen type IV by human renal fibroblasts is increased by high glucose via a TGF-β-independent pathway. Nephrol Dial Transplant. 2004;19:1694–701.

257. Xu Z, Zhao Y, Zhong P, Wang J, Weng Q, Qian Y, et al. EGFR inhibition attenuates diabetic nephropathy through decreasing ROS and endoplasmic reticulum stress. Oncotarget. 2017;8:32655–67.

10. ANNEX

10. Annex

10.1 Publications

10.1.1 Nephrology Dialysis Transplantation

Palau V, Riera M, Duran X, Valdivielso JM, Betriu A, Fernández E, et al. Circulating ADAMs are associated with renal and cardiovascular outcomes in chronic kidney disease patients. Nephrol Dial Transplant, 2018; 35:130-138.

doi: 10.1093/ndt/gfy240.

doi: 10.1093/ndt/gfy240.

doi: 10.1093/ndt/gfy240.

doi: 10.1093/ndt/gfy240.

doi: 10.1093/ndt/gfy240.

doi: 10.1093/ndt/gfy240.

doi: 10.1093/ndt/gfy240.

doi: 10.1093/ndt/gfy240.

doi: 10.1093/ndt/gfy240.

10.1.2 American Journal of Physiology – Renal Physiology

Palau V, Pascual J, Soler MJ, Riera M. Role of ADAM17 in kidney disease. Am J Physiol Renal Physiol, 2019; 317:333-342.

ANNEX

Am J Physiol Renal Physiol 317: F333–F342, 2019.
First published May 29, 2019; doi:10.1152/ajprenal.00625.2018.

REVIEW

Role of ADAM17 in kidney disease

Vanesa Palau, Julio Pascual, Maria José Soler,* and Marta Riera*
Department of Nephrology, Hospital del Mar Medical Research Institute, Barcelona, Spain

Submitted 3 January 2019; accepted in final form 23 May 2019

Palau V, Pascual J, Soler MJ, Riera M. Role of ADAM17 in kidney disease. *Am J Physiol Renal Physiol* 317: F333–F342, 2019. First published May 29, 2019; doi:10.1152/ajprenal.00625.2018.—It is known that the renin-angiotensin system plays a major role in the pathophysiology of cardiovascular disease and renal injury. Within the renin-angiotensin system, angiotensin-converting enzyme 2 (ACE2) cleaves ANG II to generate ANG(1–7) peptide, which counteracts the adverse effects of ANG II accumulation. ACE2 can undergo cleavage or shedding to release the catalytically active ectodomain into the circulation by a disintegrin and metalloprotease (ADAM)17, also known as TNF-α-converting enzyme. ADAM17 is involved in many pathological processes such as cancer, inflammatory diseases, neurological diseases, cardiovascular diseases, atherosclerosis, diabetes, and hypertension. Clinical and experimental studies have shown that ADAM17 is involved in chronic kidney disease (CKD) with a proinflammatory and profibrotic role, suggesting that it could be an important mediator of CKD progression. ADAM17 inhibition attenuates fibrosis and inflammation, suggesting that its inhibition may be a possible new valuable therapeutic tool in fibrotic kidney disease treatment. In addition, in renal disease, some experimental studies have demonstrated that ADAM17 is differently expressed in the kidney. Thus, ADAM17 is highly expressed in distal renal tubules and increased in the whole kidney in diabetic models. In this article, we will review the role of ADAM17 under physiological and pathological conditions. We will mainly focus on the importance of ADAM17 in the context of CKD.

a disintegrin and metalloprotease 17; inflammation; kidney disease; renin-angiotensin system

INTRODUCTION

A disintegrins and metalloproteases (ADAMs) are membrane-anchored, cell surface, and secreted proteins containing ADAM domains. ADAMs play an important role in the regulation of cell phenotype via their effects on cell adhesion, migration, and proteolysis and in modulating cell signaling and biological responses (6, 17). In humans, only 13 of the 21 genes in the family encode functional proteases. Functional ADAMs are involved in ectodomain shedding of diverse growth factors, cytokines, receptors, and adhesion molecules (17). ADAM enzymatic activities are controlled by posttranscriptional tissue inhibitors of metalloprotease (TIMPs) (61). There are some members of the ADAM family associated with different diseases. Among them, ADAM8, ADAM9, ADAM10, ADAM15, ADAM17, or ADAM33 are altered in atherosclerosis (81). ADAM12 has been related to late-onset Alzheimer's disease and breast and bladder cancer. ADAM10 and ADAM17 are the most studied members of the ADAM family and play important roles in Alzheimer's disease, diabetes, atherosclerosis, inflammatory diseases, cancer, and sepsis (81). ADAM17 is a type I transmembrane protein with an NH_2-terminal signal sequence followed by a prodomain with a cysteine switch-like region, a metalloproteinase domain with Zn-binding domain region catalytically active, a disintegrin cysteine-rich domain, an EGF-like domain, a single transmembrane domain, and a cytoplasmic tail (25, 53, 54, 94). ADAM17 was identified predominantly in two forms: as a full-length inactive protein (100 kDa) and as a mature form lacking the prodomain, the active form (80 kDa) (Fig. 1) (22).

The ADAM17 zymogen is enzymatically inactive because of the prodomain interaction with the active site, making substrates inaccessible to the catalytic domain. The prodomain inhibits ADAM17 activity. Maturation of ADAM17 takes place in lipid rafts that are present in the medial Golgi, where furin cleaves the ADAM17 prodomain (79). The cleavage of the ADAM17 prodomain by furin is needed for its activation together with other molecular processes such as phosphorylation events (98). Activation of the ERK or p38 MAPK pathways increases phosphorylation in Thr^{735} at the cytoplasmic domain, whereas growth factor stimulation increases phosphorylation of Ser^{819} and dephosphorylation of Ser^{791} of pro-ADAM17 (15). Mutation or dephosphorylation of Ser^{791} en-

* M. J. Soler and M. Riera contributed equally to this work.
Address for reprint requests and other correspondence: M. J. Soler, Dept. of Nephrology, Hospital del Mar Medical Research Institute, Carrer Dr. Aiguader, 88, Barcelona 08003, Spain (e-mail: mjsoler01@gmail.com).

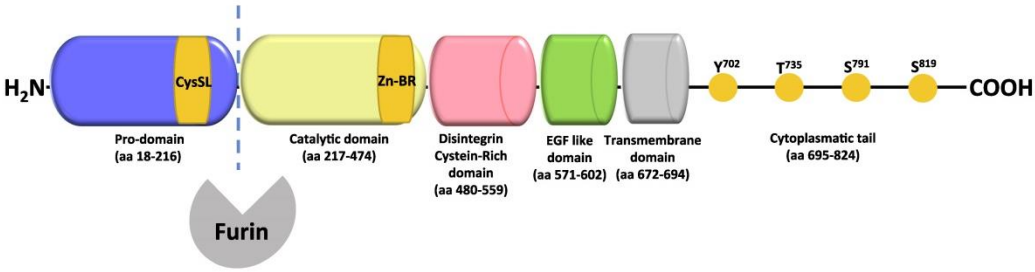

Fig. 1. Representation of a disintegrin and metalloprotease (ADAM)17 domains. The inactive pro-ADAM17 contains a prodomain, a catalytic domain, a disintegrin domain, an EGF-like domain, a transmembrane domain, and a cytoplasmatic tail. Furin is needed for ADAM17 maturation and activation. Briefly, furin cleaves the ADAM17 prodomain, and Thr^{735} at the cytoplasmatic tail is phosphorylated by MAPKs or ERK stimulation.

hance phosphorylation at Thr^{735} (95). Phosphorylation of Thr^{735} by p38 MAPK or ERK is necessary for ADAM17 maturation and regulates its cell surface levels (Fig. 2) (95).

The *ADAM17* gene is ~50 kb and contains 19 exons. Chromosomal mapping places ADAM17 on human chromosome 2p25 and mouse chromosome 12 (8a, 29). Mouse ADAM17 has 92% amino acid identity with the human protein and is ubiquitously expressed (8a). ADAM17 was initially described by Black and colleagues to specifically cleave the precursor of TNFα (pro-TNF-α) (5). Currently, it is known that ADAM17 can also release ectodomains of a diverse variety of membrane-anchored cytokines, cell adhesion molecules, receptors, ligands, and enzymes, such as transforming growth factor (TGF)-α, L-selectin, and angiotensin-converting enzyme 2 (ACE2) (23, 25, 45, 54, 69). Several substrates for ADAM17 have been involved in many pathological processes such as cancer, inflammatory diseases, neurological diseases, cardiovascular diseases, atherosclerosis, diabetes, and hypertension (45, 54, 57, 67, 68, 92, 97).

Clinical and experimental studies have shown that ADAM17 is involved in chronic kidney disease (CKD) with a proinflammatory and profibrotic role, suggesting that it could be an important mediator on CKD progression (20, 32, 56, 74). For this reason, in this review, we aimed to summarize the importance of ADAM17 under physiological and pathological conditions related to renal function.

THE IMPORTANT ROLE OF ADAM17 IN RENIN-ANGIOTENSIN SYSTEM REGULATION

The renin-angiotensin system (RAS) has a crucial role in the regulation of the cardiovascular system and renal function (65). Thus, dysregulations of this system are associated with the development of cardiovascular pathologies, including kidney injury (9). ANG II is the main molecular effector in the RAS, interacting with the ANG II type 1 receptor at the cell surface (43). ANG II induces vascular contractility, cellular transport, hypertrophy, growth factor synthesis, and reactive oxygen species generation (96). ACE forms ANG II from ANG I, whereas ACE2 cleaves ANG II to form ANG(1–7) (33), counterbalancing the ANG II-promoting effects of ACE by preventing ANG II accumulation in tissues (12, 70). The suppression of the ACE/ANG II axis of the RAS minimizes cardiovascular and renal complications (42).

ACE2 is a type I transmembrane glycoprotein with its catalytic site exposed to the extracellular surface (18, 80). When ADAM17 catalyzes ACE2 ectodomain shedding, the compensatory axis of the RAS mediated by ACE2 is compromised (Fig. 3). Increased ACE2 ectodomain into the urine has been found in diabetic mice (11, 63, 66, 91) and in patients with CKD, diabetic nephropathy (DN), and diabetic renal transplant (47, 82, 93). Interestingly, experimental studies have shown that ACE2 and ADAM17 colocalize in the apical side of

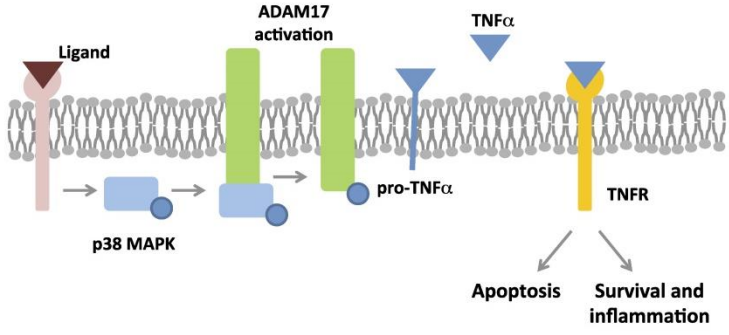

Fig. 2. Schematic representation of a disintegrin and metalloprotease (ADAM)17 phosphorylation. Activation of p38 MAPKs leads to ADAM17 phosphorylation in Thr^{735} and activation. After its activation, ADAM17 catalyzes pro-TNF-α shedding by releasing soluble TNF-α. TNF-α binds to its receptors (TNFRs) and activates apoptotic pathways and inflammatory pathways. [Adapted from Xu P et al. (95).]

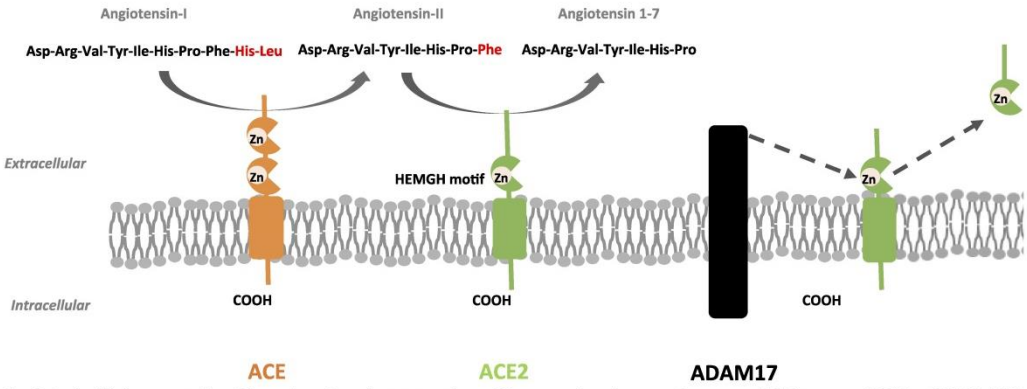

Fig. 3. A simplified representation of the renin-angiotensin system pathway. Whereas angiotensin-converting enzyme (ACE) converts ANG I to ANG II, ACE2 converts ANG II to ANG(1–7). ACE2 is cleaved by a disintegrin and metalloprotease (ADAM)17, producing a soluble form of ACE2. HEMGH motif, zinc-binding motif.

the proximal tubule brush border from diabetic Akita mice (66). Several investigators have demonstrated increased renal ADAM17 expression and urinary ACE2 excretion in diabetic mice. These levels were reversed by insulin treatment or insulin sensitizer rosiglitazone administration (11, 63, 66). Our group demonstrated, in nonobese diabetic mice, a model of type 1 diabetes, that ADAM17 expression and circulating ACE2 activity were both increased in diabetic mice compared with nondiabetic mice. In addition, paricalcitol administration could be a negative regulator of the RAS, exerting a protective role in the diabetic kidney (63).

Moreover, in patients with type 2 diabetes, urinary ACE2 activity and protein levels have been found increased compared with healthy controls (40). The authors speculated that high glucose could increase ADAM17 expression, leading to ACE2 shedding from tubular epithelial cells in patients with type 2 diabetes.

Different studies have demonstrated that ADAM17 was unable to cleave the ACE ectodomain, suggesting that ADAM17 may be involved only in the ectodomain shedding of ACE2 (26, 35, 38, 66, 84). Using TIMP proteins, specific ADAM17 inhibitors, Lambert and colleagues (35) found that ACE2 shedding in human embryonic kidney cells was only inhibited after 15 min of incubation with TIMP3; however, no inhibition was observed in the presence of TIMP1. This differential effect may be ascribed to the fact that TIMP proteins can inhibit diverse ADAM metalloproteases. Thus, while TIMP3 is a potent inhibitor of ADAM17 and ADAM10, TIMP1 can only inhibit ADAM10 activity (1, 38). Other studies conducted by Salem and colleagues demonstrated ACE2 shedding by ADAM17 using TNF-α processing inhibitor-1 (TAPI-1) a synthetic ADAM17 inhibitor, in human kidney-2 cells. By Western blot analysis, they demonstrated that ACE2 shedding into the cell medium was significantly decreased after incubating cells with TAPI-1 (66). In concordance with these two studies, Grobe and colleagues (26) also demonstrated that ADAM17 gene silencing in COS7 cells significantly reduced ACE2 protein expression in the medium compared with control cells. However, there was no significant difference in ACE2 protein expression in lysates from silenced COS7 cells compared with control cell lysates (26).

In addition, Kuruppu and colleagues (34) demonstrated that ADAM17 also participates in neprilysin (NEP) shedding. Using specific inhibitors for ADAM17 on Ea.hy926 endothelial cells, they observed that NEP activity in the cell medium was decreased.

Gutta and colleagues (27) found urinary ACE2, NEP, and ADAM17 protein levels in patients with type 2 diabetes with normo-, micro-, and macroalbuminuria. Interestingly, fragmented ACE2 and NEP bands in urine were only seen in all patients with diabetes. In contrast, neither ADAM17 nor ACE2 protein expression were detected in urine from patients without diabetes (27). These results suggest that the detection of ACE2 and NEP degradation products in urine might be used as biomarkers of kidney disease early on in DN, before the onset of microalbuminuria. Moreover, the authors speculated that ADAM17 could be responsible for ACE2 and NEP shedding from the kidney to the urine (27). These results suggest that ADAM17 would be implicated on the effectiveness of the RAS hampering the ACE2/ANG(1–7) axis and stimulating ANG II accumulation.

ADAM17 IN DIABETES

Active protein C has been shown to have endothelium-protective functions including anti-inflammatory and cytoprotective effects (19). Protein C binds to the endothelial protein C receptor (EPCR) to be active. Overexpression of active protein C reduces hyperglycemia-induced glomerular apoptosis and prevents endothelial dysfunction and apoptosis, glomerular capillary injury, and DN development in mice (30). ADAM17 is known to cleave membrane-bound EPCR, releasing soluble EPCR into the circulation. In DN, higher levels of circulating and urine EPCR were observed in patients with diabetes compared with patients without diabetes (36). In addition, increased ADAM17 glomerular levels were found in patients with diabetes. These results confirmed that, as ex-

pected in patients with diabetes, increased ADAM17 levels contributed to EPCR shedding, increasing its levels in the circulation and urine. Moreover, this study demonstrated that patients with DN presented higher cardiovascular risk factors compared with patients without DN (36). Rizza and colleagues (63a) demonstrated that increased circulating levels of VCAM-1, ICAM-1, IL-6 receptor, and TNF receptor (TNFR) type 1, other ADAM17 substrates, were associated with a significant higher rate of second cardiovascular events in a cohort of 298 patients with established vascular atherosclerosis. They also demonstrated that the increase of its substrates in the circulation depends on increased ADAM17 enzymatic activity at local inflammatory sites (63a). Renal ADAM17 activation leads to the release of proinflammatory and profibrotic markers such as cytokines, TNF-α, ICAM-1, and VCAM-1, stimulating renal inflammation and cardiovascular damage (25, 48).

In vitro experimental studies have demonstrated that high concentrations of glucose mimicking the diabetic milieu increased ADAM17 protein expression in glomerular epithelial cells or podocytes, glomerular endothelial cells, mesangial cells, and proximal tubular epithelial cells (20, 36, 78). Moreover, glucose activates ADAM17 and EGF receptor (EGFR) and regulates profibrotic TGF-β and the accumulation of matrix proteins (Fig. 4) (87–90).

Salem and colleagues (66) demonstrated increased renal and urinary ACE2 activity in Akita type 1 diabetic mice. The highest urinary ACE2 levels were associated with increased ACE2 and ADAM17 renal protein expression, demonstrating that in experimental diabetes, ADAM17 increases the ectodomain shedding of ACE2, increasing its levels in urine. Furthermore, insulin treatment in those mice normalizes hyperglycemia and attenuates urinary ACE2 shedding, albuminuria, and renal ADAM17 expression (66).

Within the kidney, increased ADAM17 expression and activity were found in the renal cortex from OVE26 mice, a model of type 1 diabetes. Pharmacological inhibition of ADAM17 with TMI-005 reduced collagen type IV, fibronectin, Nox4 protein expression, and NADPH activity in the glomeruli and tubule/interstitium from OVE26 mice (20). These results demonstrated that ADAM17 is upregulated in the diabetic kidney, contributing to matrix accumulation through upregulation of Nox4 and increasing oxidative stress, whereas its inhibition downregulated Nox4 protein expression and NADPH oxidase activity and reduced fibronectin expression.

Somineni and colleagues (72) focused on studying the effect of exercise and metformin administration in murine models of type 2 diabetes. They reported that in *db/db* mice, renal injury was associated with enhanced renal ADAM17 protein-mediated shedding of ACE2 (72). ADAM17 and ACE2 colocalized in the diabetic kidney. Moreover, ADAM17 protein expression was upregulated in the kidney from *db/db* mice, and ACE2 levels were increased in the urine of diabetic mice. Based on these data, they postulated that after early stages of kidney

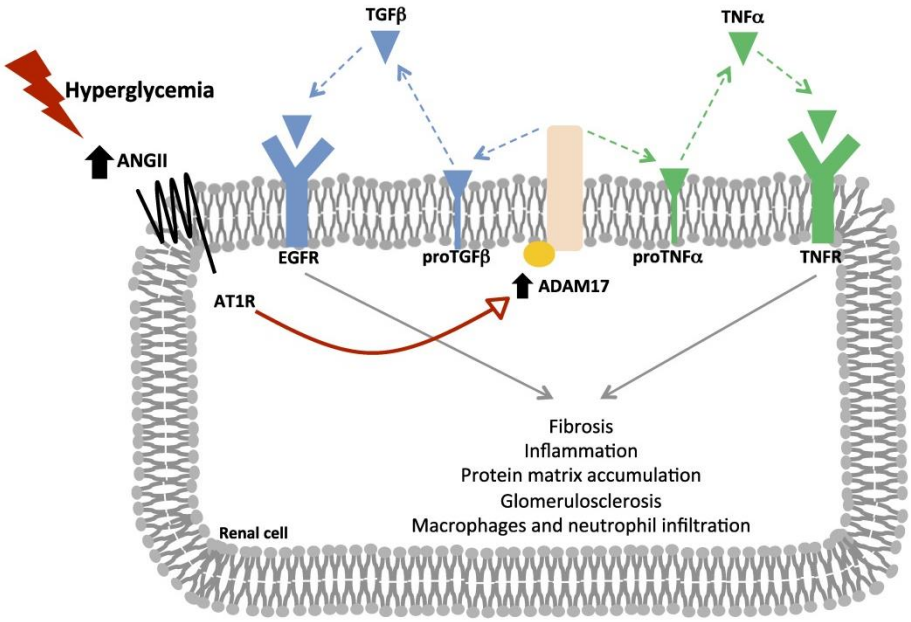

Fig. 4. Schematic representation of TNF-α and transforming growth factor (TGF)-β shedding after a disintegrin and metalloprotease (ADAM)17 upregulation during kidney injury. Kidney injury increases ANG II levels, leading to ADAM17 upregulation. ADAM17 contributes to TNF-α and TGF-β shedding, increasing fibrosis, inflammation, protein matrix accumulation, glomerulosclerosis, and macrophages and neutrophil infiltration by TNF receptor (TNFR) and EGF receptor (EGFR) signaling pathways. AT_1R, angiotensin II type 1 receptor.

damage, because of the action of ADAM17, ACE2 was shed into the urine in *db/db* mice. Thus, loss of the renoprotective enzyme ACE2 could contribute to renal damage in diabetes (11). In addition, they demonstrated that renal ACE2 activity in 8-wk-old *db/db* mice was significantly higher than in 31-wk-old *db/db* mice. These results suggested that during the progression of the disease, the kidneys are unable to keep ACE2 levels because of the increase of ADAM17 protein levels (11).

ADAM17 increases and leads to ACE2 shedding in *db/db* mice. This was associated with a higher glomerular area, glomerular and tubular basement membrane thickening, expanded mesangial matrix, and collagen deposition (71). Exercise training attenuates renal ADAM17 protein levels in the kidneys of these mice, suggesting a possible renoprotective mechanism in which decreased ADAM17 levels attenuate ACE2 shedding into urine. Furthermore, exercise training alone or in combination with metformin administration reduced blood glucose, albuminuria, glomerular and tubular thickening, and collagen depositions in *db/db* mice. Of note, metformin administration alone did not attenuate renal ADAM17 and ACE2 shedding and did not exert any effect on kidneys from diabetic mice (71).

ADAM17 AND ACUTE KIDNEY INJURY

Acute kidney injury (AKI) occurs in ~13.3 million people per year, with around 85% from developing countries, and is associated with high mortality and morbidity (50, 64). Ischemia-reperfusion injury is the leading cause of AKI, which results from generalized or localized impairment of oxygen and nutrients delivery to, and waste products removal from, kidney cells. The impairment of local tissue oxygen supply with the accumulation of waste products of metabolism injure tubular epithelial cells and cause death by apoptosis and necrosis (8, 28).

Renal ADAM17 is elevated in acute and chronic kidney injury and can activate TNF-α and EGFR ligands, leading to the synthesis and release of inflammatory and profibrotic factors (20, 31, 32, 56, 74). Experimental studies have demonstrated that EGFR inhibition attenuates renal fibrosis and renal disease progression (10, 41, 75).

ADAM17 participates in the regulation of neutrophil migration out of blood vessels at sites of inflammation. ADAM17 overactivation downregulates IL-8 receptor-β [chemokine (C-X-C motif) receptor 2] and induces neutrophil dysfunction (46). These findings suggest that ADAM17 could be used as a therapeutic target to beef up neutrophil infiltration and pathogen clearance during inflammation (46). In addition, TNF-α cleavage was reduced in the kidney of ADAM17 knockout mice and correlated with a reduction in proinflammatory markers, macrophage, and neutrophil infiltration in the kidney after AKI or in a unilateral ureteral obstruction model (32). These results demonstrated the important protective effect that ADAM17 inhibition could exert on kidney fibrosis after AKI, suggesting a central role of ADAM17 in fibrotic and inflammatory kidney diseases through the EGFR signaling pathway. TNF-α and heparin-binding EGF-like growth factor (HB-EGF), ADAM17 substrates, have been related to kidney damage in lupus nephritis, stimulating the EGFR signaling pathway and mediating kidney inflammation (7, 59). Qing and colleagues (59) found that in *Fc fragment of IgG receptor IIb* (*Fcgr2b*)$^{-/-}$ mice, a mouse experimental model of lupus nephritis, iRhom2 and ADAM17 are upregulated. Interestingly, deficiency of iRhom2 protects lupus-prone *Fcgr2b*$^{-/-}$ mice from renal inflammation by simultaneously blocking TNF-α and HB-EGF/EGFR signaling in the kidney. *Fcgr2b*$^{-/-}$ mice lacking iRhom2 did not present proteinuria, extracellular matrix depositions, infiltrated inflammatory cells, or glomerular damage (59). These results demonstrate that iRhom2 is necessary for ADAM17 activity to induce TNF-α and EGFR substrate shedding implicated in renal inflammation (39).

Bertram and colleagues (3) analyzed circulating ADAM17 activity of serum samples using the InnoZyme TACE Activity kit. They demonstrated that circulating ADAM17 levels are increased in patients with active anti-neutrophil cytoplasmic antibody-associated vasculitis, suggesting a model in which increased plasma ADAM17 correlates with enhanced proteolytic activity and disease progression. The increase in ADAM17 observed in the setting of active anti-neutrophil cytoplasmic antibody-associated vasculitis and in advanced CKD may be in part related to its direct role in inflammation (3). In concordance, different studies have demonstrated that ADAM17 is involved in inflammatory responses, playing an important role in the regulation of neutrophil influx into the peritoneal cavity (77), participating in monocyte transmigration (24), and regulating macrophage uptake of apoptotic cells (15).

Previous studies have demonstrated that ADAM17 can also shed kidney injury molecule (KIM)-1, which is responsible for transforming proximal tubular epithelial cells into phagocytes for clearance of apoptotic cells (2, 21). The efficient clearance by proximal tubular epithelial cells is inhibited by an excess of soluble KIM-1 (21). Gandhi and colleagues (21) found higher levels of soluble KIM-1 and higher cell surface expression of ADAM17 after AKI. They speculated that an excess of soluble KIM-1 might occur after AKI and could limit kidney recovery (21). Moreover, it has been shown that after AKI, ADAM17 mRNA expression, EGF ligands, TNF-α substrates, and their receptors were increased. As a consequence of ADAM17 hyperactivation, EGFR is persistently activated, leading to the synthesis and release of proinflammatory and profibrotic factors such as TGF-β, resulting in macrophages and neutrophil infiltration and fibrosis (Fig. 4) (32).

ADAM17 AND CKD

CKD is defined as an alteration in kidney structure and function with variable clinical presentation, severity, and rate of progression of the disease that is present for >3 mo. It can result from a variety of diseases, but the most common are diabetes and hypertension (62). CKD is characterized by progressive nephron loss involving tubulointerstitial fibrosis and glomerulosclerosis, leading to end-stage renal disease and a need for renal replacement therapy or kidney transplantation (13).

ADAM17 has been studied in experimental models of renal diseases and in kidney biopsies from patients with CKD, suggesting an important role on kidney fibrosis, inflammation, and disease progression (31, 32). Our group demonstrated that in plasma samples from patients with CKD without a previous history of cardiovascular disease from the NEFRONA study, circulating ADAM activity was increased in patients with CKD

stages 3–5 and was consistently increased in patients with CKD stage 5D. Interestingly, circulating ADAM activity in patients with CKD progressively increases as CKD progresses. Moreover, circulating ADAM activity was identified as a risk factor for CKD progression only in male patients and as an independent risk factor for CV events after 48 mo of followup (55).

Several studies have demonstrated that ADAM17 is increased in glomerular sclerosis and interstitial fibrosis and correlated positively with fibrotic markers in kidney biopsies (32, 44, 51). In normal human kidneys, by RNA in situ hybridization, it has been shown that ADAM17 staining was predominantly negative in the proximal tubules, glomerular mesangium, and endothelium; little staining was seen in glomerular parietal and podocytes; moderate staining was seen in renal arterial endothelial cells and smooth muscle cells; and high ADAM17 expression was detected in distal tubules (44, 51). In the same line, experimental studies have shown that the release of ADAM17 substrates such as TGF-α contributes to proteinuria, glomerulosclerosis, mononuclear cell infiltration, and fibrosis in the kidney (16, 44). In addition, high ADAM17 mRNA staining was observed in the glomerular parietal epithelium and podocytes from several renal diseases such as DN, focal segmental glomerulosclerosis, interstitial fibrosis and tubular atrophy, acute allograft rejection, and nontransplant interstitial fibrosis, among others (44, 51). ADAM17 mRNA was upregulated in the glomerular mesangium, endothelium, proximal tubules, and peritubular capillaries in the kidneys of patients with CKD (44, 51). Moreover, high ADAM17 mRNA expression was also found in interstitial inflammatory cells, the renal arterial endothelium, and smooth muscle cells in the kidneys of different renal diseases (44). In addition, ADAM17 was highly expressed in fibrotic areas and in sclerosed glomeruli from patients with Wegener granulomatosis, suggesting its important role in fibrosis and advanced CKD (44).

An in vitro study by Melenhorst and colleagues (44) demonstrated a 300-fold increase in TGF-α shedding by ADAM17 after phorbol 12-myristate 13-acetate (PMA) stimulation in podocytes. Pharmacological ADAM17 inhibition with TNF484, a TNF-α-converting enzyme inhibitor, reduced TGF-α shedding in human podocytes and proximal tubular cells (44). In concordance, Lautrette and colleagues (37) demonstrated that ANG II induces and redistributes ADAM17 to the apical membranes of distal tubules, improving TGF-α cleavages. Blockage of this pathway by overexpressing a negative isoform of EGFR, using a TGF-α inhibitor or an ADAM17 inhibitor, prevented the injury development in the kidney from ANG II-treated mice (37). In concordance, Mulder and colleagues (51) demonstrated that ADAM17 induces HB-EGF and TGF-α shedding in cultured human mesangial cells upon PMA stimulation. ADAM17 shedding was inhibited up to 82% in PMA-stimulated cells after ADAM17 inhibition with TNF484 (51). Moreover, Morgado-Pascual and colleagues (49) demonstrated that aldosterone stimulation activated the EGFR signaling pathway because of TGF-α shedding by ADAM17 in cultured human tubular epithelial cells (human kidney-2). Aldosterone increased EGFR phosphorylation, leading to its activation and resulting in upregulation of proinflammatory factors such as chemokine (C-C motif) ligand 2 and chemokine (C-C motif) ligand 5 (49). These results suggested that ADAM17 targeting could become a therapeutic tool to reduce EGFR signaling, subsequently protecting the kidney from renal fibrosis and inflammation.

EFFECT OF ADAM17 DOWNREGULATION

An efficient way to study ADAM17 function is working with knockout animal models and to assess its effect on the animal phenotype. ADAM17 knockout mice die between *embryonic day 17.5* and the first day of birth because of defects in heart development and show epithelial abnormalities in several organs (94). Thereby, *Adam17*$^{-/-}$ mice nearly mimic EGFR knockout mice, lacking the EGFR ligands TGF-α, HB-EGF, or amphiregulin, suggesting an in vivo relevance of ADAM17 in the EGFR signaling pathway (4, 6, 85). For this reason, the generation of conditional tissue-specific mutants of ADAM17 has given the opportunity to study the important role of ADAM17 in different diseases.

In ADAM17 hypomorphic mice fed with a semisynthetic diet for 16 wk to obtain a mouse model with a moderate degree of hypercholesterolemia, an increase in atherosclerotic plaque size at the aortic root was seen compared with controls. However, only in ADAM17-deficient male mice, LDL-cholesterol was lower than in controls. As expected, ADAM17 substrates such as soluble TNFR type 1, soluble TNFR type 2, and soluble IL-6 receptor were reduced in ADAM17 hypomorphic mice compared with wild-type mice (52). TNFRs are related to apoptosis and proliferation, whereas TNFR type 1 increases apoptosis and TNFR type 2 attenuates apoptosis and increases cell proliferation. In macrophages isolated from ADAM17 hypomorphic mice, they observed that TNFR type 2 levels were increased, and caspase-3 activity was reduced, demonstrating that ADAM17 deficiency attenuates apoptosis signaling pathways. TNFR type 2 deletion in ADAM17-defi-

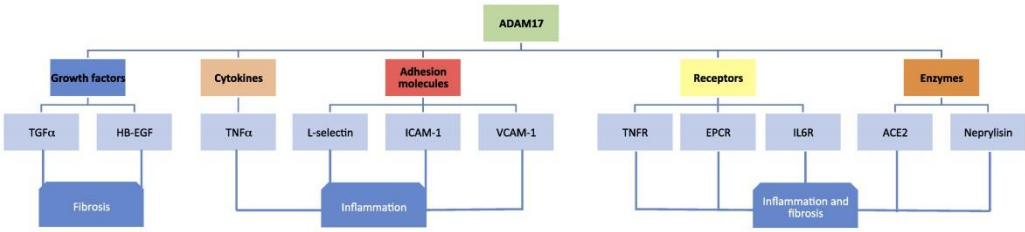

Fig. 5. A disintegrin and metalloprotease (ADAM)17 substrates. The diagram shows ADAM17 substrates confirmed by in vivo and in vitro studies. ACE2, angiotensin-converting enzyme 2; EPCR, endothelial protein C receptor; IL6R, IL-6 receptor; HB-EGF, heparin-binding EGF-like growth factor.

cient macrophages restored caspase-3 activity, leading to apoptotic and cell proliferative normal levels. The authors concluded that ADAM17 exerts a protective role in atherosclerosis, controlling apoptosis and cell proliferation levels (52).

The shedding of ADAM17 substrates leads to the release of proinflammatory cytokines, profibrotic TGF-β, and neutrophil and macrophage infiltration. After kidney injury, EGFR activation is necessary in the early phases of tubular repair. However, sustained activation of EGFR is linked to kidney fibrosis, increasing TGF-β production (10, 41, 75, 76, 83). ADAM17 releases the ectodomains of most EGFR ligands, TNF-like weak (TWEAK), and TNF-α (23, 25, 45, 54, 69). As expected, ADAM17, EGF ligand, TWEAK, and TNF-α substrates have been found increased after kidney injury in mice (32). Rayego-Mateos and colleagues (60) demonstrated that TWEAK stimulates renal inflammation by the EGFR signaling pathway and ADAM17 induces the TWEAK-EGFR pathway, which leads to the upregulation of proinflammatory factors and increasing inflammatory cell infiltration in the kidney. ADAM17 hypomorphic mice show reduced levels of TGF-β, monocyte chemoattractant protein-1 expression, proinflammatory cytokine levels, decreased macrophage ingress into the kidney, and decreased neutrophil infiltration compared with wild-type mice with unilateral ureteral obstruction injury. Moreover, mice with ADAM17-specific deletion on proximal tubular cells also presented reduced levels of macrophage and neutrophil infiltration compared with wild-type mice after ischemia-reperfusion injury (32). Taken together, ADAM17 downregulation or specific proximal ADAM17 knockout exerts a protective effect against kidney fibrosis, reducing EGFR activation.

Wilson and colleagues (86) studied the effect of endothelium-specific ADAM17 knockout and global ADAM17 knockout in mice with excision in exon 5. Global knockout mice were studied at *embryonic day 18.5* of embryogenesis because of its poor survival. They observed that endothelial ADAM17 knockout mice presented cardiomegaly postnatally but not at *embryonic day 18.5*. Instead, global knockout mice presented cardiomegaly at *embryonic day 18.5*. The cardiomegaly in endothelial knockout mice was a consequence of enlargement of the left ventricle, whereas in the global knockout model, the hearts presented perinatal enlargement of the right and left ventricles. Moreover, they found that in the aortic cusps of endothelial knockout mice, there were changes in the levels of glycosaminoglycan and proteoglycans. By transmission electron microscopy, they found that the glycosaminoglycan/proteoglycan-rich layer in cusps was enlarged with increased space between the granules compared with control mice (86). In contrast, a study by Xia et al. (92) on experimental hypertension demonstrated that knockdown of ADAM17 by siRNA attenuated DOCA-salt hypertension. These results showed that ADAM17 contributes to the maintenance of hypertension by increasing ACE2 shedding, reducing membrane-bound carboxypeptidase levels, and increasing its soluble form (92).

CONCLUDING REMARKS

ADAM17 is increased in patients with diabetes and hypertension and in experimental models of acute and chronic kidney disease. Several substrates for ADAM17 have been implicated in the main pathways involved in kidney disease progression (Fig. 5). Studies in humans have demonstrated its role in acute and chronic kidney disease with proinflammatory and profibrotic effects. ADAM17 could be an important mediator on CKD progression. Interestingly, ADAM17 deletion has been shown to be beneficial in some diseases by attenuating fibrosis, hypertension, and inflammation. Although the relevance of ADAM17 is clearly stated in this review, more studies focusing on the role of ADAM17 in the progression of renal diseases are needed.

ACKNOWLEDGMENTS

V. Palau did the study as part of her doctoral thesis at the Department de Medicina of Universitat Autònoma de Barcelona.

GRANTS

This work was made possible with ISCIII-FEDER projects PI14/00557, PI16/00617, and PI17/00257, ISCIII-FSE project FI17/00025, and ISCIII-RETICS REDinREN project RD16/0009/0013.

DISCLOSURES

M. J. Soler has received consulting fees or speaking honoraria from Boehringer Ingelheim, Janssen, AstraZeneca, Novo Nordisk, Eli Lilly, abbVie, and Esteve. None of the other authors has any conflicts of interest, financial or otherwise, to disclose.

AUTHOR CONTRIBUTIONS

V.P., M.J.S., and M.R. conceived and designed research; V.P. prepared figures; V.P., J.P., M.J.S., and M.R. drafted manuscript; V.P., J.P., M.J.S., and M.R. edited and revised manuscript; V.P., J.P., M.J.S., and M.R. approved final version of manuscript.

REFERENCES

1. **Amour A, Knight CG, Webster A, Slocombe PM, Stephens PE, Knäuper V, Docherty AJP, Murphy G.** The in vitro activity of ADAM-10 is inhibited by TIMP-1 and TIMP-3. *FEBS Lett* 473: 275–279, 2000. doi:10.1016/S0014-5793(00)01528-3.
2. **Bailly V, Zhang Z, Meier W, Cate R, Sanicola M, Bonventre JV.** Shedding of kidney injury molecule-1, a putative adhesion protein involved in renal regeneration. *J Biol Chem* 277: 39739–39748, 2002. doi:10.1074/jbc.M200562200.
3. **Bertram A, Lovric S, Engel A, Beese M, Wyss K, Hertel B, Park JK, Becker JU, Kegel J, Haller H, Haubitz M, Kirsch T.** Circulating ADAM17 level reflects disease activity in proteinase-3 ANCA-associated vasculitis. *J Am Soc Nephrol* 26: 2860–2870, 2015. doi:10.1681/ASN.2014050477.
4. **Black RA.** Tumor necrosis factor-α converting enzyme. *Int J Biochem Cell Biol* 34: 1–5, 2002. doi:10.1016/S1357-2725(01)00097-8.
5. **Black RA, Rauch CT, Kozlosky CJ, Peschon JJ, Slack JL, Wolfson MF, Castner BJ, Stocking KL, Reddy P, Srinivasan S, Nelson N, Boiani N, Schooley KA, Gerhart M, Davis R, Fitzner JN, Johnson RS, Paxton RJ, March CJ, Cerretti DP.** A metalloproteinase disintegrin that releases tumour-necrosis factor-alpha from cells. *Nature* 385: 729–733, 1997. doi:10.1038/385729a0.
6. **Blobel CP.** ADAMs: key components in EGFR signalling and development. *Nat Rev Mol Cell Biol* 6: 32–43, 2005. doi:10.1038/nrm1548.
7. **Bollée G, Flamant M, Schordan S, Fligny C, Rumpel E, Milon M, Schordan E, Sabaa N, Vandermeersch S, Galaup A, Rodenas A, Casal I, Sunnarborg SW, Salant DJ, Kopp JB, Threadgill DW, Quaggin SE, Dussaule JC, Germain S, Mesnard L, Endlich K, Boucheix C, Belenfant X, Callard P, Endlich N, Tharaux PL.** Epidermal growth factor receptor promotes glomerular injury and renal failure in rapidly progressive crescentic glomerulonephritis. *Nat Med* 17: 1242–1250, 2011. [Erratum in *Nat Med* 17: 1521, 2011.] doi:10.1038/nm.2491.
8. **Cerdá J, Lameire N, Eggers P, Pannu N, Uchino S, Wang H, Bagga A, Levin A.** Epidemiology of acute kidney injury. *Clin J Am Soc Nephrol* 3: 881–886, 2008. doi:10.2215/CJN.04961107.

8a. **Cerretti DP, Poindexter K, Castner BJ, Means G, Copeland NG, Gilbert DJ, Jenkins NA, Black RA, Nelson N.** Characterization of the cDNA and gene for mouse tumour necrosis factor α converting enzyme

(TACE/ADAM17) and its location to mouse chromosome 12 and human chromosome 2p25. *Cytokine* 11: 541–551, 1999. doi:10.1006/cyto.1998.0466.

9. **Chappell MC, Marshall AC, Alzayadneh EM, Shaltout HA, Diz DI.** Update on the angiotensin converting enzyme 2-angiotensin (1−7)-MAS receptor axis: fetal programing, sex differences, and intracellular pathways. *Front Endocrinol (Lausanne)* 4: 201, 2014. doi:10.3389/fendo.2013.00201.
10. **Chen J, Chen JK, Nagai K, Plieth D, Tan M, Lee TC, Threadgill DW, Neilson EG, Harris RC.** EGFR signaling promotes TGFβ-dependent renal fibrosis. *J Am Soc Nephrol* 23: 215–224, 2012. doi:10.1681/ASN.2011070645.
11. **Chodavarapu H, Grobe N, Somineni HK, Salem ES, Madhu M, Elased KM.** Rosiglitazone treatment of type 2 diabetic *db/db* mice attenuates urinary albumin and angiotensin converting enzyme 2 excretion. *PLoS One* 8: e62833, 2013. doi:10.1371/journal.pone.0062833.
12. **Crackower MA, Sarao R, Oudit GY, Yagil C, Kozieradzki I, Scanga SE, Oliveira-dos-Santos AJ, da Costa J, Zhang L, Pei Y, Scholey J, Ferrario CM, Manoukian AS, Chappell MC, Backx PH, Yagil Y, Penninger JM.** Angiotensin-converting enzyme 2 is an essential regulator of heart function. *Nature* 417: 822–828, 2002. doi:10.1038/nature00786.
13. **Declèves AE, Sharma K.** Novel targets of antifibrotic and anti-inflammatory treatment in CKD. *Nat Rev Nephrol* 10: 257–267, 2014. doi:10.1038/nrneph.2014.31.
14. **Díaz-Rodríguez E, Montero JC, Esparís-Ogando A, Yuste L, Pandiella A.** Extracellular signal-regulated kinase phosphorylates tumor necrosis factor α-converting enzyme at threonine 735: a potential role in regulated shedding. *Mol Biol Cell* 13: 2031–2044, 2002. doi:10.1091/mbc.01-11-0561.
15. **Driscoll WS, Vaisar T, Tang J, Wilson CL, Raines EW.** Macrophage ADAM17 deficiency augments CD36-dependent apoptotic cell uptake and the linked anti-inflammatory phenotype. *Circ Res* 113: 52–61, 2013. doi:10.1161/CIRCRESAHA.112.300683.
16. **Dusso A, González EA, Martin KJ.** Vitamin D in chronic kidney disease. *Best Pract Res Clin Endocrinol Metab* 25: 647–655, 2011. doi:10.1016/j.beem.2011.05.005.
17. **Edwards DR, Handsley MM, Pennington CJ.** The ADAM metalloproteinases. *Mol Aspects Med* 29: 258–289, 2008. doi:10.1016/j.mam.2008.08.001.
18. **Eriksson U, Danilczyk U, Penninger JM.** Just the beginning: novel functions for angiotensin-converting enzymes. *Curr Biol* 12: R745–R752, 2002. doi:10.1016/S0960-9822(02)01255-1.
19. **Finigan JH, Dudek SM, Singleton PA, Chiang ET, Jacobson JR, Camp SM, Ye SQ, Garcia JG.** Activated protein C mediates novel lung endothelial barrier enhancement: role of sphingosine 1-phosphate receptor transactivation. *J Biol Chem* 280: 17286–17293, 2005. doi:10.1074/jbc.M412427200.
20. **Ford BM, Eid AA, Göőz M, Barnes JL, Gorin YC, Abboud HE.** ADAM17 mediates Nox4 expression and NADPH oxidase activity in the kidney cortex of OVE26 mice. *Am J Physiol Renal Physiol* 305: F323–F332, 2013. doi:10.1152/ajprenal.00522.2012.
21. **Gandhi R, Yi J, Ha J, Shi H, Ismail O, Nathoo S, Bonventre JV, Zhang X, Gunaratnam L.** Accelerated receptor shedding inhibits kidney injury molecule-1 (KIM-1)-mediated efferocytosis. *Am J Physiol Renal Physiol* 307: F205–F221, 2014. doi:10.1152/ajprenal.00638.2013.
22. **Gilles S, Zahler S, Welsch U, Sommerhoff CP, Becker BF.** Release of TNF-α during myocardial reperfusion depends on oxidative stress and is prevented by mast cell stabilizers. *Cardiovasc Res* 60: 608–616, 2003. doi:10.1016/j.cardiores.2003.08.016.
23. **Giricz O, Calvo V, Peterson EA, Abouzeid CM, Kenny PA.** TACE-dependent TGFα shedding drives triple-negative breast cancer cell invasion. *Int J Cancer* 133: 2587–2595, 2013. doi:10.1002/ijc.28295.
24. **Gomez IG, Tang J, Wilson CL, Yan W, Heinecke JW, Harlan JM, Raines EW.** Metalloproteinase-mediated shedding of integrin β_2 promotes macrophage efflux from inflammatory sites. *J Biol Chem* 287: 4581–4589, 2012. doi:10.1074/jbc.M111.321182.
25. **Gooz M.** ADAM-17: the enzyme that does it all. *Crit Rev Biochem Mol Biol* 45: 146–169, 2010. doi:10.3109/10409231003628015.
26. **Grobe N, Di Fulvio M, Kashkari N, Chodavarapu H, Somineni HK, Singh R, Elased KM.** Functional and molecular evidence for expression of the renin angiotensin system and ADAM17-mediated ACE2 shedding in COS7 cells. *Am J Physiol Cell Physiol* 308: C767–C777, 2015. doi:10.1152/ajpcell.00247.2014.
27. **Gutta S, Grobe N, Kumbaji M, Osman H, Saklayen M, Li G, Elased KM.** Increased urinary angiotensin converting enzyme 2 and neprilysin in patients with type 2 diabetes. *Am J Physiol Renal Physiol* 315: F263–F274, 2018. doi:10.1152/ajprenal.00565.2017.
28. **Hesketh EE, Czopek A, Clay M, Borthwick G, Ferenbach D, Kluth D, Hughes J.** Renal ischaemia reperfusion injury: a mouse model of injury and regeneration. *J Vis Exp* 88: 51816, 2014. doi:10.3791/51816.
29. **Hirohata S, Seldin MF, Apte SS.** Chromosomal assignment of two ADAM genes, TACE (ADAM17) and MLTNB (ADAM19), to human chromosomes 2 and 5, respectively, and of Mltnb to mouse chromosome 11. *Genomics* 54: 178–179, 1998. doi:10.1006/geno.1998.5544.
30. **Isermann B, Vinnikov IA, Madhusudhan T, Herzog S, Kashif M, Blautzik J, Corat MA, Zeier M, Blessing E, Oh J, Gerlitz B, Berg DT, Grinnell BW, Chavakis T, Esmon CT, Weiler H, Bierhaus A, Nawroth PP.** Activated protein C protects against diabetic nephropathy by inhibiting endothelial and podocyte apoptosis. *Nat Med* 13: 1349–1358, 2007. doi:10.1038/nm1667.
31. **Kato T, Hagiyama M, Ito A.** Renal ADAM10 and 17: their physiological and medical meanings. *Front Cell Dev Biol* 6: 153, 2018. doi:10.3389/fcell.2018.00153.
32. **Kefaloyianni E, Muthu ML, Kaeppler J, Sun X, Sabbisetti V, Chalaris A, Rose-John S, Wong E, Sagi I, Waikar SS, Rennke H, Humphreys BD, Bonventre JV, Herrlich A.** ADAM17 substrate release in proximal tubule drives kidney fibrosis. *JCI Insight* 1: 87023, 2016. doi:10.1172/jci.insight.87023.
33. **Keidar S, Kaplan M, Gamliel-Lazarovich A.** ACE2 of the heart: from angiotensin I to angiotensin (1−7). *Cardiovasc Res* 73: 463–469, 2007. doi:10.1016/j.cardiores.2006.09.006.
34. **Kuruppu S, Rajapakse NW, Minond D, Smith AI.** Production of soluble neprilysin by endothelial cells. *Biochem Biophys Res Commun* 446: 423–427, 2014. doi:10.1016/j.bbrc.2014.01.158.
35. **Lambert DW, Yarski M, Warner FJ, Thornhill P, Parkin ET, Smith AI, Hooper NM, Turner AJ.** Tumor necrosis factor-α convertase (ADAM17) mediates regulated ectodomain shedding of the severe-acute respiratory syndrome-coronavirus (SARS-CoV) receptor, angiotensin-converting enzyme-2 (ACE2). *J Biol Chem* 280: 30113–30119, 2005. doi:10.1074/jbc.M505111200.
36. **Lattenist L, Ochodnický P, Ahdi M, Claessen N, Leemans JC, Satchell SC, Florquin S, Gerdes VE, Roelofs JJ.** Renal endothelial protein C receptor expression and shedding during diabetic nephropathy. *J Thromb Haemost* 14: 1171–1182, 2016. doi:10.1111/jth.13315.
37. **Lautrette A, Li S, Alili R, Sunnarborg SW, Burtin M, Lee DC, Friedlander G, Terzi F.** Angiotensin II and EGF receptor cross-talk in chronic kidney diseases: a new therapeutic approach. *Nat Med* 11: 867–874, 2005. doi:10.1038/nm1275.
38. **Lee MH, Verma V, Maskos K, Nath D, Knäuper V, Dodds P, Amour A, Murphy G.** Engineering N-terminal domain of tissue inhibitor of metalloproteinase (TIMP)-3 to be a better inhibitor against tumour necrosis factor-alpha-converting enzyme. *Biochem J* 364: 227–234, 2002. doi:10.1042/bj3640227.
39. **Li X, Maretzky T, Weskamp G, Monette S, Qing X, Issuree PDA, Crawford HC, McIlwain DR, Mak TW, Salmon JE, Blobel CP.** iRhoms 1 and 2 are essential upstream regulators of ADAM17-dependent EGFR signaling. *Proc Natl Acad Sci USA* 112: 6080–6085, 2015. doi:10.1073/pnas.1505649112.
40. **Liang Y, Deng H, Bi S, Cui Z, A L, Zheng D, Wang Y.** Urinary angiotensin converting enzyme 2 increases in patients with type 2 diabetic mellitus. *Kidney Blood Press Res* 40: 101–110, 2015. doi:10.1159/000368486.
41. **Liu N, Guo JK, Pang M, Tolbert E, Ponnusamy M, Gong R, Bayliss G, Dworkin LD, Yan H, Zhuang S.** Genetic or pharmacologic blockade of EGFR inhibits renal fibrosis. *J Am Soc Nephrol* 23: 854–867, 2012. doi:10.1681/ASN.2011050493.
42. **Mallat SG.** Dual renin-angiotensin system inhibition for prevention of renal and cardiovascular events: do the latest trials challenge existing evidence? *Cardiovasc Diabetol* 12: 108, 2013. doi:10.1186/1475-2840-12-108.
43. **Mehta PK, Griendling KK.** Angiotensin II cell signaling: physiological and pathological effects in the cardiovascular system. *Am J Physiol Cell Physiol* 292: C82–C97, 2007. doi:10.1152/ajpcell.00287.2006.
44. **Melenhorst WB, Visser L, Timmer A, van den Heuvel MC, Stegeman CA, van Goor H.** ADAM17 upregulation in human renal disease: a role in modulating TGF-α availability? *Am J Physiol Renal Physiol* 297: F781–F790, 2009. doi:10.1152/ajprenal.90610.2008.

45. **Menghini R, Fiorentino L, Casagrande V, Lauro R, Federici M.** The role of ADAM17 in metabolic inflammation. *Atherosclerosis* 228: 12–17, 2013. doi:10.1016/j.atherosclerosis.2013.01.024.
46. **Mishra HK, Long C, Bahaie NS, Walcheck B.** Regulation of CXCR2 expression and function by a disintegrin and metalloprotease-17 (ADAM17). *J Leukoc Biol* 97: 447–454, 2015. doi:10.1189/jlb.3HI0714-340R.
47. **Mizuiri S, Aoki T, Hemmi H, Arita M, Sakai K, Aikawa A.** Urinary angiotensin-converting enzyme 2 in patients with CKD. *Nephrology (Carlton)* 16: 567–572, 2011. doi:10.1111/j.1440-1797.2011.01467.x.
48. **Morange PE, Tregouet DA, Godefroy T, Saut N, Bickel C, Rupprecht HJ, Lackner K, Barbaux S, Poirier O, Peiretti F, Nalbone G, Juhan-Vague I, Blankenberg S, Tiret L.** Polymorphisms of the tumor necrosis factor-alpha (TNF) and the TNF-alpha converting enzyme (TACE/ADAM17) genes in relation to cardiovascular mortality: the AtheroGene study. *J Mol Med (Berl)* 86: 1153–1161, 2008. doi:10.1007/s00109-008-0375-6.
49. **Morgado-Pascual JL, Rayego-Mateos S, Valdivielso JM, Ortiz A, Egido J, Ruiz-Ortega M.** Paricalcitol inhibits aldosterone-induced pro-inflammatory factors by modulating epidermal growth factor receptor pathway in cultured tubular epithelial cells. *BioMed Res Int* 2015: 783538, 2015. doi:10.1155/2015/783538.
50. **Morigi M, Rota C, Remuzzi G.** Mesenchymal stem cells in kidney repair. *Methods Mol Biol* 1416: 89–107, 2016. doi:10.1007/978-1-4939-3584-0_5.
51. **Mulder GM, Melenhorst WB, Celie JW, Kloosterhuis NJ, Hillebrands JL, Ploeg RJ, Seelen MA, Visser L, van Dijk MC, van Goor H.** ADAM17 up-regulation in renal transplant dysfunction and non-transplant-related renal fibrosis. *Nephrol Dial Transplant* 27: 2114–2122, 2012. doi:10.1093/ndt/gfr583.
52. **Nicolaou A, Zhao Z, Northoff BH, Sass K, Herbst A, Kohlmaier A, Chalaris A, Wolfrum C, Weber C, Steffens S, Rose-John S, Teupser D, Holdt LM.** Adam17 Deficiency promotes atherosclerosis by enhanced TNFR2 signaling in Mice. *Arterioscler Thromb Vasc Biol* 37: 247–257, 2017. doi:10.1161/ATVBAHA.116.308682.
53. **Niu A, Wang B, Li YP.** TNFα shedding in mechanically stressed cardiomyocytes is mediated by Src activation of TACE. *J Cell Biochem* 116: 559–565, 2015. doi:10.1002/jcb.25006.
54. **Ohtsu H, Dempsey PJ, Frank GD, Brailoiu E, Higuchi S, Suzuki H, Nakashima H, Eguchi K, Eguchi S.** ADAM17 mediates epidermal growth factor receptor transactivation and vascular smooth muscle cell hypertrophy induced by angiotensin II. *Arterioscler Thromb Vasc Biol* 26: e133–e137, 2006. doi:10.1161/01.ATV.0000236203.90331.d0.
55. **Palau V, Riera M, Duran X, Valdivielso JM, Betriu A, Fernández E, Pascual J, Soler MJ.** Circulating ADAMs are associated with renal and cardiovascular outcomes in chronic kidney disease patients. *Nephrol Dial Transplant* 2018: gfy240, 2018. doi:10.1093/ndt/gfy240.
56. **Perna AF, Pizza A, Di Nunzio A, Bellantone R, Raffaelli M, Cicchella T, Conzo G, Santini L, Zacchia M, Trepiccione F, Ingrosso D.** ADAM17, a new player in the pathogenesis of chronic kidney disease-mineral and bone disorder. *J Ren Nutr* 27: 453–457, 2017. doi:10.1053/j.jrn.2017.05.007.
57. **Peschon JJ, Slack JL, Reddy P, Stocking KL, Sunnarborg SW, Lee DC, Russell WE, Castner BJ, Johnson RS, Fitzner JN, Boyce RW, Nelson N, Kozlosky CJ, Wolfson MF, Rauch CT, Cerretti DP, Paxton RJ, March CJ, Black RA.** An essential role for ectodomain shedding in mammalian development. *Science* 282: 1281–1284, 1998. doi:10.1126/science.282.5392.1281.
59. **Qing X, Chinenov Y, Redecha P, Madaio M, Roelofs JJ, Farber G, Issuree PD, Donlin L, McIlwain DR, Mak TW, Blobel CP, Salmon JE.** iRhom2 promotes lupus nephritis through TNF-α and EGFR signaling. *J Clin Invest* 128: 1397–1412, 2018. doi:10.1172/JCI97650.
60. **Rayego-Mateos S, Morgado-Pascual JL, Sanz AB, Ramos AM, Eguchi S, Batlle D, Pato J, Keri G, Egido J, Ortiz A, Ruiz-Ortega M.** TWEAK transactivation of the epidermal growth factor receptor mediates renal inflammation. *J Pathol* 231: 480–494, 2013. doi:10.1002/path.4250.
61. **Reiss K, Ludwig A, Saftig P.** Breaking up the tie: disintegrin-like metalloproteinases as regulators of cell migration in inflammation and invasion. *Pharmacol Ther* 111: 985–1006, 2006. doi:10.1016/j.pharmthera.2006.02.009.
62. **Rewa O, Bagshaw SM.** Acute kidney injury-epidemiology, outcomes and economics. *Nat Rev Nephrol* 10: 193–207, 2014. doi:10.1038/nrneph.2013.282.
63. **Riera M, Anguiano L, Clotet S, Roca-Ho H, Rebull M, Pascual J, Soler MJ.** Paricalcitol modulates ACE2 shedding and renal ADAM17 in NOD mice beyond proteinuria. *Am J Physiol Renal Physiol* 310: F534–F546, 2016. doi:10.1152/ajprenal.00082.2015.

63a. **Rizza S, Copetti M, Cardellini M, Menghini R, Pecchioli C, Luzi A, Di Cola G, Porzio O, Ippoliti A, Romeo F, Pellegrini F, Federici M.** A score including ADAM17 substrates correlates to recurring cardiovascular event in subjects with atherosclerosis. *Atherosclerosis* 239: 459–464, 2015. doi:10.1016/j.atherosclerosis.2015.01.029.

64. **Rodríguez E, Arias-Cabrales C, Bermejo S, Sierra A, Burballa C, Soler MJ, Barrios C, Pascual J.** Impact of recurrent acute kidney injury on patient outcomes. *Kidney Blood Press Res* 43: 34–44, 2018. doi:10.1159/000486744.
65. **Roscioni SS, Heerspink HJ, de Zeeuw D.** The effect of RAAS blockade on the progression of diabetic nephropathy. *Nat Rev Nephrol* 10: 77–87, 2014. [Erratum in *Nat Rev Nephrol* 10: 243, 2014.] doi:10.1038/nrneph.2013.251.
66. **Salem ES, Grobe N, Elased KM.** Insulin treatment attenuates renal ADAM17 and ACE2 shedding in diabetic Akita mice. *Am J Physiol Renal Physiol* 306: F629–F639, 2014. doi:10.1152/ajprenal.00516.2013.
67. **Sandgren EP, Luetteke NC, Palmiter RD, Brinster RL, Lee DC.** Overexpression of TGF α in transgenic mice: induction of epithelial hyperplasia, pancreatic metaplasia, and carcinoma of the breast. *Cell* 61: 1121–1135, 1990. doi:10.1016/0092-8674(90)90075-P.
68. **Scheller J, Chalaris A, Garbers C, Rose-John S.** ADAM17: a molecular switch to control inflammation and tissue regeneration. *Trends Immunol* 32: 380–387, 2011. doi:10.1016/j.it.2011.05.005.
69. **Schlöndorff J, Becherer JD, Blobel CP.** Intracellular maturation and localization of the tumour necrosis factor α convertase (TACE). *Biochem J* 347: 131–138, 2000. doi:10.1042/bj3470131.
70. **Shaltout HA, Westwood BM, Averill DB, Ferrario CM, Figueroa JP, Diz DI, Rose JC, Chappell MC.** Angiotensin metabolism in renal proximal tubules, urine, and serum of sheep: evidence for ACE2-dependent processing of angiotensin II. *Am J Physiol Renal Physiol* 292: F82–F91, 2007. doi:10.1152/ajprenal.00139.2006.
71. **Somineni HK, Boivin GP, Elased KM.** Daily exercise training protects against albuminuria and angiotensin converting enzyme 2 shedding in *db/db* diabetic mice. *J Endocrinol* 221: 235–251, 2014. doi:10.1530/JOE-13-0532.
72. **Soond SM, Everson B, Riches DW, Murphy G.** ERK-mediated phosphorylation of Thr735 in TNFalpha-converting enzyme and its potential role in TACE protein trafficking. *J Cell Sci* 118: 2371–2380, 2005. doi:10.1242/jcs.02357.
74. **Tang J, Frey JM, Wilson CL, Moncada-Pazos A, Levet C, Freeman M, Rosenfeld ME, Stanley ER, Raines EW, Bornfeldt KE.** Neutrophil and macrophage cell surface colony-stimulating factor 1 shed by ADAM17 drives mouse macrophage proliferation in acute and chronic inflammation. *Mol Cell Biol* 38: e00103–e00118, 2018. doi:10.1128/MCB.00103-18.
75. **Tang J, Liu N, Tolbert E, Ponnusamy M, Ma L, Gong R, Bayliss G, Yan H, Zhuang S.** Sustained activation of EGFR triggers renal fibrogenesis after acute kidney injury. *Am J Pathol* 183: 160–172, 2013. doi:10.1016/j.ajpath.2013.04.005.
76. **Tang J, Liu N, Zhuang S.** Role of epidermal growth factor receptor in acute and chronic kidney injury. *Kidney Int* 83: 804–810, 2013. doi:10.1038/ki.2012.435.
77. **Tang J, Zarbock A, Gomez I, Wilson CL, Lefort CT, Stadtmann A, Bell B, Huang LC, Ley K, Raines EW.** Adam17-dependent shedding limits early neutrophil influx but does not alter early monocyte recruitment to inflammatory sites. *Blood* 118: 786–794, 2011. doi:10.1182/blood-2010-11-321406.
78. **Taniguchi K, Xia L, Goldberg HJ, Lee KW, Shah A, Stavar L, Masson EA, Momen A, Shikatani EA, John R, Husain M, Fantus IG.** Inhibition of Src kinase blocks high glucose-induced EGFR transactivation and collagen synthesis in mesangial cells and prevents diabetic nephropathy in mice. *Diabetes* 62: 3874–3886, 2013. doi:10.2337/db12-1010.
79. **Tellier E, Canault M, Rebsomen L, Bonardo B, Juhan-Vague I, Nalbone G, Peiretti F.** The shedding activity of ADAM17 is sequestered in lipid rafts. *Exp Cell Res* 312: 3969–3980, 2006. doi:10.1016/j.yexcr.2006.08.027.
80. **Tipnis SR, Hooper NM, Hyde R, Karran E, Christie G, Turner AJ.** A human homolog of angiotensin-converting enzyme. Cloning and functional expression as a captopril-insensitive carboxypeptidase. *J Biol Chem* 275: 33238–33243, 2000. doi:10.1074/jbc.M002615200.

81. **van der Vorst EPC, Weber C, Donners MMPC.** A Disintegrin and Metalloproteases (ADAMs) in cardiovascular, metabolic and inflammatory diseases: aspects for theranostic approaches. *Thromb Haemost* 118: 1167–1175, 2018. doi:10.1055/s-0038-1660479.
82. **Wang G, Lai FM, Lai KB, Chow KM, Kwan CH, Li KT, Szeto CC.** Urinary mRNA expression of ACE and ACE2 in human type 2 diabetic nephropathy. *Diabetologia* 51: 1062–1067, 2008. doi:10.1007/s00125-008-0988-x.
83. **Wang Z, Chen JK, Wang SW, Moeckel G, Harris RC.** Importance of functional EGF receptors in recovery from acute nephrotoxic injury. *J Am Soc Nephrol* 14: 3147–3154, 2003. doi:10.1097/01.ASN.0000098681.56240.1A.
84. **Warner FJ, Lew RA, Smith AI, Lambert DW, Hooper NM, Turner AJ.** Angiotensin-converting enzyme 2 (ACE2), but not ACE, is preferentially localized to the apical surface of polarized kidney cells. *J Biol Chem* 280: 39353–39362, 2005. doi:10.1074/jbc.M508914200.
85. **Weber S, Saftig P.** Ectodomain shedding and ADAMs in development. *Development* 139: 3693–3709, 2012. doi:10.1242/dev.076398.
86. **Wilson CL, Gough PJ, Chang CA, Chan CK, Frey JM, Liu Y, Braun KR, Chin MT, Wight TN, Raines EW.** Endothelial deletion of ADAM17 in mice results in defective remodeling of the semilunar valves and cardiac dysfunction in adults. *Mech Dev* 130: 272–289, 2013. doi:10.1016/j.mod.2013.01.001.
87. **Wolf G, Hamann A, Han DC, Helmchen U, Thaiss F, Ziyadeh FN, Stahl RA.** Leptin stimulates proliferation and TGF-β expression in renal glomerular endothelial cells: potential role in glomerulosclerosis. *Kidney Int* 56: 860–872, 1999. doi:10.1046/j.1523-1755.1999.00626.x.
88. **Wu D, Peng F, Zhang B, Ingram AJ, Gao B, Krepinsky JC.** Collagen I induction by high glucose levels is mediated by epidermal growth factor receptor and phosphoinositide 3-kinase/Akt signalling in mesangial cells. *Diabetologia* 50: 2008–2018, 2007. doi:10.1007/s00125-007-0721-1.
89. **Wu D, Peng F, Zhang B, Ingram AJ, Kelly DJ, Gilbert RE, Gao B, Krepinsky JC.** PKC-beta1 mediates glucose-induced Akt activation and TGF-beta1 upregulation in mesangial cells. *J Am Soc Nephrol* 20: 554–566, 2009. doi:10.1681/ASN.2008040445.
90. **Wu D, Peng F, Zhang B, Ingram AJ, Kelly DJ, Gilbert RE, Gao B, Kumar S, Krepinsky JC.** EGFR-PLCgamma1 signaling mediates high glucose-induced PKCbeta1-Akt activation and collagen I upregulation in mesangial cells. *Am J Physiol Renal Physiol* 297: F822–F834, 2009. doi:10.1152/ajprenal.00054.2009.
91. **Wysocki J, Batlle D.** Reduced plasma ACE2 activity in dialysis patients: another piece in the conundrum of factors involved in hypertension and cardiovascular morbidity? *Nephrol Dial Transplant* 28: 2200–2202, 2013. doi:10.1093/ndt/gft240.
92. **Xia H, Sriramula S, Chhabra KH, Lazartigues E.** Brain angiotensin-converting enzyme type 2 shedding contributes to the development of neurogenic hypertension. *Circ Res* 113: 1087–1096, 2013. doi:10.1161/CIRCRESAHA.113.301811.
93. **Xiao F, Hiremath S, Knoll G, Zimpelmann J, Srivaratharajah K, Jadhav D, Fergusson D, Kennedy CRJ, Burns KD.** Increased urinary angiotensin-converting enzyme 2 in renal transplant patients with diabetes. *PLoS One* 7: e37649, 2012. doi:10.1371/journal.pone.0037649.
94. **Xu J, Mukerjee S, Silva-Alves CR, Carvalho-Galvão A, Cruz JC, Balarini CM, Braga VA, Lazartigues E, França-Silva MS.** A disintegrin and metalloprotease 17 in the cardiovascular and central nervous systems. *Front Physiol* 7: 469, 2016. doi:10.3389/fphys.2016.00469.
95. **Xu P, Derynck R.** Direct activation of TACE-mediated ectodomain shedding by p38 MAP kinase regulates EGF receptor-dependent cell proliferation. *Mol Cell* 37: 551–566, 2010. doi:10.1016/j.molcel.2010.01.034.
96. **Xu S, Touyz RM.** Reactive oxygen species and vascular remodelling in hypertension: still alive. *Can J Cardiol* 22: 947–951, 2006. doi:10.1016/S0828-282X(06)70314-2.
97. **Zhan M, Jin B, Chen SE, Reecy JM, Li YP.** TACE release of TNF-alpha mediates mechanotransduction-induced activation of p38 MAPK and myogenesis. *J Cell Sci* 120: 692–701, 2007. doi:10.1242/jcs.03372.
98. **Zhang Z, Kolls JK, Oliver P, Good D, Schwarzenberger PO, Joshi MS, Ponthier JL, Lancaster JR Jr.** Activation of tumor necrosis factor-alpha-converting enzyme-mediated ectodomain shedding by nitric oxide. *J Biol Chem* 275: 15839–15844, 2000. doi:10.1074/jbc.M000604200.

10.2 Participation in congresses

10.2.1 International congresses

Palau V, Riera M, Benito D, Duran X, Valdivielso JM, Rodriguez E, et al. Role of circulating ADAM17 activity in chronic kidney disease (Abstract). Nephrol Dial Transplant. 2018; 33(suppl_1):i46.

Nephrology Dialysis Transplantation

FO065 **ROLE OF CIRCULATING ADAM17 ACTIVITY IN CHRONIC KIDNEY DISEASE**

Vanesa Palau[1], Marta Riera[1], David Benito[1], Xavier Duran[4], José Manuel Valdivielso[5], Eva Rodriguez[3], Maria Angeles Betriu[2], Elvira Fernández[5], Julio Pascual[1], Maria José Soler[2]

[1]Nephrology, Hospital del Mar-Institut Hospital del Mar d'Investigacions Mèdiques, Barcelona, Spain, [2]Nephrology, Instituto Carlos III, PI14/00557. FEDER., Hospital del Mar-Institut Hospital del Mar d'Investigacions Mèdiques, Barcelona, Spain, [3]Nephrology, Hospital del Mar-Institut Hospital del Mar d'Investigacions Mèdiques, Nephrology, Barcelona, Spain, [4]Statistics, Hospital del Mar-Intitut Hospital del Mar d'Investigacions Mèdiques, Barcelona, Spain and [5]Nephrology Research Laboratory, Institut de Recerca Biomèdica de Lleida, Lleida, Spain

INTRODUCTION AND AIMS: Several substrates for ADAM17 have been identified, including TNF-α, epidermal growth factor receptor (EGFR) ligands, L-selectin, vascular cell adhesion molecule 1 (VCAM-1) and angiotensin converting enzyme (ACE2). We now have studied circulating ADAM17 in chronic kidney disease (CKD) patients from the NEFRONA cohort study.

METHODS: 2032 patients without history of CV disease from an observational and multicenter study (NEFRONA project) divided in two groups: non-dialysis CKD stage 3-5 patients (CKD3-5, n=1463) and control patients (CONT, n=569) were studied. Baseline circulating ADAM17 activity was analyzed using a fluorimetric assay in plasma samples. ADAM17 levels according to presence of plaques, hypertension, age, smoking and treatments with ACE inhibitors or angiotensin II receptor blockers (ARBs) at baseline were studied. Increased serum creatinine and dialysis requirement after 24 months of follow-up depending on basal circulating ADAM17 activity were also studied. Logistic regression analysis was used to identify predictors of increasing serum creatinine and risk of dialysis requirement.

RESULTS: Circulating ADAM17 activity was significantly increased in CKD3-5 patients as compared to CONT. In CONT group, patients with plaques or patients on ACEi and ARBs therapy had increased ADAM17 activity as compared to those without plaques or therapy. Hypertension was also associated with higher ADAM17 activity in CKD3-5 patients. Smokers in both groups showed increased ADAM17. Baseline circulating ADAM17 activity was higher in patients with a 30% increase in serum creatinine levels after 2 years ($p<0.05$). Circulating ADAM17 activity was also higher in patients that needed dialysis after 2 years, in comparison with patients that maintained kidney function ($p<0.05$). In the multivariate model, after adjusting by age, diabetes, smoking and gender, increased circulating ADAM17 activity and age were independent predictors of increasing serum creatinine, whereas increased circulating ADAM17 activity, gender and age were independent predictors of dialysis requirement.

CONCLUSIONS: Circulating ADAM17 activity was increased in CKD. Smoking, presence of plaques and ACEi or ARBs therapies were associated with increased ADAM17 in CONT. Smoking and hypertension were associated with higher levels of circulating ADAM17 activity in patients in CKD3-5. Circulating ADAM17 activity was also increased in patients that doubled serum creatinine and/or patients that need dialysis therapy being an independent predictor of worsening renal function.

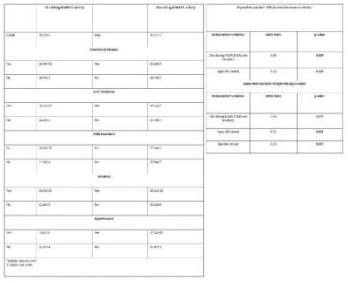

Palau V, Riera M, Benito D, Duran X, Valdivielso JM, Betriu MA, et al. Circulating ADAM17 activity as a marker of CV events in CKD patients (Abstract). Nephrol Dial Transplant. 2018; 33(Suppl_1):i131. *(Abstract awarded with the ERA-EDTA Travel Award).*

Nephrology Dialysis Transplantation

independent predictor for CV events and CV events and/or all mortality causes in CKD patients without previous history of CV disease.

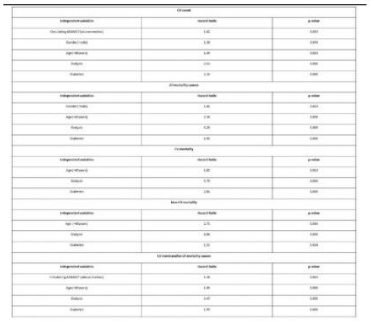

FP296 **CIRCULATING ADAM17 ACTIVITY AS A MARKER OF CV EVENTS IN CKD PATIENTS**

Vanesa Palau[1], Marta Riera[1], David Benito[1], Xavier Duran[3], José Manuel Valdivielso[4], Maria Angeles Betriu[4], Elvira Fernández[4], Julio Pascual[1], Maria José Soler[2]

[1]Nephrology, Hospital del Mar-Institut Hospital del Mar d'Investigacions Mèdiques, Barcelona, Spain, [2]Nephrology. Instituto Carlos III. PI14/00557. FEDER., Hospital del Mar-Institut Hospital del Mar d'Investigacions Mèdiques, Barcelona, Spain, [3]Statistics, Hospital del Mar-Institut Hospital del Mar d'Investigacions Mèdiques, Barcelona, Spain and [4]Nephrology Research Laboratory, Institut de Recerca Biomèdica de Lleida, Lleida, Spain

INTRODUCTION AND AIMS: Previous studies demonstrated a positive correlation between ADAM17 and TNFα in cardiovascular disorder. Increased expression of TNFα and ADAM17 had important implications in advanced cardiac dysfunction. We now studied the relation between baseline circulating ADAM17 activity, cardiovascular event and mortality in CKD patients from NEFRONA study after 48 months of follow-up.

METHODS: 2570 patients without history of CV disease from an observational and multicenter study (NEFRONA project) were divided in three groups: non-dialysis CKD stage 3-5 patients (CKD3-5, n=1463), hemodialysis or peritoneal dialysis patients (CKD5D, n=538) and control patients (CONT, n=569). Baseline circulating ADAM17 activity was analyzed using a fluorimetric assay of plasma samples. Survival was analyzed by Kaplan-Meier curves for the following events: CV event, CV mortality, non-CV mortality and all mortality causes according to ADAM17 activity, diabetes, age, smoking and dialysis requirement. A Cox regression was used to identify risk factors for these events.

RESULTS: Circulating ADAM17 activity was higher in patients with CV events and in patients with CV mortality, non-CV mortality and all-cause mortality ($p<0.05$). Circulating ADAM17 activity, diabetes, male gender, older age (>65 years), those who need dialysis and smoking were risk factors for CV events in CKD patients. Circulating ADAM17 activity, diabetes, older age and those who need dialysis were risk factors for CV mortality and all mortality causes in CKD patients. Diabetes, older age and those who need dialysis but no ADAM17 were risk factors for non-CV mortality. In the multivariate Cox regression model, circulating ADAM17 activity, older age, diabetes and dialysis were identified as independent risk factors for CV events and CV events and/or all mortality causes.

CONCLUSIONS: Higher levels of circulating ADAM17 activity, diabetes, older age and dialysis requirement correlated with a worst survival rate in patients with CV events, CV death and all mortality causes. Circulating ADAM17 activity could be an

doi:10.1093/ndt/gfy104 | i131

Palau V, Riera M, Benito D, Valdivielso JM, Betriu MA, Fernandez E, et al. ADAM17 as a predictor of CV events in CKD patients (Abstract). J Am Soc Nephrol. 2018; 29:238.

TH-PO463

The Cut-Off Value of NT-Pro BNP to Diagnose Cardiac Insufficiency with Both Decreased and Preserved Ejection Fraction Value in Patients with Stage 3 to 5D CKD

Zi Li. *Department of Medicine-Nephrology, West China Hospital of Sichuan University, Chengdu, China.*

Background: BNP and NT-Pro-BNP are widely used in clinical work for the diagnosis of heart failure even in patients with chronic kidney disease(CKD). Previous research focused on the heart failure with decreased ejection fraction (EF). However, heart failure/ insufficiency with preserved EF occurs in a large amount CKD patients especially in the early period. This research is to explore the diagnosis cut-off value of NT-Pro BNP for cardiac insufficiency in CKD patients with stage 3 to 5D, and to analyze its probable influential factors.

Methods: CKD patients with 3 to 5D stages who were hospitalized in the department of nephrology, which belongs to an affiliated hospital of our university, from April 2016 to April 2017 were enrolled. All the patients measured plasma NT-Pro BNP and completed echocardiography within 1 month. Criteria for heart insufficiency included both the patients' symptoms, the 2013 ACCF/AHA heart failure guideline and recommendations and the American Society of Echocardiography as well. Informations of age, sex, weight, height, BMI, blood pressure, NT-ProBNP, GFR, serum electrolytes, index of echocardiography were collected. According to GFR, the patients are divided into three groups: CKD3, CKD4, CKD5 (non-dialysis, hemodialysis, and peritoneal dialysis). SPSS software is used for data analysis.

Results: (1) A total of 396 patients met our inclusion crtieria. NT-Pro BNP was negatively correlated with GFR, EF, sodium, potassium or chloride and positively correlated with E/A, LV, LA, RV, RA, IVS, LVPW, EDD, ESD, EDV, ESV and CKD stages ($p<0.05$). (2) Linear correlation analysis showed ESV, EF, ESD, EDV, E/A, NT-Pro BNP, LV, LA, E/e' correlated with heart failure; multi-factor logistic regression analysis showed that the factors affecting heart failure included E/A, ESV and NT-pro BNP. The diagnostic cut-point value of NT-pro BNP for heart insufficiency increased with the increase of CKD stage (CKD stage 3: 3654.0pg/ml; CKD stage 4: 7584.5pg/ml; CKD stage 5 non-dialysis: 9465.5pg/ml; peritoneal dialysis: 18667.5pg/ml; hemodialysis: 29362.0pg/ml).

Conclusions: NT-Pro BNP cut-off values for cardiac insufficiency should be established according to different CKD stages and considering both decreased and preserved EF value in order to improve early diagnosis and treatment of heart insufficiency.

TH-PO464

N-Terminal Pro-B-Type Natriuretic Peptide and Cardiac Troponin T for Detection of Left Ventricular Hypertrophy in Non-Dialysis CKD Patients

Han Zhang, Jing Chen. *Zhongshan Hospital, Fudan University, Shanghai, China.*

Background: The mortality of cardiovascular disease (CVD) in the patients with chronic kidney disease (CKD) is significantly higher than in the general population. Plasma N-terminal pro-B-type natriuretic peptide (NT-proBNP) and cardiac troponin T (cTnT) have been shown to be powerful predictors of cardiovascular mortality. In subjects with albuminuria or impaired renal function, the use of these cardiac biomarkers has been debated. In this cross-section study, we tried to investigate whether these two biomarkers could predict left ventricular hypertrophy (LVH) in subjects with CKD patients and the prediction power of both.

Methods: A total of 1320 pre-dialysis CKD patients were recruited in this study. NT-pro-BNP and cTnT were all measured on the Roche cobas E602 (Roche Diagnostics). Left ventricular mass index (LVMI) were determined by an echocardiographic examination.

Results: Participants in high NT-proBNP group, as well as participants in high cTnT group, had a worse cardiovascular risk profile and had more LVH. Participants with high cardiac biomarkers had also more often a lower eGFR and higher proteinuria. Multivariable-adjusted association of NT-proBNP level and LVH was OR 1.233(95%CI 1.131 to 1.345) for per 1000pg/ml increase. Multivariable-adjusted association of cTnT level and LVH was OR 1.005(95%CI 1.001 to 1.010)for per 100ng/L increase. Then we identified optimal threshold value for NT-ProBNP and cTnT. The 90th percentile of NT-proBNP had moderately high positive likehood ratios for detecting LVH, 50th percentile of NT-proBNP had moderately low negtive likehood ratios for detecting LVH. The 90th percentile and 50th percentile of cTnT had optimal positive likehood ratios and negtive likehood ratios separately for detecting LVH.

Conclusions: NT-proBNP and cTnT both are independent factors associated with the echocardiographic parameters of LVH in CKD patients. The diagnostic performance of NT-proBNP is significantly superior than cTnT.

Association of NT-proBNP and cTnT with LVH

Variables	NT-proBNPper 1000pg/ml)	cTnTper 100ng/L)
Demographic-adjusted	1.373(1.262-1.495)**	1.014(1.009-1.020)**
Multivariate-adjusted	1.233(1.131-1.345)**	1.005(1.001-1.010)*

Data are presented as OR (95% CI).*P<0.05, **P<0.001.

Left ventricular hypertrophy was defined as LVM/height2.7 >47 g/m2.7 for women and >50 g/m2.7 for men.

TH-PO465

ADAM17 as a Predictor of CV Events in CKD Patients

Vanesa Palau,[1] Marta Riera,[1] David Benito,[1] Jose M. Valdivielso,[3] Angels Betriu,[3] Elvira Fernandez,[3] Julio Pascual,[1,2] Maria Jose Soler.[1,2] *[1]Hospital del Mar Medical Research Institute (IMIM), Barcelona, Spain; [2]Parc de Salut Mar. Fundació IMIM, Barcelona, Spain; [3]IRB LLEIDA, LLEIDA, Spain.*

Background: Previous studies have demonstrated a positive correlation between ADAM17 and TNFα in cardiovascular (CV) disease. Increased expression of TNFα and ADAM17 has important implications in advanced cardiac dysfunction. We studied the relationship between baseline circulating ADAM17 activity, cardiovascular events and mortality in CKD patients from the NEFRONA study after 48 months of follow-up.

Methods: 2,570 patients without history of previous CV disease from the observational and multicenter NEFRONA study were divided into three groups: non-dialysis CKD stage 3-5 patients (CKD3-5, n=1,463), hemodialysis or peritoneal dialysis patients (CKD5D, n=538) and control patients (CONT, n=569). Baseline circulating ADAM17 activity was analyzed using a fluorimetric assay in plasma samples. Survival was analyzed by Kaplan-Meier curves for the following events: CV event, CV mortality, non-CV mortality and all mortality causes according to ADAM17 activity, diabetes, age, smoking and dialysis requirement. Cox regression analyses were used to identify risk factors for these events.

Results: Circulating ADAM17 activity was higher in patients with CV events and in patients with CV mortality, non-CV mortality and all-cause mortality ($p<0.05$). In the unadjusted Cox model, circulating ADAM17 activity was a risk factor for CV events, CV mortality and all-cause mortality in CKD patients. However, circulating ADAM17 was not a risk factor for non-CV mortality. In the multivariate Cox regression model, circulating ADAM17 activity, older age, male sex, diabetes and dialysis were identified as independent risk factors for CV events.

Conclusions: Higher levels of circulating ADAM17 activity correlated with a worst survival rate in patients with CV events, CV death and all mortality causes. Circulating ADAM17 activity could be an independent predictor for CV events in CKD patients without previous history of CV disease.

Funding: Government Support - Non-U.S.

CV events				
	Unadjusted HR (95% CI)	P-value	Adjusted HR (95%CI)	P-value
sADAM17 median(≥14.9)	1.89(1.38-2.59)	**0.000**	1.71(1.22-2.40)	**0.002**
Sex (male)	1.59(1.15-2.20)	**0.005**	1.53(1.10-2.12)	**0.011**
Diabetes	2.31(1.72-3.10)	**0.000**	2.15(1.58-2.91	**0.000**
Hypertension	1.01(0.84-1.22)	0.921	1.18(0.70-2.02)	0.548
Age(≥65 years)	1.75(1.29-2.37)	**0.000**	1.65(1.20-2.26)	**0.002**
CKD stages CKD3-5 Dialysis	2.69(1.98-3.67)	**0.000**	2.60(1.87-3.61)	**0.000**
Smoking	1.25(0.88-1.77)	0.205	1.30(0.91-1.86)	0.148

TH-PO466

α-Adducin Polymorphism's Influence on Ischemic Strokes

Paola Casanova, Lino Merlino, Chiara Lanzani, Laura Zagato, Simona Delli carpini, Elisabetta Messaggio, Paolo Manunta, Marco Simonini. *San Raffaele Scientific Institute, Milan, Italy.*

Background: rs4961 Gly460Trp variant of the alpha Adducin gene (ADD1) has been associated with renal sodium retention and salt sensitive hypertension. Previous studies indicated ADD1 Gly460Trp as associated to higher risk of cardiovascular diseases. The aim of this study is to assess whether there is a correlation between this ADD1 variant and the development of ischemic strokes

Methods: 212 patients with ischemic stroke (IS) were recruited from San Raffaele Hospital in Milan and divided into four categories according to Oxford Classification. These patients were compared to a cohort of elder general population (EGP, 128 patients) and a cohort of hypertensive patients (HYP, 2404 patients), both with no history of strokes.

Results: In IS group mean age at strokes' diagnosis was 72.34±11.9, 61% men, 39% women. The incidence of CV risk factors was: hypertension 66%, diabetes 22%, hypercholesterolemia 40% and hypertriglyceridemia 13%, previous stroke 14%, CKD 16%. Two comparable populations were selected with similar age (71.28±6.9 years for EGP) and with the same incidence of risk factors (for HYP population). Notably, the presence of subjects homozygous for ADD1 mutated allele (rs4961 TrpTrp) is more than double in patients bearing ischemic stroke than in the two others (6.1% IS vs. 2.3% EP, $p=0.049$; 6.1% IS vs. 2.2 HYP, $p=0.009$; fig.1). There was no statistically difference among the various types of stroke.

Conclusions: These data suggest a correlation between mutated alpha-Adducin and the increased incidence of all types of ischemic stroke. No correlation was found with the other hypertension-related genes analysed (as ADD2, ADD3). rs4961 alpha-Adducin polymorphism should be considered as an independent risk factor for ischemic strokes, even if these events donot appear directly linked to hypertension. Finally, alpha-Adducin polymorphism itself might be a candidate gene in the pathogenesis of stroke.

Palau V, Riera M, Benito D, Valdivielso JM, Betriu MA, Fernandez E, et al. Circulating ADAM17 activity as a marker of CKD progression (Abstract). J Am Soc Nephrol. 2018; 29:462.

continuation group was eGFR of 47.9 ml/min/1.73 m^2 and 50.7 ml/min/1.73 m^2 in the PPI discontinuation group. Final eGFR in the PPI continuation group was significantly higher at 51.1 ml/min/1.73m^2 (p=0.01). Final eGFR in the PPI discontinuation group was 51.8 ml/min/1.73m^2 (p=0.3). The average time between baseline and final eGFRs was 270 days in the PPI continuation group and 301 days in the PPI discontinuation group. There was no statistically significant difference in the change in eGFRs between groups (95% CI -5.48-2.03; p=0.37).

Conclusions: Discontinuing a PPI after one year of continuous use in patients with CKD did not impact change in renal function after one year.

FR-PO167

Determining the Association of Allopurinol Prescription on Progression of Renal Dysfunction and Progression to Renal Replacement Therapy in Patients with CKD

Andrew J. Mallett,[1,2] Andrew S. Jeyaruban,[1,2] Anne Cameron (Salisbury),[2] Jianzhen Zhang,[2] Helen G. Healy,[1,2] Wendy E. Hoy,[2] on behalf of the CKD.QLD consortium *[1]Kidney Health Service, Royal Brisbane and Women's Hospital, Brisbane, QLD, Australia; [2]CKD.QLD and the NHMRC CKD.CRE, The University of Queensland, Brisbane, QLD, Australia.*

Background: Reports in the literature link hyperuricaemia with incident chronic kidney disease CKD. However, the relationship between allopurinol prescription and progression of renal dysfunction is not well understood. We aimed to determine the association of allopurinol prescription and changes in kidney function amongst patients with CKD.

Methods: A retrospective cohort study of 1,123 patients of a tertiary teaching hospital registered in the CKD.QLD registry between January 2011 and August 2017 (minimum of 2 years follow-up). Subject demographics (age), health data (BMI, comorbidities, laboratory test results) and allopurinol prescription were extracted from integrated medical records. Delta eGFR (CKD-EPI)was calculated as the difference between latest eGFR and initial eGFR. Subjects were stratified into two groups based on prescription of allopurinol.

Results: Subjects prescribed allopurinol were older (70.7 vs 65.8; p<0.01), had higher BMI (32.3kg/m^2 vs 30.5kg/m^2; p<0.01), worse renal function (35.2mL/min/1.73m^2 vs 43.6mL/min/1.73m^2; p<0.01), higher urate level (0.47mmol/L vs 0.42mmol/L; p<0.01) as well as higher proportion of diabetes (54% vs 46%; p=0.04), dyslipidaemia (54% vs 41%; p<0.01), hypertension (84% vs 72%, p<0.01) and gout (54% vs 11%; p<0.01). The proportion of subjects treated with allopurinol increased with CKD stage; stage 1:1.5%, stage 2:7.1%, stage 3: 21.7%, stage 4: 21.4% stage 5:17.3%. Prescription of allopurinol did not have a significant association with delta eGFR in patients with hyperuricaemia (1.8mL/min/1.73m^2/yearvs 1.6mL/min/1.73 m^2/year; p=0.2) or gout (2.2mL/min/1.73m^2/year vs 1.8mL/min/1.73m^2/year; p=0.5). Nor was allopurinol prescription in the subgroup with serum urate level < 0.36mmol/L associated with a significant change in delta eGFR (3.5mL/min/1.73m^2/year vs 1.6mL/min/1.73m^2/year;p=0.17). Multivariate analysis adjusting for age and comorbidities found no significant association of allopurinol prescription with either delta eGFR or progression to kidney replacement therapy (p>0.05).

Conclusions: Allopurinol prescription was more prevalent in advanced CKD. However, it did not appear to be independently associated with deterioration of kidney function.

FR-PO168

Association Between Plasma Myostatin Levels and Loop Diuretic Use in Non-Dialysis-Dependent CKD Patients

Seiko Ishikawa,[1,2] Shotaro Naito,[2] Soichiro Iimori,[2] Kiyoshi Isobe,[2] Naohiro Nomura,[2] Eisei Sohara,[2] Tomokazu Okado,[2] Tatemitsu Rai,[2] Shinichi Uchida.[2] *[1]Tokyo Kyosai Hospital, Tokyo, Japan; [2]Department of Nephrology, Tokyo Medical and Dental University, Tokyo, Japan.*

Background: Myostatin (MSTN) is mainly synthesized in skeletal muscles and acts as a negative regulator of skeletal muscle mass. It is up-regulated in patients with chronic kidney disease (CKD) and considered to be associated with the development of sarcopenia. Recently, we have reported that loop diuretics, commonly used in patients with advanced CKD, suppress skeletal muscle differentiation (Mandai S. Sci Rep. 2017). So far, the association between serum MSTN (sMSTN) levels and loop diuretic use is unknown.

Methods: We conducted a cross-sectional study comprised of 362 non-dialysis-dependent CKD patients over 20 years of age. The primary outcome was sMSTN levels. Multiple linear regression analyses were conducted to assess the associations between sMSTN levels (logarithmically transformed) and baseline characteristics including skeletal mass index (SMI). Interaction between loop diuretic use and SMI to sMSTN levels was estimated after stratifying patients by loop diuretic use. We calculated SMI as follows: Total body skeletal muscle mass measured by DEXA was divided by height squared.

Results: Median age was 71 years, 64.4% were male, mean SMI was 6.49 kg/m^2, mean eGFRcysC was 39.0 ml/min/1.73m^2, median sMSTN level was 1130 pg/ml, and 14.6% were treated with loop diuretics. Multivariate analysis showed that sMSTN levels were positively correlated with SMI (β=0.128, *P*<0.001), and negatively with eGFRcysC and loop diuretic use (β=-0.004, *P*=0.005 and β=-0.231, *P*<0.001, respectively). When stratified by loop diuretic use, adjusted coefficient β of SMI for sMSTN was higher in patients treated with loop diuretics than in patients not treated with loop diuretics (β=0.237, *P*=0.001 and β=0.118 *P*<0.001), respectively).

Conclusions: Loop diuretic use was independently associated with lower sMSTN levels. This result indicates that loop diuretics serve as negative regulator of skeletal muscle mass and therefore sMSTN levels may be attenuated by negative feedback. However, the increase of sMSTN level associated with SMI among the patients treated with loop diuretics was larger than those without loop diuretics. Other potential factors which elevate sMSTN levels in patients treated with loop diuretics are suggested to affect the relationship between sMSTN levels and SMI.

FR-PO169

Circulating ADAM17 Activity as a Marker of CKD Progression

Vanesa Palau,[1] Maria Jose Soler,[1,2] David Benito,[1] Jose M. Valdivielso,[3] Angels Betriu,[3] Elvira Fernandez,[3] Julio Pascual,[1,2] Marta Riera.[1] *[1]Hospital del Mar Medical Research Institute (IMIM), Barcelona, Spain; [2]Parc de Salut Mar. Fundació IMIM, Barcelona, Spain; [3]IRB LLEIDA, LLEIDA, Spain.*

Background: Several substrates for ADAM17 have been identified, including TNF-α, EGFR ligands, L-selectin, VCAM-1 and angiotensin converting enzyme(ACE)2. We have studied circulating ADAM17 in chronic kidney disease(CKD) patients from the NEFRONA cohort study.

Methods: 2032 patients without history of CV disease from an observational and multicenter study (NEFRONA project) divided into two groups: non-dialysis CKD stage 3-5 patients and control patients were studied. Baseline circulating ADAM17 activity was analyzed using a fluorimetric assay in plasma samples. Increased serum creatinine and dialysis requirement after 24months of follow-up depending on basal circulating ADAM17 activity were studied. Logistic regression analyses were used to identify predictors of increasing serum creatinine and risk of dialysis requirement.

Results: Circulating ADAM17 activity was significantly increased in CKD3-5 patients as compared to CONT(p<0.05). Baseline circulating ADAM17 activity was higher in patients with a 30% increase in serum creatinine levels after 2 years(p<0.05). Circulating ADAM17 activity was also higher in patients that needed dialysis in comparison with patients that maintained kidney function(p<0.05). After multivariate logistic regression analysis we found an interaction between sex and sADAM17 activity for increasing 30% serum creatinine, dialysis requirement and composite renal outcome(p<0.05). Therefore, we decided to perform the analysis stratifying by sex. Increased ADAM17 activity was independently associated with CKD progression regarding 30% increase in serum creatinine, dialysis requirement and composite renal end point but only in males. In females, ADAM17 activity was not associated with CKD progression.

Conclusions: Circulating ADAM17 activity was increased in CKD patients. Circulating ADAM17 activity was increased in patients that doubled serum creatinine and/or patients that need dialysis therapy being an independent predictor of worsening renal function in males.

Funding: Government Support - Non-U.S.

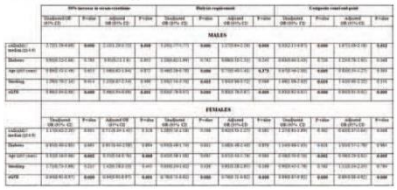

FR-PO170

Association of Serum Uromodulin with ESRD and Kidney Function Decline in the Elderly – The Cardiovascular Health Study

Dominik Steubl,[1] Petra Buzkova,[8] Pranav S. Garimella,[2] Joachim H. Ix,[2] Prasad Devarajan,[3] Michael R. Bennett,[4] Paulo H. Chaves,[7] Michael Shlipak,[5] Mark J. Sarnak.[6] *[1]Tufts Medical Center, Tufts University, Boston, MA; [2]UCSD, San Diego, CA; [3]Cincinnati Children's Hospital, Cincinnati, OH; [4]Cincinnati Children's Hospital Medical Center, Cincinnati, OH; [5]San Francisco VA Medical Center, San Francisco, CA; [6]Tufts Medical Center, Boston, MA; [7]Florida International University, Miami, FL; [8]UW, Seattle, WA.*

Background: Uromodulin is released by tubular epithelial cells into the serum (sUMOD) and low levels are associated with tubular atrophy and interstitial fibrosis (IF/TA). However, little is known about the association of sUMOD with long-term kidney outcomes in the elderly, a population with a high prevalence of IF/TA.

Methods: We assessed the association of sUMOD with end-stage-renal-disease (ESRD) in a random subcohort (n=933) plus all additional cases of ESRD in the Cardiovascular Health Study using a modified Cox regression analysis. We also evaluated the association of sUMOD with kidney function decline (≥30% decline of estimated glomerular filtration rate (eGFR) at 10 years of follow up) using logistic regression. Sampling for the latter was from the random subcohort as well as all additional cases. Models were adjusted for demographics, eGFR, albuminuria and other risk factors.

Results: Mean age of the random subcohort was 78 years, 40% were male, and 15% were non-white. Mean±SD sUMOD level was 127±64 ng/ml and eGFR was 63±19 ml/min/1.73 m^2. 53 participants experienced ESRD during a median follow-up 9.9 years. Higher sUMOD was associated with lower hazard for ESRD in univariate analysis (Figure). In multivariable analysis each 1 SD higher sUMOD was associated with a 63% lower risk of ESRD (HR 0.37 (95%-CI 0.14-0.95)). 179 participants experienced kidney function decline. In demographic adjusted analyses, higher sUMOD was associated with lower

Palau V, Riera M, Benito D, Pascual J, Soler MJ. Endothelial ADAM17 deletion attenuates diabetic nephropathy damage through PI3K/AKT signaling pathway (Abstract). Nephrol Dial Transplant. 2019; 34(Suppl_1):i23.

Nephrology Dialysis Transplantation 34 (Supplement 1): i23–i25, 2019
doi:10.1093/ndt/gfz096

FO050 **ENDOTHELIAL ADAM17 DELETION ATTENUATES DIABETIC NEPHROPATHY DAMAGE THROUGH PI3K/AKT SIGNALING PATHWAY**

Vanesa Palau[1], Marta Riera[1], David Benito[1], Julio Pascual[1], Maria José Soler[2]
[1]*Institut Hospital del Mar d'Investigacions Mèdiques IMIM, Barcelona, Spain and*
[2]*Institut Hospital del Mar d'Investigacions Mèdiques IMIM. pi17/00257, Barcelona, Spain*

INTRODUCTION: ADAM17 is a disintegrin and metalloproteinase initially described to cleave the tumor necrosis factor α (TNFα). It is known that it can also release ectodomains of diverse molecules such as, transforming growth factor α (TGFα), L-selectin, and angiotensin-converting enzyme 2 (ACE2). Renal ADAM17 is increased in diabetic mice and insulin treatment attenuates its expression. We now studied the effect of specific endothelial ADAM17 deletion in diabetic nephropathy.

METHODS: Diabetes was induced by streptozotocin (STZ) injection on inducible endothelial ADAM17 knockout mice. Renal weight/body weight (RW/BW) ratio, heart weight/body weight (HW/BW) ratio, and urinary albumin excretion (UAE) were determined. Glomerular lesions were evaluated by mesangial matrix expansion and podocyte number. TNFR gene expression was determined and pAKT/AKT ratio was analyzed as pAKT versus AKT expression ratio. Circulating and renal ACE and ACE2 activity were analyzed.

RESULTS: Diabetic mice presented higher RW/BW ratio and higher UAE as compared with control mice. Endothelial ADAM17 knockout mice exhibited higher HW/BW ratio than wild-type mice. Diabetes reduced podocyte number, increased glomerular area and mesangial matrix expansion in wild-type mice. ADAM17 deletion attenuated mesangial matrix expansion in diabetic mice. All diabetic mice presented higher TNFR1 and TNFR2 gene expression in comparison with non-diabetic mice. TNFR1 gene expression was increased in knockout diabetic mice compared with diabetic wild-type mice. pAkt/Akt ratio was increased only in diabetic wild-type mice compared with non-diabetic mice. ADAM17 deletion prevented this increase. Diabetic groups presented higher circulating ACE2 enzymatic activity. At renal level ACE2 activity was significantly increased in diabetic knockout mice as compared with diabetic wild-type mice. Renal ACE activity was decreased in all diabetic groups.

CONCLUSIONS: Endothelial ADAM17 deletion attenuates diabetic nephropathy through pAkt/Akt signaling pathway. In addition, ADAM17 deletion exacerbates TNFR1 gene increase in diabetic mice ascribed to the reduced endothelial ADAM17 shedding. ADAM17 and TNFα signaling pathway at endothelial level are implicated in diabetic nephropathy progression.

	WT-NoDB	WT-DB	KO-NoDB	KO-DB
RW/BW	0.97±0.1	1.45±0.2*	1.00±0.0	1.49±0.1*
HW/BW	0.44±0.02	0.37±0.02	0.52±0.03$	0.47±0.02$
UAE (µg Alb/mg Crea)	59.22±24.04	457.9±175.73*	28.44±5.05	270.23±100.78*
WT-1	8.71±0.23	8.05±0.17*	9.34±0.26$	8.54±0.20*
Glomerular area (µm^2)	3517.23±252.20	4378.06±247.04*	3925.65±169.53	3805.01±176.26
Mesangial area (µm^2)	1137.23±83.04	1651.73±94.69*	1183.68±65.73	1344.35±94.04$
TNFR1 gene expression	0.96±0.07	1.45±0.06*	1.12±0.07	2.05±0.16*$
TNFR2 gene expression	0.94±0.10	1.85±0.24*	1.30±0.15	2.12±0.33*
pAkt/Akt	0.67±0.08	1.21±0.16*	0.84±0.05	0.92±0.10
Circulating ACE2 activity (RFU/µl)	290.58±10.14	624.76±90.99*	298.5±17.22	668.63±58.57*
Renal ACE2 activity (RFU/µg/h)	481.31±32.70	568.66±47.71	511.98±62.25	733.69±53.71*$
Circulating ACE activity (RFU/µl)	35354.74±2176.48	36706.86±2052.20	40935.67±4445.26	32482.83±2871.14
Renal ACE activity (RFU/µg/h)	5543.21±1127.74	2566.08±591.36*	6569.44±1600.59	2548.00±938.67*

* p≤0.05 DB vs NoDB $ p≤0.05 KO vs WT

FO050 Table

Palau V, Nugraha B, Emmert M, Hoerstrup S, Pascual J, Soler MJ, et al. Human kidney proximal tubular 3D spheroids to study the role of ADAM17 in diabetic nephropathy (Abstract). Nephrol Dial Transplant. 2020; 35(Suppl_3):iii31. *(Abstract awarded with the 2020 ERA-EDTA Virtual Access Grants)*.

Nephrology Dialysis Transplantation

SO026 **HUMAN KIDNEY PROXIMAL TUBULAR 3D SPHEROIDS TO STUDY THE ROLE OF ADAM17 IN DIABETIC NEPHROPATHY**

Vanesa Palau[1], Bramasta Nugraha[2], Maximilian Emmert[3], Simon Hoerstrup[3], Julio Pascual Santos[1], Maria Jose Soler Romeo[4], Marta Riera[1]

[1]IMIM, Nephrology, Barcelona, Spain, [2]Institut für Parasitologie Universität ZH, Zürich, Switzerland, [3]Institute for Regenerative Medicine - IREM, Schlieren, Switzerland and [4]VHIR - Vall d'Hebron Institut de Recerca, Nephrology, Barcelona, Spain

Background and Aims: ADAM17 is a disintegrin and metalloproteinase initially described to cleave the tumor necrosis factor α (TNFα). Currently, it is known that it can also release ectodomains of a diverse variety of molecules such as, transforming growth factor α (TGFα), L-selectin, and angiotensin-converting enzyme 2 (ACE2). It has been shown that ADAM17 protein expression increases in kidney mesangial cells after incubation with high glucose media mimicking what has been observed in diabetic patients and experimental models of diabetic nephropathy. We now studied the effect ADAM17 deletion on human kidney cells (HKC-8) in a 3D spheroids *in vitro* cell culture incubated with high glucose, low glucose and mannitol medium resembling the *in vivo* human kidney diabetic environment.

Method: ADAM17 deletion was performed using the CRISPR/Cas9 technology. HKC8 cells grew inside a RGD-functionalized dextran hydrogel to obtain 3D spheroids. 13 days post-seeding, the spheroids were incubated with 35mM of D-glucose (HG), 5mM of D-glucose (LG) or 35mM of mannitol as osmotic control for 6h, 24h or 72h. The quality of the established 3D cell culture of mature HKC-8 spheroids was assessed by Aquoporin-1 and Glut-1 staining. After incubations quantitative-PCR analyses were performed for fibrotic and inflammatory markers. Immunofluorescence for fibrotic markers was performed on HKC-8 spheroids incubated for 72h.

Results: High glucose (HG) medium induced CCL5 gene expression on wild-type HKC-8 spheroids after 6h and 24h of incubation in comparison with the control group. Interestingly, in the ADAM17-deleted spheroids, CCL5 gene expression maintained similar to control after 6h of incubation with HG medium and tended to decrease after 24h of incubation in comparison with the wild-type. Collagen IV gene expression was increased in the wild-type spheroids incubated with HG in comparison with the control group. In ADAM17-deleted spheroids, Collagen IV gene expression was significantly decreased in the cells incubated with HG in comparison with the wild-type cells incubated with HG. HG increased the expression of α-SMA, fibronectin and Collagen IV in wild-type spheroids. Adam17 deletion blocked the increase of α-SMA, fibronectin and Collagen IV expression compared with wild-type cells after 72h of incubation.

Conclusion: ADAM17 blockade protects against fibrosis and inflammation in human kidney tubular spheroids under high glucose.

Table 1

	CCL5		Collagen IV	
	6h	24h	6h	24h
LG-WT	1.47±0.77	1.23±0.39	1.00±0.22	1.10±0.26
HG-WT	4.70±2.19*	5.64±1.67*	1.44±0.61	13.97±1.54*
M-WT	1.21±0.67	1.15±0.75#	1.43±0.23	0.72±0.26#
LG-KO	1.96±0.93	1.44±0.41	0.62±0.12	2.20±0.44
HG-KO	1.04±0.28	2.73±0.24*	1.00±0.59	3.21±1.43$
M-KO	0.77±0.14	1.56±0.74	1.01±0.10	1.27±0.54

*p<0.05 HG vs. LG;
$p<0.05 KO vs. WT;
#p<0.05 M vs. HG

	CCL5		Collagen IV	
	6h	24h	6h	24h
LG-WT	1.47±0.77	1.23±0.39	1.00±0.22	1.10±0.26
HG-WT	4.70±2.19*	5.64±1.67*	1.44±0.61	13.97±1.54*
M-WT	1.21±0.67	1.15±0.75#	1.43±0.23	0.72±0.26#
LG-KO	1.96±0.93	1.44±0.41	0.62±0.12	2.20±0.44
HG-KO	1.04±0.28	2.73±0.24*	1.00±0.59	3.21±1.43$
M-KO	0.77±0.14	1.56±0.74	1.01±0.10	1.27±0.54

*p<0.05 HG vs. LG; $p<0.05 KO vs. WT; #p<0.05 M vs. HG

Immunofluorescence Collagen IV

Immunofluorescence α-SMA

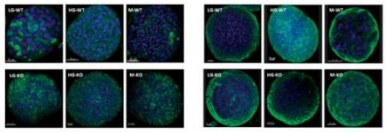

Immunofluorescence Fibronectin

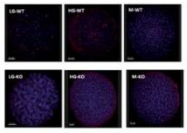

Figure:

doi:10.1093/ndt/gfaa139 | iii31

10.2.2 National congresses

Palau V, Riera M, Benito D, Pascual J, Soler MJ. La deleción específica del ADAM17 en endotelio protege ante la nefropatía diabética (Abstract). Nefrología. 2018; 38(suppl_1):5.

Diabetes

1 ••• RELACIÓN DE LOS NIVELES CIRCULANTES DE LA METALOPROTEINASA-10 (MMP-10) Y SU INHIBIDOR TIMP-1 CON LA ENFERMEDAD RENAL EN PACIENTES CON DIABETES MELLITUS TIPO 2

O.I. GONZALEZ[1], J.M. MORA[1], C.I. ALFARO[1], J. ESCALADA[2], J.A. PARAMO[3], F. SLON[4], M.J. SOLER[5], F.J. LAVILLA[1], P.L. MARTIN[1], N. GARCIA-FERNANDEZ[1]

[1]NEFROLOGIA. CLINICA UNIVERSIDAD DE NAVARRA (PAMPLONA), [2]ENDOCRINOLOGÍA. CLINICA UNIVERSIDAD DE NAVARRA (PAMPLONA), [3]HEMATOLOGIA Y ATEROTROMBOSIS. CLINICA UNIVERSIDAD DE NAVARRA (PAMPLONA), [4]NEFROLOGIA. COMPLEJO HOSPITALARIO DE NAVARRA (PAMPLONA), [5]NEFROLOGIA. HOSPITAL DEL MAR (BARCELONA)

Introducción: La diabetes mellitus tipo 2 (DM2) es la primera causa de enfermedad renal crónica en nuestro medio. Entre los mecanismos de daño renal en esta nefropatía se describe un desequilibrio entre la síntesis y degradación de la matriz extracelular (MEC). Las metaloproteinasas (MMPs) y sus inhibidores, que intervienen en ese remodelado de la MEC, podrían estar involucradas en el daño tisular renal de los pacientes con DM2.

Objetivo: Estudiar los niveles séricos de MMP-10 y su inhibidor TIMP-1 en pacientes con DM2 con distintos grados de nefropatía como marcadores precoces de enfermedad.

Métodos: Estudiados 268 pacientes con DM2 y 111 sanos. En todos ellos se midió en suero MMP-10 y TIMP-1 mediante ELISA (Quantikine; R&D Systems, Abingdon, UK). Además, se recogieron datos clínicos y demográficos. Los pacientes se clasificaron en cuatro grupos de acuerdo a la estimación de filtrado glomerular por MDRD-4 (sGFR) y en tres grupos según grado de albuminuria (A1: 300 mg/g). Se realizaron estudios de comparación de muestras, análisis de covarianza (ANCOVA) y correlaciones. El análisis estadístico se realizó mediante el software R (The R Foundation for Statistical Computing, version 3.0.3).

Resultados: Los pacientes diabéticos respecto a los sanos mostraron niveles séricos superiores de MMP-10 (473 ± 274 pg/mL vs 332 ± 151 pg/mL, p<0.01) y de TIMP-1 (573 ± 296 ng/mL vs 375 ± 317 ng/mL; p<0.001). Por otro lado, ambos biomarcadores, MMP-10 y TIMP-1, aumentaban con la progresión de la nefropatía tanto por estimación del filtrado glomerular (Figura 1A y 1B) como por albuminuria (Figura 1C y 1D).

Conclusión: En los pacientes con DM 2, los niveles séricos de MMP-10 y TIMP-1 podrían ser marcadores precoces de enfermedad renal y predictores de progresión de la nefropatía.

Figura 1. Niveles séricos de MMP-10 y TIMP-1 en pacientes controles y diabéticos tipo 2 con diferente grado de función renal y albuminuria.

Figure 1A y 1B. Grupos de pacientes definidos por filtrado glomerular (eGFR por MDRD-4): G1: >90; G2: 90-60; G3: 60-30; G4: <30 ml/min/1.73 m². *p<0,05, **p<0,01, ***p<0,001
Figure 1C y 1D. Grupos de pacientes definidos por albuminuria (estimada en cómo cociente albúmina-creatinina en muestra única) (mg/g): A1: <30; A2: 30-300; A3: >300. ***p<0,001

2 ••• LA DELECIÓN ESPECÍFICA DEL ADAM17 EN ENDOTELIO PROTEGE ANTE LA NEFROPATÍA DIABÉTICA

V. PALAU[1], M. RIERA[1], D. BENITO[1], J. PASCUAL[1], MJ. SOLER[1]

[1]SERVICIO DE NEFROLOGÍA. HOSPITAL DEL MAR-INSTITUT HOSPITAL DEL MAR D'INVESTIGACIONS MÈDIQUES (BARCELONA)

Introducción: ADAM17 participa en el shedding de varias moléculas incluyendo TNF-alpha, L-selectina, molécula de citoadhesión vascular- 1(VCAM1) y el enzima conversor de la angiotensina (ECA) 2. ADAM17 está aumentado en modelos murinos de diabetes y la insulina es capaz de normalizar su expresión. Nos proponemos estudiar el efecto de la deleción del ADAM17 endotelial en la nefropatía diabética.

Materiales y métodos: Se utilizaron ratones macho diabéticos tipo 1 por estreptozotocina (STZ) y knockout de ADAM17 a nivel endotelial (ADAM17Fl/Fl-CrePDGF+/+). Se determinó presión arterial (PA),cociente peso renal/peso corporal (PR/PC), peso corazón/peso corporal (PH/PC), tasa de filtración glomerular (TFG), excreción urinaria de albúmina (EUA) y se realizó tinción de Wilms Tumor-1 (WT-1) como marcador de podocitos y de ácido periódico de Schiff (PAS) para determinar expansión de la matriz mesangial.

Resultados: Los ratones diabéticos presentaban menor peso corporal y mayor cociente PR/PC, menor TFG y mayor EUA en comparación con los no diabéticos. Los ratones ADAM17KO endotelial presentaban mayor PH/PC en comparación con los wild-type. No se observaron cambios en la PA entre grupos. El grupo wild-type diabético mostró una disminución del número de podocitos, aumento del área glomerular y expansión de la matriz mesangial en comparación con los controles. En ratones ADAM17KO diabéticos y controles, no se observaron cambios en cuanto al tamaño renal. En cambio, en los ADAM17KO diabéticos la expansión de la matriz mesangial se veía disminuida comparado con los wild-type.

Conclusión: En los ratones diabéticos STZ la deleción del ADAM17 a nivel endotelial evita la aparición de hipertrofia glomerular y expansión de la matriz mesangial. ADAM17 puede tener un papel activador en la lesión renal diabética.

Tabla.

	Peso corporal (g)	Ratio peso riñón/peso corporal	Ratio peso corazón/peso corporal	TFG (µL/min)	EUA (µg Alb/mg Crea)	WT-1 (nº de podocitos)	Área glomerular (µm²)	Área mesangial (µm²)
ADAM17WT-NoDB	34,62±3,7	0,97±0,1	0,44±0,02	34,91±7,21	59,22± 24,04	8,62± 0,24	3517,23± 252,20	1137,23± 83,04
ADAM17WT-DB	26,35±1,9*	1,45±0,2*	0,37±0,02	17,15±3,58*	457,9± 175,73*	8,11± 0,18*	4378,06± 247,04*	1651,73± 94,69*
ADAM17KO-NoDB	33,09±1,2	1,00±0,0	0,52±0,03§	29,58±7,21	28,44± 5,05	9,41± 0,27§	3925,65± 169,53	1183,68± 65,73
ADAM17KO-DB	23,16±1,3*§	1,49±0,1*§	0,47±0,02§	13,28±3,27*§	270,23± 100,78*§	8,54± 0,20*§	3805,01± 176,26	1344,35± 94,04§

*ps0,05 DB vs NoDB §ps0,05 KO vs WT

3 ••• LOS PACIENTES DIABÉTICOS AFECTOS DE NEFROPATÍA DIABÉTICA TIENEN PEOR PRONÓSTICO RENAL:RESULTADOS PRELIMINARES ESTUDIO MULTICÉNTRICO ESPAÑOL BIODIAB-GLOSEN-GEENDIAB

S. BERMEJO[1], E. GONZÁLEZ[2], K. LÓPEZ[2], A. MARTÍN-GÓMEZ[3], D. LÓPEZ[3], N. ESPARZA[4], A. COLOMA[5], J. PASCUAL[1], X. FULLADOSA[6], MJ. SOLER[1]

[1]NEFROLOGÍA. HOSPITAL DEL MAR (BARCELONA), [2]NEFROLOGÍA. HOSPITAL 12 DE OCTUBRE (MADRID), [3]NEFROLOGÍA. HOSPITAL UNIVERSITARIO FUNDACIÓN ALCORCÓN (MADRID), [4]NEFROLOGÍA. HOSPITAL DE PONIENTE (ALMERÍA), [5]NEFROLOGÍA. CLÍNICA UNIVERSITARIA DE NAVARRA (PAMPLONA), [6]NEFROLOGÍA. HOSPITAL UNIVERSITARIO INSULAR DE GRAN CANARIA (LAS PALMAS DE GRAN CANARIA), [7]NEFROLOGÍA. HOSPITAL SAN PEDRO (LOGROÑO), [8]NEFROLOGÍA. HOSPITAL DE BELLVITGE (L'HOSPITALET DE LLOBREGAT)

El trabajo corresponde a un grupo de trabajo o un estudio multicéntrico: GLOSEN. GEENDIAB.

Objetivos: El paciente diabético con nefropatía muestra lesiones muy diversas en la biopsia renal, con una elevada prevalencia de lesiones no diabéticas. La supervivencia renal y del paciente diferenciando la afectación por nefropatía diabética (ND) o no-nefropatía diabética (NND) se desconoce.

Material y métodos: Estudio descriptivo retrospectivo multicéntrico español de los pacientes diabéticos con biopsia renal en el período 2002-2014. Se han estudiado un total de 18 centros incluyendo 791 pacientes, se revisaron datos clínicos, analíticos y la supervivencia renal (necesidad de terapia renal sustitutiva (TRS)) y la supervivencia del paciente.

Resultados: La cohorte de 791 pacientes incluye 584 hombres (73,8%), edad media de 61,8±12,8 años, creatinina sérica media 2,8±2,3mg/dl, hemoglobina glicosilada 6,9± 1,6% y proteinuria de 2,6 (RIQ 1,2-5,3) gr/24h. El tiempo de evolución de la DM fue de10,8±8,8años. El 24,4% (n=193) presentabanretinopatiadiabética, 17,8 %(n=141)vasculopatiaperiférica y 16,7% (n=132) cardiopatiaisquémica. 542 pacientes (68,5%)tratamiento con bloqueadores del SRAA. En la biopsia renal, 39,8%(n=315) presentaban ND, 50,1%(n=396) NND y 10,1%(n=80) ND+NND. La NND más frecuente fue nefroangioesclerosis (n=86, 11%), nefropatía IgA (n=42, 5,3%), nefritis intersticial aguda (n=40, 5%) y nefropatía membranosa(n=40, 5%). Necesitaron tratamiento sustitutivo renal un 39,4% (n=312);51,9% afectos de ND, 35,6% afectos de NND y el 12,5% afectos de ND y NND. La mortalidad global de los pacientes estudiados fue del 21,2% (n=168);de los cuales 47% con ND, 39,9% con NND y13,1% con ND y NND.

En el análisis de supervivencia mediante las curvas de Kaplan-Meier observamos que los pacientes afectos de ND o ND+NND presentaron peor pronóstico renal que los afectos de NND(p<0,001) y mayor mortalidad (p=0,01). En el análisis multivariado de Cox, ajustando por sexo, edad, creatinina entre otros se confirma como factor de riesgo independiente de TRS edad (HR 0,977; 0,962-0,992, p=0,004), peor función renal (creatinina (HR 1,17; 1,034-1,325, p=0,013) y FG(HR 0,977; 0,964-0,991, p=0,001)), mayor proteinuria(HR 1,089; 1,047-1,134, p<0,001), no seguir tratamiento con BSRAA(HR 0,581; 0,373-0,906, p=0,017) y la nefropatía diabética(HR 1,804; 1,174-2,774, p=0,007). En cuanto a la mortalidad, únicamente la edad edad avanzada se confirma como factor de riesgo independiente (HR 1,045; 1,016-1,075, p=0,002).

Conclusiones: En los pacientes diabéticos con biopsia renal, los afectos de ND tienen peor pronóstico renal que aquéllos con NND. El diagnóstico histológico de la afectación renal en el diabético puede facilitar un tratamiento eficaz y una mejoría en el pronóstico.

4 •• LIRAGLUTIDE EN DIABÉTICOS CON ENFERMEDAD RENAL G3B: EFICAZ, SEGURO CON DESCENSO DE LA ALBUMINURIA. EXPERIENCIA A 3 AÑOS

B. AVILES BUENO[1], MD. GARCÍA DE LUCAS[2], J. OLALLA SIERRA[2]

[1]NEFROLOGÍA. HOSPITAL COSTA DEL SOL (MARBELLA/ESPAÑA),[2]MEDICINA INTERNA. HOSPITAL COSTA DEL SOL (MARBELLA/ESPAÑA)

Introducción: Comunicamos la eficacia, seguridad y evolución de la función renal en pacientes obesos con diabetes tipo 2 (DM2) y enfermedad renal crónica grado 3B (ERC G3B) tratados con liraglutide durante 3 años.

Material y métodos: Estudio retrospectivo en 28 pacientes con DM2, ERC 3B, IMC > 27 kg/m2 y HbA1c > 7% tras 40 meses de tratamiento con liraglutide 1,8 mg/día. Los resultados se expresan en medias con desviación estándar.

Resultados: La antigüedad del diagnóstico de DM2 era de 17,95 (± 6,34) años. Diez paciente eran mujeres (35 %), la media de edad de 69,39 (± 7,06) años. 5 fumaban, 24 recibían antihipertensivos, 22 estatinas, 18 insulina lenta y 12 insulina prandial. 58 % tenían cardiopatía isquémica, 44 % retinopatía, 13 % ACVA, 47 % arteriopatía periférica. El índice de Charlson de 7,97 ± 1,40. Tabla 1: Las necesidades de insulina prandial y basal disminuyeron un 67.5% y 30% llegando a suspenderse en 32% y 14.2% casos respectivamente. Sólo se observó una hipoglucemia leve diurna. No se describieron efectos secundarios relevantes, ni hubo que suspender ningún tratamiento. Detectamos un descenso significativo de la albuminuria (UACR), que también podría estar en relación con el mejor control de TA, glucémico y la pérdida de peso. Y una leve mejoría del filtrado glomerular (FGe por CKD-EPI). Aunque en los grandes estudios previos con liraglutide se estima el FG por CKD-EPI o MDRD, pensamos que debería calcularse mediante aclaramiento de creatinina en orina de 24 horas al tratarse de pacientes obesos.

Tabla 1

	Inicio estudio	40 meses	p < 0,05
Peso (Kg)	98,25 ± 13,67	91,60 ± 12,16	0,0005
IMC (kg/m²)	36,38 ± 4,79	33,64 ± 4,12	0,0005
Perimetro abdominal (cm)	118,8 ± 19,14	107,46 ± 9,47	0,0005
TAS (mmHg)	125,57 ± 13,32	120,00 ± 7,07	0,029
TAD (mmHg)	73,10 ± 6,10	68,57 ± 4,87	0,002
Insu basal (UI/dia)	59,05 ± 31,29	41,55 ± 18,77	0,008
Insu prandial (UI/dia)	40,37 ± 27,83	13,0 ± 24,42	0,012
Gluc basal (mg/dl)	171,60 ± 59,24	129, 14 ± 27,56	0,005
HbA1c (%)	8,42 ± 1,80	7,09 ± 0,67	0,0005
Creat basal (mg/dl)	1,62 ± 0,40	1,43 ± 0,39	0,001
FG (ml/min/1.73m²) (CKD-EPI)	41,00 ± 9,49	47,14 ± 11,47	0,001
U_{Alb} (mg/g)	126,28 ± 169,76	84,23 ± 123,88	0,009
Hipoglucemias leves (n)	4	1	

Conclusiones: Liraglutide parece una terapia eficaz bien tolerada y segura en pacientes DM2 con ERC G3B y obesidad. Favorece la pérdida de peso, mejora el control glucémico y de la TA. Ayudaría a disminuir la albuminuria preservando la función renal. Nuestros resultados deben confirmarse en amplios estudios específicos para pacientes diabéticos obesos con enfermedad renal crónica.

••• Presentación oral •• E-póster • Póster

5

Palau V, Riera M, Valdivielso JM, Duran X, Vázquez S, Betriu A, et al. La actividad circulante del ADAM17 como biomarcador de evento cardiovascular en pacientes con ERC (Abstract). Nefrología. 2018; 38(suppl_1):94.

Hipertensión arterial, riesgo cardiovascular, hemodinámica y regulación vascular

343 ••• ESTADOS HIPERTENSIVOS DEL EMBARAZO: COMPORTAMIENTO DE LOS PARÁMETROS DE RIGIDEZ ARTERIAL, LA ECOGRAFÍA DOPPLER UTERINA Y LOS MARCADORES SEROLÓGICOS

MP. VALENZUELA MUJICA[1], A. RODRÍGUEZ VICENTE[2], M. BOLÓS CONTADOR[1], Q. SUN LIN[2], R. SALVADOR CARBÓ[1], J. COSTA PUEYO[2], L. BETANCOURT CASTELLANOS[1], M. COMAS ROVIRA[2], MJ. AMENGUAL GUEDÁN[2], J. ALMIRALL DALY[1]

[1]SERVICIO DE NEFROLOGÍA. PARC TAULÍ SABADELL. HOSPITAL UNIVERSITARI (UAB) (BARCELONA),[2]SERVICIO DE GINECOLOGÍA Y OBSTETRÍCIA. PARC TAULÍ SABADELL. HOSPITAL UNIVERSITARI (UAB) (BARCELONA), [3]UDIAT-LABORATORIO. PARC TAULÍ SABADELL. HOSPITAL UNIVERSITARI (UAB) (BARCELONA)

Introducción: La enfermedad hipertensiva del embarazo (EHE) es una patología relativamente infrecuente, aunque con una morbimortalidad materno-fetal elevada. Los métodos de screening actuales detectan solamente 1/3 de casos. Los avances en el conocimiento de su fisiopatología ha motivado la evaluación de nuevas herramientas de detección precoz.

Objetivo: Analizar el comportamiento durante la gestación de: rigidez arterial, Doppler de arterias uterinas y factores placentarios, comparando un grupo de gestantes sanas, con un grupo de gestantes con factores de riesgo para EHE.

Metodología: Estudio prospectivo descriptivo general y comparativo de cohortes. Se establecieron 2 cohortes de gestantes: cohorteFR- (sin factores de riesgo), y cohorteFR+ (con factores de riesgo para EHE). Trimestralmente se analizó: rigidez arterial, Doppler de arterias uterinas, y determinación de los factores placentarios sFlt-1 y PlGF.

Resultados: Se incluyeron 84 gestantes (43 en la cohorteFR- y 41 en la cohorteFR+), edad media: 33±4,3 años, IMC: 25,3±5,3, primíparas: 54,6%.

En relación a la presión arterial y parámetros de rigidez arterial, la cohorteFR- presentó presiones arteriales periféricas, índice aumento (IA), presiones arteriales centrales y velocidad de la onda del pulso menores en el momento basal respecto a la cohorteFR+ (p=0,012 para el IA y p=0,000 para el resto). Esta diferencia se mantuvo en el segundo y tercer trimestre (2T y 3T), sin diferencias significativas en el comportamiento evolutivo de estas variables.

Por lo que respecta a la ecografía doppler: el % de pacientes con índice de pulsatilidad de arterias uterinas (IP) patológico fue más elevado en la cohorteFR+ en el 2T y en el 3T (3T: 32,4%vs19,5%, aunque con p ns).

En cuanto a los marcadores serológicos, el PlGF aumentó sobretodo en el 2T, siendo dicho aumento menor en la cohorteFR+ (aumento PlGF 2T: 8,4vs12,3 veces su valor basal, p=0,03). La sFlt-1 aumentó en ambas cohortes, con un incremento mayor en la cohorteFR+ (incremento sFlt-1 3T: 135,9%vs62,6%, p ns). El cociente sFlt-1/PlGF aumentó entre el 2T y el 3T sólo en la cohorteFR+.

Conclusión: La presión arterial y los parámetros de rigidez arterial són inferiores en la cohorteFR- ya desde el inicio de la gestación. El comportamiento evolutivo a lo largo de la gestación de estas variables es similar en ambos grupos. El porcentaje de IP patológicos aumenta de forma más marcada en la cohorteFR+ a medida que progresa la gestación (p ns). La cohorteFR+ tiene a lo largo de la gestación, un menor incremento de PlGF, y un ascenso más marcado de sFlt-1 y cociente sFlt-1/PlGF.

344 ••• LA ACTIVIDAD CIRCULANTE DEL ADAM17 COMO BIOMARCADOR DE EVENTO CARDIOVASCULAR EN PACIENTES CON ERC

V. PALAU[1], M. RIERA[1], JM. VALDIVIELSO[2], X. DURAN[3], S. VÁZQUEZ[1], A. BETRIU[3], E. FERNÁNDEZ[3], J. PASCUAL[1], MJ. SOLER[1]

[1]SERVICIO DE NEFROLOGÍA. HOSPITAL DEL MAR-INSTITUT HOSPITAL DEL MAR D'INVESTIGACIONS MÈDIQUES (BARCELONA),[2]SERVICIO DE NEFROLOGÍA. INSTITUT DE RECERCA BIOMÈDICA DE LLEIDA (LLEIDA), [3]DEPARTAMENTO DE ESTADÍSTICA. HOSPITAL DEL MAR-INSTITUT HOSPITAL DEL MAR D'INVESTIGACIONS MÈDIQUES (BARCELONA)

Introducción: ADAM17 y TNF-alpha correlacionan con la enfermedad cardiovascular(CV). El incremento en la expresión de ADAM17 y TNF- alpha ha demostrado implicaciones en disfunción cardiaca. Estudiamos la relación entre la actividad circulante del ADAM17 basal(sADAM17) y evento CV y mortalidad en pacientes con enfermedad renal crónica(ERC) a los 48 meses de seguimiento procedentes del estudio NEFRONA.

Material y Métodos: Se determinó la actividad circulante del ADAM17 basal mediante método fluorimétrico en plasma. Se estudiaron 1994 pacientes sin historia previa de enfermedad CV divididos en 2 grupos: pacientes con ERC estadio 3-5(ERC3-5), pacientes en diálisis(ERCSD). Se estudiaron eventos a los 48 meses de seguimiento: evento CV(angina de pecho, infarto agudo de miocardio, accidente cerebrovascular isquémico, infarto cerebral, hemorragia subaracnoidea, hemorragia intracerebral, insuficiencia cardiaca, aterosclerosis de las extremidades con claudicación intermitente y aneurisma aórtico abdominal), mortalidad CV, mortalidad no-CV y mortalidad general. Se realizaron curvas de supervivencia actuarial según la mediana de sADAM17, eventos CV y mortalidad. Para identificar los factores de riesgo para estos eventos se realizaron regresiones de Cox con sADAM17 ajustadas por diabetes, edad, tabaquismo y función renal.

Resultados: sADAM17 está aumentada en pacientes con evento CV y mortalidad CV, no-CV y general (p<0,001) según las curvas de supervivencia de Kaplan-Meier. En pacientes con ERC el incremento sADAM17, la diabetes, ser hombre, tener más de 65 años y estar en programa de diálisis son factores de riesgo de mortalidad CV y general. En el modelo multivariado de Cox se observó como un incremento sADAM17, sexo masculino, edad mayor de 65 años, diabetes y estar en programa de diálisis eran factores de riesgo independientes para sufrir un evento CV.

Conclusiones: Un aumento de actividad circulante basal del ADAM17 junto con los factores de riesgo clásicos (diabetes, edad, sexo masculino y ERC avanzada) nos puede ayudar a detectar a pacientes con ERC en riesgo de presentar enfermedad CV.

Tabla.
Eventos cardiovasculares (Regresión de Cox)

	HR ajustado (IC 95%)	p-valor
Mediana ADAM17 (≥14,9)	1,68(1,20-2,36)	**0,003**
Sexo (hombre)	1,53(1,10-2,12)	**0,011**
Diabetes	2,30(1,70-3,12)	**0,000**
Edad (≥65 años)	1,87(1,36-2,57)	**0,000**
ERCSD vs ERC3-5	2,77(1,99-3,85)	**0,000**
Fumador	1,31(0,92-1,89)	0,131

345 ••• ENSAYO CLÍNICO ABIERTO RANDOMIZADO PROERCAN (NCT03195023): EFECTO DE BLOQUEANTES DEL SISTEMA RENINA-ANGIOTENSINA-ALDOSTERONA (BSRAA) EN LA PROGRESIÓN DE LA ENFERMEDAD RENAL CRÓNICA DE PACIENTES MAYORES DE 65AÑOS CON NEFROPATÍAS NO PROTEINÚRICAS. DISEÑO Y RESULTADOS PRELIMINARES

A. GARCÍA-PRIETO1, M. GOICOECHEA1, U. VERDALLES1, A. PÉREZ DE JOSÉ1, E. VERDE1, T. LINARES1, D. BARBIERI1, I. ARAGONCILLO1, E. HURTADO1, J. LUÑO1

1NEFROLOGÍA. HOSPITAL GREGORIO MARAÑÓN (MADRID)

Introducción: En la actualidad no existe suficiente evidencia para la recomendación del uso de bloqueantes del sistema renina-angiotensina-aldosterona (BSRAA) como primera línea de tratamiento antihipertensivo en pacientes de edad avanzada con enfermedad renal crónica (ERC), sin proteinuria y sin cardiopatía.

El objetivo principal del estudio es evaluar el efecto de los BSRAA en la progresión renal de pacientes de edad avanzada. Los objetivos secundarios fueron evaluar: 1) la seguridad de los BSRAA mediante la recogida del número de episodios de hiperpotasemia y de deterioro agudo de la función renal, 2) el efecto sobre el riesgo cardiovascular y 3) la mortalidad global y cardiovascular.

Métodos: Estudio prospectivo, aleatorizado, que compara la eficacia de los BSRAA frente a otros tratamientos antihipertensivos en la progresión renal en pacientes mayores de 65 años con ERC estadios 3 y 4 e índice albumina/creatinina < 30mg/g. Criterios de exclusión: diabetes, cardiopatía isquémica, insuficiencia cardiaca o hipertensión resistente o mal controlada.

Randomización 1:1 BSRAA vs tratamiento antihipertensivo estándar. Los pacientes que recibían BSRAA fueron lavados durante 1 mes antes de la randomización. El tamaño muestral estimado fue de 110 pacientes, 55 por grupo, con un tiempo de seguimiento de 3 años. Se recogieron cifras tensionales y parámetros analíticos de un año previo a la randomización y durante el seguimiento.

Resultados: Presentamos los datos de 45 pacientes (18 varones, 27 mujeres) con un tiempo de seguimiento de 20 meses, edad media de 79,2±10,8 años, randomizados 15 al grupo BSRAA y 30 al estándar. La etiología de ERC fue: 34 vascular, 6 intersticial y 5 no filiada. En el grupo de BSRAA se observó progresión de ERC durante el tiempo de seguimiento (-7,3±1,6 ml/min), mientras que en los pacientes del grupo estándar se observó un aumento del filtrado glomerular (+7,1±0,8 ml/min), p 0,01. Se evidenció un aumento significativo de los niveles de potasio en el grupo BSRAA a los 20 meses y un descenso en el grupo estándar (+0,2±0,03 vs −0,4±0,01 mmol/l), p 0,02. No se apreciaron diferencias en el control tensional, el número de fármacos antihipertensivos, las cifras de albuminuria, la incidencia de eventos cardiovasculares ni en la mortalidad.

Conclusiones: Resultados preliminares muestran que en pacientes añosos con ERC no proteinúricas el uso de BSRAA no añade beneficio a la progresión de la enfermedad renal a corto plazo y sí más efectos secundarios como la hiperpotasemia.

346 ••• UTILIZACIÓN DE SACUBITRILO/VALSARTAN EN PACIENTES CON ENFERMEDAD RENAL CRÓNICA

J. VIAN[1], Z. GÓMEZ[2], A. ESTEBAN[2], M. GONZÁLEZ[2], F. TORNERO[1], R. BOVER[2], V. LÓPEZ DE LA MANZANARA[1], JA. HERRERO[1]

[1]NEFROLOGÍA. HOSPITAL CLÍNICO SAN CARLOS (ESPAÑA), [2]CARDIOLOGÍA. HOSPITAL CLÍNICO SAN CARLOS (ESPAÑA)

Introducción: El tratamiento con inhibidores de la neprilisina asociado a antagonistas del receptor de la angiotensina II ha demostrado su eficacia en el tratamiento de la insuficiencia cardiaca congestiva con FEVI deprimida. Estos pacientes presentan frecuentemente afectación de la función renal, si bien es poca la experiencia con este fármaco en pacientes que presentan enfermedad renal crónica. El objetivo de este estudio es analizar la seguridad del sacubitrilo/valsartan en pacientes con enfermedad renal, así como evaluar la evolución de los parámetros clínicos y analíticos.

Material y métodos: Se estudiaron todos los pacientes en los que se inició tratamiento con sacubitrilo/valsartan en la unidad de insuficiencia cardiaca del Hospital Clínico San Carlos, desde junio de 2016 hasta septiembre de 2017. Se recogieron variables demográficas en la primera visita y tensión arterial, frecuencia cardiaca y parámetros analíticos (hemoglobina, creatinina, sodio, potasio, estimación del filtrado glomerular y nt- proBNP) valorando la evolución de estos parámetros en función del grado de función renal al inicio del tratamiento con sacubitrilo/valsartan, hasta el final de la titulación. Se realizó un análisis comparativo de las medias de cada uno de los parámetros entre la primera y la última visita.

Resultados: De los 156 pacientes analizados, el 72% eran varones y el 28% mujeres, con una edad media de 72 años. Un total de 76 pacientes (47,8%) presentaban un filtrado glomerular estimado por CKD-EPI >60 ml/min, 33 pacientes (21,5%) correspondían a un filtrado glomerular entre 46- 60 ml/min, 39 pacientes (25,0%), tenían un filtrado glomerular entre 30-45 ml/min y sólo 8 pacientes (5,1%) iniciaron sacubitrilo/valsartan con un filtrado glomerular estimado < 30 ml/min. En todos los grupos se objetivó un descenso de creatinina tras el inicio del fármaco (Cr 1,24 vs 1,19 mg/dL en pacientes con FG 46-60 ml/min [p >0,05], Cr 2,26 vs 2,05 ml/min en pacientes con FG <30 ml/min [p>0,05]), si bien sólo alcanzó la significación estadística el grupo de pacientes con filtrado entre 30-45 ml/min (Cr 1,6 vs 1,41 mg/dl [p =0.02]). No observamos diferencias estadísticamente significativas en ninguno de los grupos de función renal estudiados entre los valores de presión arterial sistólica y diastólica, de sodio, potasio y nt-pro BNP.

Conclusiones: El sacubitrilo/valsartan es un fármaco seguro en pacientes con enfermedad renal crónica. La introducción del fármaco no solo no produce deterioro de función renal si no que puede producir mejoría, especialmente en pacientes con enfermedad renal crónica más severa.

Palau V, Riera M, Valdivielso JM, Duran X, Vázquez S, Betriu A, et al. Actividad circulante del ADAM17 en la enfermedad renal crónica (Abstract). Nefrología. 2018; 38(suppl_1):128.

Resúmenes

Enfermedad renal crónica - Progresión de la IRC

471 COMPARACIÓN DE LOS MARCADORES DE ESTRÉS OXIDATIVO EN LOS ESTADIOS INICIALES VS FINALES DE LA ENFERMEDAD RENAL CRÓNICA

JM. GALLARDO[1], RA. ANDRADE-MORENO[2], MF. GUTIERREZ-DERAS[1], ML. VILLELA-TORRES[1], ME. GALVAN-PLATA[2], P. VALDEZ-CABALLERO[1], R. PANIAGUA[1]

[1]UNIDAD DE INVESTIGACIÓN MÉDICA EN ENFERMEDADES NEFROLÓGICAS. HE, CENTRO MÉDICO NACIONAL "SIGLO XXI", INSTITUTO MEXICANO DEL SEGURO SOCIAL (CIUDAD DE MÉXICO, MÉXICO.), [2]MEDICINA INTERNA. HE, CENTRO MÉDICO NACIONAL "SIGLO XXI", INSTITUTO MEXICANO DEL SEGURO SOCIAL (CIUDAD DE MÉXICO, MÉXICO.)

Introducción: El estrés oxidativo ha sido asociado como un contribuyente importante de la patogénesis y el desarrollo de complicaciones en enfermedades crónicas, dentro de las cuales se encuentran la enfermedad renal crónica. El propósito de este estudio fue investigar los cambios en el estado antioxidante y oxidativo inducido por la enfermedad renal crónica (ERC) en pacientes en estadio temprano (1) vs terminal (5).

Materiales y métodos: Estudio transversal analítico, donde se estudiaron diferentes marcadores de estrés oxidativo en muestras de suero de participantes divididos en dos subgrupos: (A) sujetos con ERC en estadio 1 (n=33); (B) sujetos con ERC en estadio 5 (n=32).

Se midió la actividad de dos antioxidantes (AOx): glutatión total (GSH), y vitamina C (VC) y dos oxidantes (Ox): malondialdehido (MDA) y productos finales de la glucosilación (AGEs). Paralelamente se obtuvieron valores clínicos y bioquímicos de todos los participantes. El análisis estadístico de los resultados obtenidos se realizó mediante métodos estadísticos paramétricos o no paramétricos según se requiriió (prueba t de Student o U de MannWhitney). Se buscó correlación entre la severidad de la ERC y los marcadores bioquímicos de estrés oxidativo, así como de la función renal, mediante correlación de Pearson conforme a su distribución. El valor de p<0.05 se consideró significativo.

Consideraciones éticas. El proyecto se aprobó por el comité local de investigación en salud (R-2017-3601-48). Este estudio cumplió con la normatividad de la Ley General de Salud de México y del Código de Helsinki vigentes.

Resultados y Conclusiones: El análisis mostró que los productos avanzados de la glucosilación (AGE's) se encontraron significativamente más elevados en el paciente con enfermedad renal crónica estadio 5 con respecto a pacientes en el estadio 1 (p<0.0001). El malondialheído mostró un comportamiento similar (p<0.0001). En cuanto al grupo de los antioxidantes, la vitamina C mostró una disminución importante en el paciente con enfermedad crónica en estadio 5 con respecto a pacientes en el estadio 1 (p<0.0001). Los niveles de glutatión (GSH) mostraron también una disminución marcada. (p=0.0029) Como se esperaba la creatinina se encontró considerablemente elevada en el estadio 5, que va de la mano con la disminución en la tasa de filtración glomerular en este tipo de pacientes (<0.0001). En las mediciones de rutina, se han observado también diferencias estadísticas entre el grupo 5 en comparación con el grupo 1. El resto de las mediciones permanecieron sin cambios.

472 C1Q/TNF RELATED PROTEIN 1, OBESIDAD Y PROGRESIÓN DE ENFERMEDAD RENAL CRÓNICA

D. BARBIERI MERLO[1], M. GOICOECHEA DIEZHANDINO[1], A. ORTIZ ARDUÁN[2], M. SÁNCHEZ NIÑO[3], E. VERDE MORENO[1], U. VERDALLES GUZMÁN[1], A. PÉREZ DE JOSÉ[1], A. DELGADO RODRÍGUEZ[1], A. GARCÍA PRIETO[1], J. LUÑO FERNÁNDEZ[1]

[1]NEFROLOGÍA. H. GREGORIO MARAÑÓN (MADRID/ESPAÑA), [2]NEFROLOGÍA. IIS-FUNDACIÓN JIMENEZ DIAZ UAM (MADRID/ESPAÑA),[3]BIOQUÍMICA. IIS-FUNDACIÓN JIMENEZ DIAZ UAM (MADRID/ESPAÑA)

Introducción: La obesidad es un factor para el desarrollo de enfermedad renal crónica (ERC) en la población general. Sin embargo, no todos los estudios presentan asociación entre IMC y progresión de la ERC. C1q/TNF related protein 1 (CTRP1) es una nueva adipoquina con efectos antiaterogénicos y antiinflamatorios y puede jugar un papel entre obesidad y enfermedades vasculares. Estudio observacional prospectivo que analiza los niveles de CTRP1 y su asociación en pacientes con obesidad y ERC.

Métodos: Se incluyeron pacientes con ERC estadio 3/4 sin eventos cardiovasculares previos, divididos en dos grupos según IMC. Se recogieron mediciones basales de CTRP1, función renal, albuminuria, estudio metabólico, PCR, aldosterona, renina plasmática y medicación concomitante. Se recogieron los eventos renales definidos como entrada en diálisis, duplicación de creatinina o caída de un 50% del filtrado glomerular (MDRD4).

Resultados: 71 pacientes con ERC divididos en dos grupos: 25 obesos (IMC≥30 kg/m2) y 46 no obesos. CTRP1 en plasma fue más elevada en obesos (342 ±141 vs 433±246 ng/ml, p=0,041), no encontrando una asociación con grado de ERC, diabetes, aldosterona y renina, ni presión arterial. Los obesos tuvieron mayor presión arterial sistólica (p=0,018) y mayor PCR (p=0,019) y úrico (p=0,003), sin diferencias en diabetes ni albuminuria. Durante un seguimiento medio de 63,7 meses, 14 pacientes tuvieron un evento renal. Los pacientes con CTRP1 en el tercil más bajo tuvieron más eventos renales en el global de la muestra (logRank: 5,810, p=0,016) y en los obesos (logRank: 5,405, p=0,020). Los niveles de CTRP1 más elevados (HR 0,992 (0,986-0,998), p=0,001), se asocian a progresión renal más lenta en un modelo ajustado para obesidad, albuminuria y función renal.

Conclusiones: CTRP1 aumenta en los pacientes con obesidad y ERC, con un papel probablemente protector, puesto que se asocia a progresión más lenta de la enfermedad renal a largo plazo.

Figura 1.

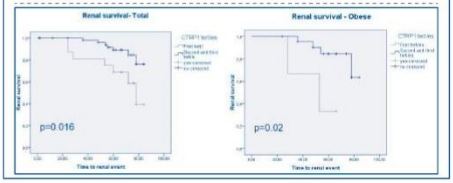

473 ACTIVIDAD CIRCULANTE DEL ADAM17 EN LA ENFERMEDAD RENAL CRÓNICA

V. PALAU[1], M. RIERA[1], JM. VALDIVIELSO[2], X. DURAN[3], S. VÁZQUEZ[1], A. BETRIU[3], E. FERNANDEZ[3], J. PASCUAL[1], MJ. SOLER[1]

[1]SERVICIO DE NEFROLOGÍA. HOSPITAL DEL MAR-INSTITUT HOSPITAL DEL MAR D'INVESTIGACIONS MÈDIQUES (BARCELONA),[2]SERVICIO DE NEFROLOGÍA. INSTITUT DE RECERCA BIOMÈDICA DE LLEIDA (LLEIDA), [3]DEPARTAMENTO DE ESTADÍSTICA. HOSPITAL DEL MAR-INSTITUT HOSPITAL DEL MAR D'INVESTIGACIONS MÈDIQUES (BARCELONA)

Introducción: ADAM17 (desintegrina y metaloproteasa) se ha asociado con la enfermedad cardiovascular(CV) entre otras. El ADAM17 circulante no se ha estudiado previamente en pacientes con enfermedad renal crónica(ERC). Nos proponemos estudiar la relación entre la actividad circulante del ADAM17(sADAM17) y la función renal en pacientes con ERC sin historia previa de enfermedad CV procedentes del estudio NEFRONA.

Materiales y métodos: La actividad circulante del ADAM17 a nivel basal se analizó por método fluorimétrico en plasma de 2570 pacientes. Estos se dividieron en 3 grupos: ERC estadio 3-5(ERC3-5), ERC estadio 5D(ERC5D) y controles. Se estudió la relación del ADAM17 con la función renal basal y posteriormente, la relación con progresión de ERC definida como incrementar 30% la creatinina sérica y/o inicio de terapia renal sustitutiva(TRS) a los 24 meses de seguimiento. Se realizaron análisis multivariados para determinar la asociación entre el ADAM17 basal y la función renal tanto basal como su progresión.

Resultados: sADAM17 se encontró significativamente incrementada en ERC3-5 en comparación con controles (mediana[IQ25- IQ75];14,37[7,99-24,79] vs 10,46[7,10-14,15]) y en ERC5D(34,40[19,90-57,60]) en comparación con controles y ERC3-5. En el análisis multivariado ajustado por edad, sexo, diabetes, dislipemia, hipertensión, tratamiento con insulina y bloqueo del Sistema Renina Angiotensina, ERC5D y ERC3-5 se asociaron de forma independiente a sADAM17 (p<0,001). Además, sADAM17 se encontró elevada en pacientes que presentaban progresión de la ERC. Mediante análisis multivariado se observó una interacción entre la sADAM17 y el sexo en pacientes que incrementaban la creatinina sérica y/o inicio TRS. Separando la población por sexo, observamos como en hombres, existía una asociación independiente entre sADAM17 y progresión de ERC, en cambio, en mujeres, no se observó.

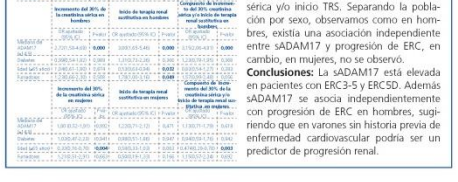

Conclusiones: La sADAM17 está elevada en pacientes con ERC3-5 y ERC5D. Además sADAM17 se asocia independientemente con progresión de ERC en hombres, sugiriendo que en varones sin historia previa de enfermedad cardiovascular podría ser un predictor de progresión renal.

474 IMPORTANCIA DE UN PROCESO SISTEMÁTICO DE DECISIÓN COMPARTIDA EN LA ELECCIÓN DE TERAPIA RENAL SUBSTITUTIVA: UN ANÁLISIS PROSPECTIVO DURANTE 4 AÑOS

S. COLLADO[1], F. BARBOSA[1], H. CAO[1], M. FERNÁNDEZ[1], E. BARBERO[1], E. JUNYENT[1], J. PASCUAL[1]

[1]NEFROLOGÍA. HOSPITAL DEL MAR (BARCELONA)

Objetivo: Analizar las opciones terapéuticas escogidas por pacientes con enfermedad renal crónica avanzada (ERCA) grados 4-5 tras la implementación de un proceso de decisión de tratamiento renal substitutivo (TRS).

Metodología: Análisis prospectivo durante 4 años (2014-2017) en pacientes con ERC G4-5 que pasaron por el proceso de elección de técnica de TRS con visitas estandarizadas a cargo de enfermería especializada y nefrólogo (n=276). Se recogió mortalidad total y cardiovascular, datos demográficos habituales, impacto sobre la terapia renal escogida y tipo de inicio.

Resultados: La edad era 71.6±15.1 años (33% >80 años) y 57.9% eran varones. Remitidos a consulta de ERCA conjunta enfermera-nefrólogo con un FGe medio de 22.7 ml/min, el tiempo medio de seguimiento fue 132.3±118.4 semanas, La etiología principal de ERC era vascular-hipertensiva (29.5%), presentando antecedentes de HTA un 98%, DM 47% e insuficiencia cardiaca 21.5%. Tras la instauración del proceso, el número de pacientes derivados a consulta ERCA ha crecido un 40%. Un 47.8% escogen hemodiálisis (HD), un 32.8% diálisis peritoneal (DP) y un 17.5% tratamiento conservador. Este proceso de elección ha permitido un mejor cribado de pacientes potencialmente trasplantables, situándose en el 48.5% del total.

Si comparamos estos datos con el periodo previo a la instauración de este proceso reglado, la elección de HD ha crecido un 14.2%, DP un 55.5%, la elección de trasplante de donante vivo como primera opción un 50% y la elección de tratamiento conservador un 85% (p=0.015).

Finalmente, 167 pacientes iniciaron TRS, evidenciándose un mayor inicio electivo tanto en HD como DP (74.5%), así como mayor control y enlentecimiento de su ERC. El inicio de TRS por agudización de la ERC se redujo de un 40% en 2014 a un 25.8% en 2017 (p<0.001) y de éstos, el 83.8% presentaban acceso vascular nativo definitivo.

Durante los 4 años se han registrado 84 éxitus (causa cardiovascular 45%, infecciosa 21%, neoplásica 13% y otras 19%), pero a pesar del aumento del porcentaje de pacientes en tratamiento conservador, la mortalidad anual se ha mantenido estable (8.3% vs 8.5%).

Conclusiones: El desarrollo de un proceso de decisiones compartidas de modalidad de TRS mejora el control de la ERC y sus complicaciones, así como el inicio electivo de TRS. En la fase inicial del proceso educacional, aumenta el número de pacientes que escogen DP, estabilizándose en años posteriores. El porcentaje de pacientes que optan por el tratamiento conservador aumenta, sobre todo en los más añosos y comórbidos.

Palau V, Soler MJ, Nurgaha B, Emmert M, Hoerstrup S, Pascual J, et al. Cultivo 3D de células tubulares renales para estudiar el papel del ADAM17 en la nefropatía diabética (Abstract). Nefrología. 2020; 40(Suppl_1):5. *(Best Oral Presentation Award)*.

Diabetes

1 LAS VESÍCULAS EXTRACELULARES DE SUERO DE PACIENTES CON NEFROPATÍA DIABÉTICA INDUCEN DISFUNCIÓN ENDOTELIAL MEDIADA POR ICAM-1 Y VCAM-1 EN UN MODELO IN VITRO

E. MONTAGUD-MARRAHI[1], S. TORRAMADE-MOIX[2], MJ. RAMÍREZ-BAJO[3], J. ROVIRA[3], E. BAÑÓN-MANEUS[3], E. HERMIDA[1], F. DIEKMANN[4], M. PALOMO[2], M. DÍAZ-RICART[3], P. VENTURA-AGUIAR[4]
[1]NEFROLOGÍA Y TRASPLANTE RENAL. HOSPITAL CLÍNIC DE BARCELONA (BARCELONA),[2]HEMATOPATOLOGÍA, CENTRO DE DIAGNÓSTICO BIOMÉDICO(IDIBAPS).INSTITUTO PARA LA INVESTIGACIÓN BIOMÉDICA AUGUST PI I SUNYER (IDIBAPS). HOSPITAL CLÍNIC DE BARCELONA (BARCELONA), [3]LABORATORIO EXPERIMENTAL DE NEFROLOGÍA Y TRASPLANTE (LENIT). INSTITUTO PARA LA INVESTIGACIÓN BIOMÉDICA AUGUST PI I SUNYER (IDIBAPS). HOSPITAL CLÍNIC DE BARCELONA (BARCELONA)[4]. NEFROLOGÍA Y TRASPLANTE RENAL/LABORATORIO EXPERIMENTAL DE NEFROLOGÍA Y TRASPLANTE (LENIT). INSTITUTO PARA LA INVESTIGACIÓN BIOMÉDICA AUGUST PI I SUNYER (IDIBAPS). HOSPITAL CLÍNIC DE BARCELONA (BARCELONA), [5]HEMATOPATOLOGÍA, CENTRO DE DIAGNÓSTICO BIOMÉDICO/INSTITUTO PARA LA INVESTIGACIÓN BIOMÉDICA AUGUST PI I SUNYER (IDIBAPS)/ JOSEP CARRERAS LEUKAEMIA RESEARCH INSTITUTE/BARCELONA ENDOTHELIUM TEAM. HOSPITAL CLÍNIC DE BARCELONA (BARCELONA), [6]HEMATOPATOLOGÍA, CENTRO DE DIAGNÓSTICO BIOMÉDICO/INSTITUTO PARA LA INVESTIGACIÓN BIOMÉDICA AUGUST PI I SUNYER (IDIBAPS)/BARCELONA ENDOTHELIUM TEAM. HOSPITAL CLÍNIC DE BARCELONA (BARCELONA)

Introducción: las vesículas extracelulares (VEs) son estructuras membranosas liberadas por las células que están formadas por diferentes compuestos citoplasmáticos y que se han descrito como potencialmente patógenas en la disfunción endotelial (DE), capaces de modificar la expresión de receptores endoteliales. Los mecanismos de la DE en pacientes con enfermedad renal crónica (ERC) y diabetes mellitus (DM) no están bien definidos, aunque las VEs pueden tener un papel fundamental.

Material y Método: estudio transversal con suero de 11 pacientes de 46±7.6 años (45% mujeres) con ERC (FGe 18±7mL/min) por nefropatía diabética (DM1),agrupados en 4 pooles. Se estudió el papel de las VEs mediante un modelo in vitro de DE con células HMEC-1 expuestas durante 72 horas a medio suplementado con a)suero del paciente (grupo 1*roja*); b)suero del paciente deplecionado de VE (grupo 2/naranja); c)suero control deplecionado al cual se añadió las VEs del paciente (grupo 3/ amarillo); Se analizaron cambios en la expresión de la proteína adhesiva vWF y los receptores de adhesión de membrana VCAM-1 e ICAM-1 en las células expuestas a las distintas condiciones, respecto al suero de donante sano.

Resultados: la expresión de los marcadores de DE (vWf, VCAM-1 e ICAM-1) en las células expuestas a suero del paciente (con o sin VE) fue superior respecto a la exposición a los sueros control (vWf, p<0.01; Fig.1A; VCAM-1 p<0.01; Fig.1B, ICAM-1, p<0.01; Fig.1C). También se identificó que la depleción de VEs disminuye de forma significativa la expresión de VCAM-1 e ICAM-1 respecto al suero del paciente (Fig.1B, p<0.01 y 1C, p<0.01), pero no de vWF.

Figure 1. Cost of complications per prevalent patient/year for years 2017 and 2018. PD= Peritoneal dialysis, HDH= Hemodialysis of patients treated in Josep Trueta Hospital, CHDC= Hemodialysis of patients treated in contracted out-patient HD center

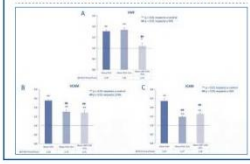

Conclusiones: las VEs incrementan el daño endotelial a través del aumento de VCAM-1 e ICAM-1, siendo ambos marcadores inflamatorios asociados a adhesión leucocitaria, constituyendo así un elemento patogénico en la DE en el paciente con DM1 y ERC. Conocer su procedencia y contenido es clave para evitar la DE.

2 EFECTO DE LA FUNCIÓN RENAL SOBRE LOS NIVELES CIRCULANTES DE SUCCINATO EN PACIENTES CON DIABETES MELLITUS TIPO 2

A. SIERRA-OCHOA[1], G. LLAURADÓ[2], E. SOLÁ-PORTA[1], E. RODRIGUEZ[1], L. SANS[1], MD. ARENAS[1], J. FLORES[1], S. FERNANDEZ-VELEDO[2], J. PASCUAL[1], C. BARRIOS[1]
[1]NEFROLOGÍA. HOSPITAL DEL MAR/INSTITUT HOSPITAL DEL MAR D'INVESTIGACIONS MÈDIQUES (IMIM) (BARCELONA/ESPAÑA),[2]ENDOCRINOLOGÍA. HOSPITAL DEL MAR (BARCELONA/ESPAÑA), [3]UNIDAD DE INVESTIGACIÓN. HOSPITAL UNIVERSITARI DE TARRAGONA JOAN XXIII (TARRAGONA/ESPAÑA)

Introducción: El succinato circulante, un metabolito producido tanto por la microbiota como por el huésped, aumenta en la hipertensión, la cardiopatía isquémica, la diabetes tipo 2 (DM2), la obesidad y se postula como marcador de riesgo cardiovascular (CV). Estudios experimentales sugieren que su acúmulo tisular y la señalización de su receptor SUCNR1 activa la respuesta celular que desencadena el daño renal en la diabetes y aumenta la liberación de renina. Se conoce poco sobre su relación práctica en la clínica con la función renal y en concreto con la enfermedad renal diabética (ERD).

Objetivo: Estudiar la relación de los niveles circulantes de succinato con la función renal y la proteinuria en una cohorte de diabéticos tipo 2.

Métodos: Los niveles de succinato se obtuvieron mediante ensayo fluorimétrico (EnzyChromTM Kit) en suero de 602 pacientes con DM2>10 años de evolución, 61,3%Hombres: 38,7%Mujeres, de 69,8±9,3 años, con distintos grados de ERD: G1-2; 53,9%, G3; 32,9%, y G4-5; 13,1% de los participantes, pertenecientes a la cohorte GenoDiabMar. El FGe se calculó mediante la fórmula CKD-EPI y se consideró ERD *si*, FGe<=60 y/o albúmina/creatinina en orina>=300mg/gr o albúmina/creatinina en orina 30-299mg/gr y retinopatía.

Resultados: El análisis no ajustado observó menores niveles de succinato en los grupos con mayor afectación renal: G1-2; 63,5±32,1µM/L, G3; 58,9±34,5µM/L y G4-5; 46,9±27,5µM/L, p<0,001. Este hallazgo fue independiente en los modelos multivariados ajustados por edad, sexo, IMC, tiempo de DM, HTA, HbAc1, cardiopatía isquémica, AVC, vasculopatía periférica y el uso de inhibidores del SRAA, donde el succinato mostró una asociación independiente con la ERD con OR: 0.97 [0.98 - 0.99] p<0,001. Detectamos, además, una relación inversa con la albuminuria: rho -0,21 p<0,001. La asociación negativa entre la proteinuria y el succinato circulante se confirma en el modelo ajustado por el resto de covariables, incluida la función renal, Coef: -1,65 [-3.27 - -.038] p=0,04.

Conclusiones: Al contrario de los esperado, el análisis ajustado muestra que grados más avanzados de enfermedad renal crónica se asocian a niveles de succinato más bajos. Este hallazgo podría explicarse por su relación, independiente del FGe, con la proteinuria. El estudio de la expresión de los receptores de succinato renal y el análisis de sus niveles urinarios, ayudarán a entender mejor la fisiopatología y su relación con esta enfermedad. Es importante valorar el efecto la función renal y las peculiaridades según su etiología, sobre los marcadores emergentes de riesgo CV.

3 LOS NIVELES ELEVADOS DE IL-6 PREDICEN LA PROGRESIÓN DE LA NEFROPATÍA DIABÉTICA

B. SÁNCHEZ ÁLAMO[1], A. SHABAKA[1], V. CACHOFEIRO[2], GM. FERNÁNDEZ JUÁREZ[1]
[1]NEFROLOGÍA. HOSPITAL UNIVERSITARIO FUNDACIÓN ALCORCÓN (MADRID), [2]DEPARTAMENTO FISIOLOGÍA. UNIVERSIDAD COMPLUTENSE (MADRID)

Introducción: La nefropatía diabética(ND) es la principal causa de enfermedad renal crónica terminal(ERCT). Existen evidencias de que la inflamación juega un papel importante en su patogénesis y progresión. En ese sentido, la interleuquina 6 (IL-6) se ha identificado como un mediador importante del daño renal. El objetivo de este estudio ha sido investigar si existe una asociación entre los niveles de IL-6 y la progresión de la ND.

Métodos: Se han analizado los niveles de IL-6 en 70 pacientes incluidos en el ensayo clínico multicéntrico randomizado PRONEDI. El objetivo primario compuesto se definió como:aumento >50% de la creatinina sérica basal, ERCT o exitus.

Resultados: Los niveles de IL-6 se correlacionaron con otros biomarcadores inflamatorios como el TNFα(r:0,29;IC95%:0,05-0,49;p=0,02), y la PCR:r=0,61;IC95% 0,44-0,74,p<0,01.Los pacientes se clasificaron en terciles según los niveles basales de IL-6. Después de una mediana de 48 meses de seguimiento, el objetivo primario fue alcanzado por 15 pacientes(65,22%) del primer tercil, 15 (62,6%) del segundo y 20 pacientes(86,96%) del tercero(p:0,001).

En el modelo de Cox, los niveles elevados de IL-6 se asociaron con el objetivo primario (HR:3,86;IC95%:1,075-13,864;p:0,038). El efecto no se modificó tras ajustar por creatinina, proteinuria y tratamiento con inhibidores del SRAA. En el modelo de análisis mixto los niveles de IL-6 no se modificaron por el tratamiento.

El área bajo la curva dependiente del tiempo mostró que la capacidad predictiva de la IL-6 para el objetivo primario fue de 0,879 al segundo año de seguimiento. Los niveles de 4,68 pg/mg tuvieron una sensibilidad del 100% y una especificidad del 78,7% para predecir el objetivo primario.

Conclusión: En pacientes con ND y proteinuria, los niveles de IL-6 se asociaron con progresión renal y no se modificaron con el bloqueo del SRAA. Por este motivo,la IL-6 es un biomarcador prometedor que podría usarse en la práctica clínica para identificar a los pacientes con alto riesgo de progresión renal.

Tabla 1.

AUC (IC 95%)	Punto de corte	Sensibilidad (IC95%)	Especificidad (CI 95%)	VPP (IC95%)	VPN (IC95%)
0,879 (0,791-0,966)	4,68 pg/mL	100% (100-100)	78,72% (66,9-90,5)	45,67% (23,2-68,1)	100% (100-100)

*Curva ROC dependiente del tiempo para el endpoint primario a los 2 años

4 CULTIVO 3D DE CÉLULAS TUBULARES RENALES PARA ESTUDIAR EL PAPEL DEL ADAM17 EN LA NEFROPATÍA DIABÉTICA

V. PALAU[1], MJ. SOLER[1], B. NUGRAHA[2], M. EMMERT[3], S. HOERSTRUP[3], J. PASCUAL[1], M. RIERA[1]
[1]NEFROLOGÍA. INSTITUTO HOSPITAL DEL MAR DE INVESTIGACIONES MÉDICAS (BARCELONA), [2]UNIVERSITY OF ZURICH. INSTITUTE FOR PARASITOLOGY (ZURICH), [3]UNIVERSITY OF ZURICH. INSTITUTE FOR REGENERATIVE MEDICINE (SCHLIEREN)

ADAM17 es una desintegrina y metaloproteinasa capaz de cortar los ectodominios de varias enzimas, receptores y ligandos. Se ha demostrado que la expresión proteica de ADAM17 aumenta en las células mesangiales renales en medio rico en glucosa de manera parecida a lo observado en pacientes diabéticos. Nos proponemos analizar el efecto de la deleción del ADAM17 en esferoides 3D de células renales humanas(HKC-8) en cultivo incubadas con medio bajo en glucosa(LG), rico en glucosa(HG) y manitol.

La deleción del ADAM17 se llevó a cabo mediante la técnica CRISPR/Cas9. Las células HKC-8 crecieron en una matriz de hidrogel de dextrano. 13 días después de la siembra, los esferoides fueron incubados con HG(35mM), LG(5,5mM) o manitol(35mM) durante 6h, 24h o 72h. Se determinó la expresión génica de marcadores fibróticos e inflamatorios a las 6h y 24h. A las 72h post-incubación, se determinó por inmunofluorescencia la expresión de varios marcadores de fibrosis.

La expresión génica de CCL5 incrementó a las 6h y 24h en los esferoides WT incubados con HG. En los esferoides con deleción del ADAM17, no se observó incremento de la expresión de CCL5 a las 6h pero sí una ligera tendencia a disminuir a las 24h comparado con el control. La expresión génica de colágeno-IV aumentó en los esferoides incubados con HG a las 24h. La deleción de ADAM17 disminuyó la expresión génica de colágeno-IV en los esferoides incubados con HG en comparación con los WT. El medio HG produjo un incremento en la acumulación de αSMA, fibronectina y colágeno-IV. En cambio, la deleción del ADAM17 disminuyó la tinción para αSMA, fibronectina y colágeno-IV en los esferoides incubados con HG durante 72h.

ADAM17 está implicado en los cambios fenotípicos de la célula tubular renal diabética. Su deleción protege frente a fibrosis e inflamación en los esferoides HKC-8 incubados con HG.

Tabla 1.

	CCL5		Colágeno -IV	
	6h	24h	6h	24h
LG-WT	1,47±0,77	1,23±0,39	1,00±0,22	1,10±0,26
HG-WT	4,70±2,19*	5,64±1,67*	1,44±0,61	13,97±1,54*
M-WT	1,21±0,67	1,15±0,75#	1,43±0,23	0,72±0,26#
LG-KO	1,96±0,93	1,44±0,41	0,62±0,12	2,20±0,44
HG-KO	1,04±0,28	2,73±0,24*	1,00±0,59	3,21±1,43$
M-KO	0,77±0,14	1,56±0,74	1,01±0,10	1,27±0,54

*p<0,05 HG vs. LG; $p<0,05 KO vs. WT, #p<0,05 M vs. HG

Figure 1. Inmunofluorescencia de Colageno-IV

Figure 2. Inmunofluorescencia de αSMA

Figure 3. Inmunofluorescencia de Fibronectina

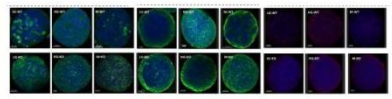

••• Presentación oral •• E-póster • Póster

10.3 Funding

This thesis was supported by funding from the following grants:

1. Fondo de Investigación Sanitaria-Instituto Carlos III-FEDER (ISCIII-FEDER PI 14/00557). Principal Investigator: Dr. María José Soler Romeo.

2. Red de Investigación Renal. Fondo de Investigación Sanitaria-Instituto Carlos III. Subprograma RETICS (ISCIII-REDinREN RD16/0009/0013). Principal Investigator: Dr. Julio Pascual Santos.

3. Ayudas predoctorales de formación en investigación en salud. Convocatoria 2017. Fondo de investigación Sanitaria-Instituto Carlos III-FEDER (ISCIII-FEDER, FI 17/00025). Principal Investigator: Dr. Julio Pascual Santos.

4. Ayudas para la movilidad de personal investigador contratado en el marco de la AES (M-AES). Convocatoria 2018. Fondo de investigación Sanitaria-Instituto Carlos III-FEDER (ISCIII-FEDER, MV18, 00031). Principal Investigator: Dr. Julio Pascual Santos.